Characterization of the Hsp40 partner proteins of *Plasmodium falciparum* Hsp70

Thesis submitted in fulfillment of the requirements for the degree of

Doctor of Philosophy
(Biochemistry)

In The Department Of Biochemistry, Microbiology and Biotechnology

Faculty of Science

RHODES UNIVERSITY

By

James Mwangi Njunge

2014

Declaration

I, James Mwangi Njunge, declare that this thesis is my own unaided work hereby submitted for the degree of Doctor of Philosophy (Biochemistry) at Rhodes University. Where the work of other researchers has been included in the thesis, the person responsible for producing such work has been appropriately acknowledged. It has not been submitted for any other degree for examination at any other university.

_____

James Mwangi Njunge

Dated this _____Day of _____ _____

Abstract

Human malaria is an economically important disease caused by single-celled parasites of the *Plasmodium* genus whose biology displays great evolutionary adaptation to both its mammalian host and transmitting vectors. This thesis details the 70 kDa heat shock protein (Hsp70) and J protein chaperone complements in malaria parasites affecting humans, primates and rodents. Heat shock proteins comprise a family of evolutionary conserved and structurally related proteins that play a crucial role in maintaining the structural integrity of proteins during normal and stress conditions. They are considered future therapeutic targets in various cellular systems including *Plasmodium falciparum*. J proteins (Hsp40) canonically partner with Hsp70s during protein synthesis and folding, trafficking or targeting of proteins for degradation. However, in *P. falciparum*, these classes of proteins have also been implicated in aiding the active transport of parasite proteins to the erythrocyte cytosol following erythrocyte entry by the parasite. This host-parasite "cross-talk" results in tremendous modifications of the infected erythrocyte, imparting properties that allow it to adhere to the endothelium, preventing splenic clearance. The genome of *P. falciparum* encodes six Hsp70 homologues and a large number of J proteins that localize to the various intracellular compartments or are exported to the infected erythrocyte cytosol. Understanding the Hsp70-J protein interactions and/or partnerships is an essential step for drug target validation and illumination of parasite biology. A review of these chaperone complements across the *Plasmodium* species shows that *P. falciparum* possesses an expanded Hsp70-J protein complement compared to the rodent and primate infecting species. It further highlights how unique the *P. falciparum* chaperone complement is compared to the other *Plasmodium* species included in the analysis. In silico analysis showed that the genome of *P. falciparum* encodes approximately 49 J proteins, 19 of which contain a PEXEL motif that has been implicated in routing proteins to the infected erythrocyte. Most of these PEXEL containing J proteins are unique with no homologues in the human system and are considered as attractive drug targets.

Very few of the predicted J proteins in *P. falciparum* have been experimentally characterized. To this end, cell biological and biochemical approaches were employed to characterize PFB0595w and PFD0462w (Pfj1) J proteins. The uniqueness of Pfj1 and the controversy in literature regarding its localization formed the basis for the experimental work. This is the first study showing that Pfj1 localizes to the mitochondrion in the intraerythrocytic stage of

development of *P. falciparum* and has further proposed PfHsp70-3 as a potential Hsp70 partner. Indeed, attempts to heterologously express and purify Pfj1 for its characterization are described. It is also the first study that details the successful expression and purification of PfHsp70-3. Further, research findings have described for the first time the expression and localization of PFB0595w in the intraerythrocytic stages of *P. falciparum* development. Based on the cytosolic localization of both PFB0595w and PfHsp70-1, a chaperone – cochaperone partnership was proposed that formed the basis for the in vitro experiments. PFB0595w was shown for the first time to stimulate the ATPase activity of PfHsp70-1 pointing to a functional interaction. Preliminary surface plasmon spectroscopy analysis has revealed a potential interaction between PFB0595w and PfHsp70-1 but highlights the need for further related experiments to support the findings. Gel filtration analysis showed that PFB0595w exists as a dimer thereby confirming in silico predictions. Based on these observations, we conclude that PFB0595w may regulate the chaperone activity of PfHsp70-1 in the cytosol while Pfj1 may play a co-chaperoning role for PfHsp70-3 in the mitochondrion. Overall, this data is expected to increase the knowledge of the Hsp70-J protein partnerships in the erythrocytic stage of *P. falciparum* development, thereby enhancing the understanding of parasite biology.

Dedication

This thesis is dedicated to Martha, the love of my life, and to Moses and Angel, for their selflessness, patience, love, kindness, and constant encouragement.

Acknowledgements

I begin by thanking my parents for always providing me with unlimited support. Many thanks go to you for your prayers, love, and constant encouragement without which I would not made it this far. I also thank Martha, my wife, and our son Moses and daughter Angel for having allowed me to be away from home to study. Many thanks for your unlimited love, prayers, constant communication, and understanding from the beginning.

Many thanks to my supervisors, Professor Gregory L. Blatch and Dr. Aileen Boshoff for their encouragement, guidance, support while undertaking the PhD studies. Many thanks also go to Dr. Eva-Rachele Pesce who has provided the much needed support in the running of the PhD project from the beginning to the end and with my supervisors, proofread this thesis. I remain inspired by their passion for science and enthusiasm towards my project as well as their motivation that always allowed me to grow as a budding scientist. Your guidance, patience and constant encouragement is highly appreciated.

I greatly thank my co-supervisor, Professor Jude Przyborski and his laboratory for having trained me during a three month research visit at Philipps University in Germany and given me further support with the cell biological work especially with the pARL2-GFP plasmid, malaria transfections, and imaging. I acknowledge the great role that Mr. Pradipta Mandal (Piddy) played in both the training and assistance with cell culture and malaria transfection.

I thank Dr. Adrienne Edkins for her support and overall administration that ensured smooth running of the project. Many thanks go to both Dr Edkins and to Dr. Caroline Knox as members of my PhD committee.

I sincerely thank Prof. Heinrich Hoppe and Dr. Earl Prinsloo for their support, expertise and novel ideas while undertaking the project and during the write up. I also thank Dr. Mike Ludewig for his bioinformatics expertise, useful ideas, and constant encouragement while undertaking the study. Many thanks also go to Dr. Mugdha Suthkanthar, Mr Mike Daniyan, Ms. Fortunate Mokoena, and Ms. Ingrid Cockburn for their constant support and encouragement.

I greatly thank past and present members of the Biomedical and Biotechnology Research Unit at Rhodes University for the great role they have played in transforming me into a well-

rounded young scientist through presentations, research meetings, positive criticism, and sharing of ideas.

Acknowledgement of funding

I acknowledge funding from the Deutsche Forschungsgemeinschaft (DFG) German-African Cooperation Projects in Infectology grant (DFG [Ref: LI 402/12-0])

Table of Contents

Declaration ii
Abstract iii
Dedication v
Acknowledgements vi
List of Figures xiii
List of Tables xvi
List of Abbreviations xvii
List of Research Outputs xxii
CHAPTER ONE 1
Literature review, Hypothesis, Broad objectives, and Approach 1

1.1 Malaria 2
1.1.1 Malaria parasites and vectors 2
1.1.2 The life cycle of malaria parasites 4
1.1.3 Clinical manifestation of malaria 5
1.1.4 Immunity to malaria 6
1.1.5 Malaria control and management 7
1.1.5.1 Vector targeted approaches 7
1.1.5.2 Parasite targeted approaches 8
1.2 Cellular homeostasis, stress and response 10
1.3 Molecular chaperones 12
1.4 Heat shock proteins 13
1.4.1 Hsp110 14
1.4.2 Hsp90 14
1.4.3 Hsp70 15
1.4.4 J proteins 18
1.4.5 Heat shock proteins in the context of malaria 18
1.5 Knowledge gap and motivation 20
1.6 Research hypothesis 22
1.7 Aims and Objectives and Approach 22
1.7.1 In silico bioinformatic analysis of the Hsp70-J protein chaperone complement across *Plasmodium* species 22
1.7.2 Characterization of PFB0595w 23

1.7.3 Characterization of Pfj1 23

CHAPTER TWO 24

Bioinformatic analysis of the Hsp70-J protein chaperone complement across *Plasmodium* species 24

2.0 Introduction 25
2.1 Objectives 26
2.2 Materials and methods 26
2.2.1 Sequences searches and comparison 26
2.2.2 Domain identification and subcellular localization 27
2.3 Results and discussion 28
2.3.1 Gene structure and protein conservation 28
2.3.1.1 Phylogenetic analysis of Hsp70 28
2.3.1.2 Hsp70 Domain organization 30
2.3.1.3 J proteins 31
2.3.1.3.1 Chromosomal localization and phylogenetic analysis 35
2.3.1.3.2 Domain organization 36
2.3.2 The intraerythrocytic *Plasmodial* Hsp70-J protein chaperone machinery 41
2.3.3 Cytoplasm and Nucleus 42
2.3.4 Endoplasmic reticulum (ER) 45
2.3.5 Mitochondrion 47
2.3.6 Apicoplast 50
2.3.7 Parasitophorous vacuole 52
2.3.8 Infected erythrocyte cytosol 52
2.4 Conclusion 58

CHAPTER THREE 59

Cell biological and biochemical characterization of Pfj1 59

3.0 Introduction 60
3.1 Objectives 61
3.2 Materials and methods 61
3.2.1 Heterologous production of recombinant Pfj1 protein 61
3.2.1.1 Plasmid construct coding for 6xHis Pfj1 protein 61
3.2.1.2 Induction studies for the production of Pfj1m 62

3.2.2 Cell biological characterization of Pfj1 and PfHsp70-3 63
3.2.2.1 Peptide directed anti-Pfj1 antibody design and production 63
3.2.2.2 Parasite culture 64
3.2.2.3 Preparation of *P. falciparum* lysates and detection of Pfj1 65
3.2.2.4 Pfj1 and PfHsp70-3 constructs for transfection 66
3.2.2.4.1 Pfj1 constructs for transfection 66
3.2.2.4.2 PfHsp70-3 construct for transfection 68
3.2.2.5 Parasite transfection 69
3.2.2.6 Live cell imaging and western analysis of transfectants 70
3.2.2.7 Indirect Immunofluorescence microscopy 70
3.2.3 Heterologous production of recombinant PfHsp70-3 protein 71
3.2.3.1 Preparation of the plasmid coding for the 6xHis PfHsp70-3 protein 71
3.2.3.1.1 Induction studies for the production of PfHsp70-3m 72
3.2.3.1.2 Solubility studies for PfHsp70-3m 72
3.2.3.1.3 Purification of PfHsp70-3m 73
3.3 Results 73
3.3.1 Approaches to the expression of Pfj1m 73
3.3.2 Peptide anti-Pfj1 antibodies unsuitable for cell-biological studies 75
3.3.3 The N-terminus of Pfj1 targets GFP to the mitochondrion 76
3.3.4 PfHsp70-3_Nterm-GFP localizes to the mitochondrion and cytoplasm 78
3.3.5 Expression and purification of PfHsp70-3m 80
3.4 Discussion 82
3.5 Conclusion 86

CHAPTER FOUR 88
Cell-biological characterization of PFB0595w 88

4.0 Introduction 89
4.1 Objectives 90
4.2 Materials and methods 90
4.2.1 Peptide directed anti-PFB0595w antibody design and production 90
4.2.2 Parasite culture 91
4.2.3 Preparation of *P. falciparum* lysates and detection of PFB0595w 91
4.2.4 PFB0595w plasmid constructs for transfection 92

4.2.5 Parasite transfection 92
4.2.6 Live cell imaging and western analysis of transfectants 93
4.2.7 Indirect immunofluorescence microscopy 93
4.2.8 Intraerythrocytic time course expression of PFB0595w 94
4.2.9 Heat shock inducibility of PFB0595w 94
4.2.10 Solubility study 95
4.3 Results 95
4.3.1 PFB0595w is expressed in the intraerythrocytic stage of parasite development 95
4.3.2 The expression of PFB0595w is slightly induced by heat shock treatment 96
4.3.3 Preparation of transfection constructs 97
4.3.4 PFB0595w and PfHsp70-1 localize to the parasite cytosol in the infected erythrocyte 99
4.3.5 PFB0595w is expressed maximally at the trophozoite stage 100
4.3.6 Solubility studies 102
4.4 Discussion 103
4.5 Conclusion 105

CHAPTER FIVE 106
Biochemical interaction studies of PFB0595w with PfHsp70-1 106

5.0 Introduction 107
5.1 Objectives 108
5.2 Materials and methods 109
5.2.1 Heterologous expression and purification of PFB0595w and PfHsp70-1 109
5.2.1.1 Expression plasmids coding for PFB0595w and PfHsp70-1 109
5.2.1.2 Induction studies for the production of PFB0595w and PfHsp70-1 109
5.2.1.3 Solubility studies for PFB0595w and PfHsp70-1 110
5.2.1.4 Heterologous purification of PFB0595w and PfHsp70-1 110
5.2.2 ATPase assay 111
5.2.3 Surface plasmon resonance spectroscopy 112
5.2.4 Size exclusion chromatography of PFB0595w 114
5.3 Results 115
5.3.1 Non-denaturing purification of PFB0595w and PfHsp70-1 115
5.3.2 PFB0595w stimulates the ATPase activity of PfHsp70-1 118

5.3.3 PFB0595w interacts with PfHsp70-1 as depicted by SPR spectroscopy.....119
5.3.4 PFB0595w exists as a homodimer 121
5.4 Discussion 123
5.5 Conclusion 125

CHAPTER SIX 127
Conclusions and Future perspectives.....127
References.....135
APPENDICES.....171
Appendix A: Amino Acid and Nucleotide Nomenclature 172
Appendix B: Nucleotide sequences in Fasta format 173
Appendix C: Amino acid sequences in Fasta format.....174
Appendix D: Recipes.....174

Yeast-Tryptone (YT) Broth growth medium.....174
Yeast-Tryptone (YT) Agar 175

Appendix E: Organisms 175
Appendix F: common protocols for standard molecular biology techniques 176

F1: Isolation of plasmid DNA.....176
F2: DNA digestion with restriction enzymes 176
F3: Agarose gel electrophoresis 176
F4: Extraction and purification of DNA from an agarose gel 177
F5: Ligation of DNA fragments 177
F6: DNA sequencing.....177
F7: Preparation of competent *E. coli* cells 178
F8: Transformation of competent *E. coli* cells.....178
F9: Sodium dodecyl sulphate – polyacrylamide gel electrophoresis (SDS-PAGE)....178
F10: Protein detection by western analysis.....179
F11: analysis of recombinant protein expression.....179

Appendix F: Output.....180

List of Figures

Chapter One: Literature review, Hypothesis, Broad objectives, and Approach **1**

Figure 1.1 A diagrammatic representation of the life cycle of the malaria parasite, *P. falciparum*. 4

Figure 1.2 Protein fates in the molecular chaperone proteostasis network.

Figure 1.3 Domain organization of the Hsp70 and J proteins (upper panel) and a model depicting the interaction cycle of Hsp70 with J proteins, NEF, and client proteins (lower panel). 16

Chapter Two: Bioinformatic analysis of the Hsp70-J protein chaperone complement across Plasmodium species **23**

Figure 2.1 Phylogenetic analysis of the Hsp70 homologues across the *Plasmodium* species. 28

Figure 2.2 Schematic representation of the domain architecture of the *P. falciparum* Hsp70 complement. 29

Figure 2.3 Chromosomal localization of the *P. falciparum* Hsp70s and J proteins. 30

Figure 2.4 Schematic representation of the domain architecture of the *P. falciparum* J protein complement showing parasite resident J proteins followed by exported J proteins. 36

Figure 2.5 Phylogenetic clustering analysis of the J protein complement. 37

Figure 2.6 Alignment of the conserved 41 amino acid motif identified using the Multiple Expectation Maximization for Motif Elicitation (MEME) suite (http://meme.nbcr.net). 39

Figure 2.7 A diagrammatic representation of an infected erythrocyte depicting the various compartments and organelles present. 41

Figure 2.8 The roles of several J proteins in the cytoplasmic and nucleus. 42

Figure 2.9 Protein co-translational translocation and retro-translocation between the cytoplasm and the ER. 45

Figure 2.10 Protein import and refolding in the mitochondrion. 48

Figure 2.11 Protein import and refolding in the apicoplast. 50

Figure 2.12 A diagrammatic representation of the structural components and protein trafficking machinery from parasite's cytoplasm to infected erythrocyte compartment. 53

Chapter Three: Cell biological and biochemical characterization of Pfj1 **58**

Figure 3.1 The amino acid sequence depicting the conserved domains and the identification of the unique peptide for the design of the Pfj1 antibody. 63

Figure 3.2 Schematics representation depicting the design of transfection constructs for Pfj1 and PfHsp70-3. 65

Figure 3.3 Heterologous expression of Pfj1m. 73

Figure 3.4 Pfj1-specific peptide based antibody detects native and recombinant Pfj1 proteins. 74

Figure 3.5 Pfj1 plasmids used for transfection. 76

Figure 3.6 Microscopy images of the Pfj1-Nterm-GFP transfectants depicting the mitochondrial localization of Pfj1. 77

Figure 3.7 PfHsp70-3 plasmids used for transfection. 79

Figure 3.8 PfHsp70-3 localizes to the Mitochondrion. 79

Figure 3.9 Heterologous expression and purification of PfHsp70-3m. 80

Chapter Four: Cell-biological characterization of PFB0595w **87**

Figure 4.1 The amino acid sequence depicting the conserved domains and the identification of the unique peptide with potential for design of the PFB0595w antibody. 90

Figure 4.2 PFB0595w is expressed in the intraerythrocytic stage of *P. falciparum* development. 95

Figure 4.3 PFB0595w is slightly upregulated following heat-shock. 96

Figure 4.4 PFB0595w constructs used for transfection. 97

Figure 4.5 PFB0595w localizes to the parasite cytosol as PfHsp70-1 in the infected erythrocyte. 99

Figure 4.6 Time course expression of PFB0595w and PfHsp70-1 in the intraerythrocytic cycle of parasite development. 101

Figure 4.7 Solubility study of PFB0595w. 102

Chapter Five: Biochemical interaction studies of PFB0595w with PfHsp70-1 **105**

Figure 5.1 The immobilization of PfHsp70-1 on the surface of the GLC sensor chip. 111

Figure 5.2 Plasmid maps and associated diagnostic restriction analyses of pQE30-PFB0595w and pQE30-PfHsp70-1 plasmids. 114

Figure 5.3 Heterologous over-expression and purification of PFB0595w (upper panel) and PfHsp70-1 (lower panel). 115

Figure 5.4 Bar graph showing that PFB0595w stimulated the ATPase activity of PfHsp70-1 117

Figure 5.5 PFB0595w and not BSA intearcts with immobilized PfHsp70-1 in the presence and absence of ATP. 119

Figure 5.6 PFB0595w, at differing concentrations, interacts with PfHsp70-1 in the presence of ATP. 120

Figure 5.7 Gel filtration analysis of purified PFB0595w. 121

List of Tables

Table 2.1	Comprehensive list of J proteins across the *Plasmodium* species analyzed.	33
Table 2.2	Comprehensive list of proteins possessing the 41aa unknown domain.	40
Table 3.2	The Hsp70 and the Hsp40 complement in mature uninfected erythrocytes.	52

List of Abbreviations

α	Alpha
β	Beta
°C	Degrees Celsius
µ	Micro
µg	Microgram(s)
µl	Microlitre(s)
µM	Micromolar
µmol	Micromole(s)
A	Absorbance
ACT	artemisinin-based combination therapy
A_{600}	Absorbance at 600 nm
A. gambiae	*Anopheles gambiae*
A. tumefaciens	*Agrobacterium tumefaciens*
ADP	Adenosine diphosphate
AmpR	Ampicillin resistance (β-lactamase gene)
A-T	Adenosine - Thymine
ATP	Adenosine triphosphate
ATPase	Adenosine triphosphatase
APS	Ammonium Persulphate
BLAST	Basic Local Alignment Search Tool
BSA	Bovine Serum Albumin
bp	Base pairs
C-	COOH-terminal
CAAX	C – Cysteine, A – Aliphatic Residue, X – Any Residue
CbpB	Curved DNA binding protein Beta
CHIP	Carboxyl terminus of the Hsc70 Interacting Protein
DAPI	4',6-diamidino-2-phenylindole

DNA	Deoxyribonucleic Acid
DnaJ	Prokaryotic Hsp40
DnaK	Prokaryotic Hsp70
dNTP	Deoxyribonucleotide Triphosphate
DSG	15-Deoxyspergualin
DTT	Dithiothreitol
E. coli	*Escherichia coli*
EDTA	Ethylene diamine tetra-acetic acid
EGTA	Ethylene glycol tetra-acetic acid
ER	Endoplasmic reticulum
g	Gram
GF-Region	Glycine-Phenylalanine rich region
GFP	Green Fluorescent Protein
H. sapiens	*Homo sapiens*
Hepes	N-2-hydroxyethyl-piperrazine-N'-2-ethanesulfonic acid
HIV	Human immunodeficiency virus
Hip	Hsc70 interacting protein
6xHis	Hexahistidine tag
Hop	Hsp70/Hsp90 organising protein
HPD motif	Histidine-Proline-Aspartic acid motif
HRP	Horse Radish Peroxidase
HSF	Heat Shock Factor
Hsc70	70 kDa Heat shock cognate protein
Hsp	Heat shock protein
Hsp110	110 kDa Heat shock protein
Hsp90	90 kDa Heat shock protein
Hsp70	70 kDa Heat shock protein
Hsp60	60 kDa Heat shock protein
Hsp40	40 kDa Heat shock protein

HT	Host Targeting Signal
IUBMB	International Union of Biochemistry and Molecular Biology
IUPAC	International Union of Pure and Applied Chemistry
IPTG	Isopropyl-β-D-thiogalactopyranoside
ITNs	Insecticide Treated Nets
iRBC	Infected Red Blood Cell
IRS	Indoor Residual Spraying
KanR	Kanamycin resistance
kb	kilo base pairs
kDa	Kilo Daltons
LB	Luria-Bertani media
LLINs	Long-lasting insecticidal nets
m	Milli
M	Molar
mAb	Monoclonal antibody
MC	Maurer's Clefts
MESA	Mature parasite-infected Erythrocyte Surface Antigen
mol	Mole(s)
mg	Milligram(s)
ml	Millilitre(s)
mM	Millimolar
n	Nano
NaCl	Sodium chloride
NBD	Nucleotide Binding Domain
NEF	nucleotide exchange factor
SBD	Substrate Binding Domain
SPR	Surface Plasmon Resonance Spectroscopy
Ni-NTA	Nickel nitrilotriacetic acid
ng	Nanogram(s)

nmol	Nanomole(s)
nM	Nanomolar
N-	NH_2-terminal
N.D.	Not determined
NEF	Nucleotide Exchange Factor
pI	Isoelectric point
Pi	Inorganic phosphate
P. berghei	*Plasmodium berghei*
P. chabaudi	*Plasmodium chabaudi*
P. falciparum	*Plasmodium falciparum*
P. knowlesi	*Plasmodium knowlesi*
P. malariae	*Plasmodium malariae*
P. vivax	*Plasmodium vivax*
P. ovale	*Plasmodium ovale*
P. yoelii	*Plasmodium yoelii yoelii*
PBS	Phosphate Buffer Saline
PCR	Polymerase Chain Reaction
PDI	Protein Disulphide Isomerase
PEXEL	Plasmodium Export Element
PEI	Polyethyleneimine
PfBiP	*P. falciparum* binding protein
PHIST	*Plasmodium* helical interspersed subtelomeric family
PMSF	Phenyl Methyl Sulfonyl Fluoride
PV	Parasitophorous Vacuole
RESA	Ring-infected Erythrocyte Surface Antigen
RNA	Ribonucleic Acid
rpm	Revolutions per minute
S. cerevisiae	*Saccharomyces cerevisiae*
SDS	Sodium Dodecyl Sulphate

SDS-PAGE	Sodium Dodecyl Sulphate – Polyacrylamide Gel Electrophoresis
sHsp	Small Heat shock protein
SP	Signal Peptide
T. gondii	*Toxoplasma gondii*
TBE	Tris Borate EDTA buffer
TBS	Tris-Buffered Saline
TBS-T	Tris Buffer Saline – Tween 20
TE	Tris-EDTA buffer
TEMED	N,N,N',N'-tetramethylethylenediamine
TMD	Transmembrane domain
TPR	Tetratricopeptide Repeat
Tris	Tris-2-amino-2-hydroxymethyl-1,3-propanol
TRITC	Tetramethyl Rhodamine Iso-Thiocyanate
U	Unit(s)
UV	Ultraviolet
V	Volts
WHO	World Health Organization
WHOPES	WHO Pesticide Evaluation Scheme
v/v	Volume to volume ratio
w/v	Weight to volume ratio
YT	Yeast-Tryptone media
xg	Gravitational force

List of Research Outputs

Publication:

- James M. Njunge, Michael H. Ludewig, Aileen Boshoff, Eva-Rachele Pesce, and Gregory L. Blatch. Hsp70s and J Proteins of *Plasmodium* Parasites Infecting Rodents and Primates: Structure, Function, Clinical Relevance, and Drug Targets. Current Pharmaceutical Design, 2013, 19, 387-403.

Conferences:

- 4th Molecular Approaches to Malaria 2012 (MAM 2012), Lorne, Australia
  Njunge JM, Mandal P, Przyborski J, Pesce E-R, Boshoff A, Blatch GB. The characterization of an Hsp40 partner protein of *P. falciparum* Hsp70. [Poster]
- German Research Foundation (DFG) conference of African-German partnerships on neglected diseases. Accra, Ghana. Characterization of the protein interactors of *P.falciparum* Hsp70-1: towards the development of small-molecule inhibitors of PfHsp70-1 chaperone function. 2011. Progress report on a joint DFG collaborative project between Rhodes University, South Africa, University of Zululand, South Africa, and Philipps University, Germany. [Presentation]

CHAPTER ONE

Literature review, Hypothesis, Broad objectives, and Approach

1.1 Malaria

Recent estimates indicate that human malaria, a disease caused by *Plasmodium* parasites and transmitted by mosquitoes, continues to be a major cause of morbidity and mortality (Murray, et al., 2012; WHO, 2011a). Statistics show that while approximately 3.3 billion people are at risk of malaria, an estimated 250 million people get infected and more than half a million die of the disease every year (WHO, 2010a; WHO, 2011a). In regions of high malaria transmission, such as sub-Saharan Africa, children below the age of five years and pregnant women, particularly during their first and second pregnancies, are the most at risk and heavily afflicted by the disease (WHO, 2003; WHO, 2005). Many resources, including manpower, are diverted towards the management of malaria associated morbidity and mortality thereby affecting the overall economic output of these endemic areas. It is not surprising therefore that the inhabitants of these malaria endemic areas are heavily affected by poverty (Breman, et al., 2001; Gallup and Sachs, 2001; Sachs and Malaney, 2002).

Mapping studies have shown that there is a wide variation in malaria transmission patterns and disease amongst different geographical regions including the Americas, Asia, and Africa, and also within individual countries (Gething, et al., 2011). This variation is mainly related to differences in the local species of circulating parasites and vectors, the ecological conditions, and the approaches used in the malaria management and control (WHO, 2005; WHO, 2011a). Malaria control and management relies on the correct usage of insecticidal nets, indoor residual spraying, and chemotherapy since no vaccine has been licensed to date (Grimberg and Mehlotra, 2011). While a vaccine would be the most efficient and potentially cost-effective way to eliminate malaria, prompt chemotherapy has effectively reduced human suffering, saved lives, and helped reduce the overall parasite burden in a community. However, the rise and geographical spread of resistance of parasites to chemotherapeutic agents and of vectors to insecticides and the apparent lack of effective management and control programs has continued to aggravate the current malaria situation (Alonso, et al., 2011; Greenwood, et al., 2008).

1.1.1 Malaria parasites and vectors

Plasmodium parasites, the unicellular eukaryotes responsible for malaria, fall under the phylum *Apicomplexa* and were first identified as the cause of malaria from a patient in

Algeria (Cavalier-Smith, 1993; Haas, 1999). There are over a hundred *Plasmodium* species known and five cause malaria in humans: *P. falciparum*, *P. vivax*, *P. ovale*, *P. malariae,* and *P. knowlesi*. *P. falciparum* accounts for most of the morbidity and mortality associated with malaria. *P. vivax*, on the other hand, is less dangerous but more widespread and the treatment is complicated by clinical relapses (Wells, et al., 2010). Other examples of members present in this phylum include the genera *Toxoplasma*, *Cryptosporidium*, and *Theileria*, which also cause serious diseases. Most members in this phylum infect a variety of hosts where they undergo complex lifecycles characterized by various stages that are morphologically different (Plattner and Soldati-Favre, 2008). Additionally, they possess organelles such as rhoptries, micronemes, and dense granules, that are vital for host invasion (Plattner and Soldati-Favre, 2008). These organelles are secretory vesicles that store proteins which are released through the apical complex during host cell attachment and invasion processes (Carruthers and Sibley, 1997; Sibley, 2004). An additional organelle found in all members of this phylum except *Cryptosporidium* and *Gregarina* species is the apicoplast, a unique yet essential non-photosynthetic plastid (Fast, et al., 2001; Toso and Omoto, 2007; Zhu, et al., 2000).

Malaria parasites are transmitted exclusively by mosquitoes of the genus *Anopheles* with the rare exception of transplacental and blood transfusion associated transmission. It has to be noted that while not every mosquito transmits malaria, of those that transmit, some are of minor or incidental importance. Recent mapping studies on the global distribution of approximately 40 malaria vectors showed that many regions of the world have few important vectors with the *Anopheles gambiae* complex being the most efficient (Coetzee, 2004; Sinka, et al., 2012). For example, while the endemic regions of Africa have three main malaria associated vectors including *Anopheles gambiae*, *A. arabiensis*, and *A. funestus*, Southeast Asia has approximately ten (Sinka, et al., 2010). The combination of the most efficient transmitting mosquito vectors with the deadly malaria parasite *P. falciparum* in sub-Saharan Africa has acted as a major thrust for the observed morbidity and mortality in this region. Apart from malaria, mosquito vectors have been shown to transmit other diseases of clinical and economic importance such as chikungunya and Japanese encephalitis (Rozendaal, 1997).

1.1.2 The life cycle of malaria parasites

In humans and other mammals, malaria infection begins when sporozoites present in the salivary glands of an infected *Anopheles* mosquito are inoculated into a vertebrate host during a blood-meal (Vaughan, et al., 2008) (Figure 1.1). The sporozoites are transported via the bloodstream to the liver where they migrate through Kupffer cells and infect hepatocytes (Ishino, et al., 2004; Mota, et al., 2002; Stewart, et al., 1986). Here, the sporozoites multiply asexually and differentiate into hundreds of merozoites clustered together within the hepatocyte membrane (commonly referred to as merosomes) that are then released into the bloodstream (Baer, et al., 2007; Sturm, et al., 2006).

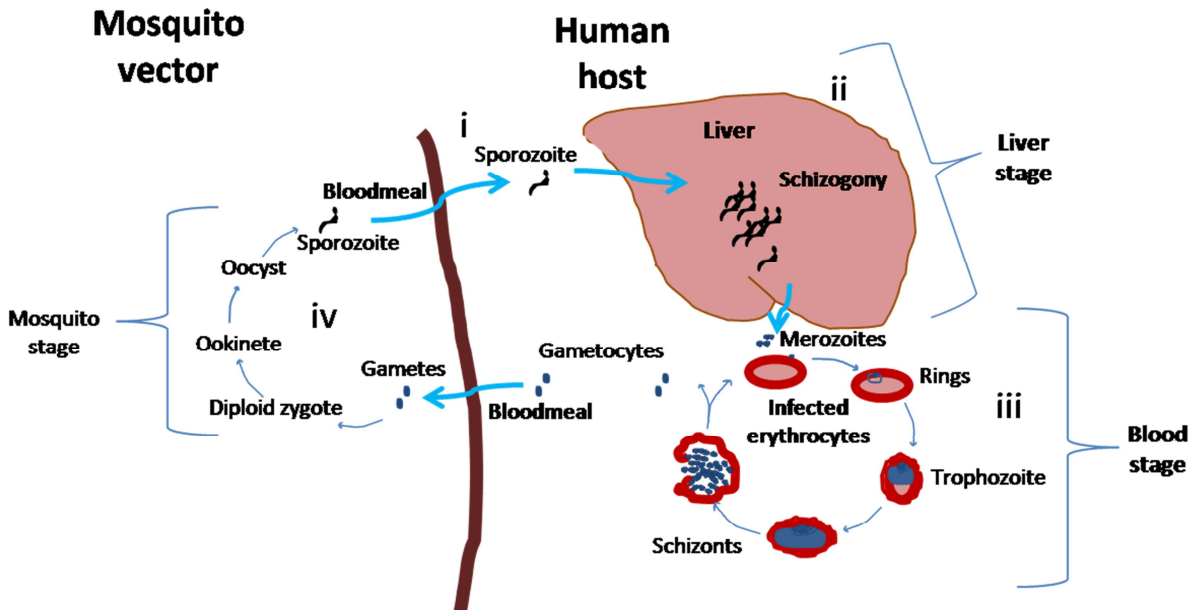

Figure 1.1: A diagrammatic representation of the life cycle of the malaria parasite, *P. falciparum*. (i) Human infection is initiated when sporozoites are inoculated into the bloodstream by an infected mosquito. (ii) The sporozoites migrate to the liver where they multiply asexually and differentiate into merozoites in a process called schizogony. (iii) The blood stage occurs when free merozoites invade erythrocytes and multiply asexually and release new invasive merozoites. (iv) Mosquito takes up gametocytes during a blood-meal from an infected host allowing parasite development into sporozoites in the vector.

The blood stage of the parasite's development is initiated when free merozoites present in the bloodstream quickly invade erythrocytes (Cowman and Crabb, 2006). Upon invasion, the parasite undergoes another asexual amplification (Figure 1.1) with the intraerythrocytic cycle lasting approximately 48 hours in *P. falciparum* but varies among other *Plasmodium* species. The parasite transforms in morphology and size from ring to schizont which subdivides to yield new merozoites that are then released into the bloodstream and invade uninfected

erythrocytes (Figure 1.1). Some intraerythrocytic parasites differentiate into male or female gametocytes in a process referred to as gametocytogenesis (Baker, 2010) and circulate in the peripheral blood. Circulating gametocytes are then transferred to the vector's midgut during a blood-meal from an infected host (Matuschewski, 2006) (Figure 1.1). Here, they differentiate into gametes which combine to form a diploid zygote that in turn differentiates into an ookinete which invades the mosquito gut and establishes itself on the midgut wall. The ookinete then differentiates into a replicative oocyst and produces sporozoites. Upon rupture of a mature oocyst, the sporozoites are released and actively migrate and invade the mosquito salivary glands where they rest awaiting injection into another host during a blood-meal (Fujioka and Aikawa, 2002; Matuschewski, 2006).

1.1.3 Clinical manifestation of malaria

Malaria is a complex disease and prognosis, manifestation, and severity depend on a variety of factors (Collins and Paskewitz, 1995; Warrell and Gilles, 2002). These factors include: infecting parasite (species and strain), geographical location (transmission intensity, disease incidence, and parasite prevalence rates), host factors (age, genetic constitution, level of natural and acquired immunity, general health and nutritional status, the effects of any chemoprophylaxis or chemotherapy), amongst others (Schofield and Grau, 2005; Snow and Omumbo, 2006). As mentioned previously, infections by *P. falciparum* are almost always severe especially in non-immune individuals while those by *P. vivax* are less dangerous especially in healthy individuals. *P. malariae* and *P. ovale*, on the other hand, cause asymptomatic infections and almost no morbidity or associated mortality.

The relation between transmission intensity, as determined by the frequency of parasite exposure, and disease outcome is quite complex (Snow and Marsh, 2002). In regions of intense transmission, severe cases are reportedly from infants below the age of 1 year and the majority of infections in the other age groups are less complicated (Marsh, et al., 1995; Schofield and Grau, 2005). However, severe symptoms including severe anemia, coma, and death, may also be observed in women in their first or second pregnancy, HIV co-infected individuals, and non-immune travellers to malaria endemic areas (Ayisi, et al., 2003; Chirenda, et al., 2000). Through infective bites, older children and adults in endemic regions can acquire partial immunity to the disease that often reduces the frequency of clinical attacks

but not infection (Cox, et al., 1994). In contrast, severe malarial disease mainly affects children between the ages of one to five years in lower transmission areas and cerebral malaria is a common clinical complication. Overall, malaria infection can manifest in an individual as asymptomatic parasitemia or as clinical malaria that may present as fever episodes with parasitemia or as severe and complicated malaria characterized by anemia, neurologic syndromes, coma, and death (Laishram, et al., 2012; Marsh, et al., 1995; Perkins, et al., 2011). Other associated clinical features range from mild conditions such as low-level fever and headache to more severe symptoms such as prostration, coma, acidosis, and epileptic seizures (Murphy and Breman, 2001; Waruiru, et al., 1996). Additionally, malaria can also manifest as myalgia, joint pain, vomiting, and associated metabolic complications (Planche, et al., 2005; Planche and Krishna, 2006).

1.1.4 Immunity to malaria

Immunity to malaria is complex and is specific to the infecting *Plasmodium* species and stage of parasite development (Stevenson and Riley, 2004). It is dependent on the host's genetic make-up, parasite properties, and exposure through infective bites amongst other factors. Acquired protective immunity only develops through infectious bites and is generally not life-long and requires repeated infections to be maintained (Achtman, et al., 2005). It is commonly observed that the age at which protective immunity develops varies but often depends on transmission intensity with immunity developing much earlier and more rapidly in areas of high transmission (Snow, et al., 1997). In high transmission areas, older children and adults are protected by the acquired immunity against severe disease with mortality being restricted to early childhood (Gupta, et al., 1999). However, infants born to mothers residing in these areas, although exposed to infective bites, are protected against severe disease for about six months after birth by maternal antibodies (Zinkernagel, 2001). During this period their immune system develops with acquired immunity to malaria being related to infectious bites from local circulating parasites. In areas of moderate transmission, children acquire associated immunity over the first five years of life and even though they may retain relatively high parasitemia, they often show reduced disease symptoms (Snow and Marsh, 2002). Non-immune travellers and people in areas of low transmission rarely experience infectious bites and are likely to suffer more from severe malaria irrespective of age, due to lack of protective immunity (Doolan, et al., 2009; Struik and Riley, 2004).

The relative slow development and lack of memory associated with acquired antimalarial immunity compared to bacterial or viral pathogens can be explained partly by the observation that in malaria, immunity may be specific to the local strains (Good, et al., 1998). Indeed, infection with different parasite strains or genotypes may be required in order to develop protective immunity against most parasite variants circulating in an area (Gatton and Cheng, 2004). It has been observed that the speed at which people acquire protective immunity largely depends on the number of infecting parasites and the genetic diversity of the parasite population in a particular geographical locality (Ferreira, et al., 2004).

1.1.5 Malaria control and management

Although malaria continues to be a leading cause of death and disease worldwide, the clinical course after an infection can be predicted and the disease can be prevented or treated using available antimalarials. Indeed, preventive methods and drugs are available for the control of malaria. Over the years, WHO has provided guidelines to combat malaria and countries afflicted by malaria have adopted various strategies for malaria prevention and treatment, mainly depending on the available tools and the disease situation. Broadly speaking, the fight against malaria is multifaceted and complementary in approaches used and continues to be fought with every available arsenal. This all inclusive approach is mainly advocated by the development of resistance to common prophylactic and chemotherapeutic agents and to pesticides used for vector control, thereby posing a big threat to control and management efforts.

1.1.5.1 Vector targeted approaches

Long-lasting insecticidal nets (LLINs) and indoor residual spraying (IRS) are currently among the preferred primary vector targeted approaches to suppress malaria transmission by eliminating associated vectors (Karunamoorthi, 2011). In many cases, both methods are used together in the same locality. IRS refers to the application of chemicals in domestic areas intended to kill insects including mosquitoes that land or rest on these areas (WHOPES, 2009). The insecticides used for IRS repel the entry of mosquito into houses and also kill

those resting inside houses before and after a blood-meal. The mass repelling and killing of vectors effectively reduces malaria transmission and is one of the main methods used to control and eliminate malaria on a large scale from different global localities (Lengeler and Sharp, 2003; Pluess, et al., 2010). However, malaria control strategies based on insecticides use are faced with challenges such as economic costs and sustainability in poor countries, the environmental impact, possible long-term effects on human and animal health and development of vector resistance to insecticides amongst others (Mills, et al., 2008; Ramirez, et al., 2009).

The use of insecticidal nets for prevention of malaria especially for the vulnerable population (young children and pregnant women) is one of the pillars in malaria control. Insecticidal nets including the insecticide treated nets (ITNs), the long lasting insecticidal nets (LLINs), and curtains act as physical barriers for personal protection against mosquitoes and are recommended by WHO as an effective malaria transmission control tool (WHO, 2003). They have been documented to reduce malaria morbidity and mortality in the general population, children, and pregnant women in varying transmission localities (Gamble, et al., 2007; Lengeler, 2004; Lengeler, et al., 1998; Lengeler and Snow, 1996). It has also been established that insecticidal nets provide protection both to individuals sleeping under them and to other community members (Hawley, et al., 2003). The significant impact of insecticidal nets makes them one of the most promising and cost-effective malaria prevention measures resulting in large-scale distribution and usage in sub-Saharan Africa, Asia and Latin America (Lengeler, 2004). However, sustainability, cost, and scaling up are some of the concerns that may need to be addressed if the observed benefits are to be sustained.

1.1.5.2 Parasite targeted approaches

While several strategies are used in the fight against malaria, chemotherapy remains the mainstay for both prophylaxis and treatment since there is no licensed vaccine. Chemotherapy may vary depending on the age, disease severity, genetic factors, pregnancy, and geographical location among others. A wide range of antimalarial monotherapies have been widely used for the treatment of uncomplicated malaria including quinine, chroloquine, sulfadoxine-pyrimethamine, and artemisinins (Delves, et al., 2012). Chloroquine, for example, was the main-stay for the treatment of uncomplicated malaria in many malarious

areas from the 1950s (WHO, 1999). It was thereafter replaced with sulfadoxine-pyrimethamine in the 1980s and 90s in different geographical regions due to parasite resistance (Bloland, et al., 1993). However, parasite resistance to sulfadoxine-pyrimethamine developed and spread more quickly than chroloquine prompting replacement with artemisin monotherapies and thereafter, combined therapies (Mutabingwa, 2005; Rønn, et al., 1996). Currently, monotherapies are no longer recommended following associated clinical treatment failures and recrudescence related to parasite drug resistance (Fidock, et al., 2008; Trape, 2001; WHO, 2010b). This has led to the advocacy for artemisinin-based combination therapies (ACT) (Olliaro and Wells, 2009; White, 1999a; WHO, 2010b). ACTs are more effective and are associated with a lower malaria incidence and reduced chance of developing and spreading resistance (Mutabingwa, 2005; White, 1999a; White, 1999b; White and Olliaro, 1996). Examples of drug combinations used in ACT include artemether-lumefantrine, artesunate–amodiaquine, artesunate–mefloquine, artesunate–sulfadoxine–pyrimethamine, artesunate–sulfalene–pyrimethamine and dihydroartemisinin–piperaquine (WHO, 2011b).

The development of an effective antimalarial vaccine has proven to be quite a difficult objective since, to date, there is none commercially available despite many years of research (Bairwa, et al., 2012; White, 2011). A working antimalarial vaccine is considered to be the most effective way to control and manage malaria. Malaria vaccine efforts have largely targeted three parasite stages and can be broadly categorized as pre-erythrocytic vaccines, blood stage vaccines, and transmission-blocking vaccines (Moorthy, et al., 2004; Thera and Plowe, 2012). Vaccines designed against the pre-erythrocytic stage target the sporozoites to prevent them from entering the liver stage or to destroy them once inside the hepatocytes (Schwenk and Richie, 2011). They mainly protect against infection but do not prevent transmission. The lead candidate vaccine in this group is RTS,S/AS01- a recombinant protein vaccine that has entered phase III clinical trials and shows great promise (Alonso, et al., 2004; Stoute, et al., 1997; White, 2011). Blood stage vaccines are based on antigens that coat the surface of merozoites and/or malaria antigens expressed on the surface of infected erythrocytes that aim to mimic naturally acquired immunity and reduce disease (Ellis, et al., 2010; Good, 2001). Of the several proteins on the merozoite surface, the merozoite surface protein 1 (MSP1) is considered one of the leading and best characterized molecules for blood stage vaccine development (Holder, 2009). Transmission-blocking vaccines are based on antibodies against gametocyte antigens that can prevent fertilization in the mosquito

following a blood meal (Dinglasan and Jacobs-Lorena, 2008; Hirai and Mori, 2010; Lavazec and Bourgouin, 2008). The premise relies on dual ingestion of the fertilization blocking antibodies and gametocytes (Carter, 2001). The prevention of sexual stage development in the vector should prevent further spread of the disease and hence offer protection.

A complementary strategy to the subunit vaccines strategy discussed here is the use of whole parasites attenuated through irradiation, drugs, or genetic modification (Hoffman, et al., 2002; Nussenzweig, et al., 1967; Vaughan, et al., 2010). In this approach, attenuated whole parasites of diverse strains or at different stages of development offers an opportunity for immune response against an enormous range of antigens that could translate into protection. Overall, the development of an effective malaria vaccine has been hampered by a variety of obstacles. As mentioned above, antimalarial immunity is never long-lived and often requires repeated infection to be sustained. Secondly, parasites have been shown to evade the immune system through adherence to vascular tissues (Ho and White, 1999). As discussed above, vaccines are designed based mostly on surface antigens some of which have been shown to be polymorphic in different isolates found in different geographical areas while others rapidly switch preventing detection by the immune system (Ranjit and Sharma, 1999; Scherf, et al., 2008).

1.2 Cellular homeostasis, stress and response

Environmental changes that alter the acceptable range of maximal performance often affect an organism's physiology and prompt it to adjust and maintain its physiology at conditions that favor viability, fitness, and maximal performance (Hofmann and Todgham, 2010). These tendencies to maintain a favorable internal equilibrium, often referred as cellular homeostasis, are critical for proper macromolecular functionality and cell survival. The shift from homeostasis often leads to stress in a cellular system that can translate into perturbed development and reproduction (Johnson, et al., 1992; Kassahn, et al., 2009). While the spectrum of cellular stress is wide, ranging from mild and/or acute to chronic, cells initially respond by promoting stress defense and survival mechanisms (Kültz, 2003; Kültz, 2005). However, depending on the nature and strength of the stress, cells may also activate programmed cell death to eliminate damaged cells (Fulda, et al., 2010).

Environmental stressors often perturb the integrity of cellular macromolecules such as proteins and nucleic acids. Such stressors include thermal stress, oxidative stress, hypoxia, chemicals and heavy metals, ionizing radiation, pathogenic infections, tissue injury, pH changes, among others (Carpenter, et al., 2002; Lindquist, 1986; Ray, et al., 2012; Sonna, et al., 2002; Zhang, et al., 2011). Additionally, pathological conditions such as cancer, metabolic stresses (associated with nutrient balance, production of reactive oxygen species, and mitochondrial dysregulation), and aging do affect the integrity of cellular macromolecules (Haigis and Yankner, 2010). Cellular systems appear to have an evolutionary conserved and generalized protective response towards most environmental stressors referred to as the environmental stress response (ESR), and allows for adaptive cellular responses (Voisine, et al., 2010).

Apart from the external and internal cellular stress influences, proteins on their own have a high propensity to misfold and aggregate or to fail reaching and maintaining their functional conformation (Dobson, 2004). This tendency is more pronounced for large single and multimeric proteins in cellular environments due to molecular crowding which is a major constraint to in vivo protein folding (Elcock, 2010; Zhou, et al., 2008). Indeed, while the primary protein structure is determined by the amino acid sequence (Anfinsen, 1973), attaining a thermodynamically favored tertiary structure in vivo is often slow. Misfolded proteins may inappropriately interact with cellular components and lead to accumulation of potentially toxic protein inclusions that compromise cellular homeostatic balance thereby risking cell viability (Lansbury and Lashuel, 2006). In some instances, protein misfolding results in aberrant aggregation and conformations that present as medical conditions. Such examples include Parkinson’s disease, amyotrophic lateral sclerosis, Huntington’s disease and other neurodegenerative diseases (Barral, et al., 2004; Dobson, 2001; Muchowski, 2002; Sakahira, et al., 2002; Thomas, et al., 1995). It is not surprising therefore that cellular systems have established an evolutionarily conserved, yet elaborate machinery, comprised of molecular chaperones for protein quality control that is crucial for cell survival and an organism’s well-being (Gething and Sambrook, 1992).

1.3 Molecular chaperones

Molecular chaperones manage protein conformational maturation and stability during normal house-keeping and also in response to stress. They play a critical role in recognizing and determining the fate of misfolded proteins in the cell (Hartl and Hayer-Hartl, 2002; Hartl and Hayer-Hartl, 2009; McClellan, et al., 2005). Originally, they were defined as a group of unrelated proteins that interact, stabilize and/or help other proteins in processes that lead to their native conformations during normal and stressful conditions but are not part of the mature native conformations (Ellis, 1987; Hartl, 1996). This definition however changed with the realization that chaperones are involved in processes other than protein folding. They have been redefined as proteins that function through controlled binding and release of non-native polypeptides intended to prevent incorrect interactions and stabilize unstable protein conformations, thereby facilitating the fate of proteins in vivo (Hartl, 1996). Due to their essential cellular roles, chaperones are widely distributed and evolutionarily conserved and generally play a vital role in protein folding, oligomeric assembly, trafficking, unfolding and degradation (Figure 1.2) (Ellis, 1987; Ellis and van der Vies, 1991; Hartl, et al., 2011; Lindquist and Craig, 1988). The expression of many members present in this superfamily is upregulated under stressful conditions, such as heat, that lead to an increase in the levels of misfolded or aggregated proteins. Among the molecular chaperone superfamily are the heat shock proteins which are highly abundant and generally conserved. They were first identified and named so in *Drosophila melanogaster* following their upregulated expression in cells exposed to heat stress (Ritossa, 1962; Ritossa, 1996). Beyond the confines of single cells, molecular chaperones have been shown to be secreted into the extracellular environment or exist on the outer plasma membrane where they probably play signaling functions (Henderson, 2010; Tamura, et al., 2012; Tamura, et al., 2012).

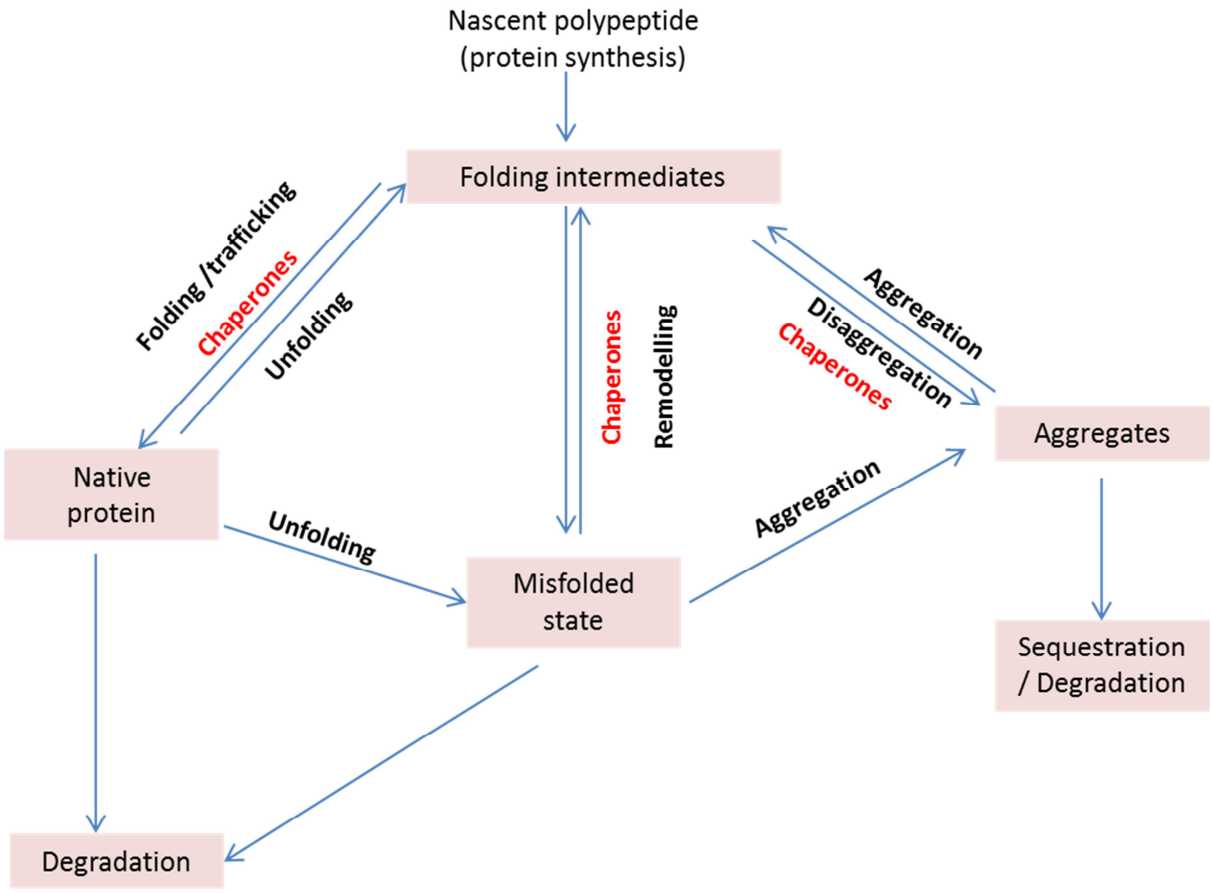

Figure 1.2: Protein fates in the molecular chaperone proteostasis network. The chaperone proteostasis network integrates pathways for the folding of newly synthesized proteins, for the remodelling of misfolded states and for disaggregation of aggregated proteins. (Adapted and modified from (Hartl, et al., 2011))

1.4 Heat shock proteins

Heat shock proteins (Hsps) comprise a large family of evolutionary conserved and structurally related proteins within the molecular chaperone superfamily that often display stress induced expression (Lindquist, 1986; Lindquist and Craig, 1988; Ritossa, 1962; Tyedmers, et al., 2010). In the cellular environment, they help proteins acquire proper conformations while mitigating non-specific interactions that often lead to aggregation (Gething and Sambrook, 1992). On the basis of sequence homology and molecular mass, Hsps can be assigned into several subfamilies which include Hsp110/Grp170, Hsp104, Hsp90, Hsp70, Hsp60, J proteins (DnaJ/Hsp40), and small heat shock proteins (sHsps) families (Feder and Hofmann, 1999; Lindquist and Craig, 1988). In eukaryotes, these families often comprise multiple members that differ in stress associated upregulation, function, and

intracellular localization. Through regulated association with and/or hydrolysis of nucleotides, Hsps broadly recognize and transiently bind to non-native proteins during protein synthesis and folding (Deuerling and Bukau, 2004; Eggers, et al., 1997), oligomeric assembly (Zylicz, et al., 1989), trafficking or targeting for degradation (Bukau, et al., 2006; Feder and Hofmann, 1999; Lee and Tsai, 2005). They functionally interact as oligomers and/or complexes of several different chaperones, cochaperones, and/or nucleotide exchange factors forming efficient proteostatic chaperone machinery (Mayer, 2010). It is notable that although the term Hsp is often used to refer to only the stress induced proteins, the cellular Hsp complement displays either constitutive (housekeeping) functions or stress-inducible roles or both (Feder and Hofmann, 1999).

1.4.1 Hsp110

The Hsp110 and Grp170 families comprise a relatively conserved group of molecular chaperones widely found in eukaryotes (Easton, et al., 2000). They are the atypical or divergent relatives of classical Hsp70s based on differences in several features such as sequence length, significantly larger molecular masses, sequence identity and similarity of their C-terminal regions, as well as structure and function (Polier, et al., 2008). They rank third or fourth in eukaryotic cellular Hsp abundance (Easton, et al., 2000). They have been identified in eubacteria and organelles of prokaryotic origin (Harrison, et al., 1997), as well as in eukaryotes (Dragovic, et al., 2006; Kabani, et al., 2002; Shomura, et al., 2005). Structurally, Hsp110 proteins consist of a nucleotide binding domain (NBD) that is linked to a β sandwich domain followed by a three α helix bundle domain (3HBD) (Polier, et al., 2008). They provide a powerful nucleotide-exchange activity to canonical Hsp70s and act as holdases for non-native proteins thereby providing synergistic co-chaperoning roles for Hsp70s (Dragovic, et al., 2006; Polier, et al., 2008; Shaner and Morano, 2007).

1.4.2 Hsp90

The 90 kDa heat shock protein (Hsp90) family is a highly abundant, essential, and widespread class of molecular chaperones found in bacteria and all eukaryotes (Buchner, 1999; Johnson, 2012). Indeed, while bacteria have only one Hsp90 homologue termed HtpG

(High temperature protein G), yeast has one to two homologues and humans possess four isoforms. Many eukaryotes possess multiple Hsp90 homologues that localize in the cytosol (Hsp90) and major subcellular compartments including endoplasmic reticulum (GRP94 for 94 kDa glucose-regulated protein), mitochondria (TRAP1 for tumor necrosis factor receptor-associated protein 1), and chloroplasts (Hsp90C) (Altieri, et al., 2012; Marzec, et al., 2012). Hsp90 is involved in the maturation and activation of numerous clients involved in signal transduction pathways that control cell homeostasis, proliferation, differentiation and cell death in both housekeeping and stress induced cellular conditions (Pearl and Prodromou, 2006; Taipale, et al., 2010).

Structurally, Hsp90 possesses an N-terminal domain (NTD, also referred to as ATPase domain), the middle catalytic loop and client protein binding domain, and the C-terminal domain that includes a dimerization domain and an EEVD motif implicated in binding to cochaperones (Jackson, 2012; Pearl and Prodromou, 2006). Hsp90 functions as a dimer and its structure cycles between the open and closed conformation that is highly regulated by nucleotide binding, cochaperone interaction, and client binding and release (Jackson, 2012; Li, et al., 2012). While the NTD binds cochaperones such as p23, the ATP binding pocket has been under extensive research concerning small molecule inhibitors such as geldanamycin (Roe, et al., 1999; Shiau, et al., 2006). The Hsp90-dependent folding and activation of client proteins depends on prior interaction and/or bridging with a number of different cochaperones, forming sequential dynamic multiprotein chaperone complexes (Johnson, 2012; Pearl and Prodromou, 2006; Pratt, et al., 2004; Pratt and Toft, 2003). Some of these cochaperones play a crucial role in regulating Hsp90 ATPase activity while others have specialized roles such as client protein interactions, localization and trafficking (Pratt, et al., 2004; Prodromou, et al., 1999; Riggs, et al., 2004). Tetratricopeptide containing cochaperones such as the Hsp70-Hsp90 organizing protein (Hop) provides a physical link between Hsp90 and Hsp70 during client protein transfer (Scheufler, et al., 2000).

1.4.3 Hsp70

The 70 kDa heat shock protein (Hsp70) family is highly conserved and ubiquitous. In eukaryotes, Hsp70 members are found in several subcellular compartments (Boorstein, et al., 1994; Kampinga and Craig, 2010; Karlin and Brocchieri, 1998; Shonhai, et al., 2007). While

Hsp70s are some of the most abundant chaperones in the cell involved in general housekeeping, most members are often highly induced during stress to enhance protein quality control. This protein family specializes in the folding and refolding of nascent and/or misfolded proteins, assists in their translocation across membranes, and degradation of the terminally misfolded or aggregated proteins, among others (Mayer and Bukau, 2005). Structurally, Hsp70s are comprised of an N-terminal nucleotide binding domain (NBD) that is connected to the substrate binding domain (SBD) by a linker region and followed by a C-terminal domain (Figure 1.3A) (Mayer and Bukau, 2005). Through nucleotide dependent substrate binding and release cycles, Hsp70 functionally interacts with client proteins via binding to short hydrophobic stretches present in these substrates (Mayer and Bukau, 2005)**.** To efficiently interact with client proteins Hsp70s often require cochaperones including J proteins and nucleotide exchange factors (NEFs) (Figure 1.3B). The basal ATPase activity of Hsp70 is low and its affinity for client proteins is high in the ADP-bound conformation unlike the ATP-bound state (Dragovic, et al., 2006; Kampinga and Craig, 2010). J proteins stimulate the ATPase activity of Hsp70s, deliver client substrates, and can also recruit Hsp70 to specific cellular sites. NEFs facilitate the release of ADP from Hsp70 resulting in a conformation change that allows substrate dissociation and primes Hsp70 for another cycle of substrate binding (Figure 1.3B) (Dragovic, et al., 2006; Steel, et al., 2004).

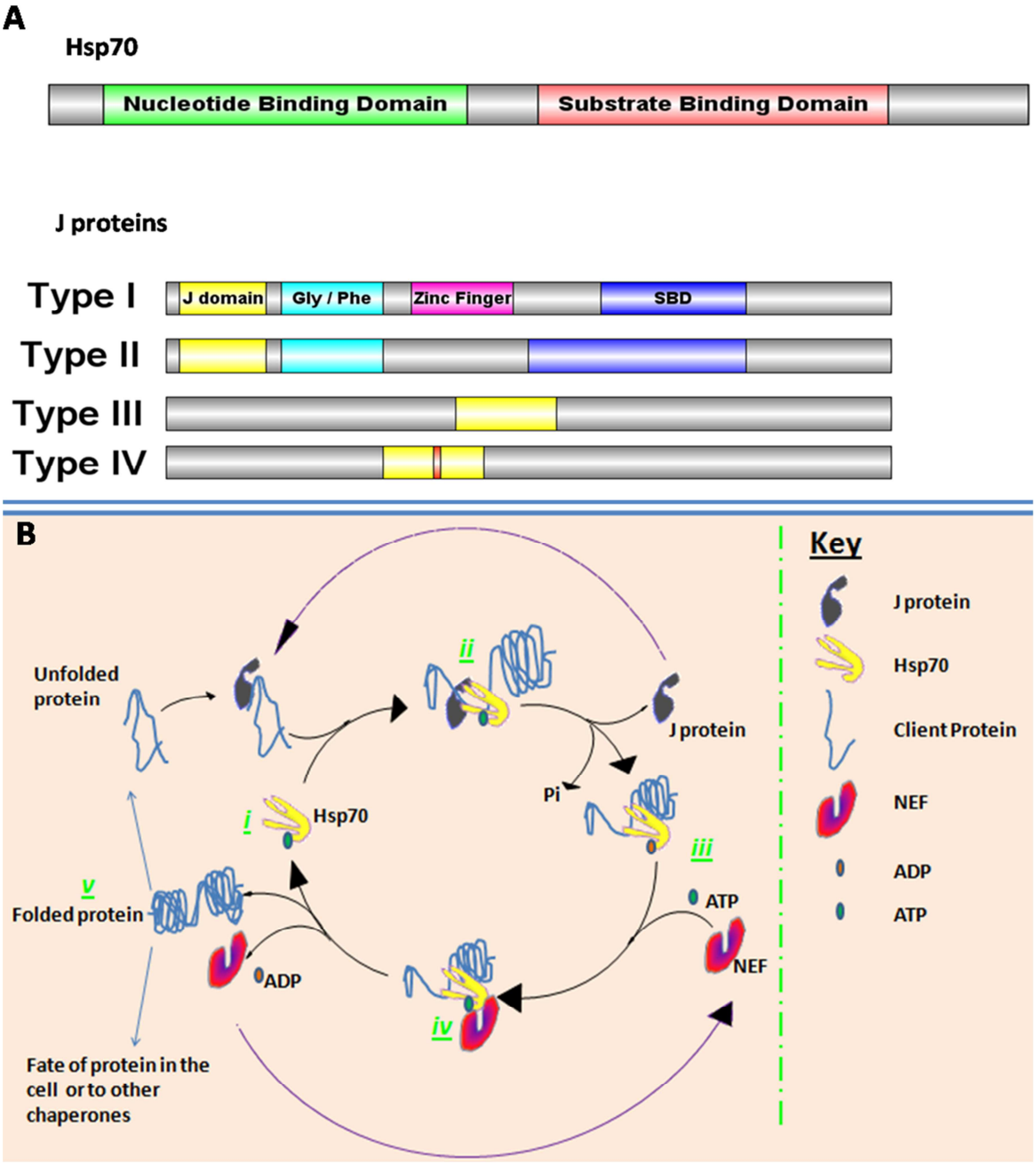

Figure 1.3: Domain organization of the Hsp70 and J proteins (upper panel) and a model depicting the interaction cycle of Hsp70 with J proteins, NEF, and client proteins (lower panel). A). Domain schematics of the Hsp70 and J proteins are represented as open bars. The domains present are indicated and are color coded for J proteins. The corrupted HPD motif is highlighted in the J domain of type IV J proteins. B) *i*) Hsp70 in the ATP bound state has low affinity for client proteins. *ii*) A J protein binds client proteins and transfers them to Hsp70 coupled to hydrolysis of the bound ATP. *iii*) Hsp70 in its ADP bound state bound to an unfolded client allowing it to fold or refold. *iv*) NEF facilitates the release of ADP and the binding of ATP thereby allowing release of the folded client protein. *v*) The fate of the folded client protein to other cellular pathways or for partially folded clients to repeat the folding cycle.

1.4.4 J proteins

J proteins are more diverse in number, structure, and function and are also less abundant relative to Hsp70 (Botha, et al., 2007; Kampinga and Craig, 2010; Walsh, et al., 2004). Although most J proteins have diverged from the *Escherichia coli* J protein, DnaJ, sequence alignment and structural studies showed that they share a highly conserved J-domain that is approximately 70 to 80 amino acids long (Cheetham and Caplan, 1998) (Figure 1.3A). This domain exhibits four α-helices (I-IV) and a highly conserved signature histidine-proline-aspartate (HPD) tripeptide motif in the loop region between helices II and III (Greene, et al., 1998; Hill, et al., 1995) that is vital for stimulation of Hsp70 ATPase activity (Genevaux, et al., 2002; Hennessy, et al., 2005; Wittung-Stafshede, et al., 2003). Indeed, it is through the HPD motif present in the J-domain that J proteins stimulate the ATPase activity of Hsp70. J proteins have canonically been classified as type I, II, III, and IV (Botha, et al., 2007; Cheetham and Caplan, 1998) (Figure 1.3A). This classification is however not definitive of their biochemical functions (Cheetham and Caplan, 1998; Kampinga and Craig, 2010) and most are highly divergent possessing additional domains (Kampinga and Craig, 2010; Rajan and D'Silva, 2009). The diversity of the additional domains potentially allows them to interact with a wide range of substrates and to perform specialized functions. Type I J proteins possess an N-terminal J-domain, an adjacent glycine and phenylalanine rich region (Gly/Phe-rich region), followed by a cysteine/glycine repeat zinc finger domain, and a variable C-terminal domain. Type II J proteins lack the zinc finger domain while type III have the J-domain located anywhere in the protein. Type IV J proteins possess a J-domain with variations of the canonical HPD motif (Botha, et al., 2007).

1.4.5 Heat shock proteins in the context of malaria

The lifecycle of the malaria parasite requires both a mammalian host and a mosquito vector where it undergoes extensive morphological changes and shows multiple tissue adaptations to both environments. During these transitions, the parasite is thought to be subjected to various stressors, such as temperature, that may lead to protein misfolding and aggregation and ensuring the stability and functionality of cellular macromolecules is critical and vital for parasite survival. As mentioned previously, molecular chaperones help buffer against cellular stress by promoting productive folding of cellular proteins and preventing their misfolding and aggregation (Riezman, 2004). *P. falciparum* dedicates a significant portion of its genome

(approximately 2% of the total genes) to encode chaperones (Acharya, et al., 2007). This chaperone complement is thought to play an important role in ensuring protein homeostasis during several stages of development and host-vector transitions.

Data from comparative analysis of the molecular chaperone families shows that whilst these families are generally conserved across the *Plasmodium* species, there are several members that are species-specific (Wasmuth, et al., 2009), lineage-specific (Aravind, et al., 2003; Külzer, et al., 2012; Sargeant, et al., 2006) or stage-specific (Florens, et al., 2002; Khan, et al., 2005; Lasonder, et al., 2008). Of the several stages of *Plasmodium* development, the blood stage is the best studied where members of the Hsps have been shown to be intimately involved in malaria pathogenesis (Daily, et al., 2007; Maier, et al., 2009; Maier, et al., 2008; Pallavi, et al., 2010). Indeed, while some of these Hsps play housekeeping proteostasis role within the parasite, some members have been shown to be exported to the host cell cytoplasm where they are proposed to chaperone exported proteins (Acharya, et al., 2012; Külzer, et al., 2012; Maier, et al., 2008). This unique protein complement is thought to fulfill parasite-specific functions and forms a good basis for drug targeting (Pesce, et al., 2010; Shonhai, 2010).

The genome of *P. falciparum* encodes four Hsp90 and six Hsp70 homologues and a large number of J proteins that localize to the various intracellular compartments or are exported to the infected erythrocyte cytosol (Acharya, et al., 2007; Botha, et al., 2007; Shonhai, et al., 2007). Several members have been shown to be unique to the parasite as there are no homologues present in the human system and are therefore considered as drug targets. Data from Hsp90 inhibition with benzoquinone ansamycins, such as geldanamycin and radiciol and associated geldanamycin derivatives such as 17 allylamino-17 demethoxygeldanamycin (17-AAG) and 17 dimethylaminoethylamino-17-demethoxygeldanamycin (17-DMAG), has shown therapeutic promise from clinical trials in cancer treatment (Den and Lu, 2012; Uehara, 2003; Whitesell, et al., 1994). Treatment of *P. falciparum* parasites in culture with geldanamycin leads to arrest in parasite growth thereby highlighting the importance of Hsp90 to the parasite's development (Banumathy, et al., 2003; Pallavi, et al., 2010). However, while Hsp90 inhibition has given positive results resulting in clinical trials, inhibiting Hsp70 has been quite a challenge (Goloudina, et al., 2012). Small molecule inhibitors have been tested on some *P. falciparum* Hsp70s and showed promising results (Chiang, et al., 2009; Ramya, et al., 2007; Ramya, et al., 2006). Overall, the essential role played by molecular chaperones

provides avenues for enhancing our understanding of the biology of the parasite and identification of novel drug targets which are an important priority to malaria control efforts.

1.5 Knowledge gap and motivation

Comparative analysis of the genomes of the human host and the malaria parasites has revealed unique and novel characteristics possessed by these intracellular parasites (Frech and Chen, 2011; Winzeler, 2008). The unique traits are considered exploitable and may provide a major thrust in finding new therapeutics in the face of increasing development and geographical spread of drug resistance. Heat shock proteins including Hsp90s, Hsp70s, and J proteins are considered potential drug targets in various cellular systems including malaria (Cockburn, et al., 2011; Kondoh and Osada, 2012; Pesce, et al., 2010; Shonhai, 2010). Data arising from several studies on these protein families suggests that they have potential for being targeted with small molecules and peptidomimetics (Brodsky, 1999; Evans, et al., 2010; Fewell, et al., 2004). Indeed, several small molecules have been tested as inhibitors on a plasmodial Hsp70 (Botha, et al., 2011; Chiang, et al., 2009; Cockburn, et al., 2011). The inhibitory and/or stimulatory effects of these molecules can be well understood by studying the partnerships, localizations and interaction of chaperones with their cochaperones and client proteins. Such information can be used in the development of assays for testing small molecules and further enhance the understanding of the parasite biology. However, characterization of the roles of these proteins in the chaperoning process, which is crucial for drug targeting, is still at its infancy in *Plasmodium* parasites.

While Hsp90 and Hsp70 families in *P. falciparum* appear to be generally conserved with respect to homologues present in other cellular systems, very little is known about their partnerships with the cochaperone complement including J proteins. Additionally, studies on chaperones have neglected the rodent and primate infecting *Plasmodium* species that serve as experimental models or research tools in immunology, pathogenesis, basic discovery, drug testing and vaccine development (Fidock, et al., 2004; Langhorne, et al., 2011). To date, significant progress has been made in several areas including continued genome sequencing and annotation, development of several *Plasmodium* specific software and database resources, and continuous experimentation. Such resources motivate for comparative studies that can inform on some of the similarities and differences in host-parasite interactions and

virulence. They may also provide insights into the evolution of proteins, protein families, and protein interaction networks (Juan, et al., 2008; Lewis, et al., 2010) in malaria parasites. This study includes a detailed review of the Hsp70 and J proteins in *Plasmodium* parasites.

PfHsp70-1 is a cytosolic *P. falciparum* Hsp70 homologue that shuttles to the nucleus and is a considered a crucial player in protein homeostasis during physiological, morphological and temperature associated transitions in the parasite lifecycle (Botha, et al., 2011; Pesce, et al., 2008). PfHsp70-1 is at the center stage of chaperoning cytosolic proteins and its expression may be increased in response to several antimalarial treatments (Aunpad, et al., 2009). It therefore plays a crucial role geared towards parasite survival and is considered a novel drug target (Pesce, et al., 2010). Characterization of the interactions between PfHsp70-1 and J proteins and the identification of client proteins is essential for drug target validation. However, the subcellular localization of most J proteins has not been experimentally validated which is crucial if any inferences on partnership and function are to be made. Of the several J proteins predicted to reside in the cytosol, only two have been studied experimentally and implicated as cochaperones of PfHsp70-1 (Botha, et al., 2011; Pesce, et al., 2008). PFB0595w is a typical type II J protein that does not have a topogenic signal and is predicted to reside in the cytoplasm and act as a cochaperone to PfHsp70-1. In silico studies depict it to be highly conserved with yeast Sis1p homologues in most cellular systems and its characterization was prioritized to enhance the understanding of PfHsp70-1 chaperone machinery in the cytosol. Since PFB0595w is highly conserved, data obtained from studying its interaction with PfHsp70-1 may be extrapolated across other *Plasmodium* species and compared with other closely related cellular systems. As such, the cell biological and biochemical properties of PFB0595w from *P. falciparum* needs to be determined.

Another goal for this study was to characterize PFD0462w (Pfj1) which is an atypical type I J protein with an extended N-terminal domain possibly depicting a signal presequence before the J-domain. Pfj1 also has an extended C-terminal domain that has little or no significant homology with other proteins; a characteristic that allowed it to be considered a drug target (Botha, et al., 2007; Pesce, et al., 2010). Pfj1 was argued to reside in the mitochondria following the in silico identification of a mitochondrial import signal (Watanabe, 1997). It was however shown to localize in the apicoplast where it was hypothesized to play a role in the replication of the apicoplast genome with little or no chaperone roles (Kumar, et al., 2010). Complementation experiments in DnaJ *cbpA* mutant *Escherichia coli* strain have shown that Pfj1 has a functional J domain (Nicoll, et al., 2007). Additionally, Pfj1 was shown

to functionally interact with PfHsp70-1 in vitro thereby raising questions about its localization and potential cochaperone properties with Hsp70s in *P. falciparum* (Misra and Ramachandran, 2009). To date, none of the Hsp70s encoded by the *P. falciparum* genome has been localized in the apicoplast. It was expected that Pfj1 would potentially co-localize with an Hsp70 partner due to these mentioned chaperone associated properties. It is against this background that the confirmation of the localization of Pfj1 was prioritized.

1.6 Research hypothesis

This dissertation attempts to illuminate the Hsp70-J protein partnerships in the malaria parasite, *P. falciparum*. This study therefore hypothesizes that:

i. PFB0595w is a cytosolic J protein that potentially regulates the PfHsp70-1 chaperone activity.
ii. Pfj1 does not localize to the apicoplast and may potentially have an Hsp70 chaperone partner.

1.7 Aims and Objectives and Approach

1.7.1 In silico bioinformatic analysis of the Hsp70-J protein chaperone complement across *Plasmodium* species

The study aimed to identify all the Hsp70 and J proteins across the *Plasmodium* species including the human- and primate- (*P. falciparum 3D7* and *P. vivax SaI-1*, *P. knowlesi strain H*), and rodent-infecting species (*P. berghei ANKA*, *P. chabaudi chabaudi*, and *P. yoelii yoelii 17XNL*). The study additionally aimed at providing a review of literature on Hsp70s and J proteins in the mentioned *Plasmodium* species. Chromosomal localization, protein domain mapping, and phylogenetic analysis was also carried out for *P. falciparum*. The predicted nucleotide and protein sequences were retrieved from PlasmoDB version 8.1 (Aurrecoechea, et al., 2009). The J protein complement was identified through a search criterion that included using gene IDs from available literature, database searching through search-terms including “heat shock protein 40”, “DnaJ”, and “chaperone”. Additionally, the J-domain of the *E. coli* DnaJ was used to search the entire genome of the *Plasmodium* species

using the standard protein blast (blastp) option in the PlasmoDB genome resource. Protein domains and associated features were identified using a combination of different software. Further, the organelle distribution of the several J proteins was also analyzed, in the absence of experimental data, using bioinformatic tools. J proteins were predicted as exported to the infected erythrocyte based on the presence of the PEXEL motif (Hiller, et al., 2004; Marti, et al., 2004).

1.7.2 Characterization of PFB0595w

Another aim of this study was to determine the presence and localization of PFB0595w through transfection and fluorescence imaging approaches. Antibodies specific to PFB0595w were designed and commercially raised in mice and used for detection both under normal and heat stress conditions. Additionally, the expression profile of PFB0595w relative to PfHsp70-1 throughout the intraerythrocytic stage of parasite development was determined. The localization of PFB0595w was demonstrated through fluorescent imaging of parasites transfected with plasmids expressing PFB0595w tagged to GFP as well as immunofluorescence imaging. The study also aimed to study the potential for heterologously purified PFB0595w to play a role as a cochaperone for PfHsp70-1 and this was assessed through ATPase assays. The interaction dynamics between these two proteins was additionally assessed through surface plasmon resonance spectroscopy.

1.7.3 Characterization of Pfj1

The aim here was to validate the localization and expression of Pfj1 through transfection technology and fluorescent imaging approaches. Antibodies specific to Pfj1 were designed and commercially raised in mice and used for detection in the intraerythrocytic stage of parasite development. Through the transfection and immunofluorescence imaging approach, its localization has been determined. Further, preliminary studies of its potential Hsp70 partner have been conducted paving the way for functional characterizations through in vitro approaches.

CHAPTER TWO

Bioinformatic analysis of the Hsp70-J protein chaperone complement across *Plasmodium* species

Note: some of the work described in this chapter has been published in the following article;

> **James M. Njunge**, Michael H. Ludewig, Aileen Boshoff, Eva-Rachele Pesce, and Gregory L. Blatch. **Hsp70s and J Proteins of *Plasmodium* Parasites Infecting Rodents and Primates: Structure, Function, Clinical Relevance, and Drug Targets.** *Current Pharmaceutical Design*, 2013, 19, 387-403.

The published data has been reproduced as part of this thesis with written permission of the publishers of the article (Bentham Science Publishers).

2.0 Introduction

Chaperone studies in malaria have mainly focused on *P. falciparum*, the malaria parasite that accounts for the most severe form of human malaria, and neglected the rodent and primate infecting counterparts. The latter species have been widely used as experimental study models in malaria immunology, pathogenesis, basic discovery and testing, and vaccine development (Fidock, et al., 2004; Langhorne, et al., 2011). Previously, it has been shown that there is a high level of genome conservation (Carlton, et al., 2008; Carlton, et al., 2002; Pain, et al., 2008) and resemblance among *Plasmodium* species infecting humans, primates and rodents (Carter and Diggs, 1977). Indeed, comparative studies that focus on the genomes, transcriptomes, and proteomes of closely related parasitic species are quite informative of similarities and differences present in parasite populations. Information generated from such studies can be used to inform differences in host-parasite interactions and virulence amongst other traits. Thus, the level of conservation of the Hsp70 and J protein chaperone system among *Plasmodium* species may contribute to the understanding of the similarities and differences in host-parasite interactions, virulence, and provide avenues for drug targeting. It may also provide insights into the evolution of proteins, protein families, and protein interaction networks (Juan, et al., 2008; Lewis, et al., 2010) in the malaria parasites.

Several reviews have been written on Hsp70s and J proteins in *P. falciparum* (Acharya, et al., 2007; Botha, et al., 2007; Pesce, et al., 2010; Rug and Maier, 2011). However, no comprehensive assessment of Hsp70-J protein chaperone system has been made across the rodent- and primate-infecting *Plasmodium* species. It is worth noting that within the last few years, significant progress has been made in several areas including continued genome sequencing and annotation, development of several *Plasmodium* specific software and database resources, and continuous experimentation. This chapter intends to further previous analyses of the *P. falciparum* Hsp70s and J proteins by examining how conserved this complement is among a number of *Plasmodium* species. Additionally, it compiles chromosomal locus and protein domain maps for *P. falciparum* Hsp70s and J proteins and highlights the yeast and human orthologues. *Plasmodium* species assessed include the human- and primate- (*P. falciparum 3D7* and *P. vivax SaI-1, P. knowlesi strain H*), and rodent-infecting species (*P. berghei ANKA, P. chabaudi chabaudi*, and *P. yoelii yoelii 17XNL*). It has to be noted that unlike *P. falciparum*, the genome sequencing and annotation of *P. knowlesi*, *P. berghei*, and *P. chabaudi*, have a noncontiguous finished draft while those

of *P. yoelii* and *P. vivax* have an improved high-quality genome draft (Logan-Klumpler, et al., 2011). Overall, the chapter provides an overview of the Hsp70-J protein machinery in the above mentioned *Plasmodium* species with emphasis on the intraerythrocytic stage of parasite development.

2.1 Objectives

An in silico comparative analysis was undertaken to identify all the Hsp70 and J proteins across the *Plasmodium* species. The analysis included the human- and primate- (*P. falciparum 3D7* and *P. vivax SaI-1*, *P. knowlesi strain H*), and rodent-infecting species (*P. berghei ANKA*, *P. chabaudi chabaudi*, and *P. yoelii yoelii 17XNL*). The specific objectives include:

i. To provide an update of all the Hsp70 and J proteins across the above mentioned *Plasmodium* species.
ii. To investigate the similarities and differences in the Hsp70 and J protein complements of these species.
iii. To identify human and yeast homologues of the Hsp70s and J proteins in *P. falciparum*.
iv. To provide chromosomal localization and protein domain maps for *P. falciparum* Hsp70s and J proteins.
v. To provide an updated prediction of localization, interactions, and possible cellular roles of the Hsp70-J protein complement in *P. falciparum*.

2.2 Materials and methods

2.2.1 Sequences searches and comparison

All the predicted genomic and amino acid sequences used to assess the gene structure of the Hsp70s and J proteins among *Plasmodium* species were retrieved from PlasmoDB version 8.1 (http://plasmodb.org/plasmo/) (Aurrecoechea, et al., 2009). To identify the J protein complement, a search criterion was used including using gene IDs from available literature, database searching through search-terms including “heat shock protein 40”, “DnaJ”, and

"chaperone". Additionally, the J-domain of the *Escherichia coli* DnaJ was used to search the entire genome of the *Plasmodium* species using the standard protein blast (blastp) option in the PlasmoDB genome resource. It has to be noted that gene chromosomal context has been completed for all the *Plasmodium* species except for *P. yoelii*. Multiple protein sequence alignments were carried out using ClustalW (Larkin, et al., 2007) followed by phylogenetic analysis. Pairwise amino acid identities and similarities were calculated using GeneDoc version 2.6 (Nicholas, et al., 1997) using the Blosum 62 model.

2.2.2 Domain identification and subcellular localization

The predicted protein characteristics comparatively assessed in this study include: molecular masses, predicted signal sequences, transmembrane and other domains, isoelectric point, and number of amino acids. Protein domains and associated features were identified using a combination of different software such as Prosite (http://prosite.expasy.org/) (Sigrist, et al., 2010), SMART 7 (Simple Modular Architecture Research Tool; http://smart.embl-heidelberg.de/) (Letunic, et al., 2012), Phobius (http://phobius.sbc.su.se/) (Käll, et al., 2004), PrePs (Prenylation Prediction Suite; http://mendel.imp.ac.at/PrePS/) (Maurer-Stroh and Eisenhaber, 2005), HAMAP (High-quality Automated and Manual Annotation of microbial Proteomes; http://hamap.expasy.org/) (Lima, et al., 2009), and Multiple Expectation Maximization for Motif Elicitation (MEME; http://meme.nbcr.net/) suite (Bailey and Elkan, 1994; Bailey, et al., 2006). The organelle distribution of several J proteins were analyzed, in the absence of experimental data, using several bioinformatic tools such as Prediction of apicoplast targeting signals (PlasmoAP; rule based: http://v4-4.plasmodb.org/restricted/PlasmoAPcgi.shtml and PATs; neural network based: http://gecco.org.chemie.uni-frankfurt.de/pats/pats-index.php) (Foth, et al., 2003; Zuegge, et al., 2001) algorithms to predict apicoplast-target sequences, PlasMit (http://gecco.org.chemie.uni-frankfurt.de/plasmit/) for prediction of *P. falciparum* mitochondrial transit peptides (Bender, et al., 2003). J proteins were predicted as exported to the infected erythrocyte based on the presence of the PEXEL motif (Hiller, et al., 2004; Marti, et al., 2004).

2.3 Results and discussion

2.3.1 Gene structure and protein conservation

2.3.1.1 Phylogenetic analysis of Hsp70

Sequence searches from the PlasmoDB genome resource revealed that the *Plasmodium* species analyzed in this study possess five Hsp70 homologues except *P. falciparum* that possesses six as previously shown (Shonhai, et al., 2007). This number is significantly smaller relative to other eukaryotes like yeast (*Saccharomyces cerevisiae*) and humans (*Homo sapien*) both of which encode fourteen Hsp70 members (Kampinga and Craig, 2010). Overall phylogenetic analysis displayed a high level of Hsp70 conservation among the *Plasmodium* species as shown in Figure 2.1. Five distinct phylogenetic clusters were observed and each cluster showed conservation of both protein sequence and domain architecture (shown in Figure 2.2 for *P. falciparum* Hsp70s). Two of these clusters namely; the PfHsp70-y cluster and PfHsp70-z cluster, are members of the Hsp110/SSE family and have been proposed to function as nucleotide exchange factors (NEFs) (Shonhai, et al., 2007). As expected, in each group, the human-infecting *P. vivax* and the primate- and human-infecting *P. knowlesi* Hsp70s cluster together. Similarly, *P. berghei* and *P. yoelii* and to a certain extent *P. chabaudi* Hsp70s cluster together (Figure 2.1). However, *P. falciparum* Hsp70 homologues deviated from this trend localizing in differing chromosomes from the other human infecting *Plasmodium* species in all the clusters, probably reflecting a greater evolutionary distance from the rest. With the exception of MAL7P1.228 (PfHsp70-x) and PF07_0033 (PfHsp70-z), a high level of conservation was observed in gene structure and synteny in each cluster. For example, at the nucleotide level, the position and possession of spliceosomal introns in these genes is highly conserved. However, the intron composition and length varies across the *Plasmodium* species. At the protein level, the number of amino acids and the various protein motifs and domains are highly conserved (Figure 2.1). PfHsp70-x falls in the same phylogenetic clade as PF08_0054 (PfHsp70-1), but lacks equivalent syntenic homologues in the *Plasmodium* species considered in this review (Figure 2.1). Unlike the other Hsp70 genes in the same cluster, PfHsp70-x is uniquely localized in the subtelomeric region of chromosome 8 (Figure 2.3) after the synteny breakpoint.

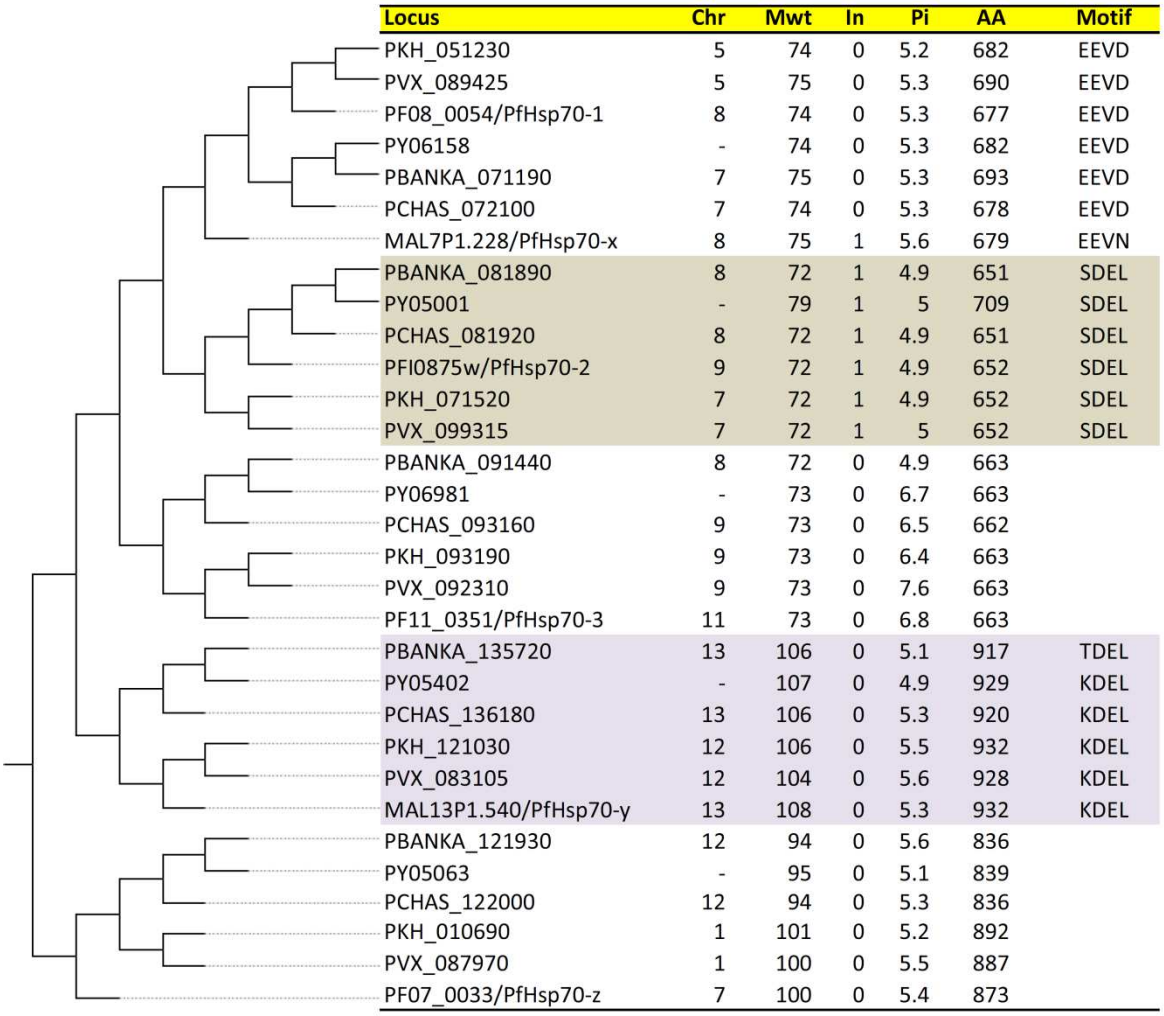

Locus	Chr	Mwt	In	Pi	AA	Motif
PKH_051230	5	74	0	5.2	682	EEVD
PVX_089425	5	75	0	5.3	690	EEVD
PF08_0054/PfHsp70-1	8	74	0	5.3	677	EEVD
PY06158	-	74	0	5.3	682	EEVD
PBANKA_071190	7	75	0	5.3	693	EEVD
PCHAS_072100	7	74	0	5.3	678	EEVD
MAL7P1.228/PfHsp70-x	8	75	1	5.6	679	EEVN
PBANKA_081890	8	72	1	4.9	651	SDEL
PY05001	-	79	1	5	709	SDEL
PCHAS_081920	8	72	1	4.9	651	SDEL
PFI0875w/PfHsp70-2	9	72	1	4.9	652	SDEL
PKH_071520	7	72	1	4.9	652	SDEL
PVX_099315	7	72	1	5	652	SDEL
PBANKA_091440	8	72	0	4.9	663	
PY06981	-	73	0	6.7	663	
PCHAS_093160	9	73	0	6.5	662	
PKH_093190	9	73	0	6.4	663	
PVX_092310	9	73	0	7.6	663	
PF11_0351/PfHsp70-3	11	73	0	6.8	663	
PBANKA_135720	13	106	0	5.1	917	TDEL
PY05402	-	107	0	4.9	929	KDEL
PCHAS_136180	13	106	0	5.3	920	KDEL
PKH_121030	12	106	0	5.5	932	KDEL
PVX_083105	12	104	0	5.6	928	KDEL
MAL13P1.540/PfHsp70-y	13	108	0	5.3	932	KDEL
PBANKA_121930	12	94	0	5.6	836	
PY05063	-	95	0	5.1	839	
PCHAS_122000	12	94	0	5.3	836	
PKH_010690	1	101	0	5.2	892	
PVX_087970	1	100	0	5.5	887	
PF07_0033/PfHsp70-z	7	100	0	5.4	873	

Figure 2.1: Phylogenetic analysis of the Hsp70 homologues across the *Plasmodium* species. Ch and Mw represents the chromosomal localization and the molecular mass respectively. In indicates the number of intron(s) present. Pi and AA represents the isoelectric point and the number of amino acids respectively. The alphabetical letters in the locus column depict the *Plasmodium* specie: PF; *P. falciparum*, PBANKA; *P. berghei*, PY; *P. yoelii*, PCHAS; *P. chabaudi*, PVX; *P. vivax*, PKH; *P. knowlesi*. The amino acid sequences used in this figure were retrieved from PlasmoDB version 8.1 (www.plasmodb.org) (Aurrecoechea, et al., 2009). Multiple protein sequence alignments were carried out using ClustalW (Larkin, et al., 2007) followed by phylogenetic tree construction. Pairwise amino acid identities and similarities were calculated with GeneDoc version 2.6 (Nicholas, et al., 1997) using the Blosum 62 model. Note: The gene chromosomal locus for *P. yoelii* has not been yet assigned and is indicated by the – (dash) sign.

Additional unique features relative to the other Hsp70s in the same cluster include the presence of a short N-terminal extension predicted to be a signal sequence (Figure 2.2), lack of GGMP repeats at the C-terminus, and possession of an EEVN motif instead of an EEVD. The presence of a predicted signal motif potentially raised doubts as to its previously suggested cytosolic and nuclear localization (Shonhai, et al., 2007). Recently, PfHsp70-x was

shown to reside in both the parasitophorous vacuole (PV) lumen and exported to the infected erythrocyte through non-PEXEL mediated mechanisms (Külzer, et al., 2012). Additionally, Kulzer and colleagues hypothesized that PfHsp70-x may have arisen from a gene duplication event of PfHsp70-1. It has been recently shown that almost all unique genes in *P. falciparum* possess introns (Sharma, et al., 2010) and this is consistent with the observed lineage specific evolution of *P. falciparum* genes (Sargeant, et al., 2006).

2.3.1.2 Hsp70 Domain organization

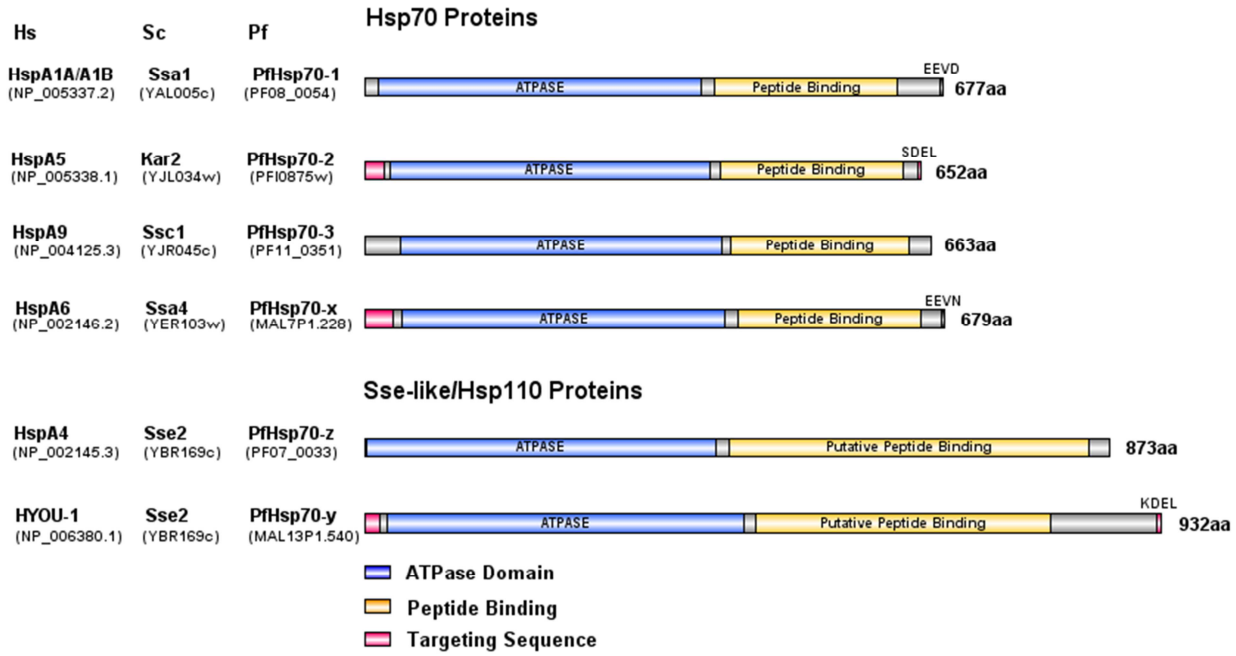

Figure 2.2: Schematic representation of the domain architecture of the *P. falciparum* Hsp70 complement. Each protein sequence is represented by an open bar with the protein locus indicated on the left hand side along with the human (*H. sapien*/Hs) and yeast (*Saccharomyces cerevisiae*/Sc) orthologues. The number of amino acids in each protein is shown on the right hand side of the protein bar. The various domains are depicted by blocks within the protein sequence bar using different colors. The key provides a short description of the various domains and their corresponding color code. Protein domains and associated features were identified using a combination of different software including Prosite (Sigrist, et al., 2010), SMART 7 (Simple Modular Architecture Research Tool) (Letunic, et al., 2012), and Phobius (Käll, et al., 2004).

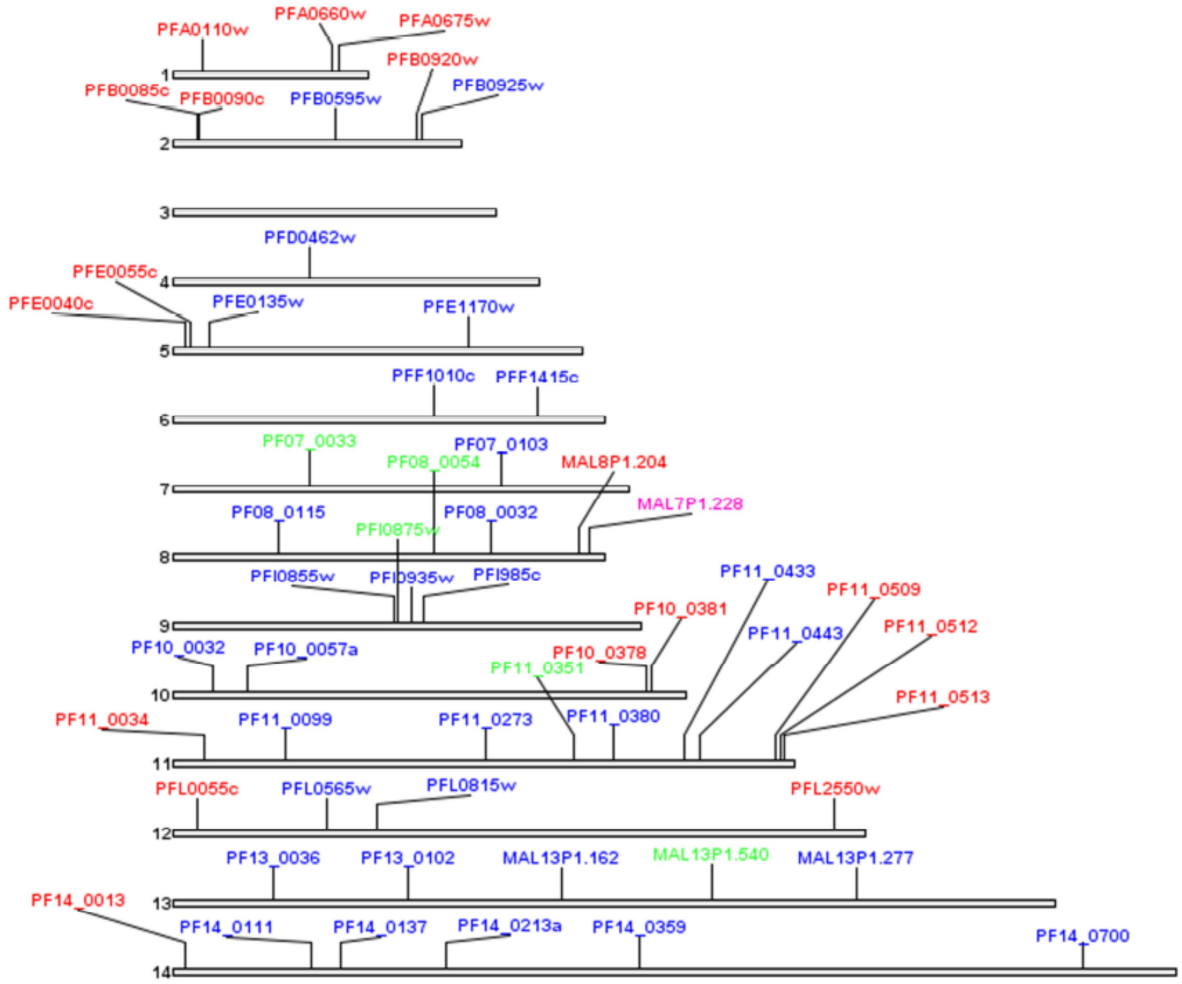

Figure 2.3: Chromosomal localization of the *P. falciparum* Hsp70s and J proteins. Each chromosome is represented by an open bar with the chromosome number indicated on the left hand side and the heat shock proteins annotated above. The Hsp70s are depicted in green except for MAL7P1.228 shown in pink. Parasite resident and exported J proteins are depicted in blue and red colors respectively.

2.3.1.3 J proteins

A search for the entire J protein complement identified a total of 49 J proteins in *P. falciparum* relative to *P. vivax*; (*n = 32*), *P. knowlesi*; (*n = 31*), *P. chabaudi*; (*n = 29*), *P. berghei*; (*n = 31*), and *P. yoelii*; (*n = 28*) (Table 2.1). Previously *P. falciparum* had been reported to possess 43 J proteins while few homologues had been identified in the other *Plasmodium* species (Acharya, et al., 2007; Botha, et al., 2007; Sargeant, et al., 2006). Of the 49 *P. falciparum* J proteins, eight (PF14_0213, MAL13P1.162, MAL8P1.204, PF10_0057a, PF11_0433, and PF14_0111, PFI0855w, and PFF1010c) were newly identified and/or are listed as DnaJ proteins in PlasmoDB (Aurrecoechea, et al., 2009). Additionally, this study

observed that the current protein models for PFF1290c and PF10_0058 which were previously considered as J proteins, do not display a J-domain and were therefore excluded. Consistent with a previous study (Botha, et al., 2007), *P. falciparum* has the highest number of J proteins relative to other *Plasmodium* species (Table 2.1). The increase in the number of J proteins identified relative to those previously reported can be attributed to the ongoing annotation of *Plasmodium* genomes. There are however 22 J proteins in yeast (Walsh, et al., 2004), 41 in humans (Kampinga and Craig, 2010), 36 in *T. gondii*, and approximately 65 members in *Trypanosomes*.

Many proteins in *Plasmodium* that have been shown to be exported to the infected erythrocyte compartment contain a short N-terminus sequence referred to as the *Plasmodium* export element (PEXEL) or vacuolar transport signal (VTS) (Hiller, et al., 2004; Marti, et al., 2004). This motif is responsible for targeting parasite proteins to the infected erythrocyte and is conserved across *Plasmodium* species (Sargeant, et al., 2006). Several J proteins possess a PEXEL motif and therefore the *P. falciparum* J proteins were categorized into parasite resident and exported J proteins on the basis of its presence in the protein sequence. Of the 49 members of the *P. falciparum* J protein complement, 19 possess a PEXEL motif and were therefore considered to be exported. Sequence alignments revealed that parasite resident J proteins are highly conserved with almost all *P. falciparum* J proteins having homologues in the other *Plasmodium* species (Table 2.1). Additionally, several have putative orthologues in both yeast and humans (Figure 2.4). Multiple protein sequence alignments of each J protein with orthologues across *Plasmodium* showed a high level of similarity and identity implying high structural and functional conservation. Comparative analysis of J proteins across the *Plasmodium* species showed that *P. falciparum* possesses the highest number (*n = 19*) of exported J proteins (Table 2.1). The observation that most of the exported J proteins are present only in *P. falciparum* is consistent with the existence of an expanded exportome in *P. falciparum* relative to the other *Plasmodium* species (Sargeant, et al., 2006; van Ooij, et al., 2008). With the exception of five exported J proteins that possess more than one intron, all the others contain a single intron (Data not shown). Previously, it has been observed that most parasite exported proteins, including exported J proteins, have similar gene structures with the first intron occurring in the stretch encoding the spacer region between the signal sequence and the PEXEL motif, or, less commonly, downstream in the hydrophobic signal section (Sargeant, et al., 2006). However, it has to be noted that there are a number of

exported *Plasmodial* proteins that lack a PEXEL sequence (Spielmann and Gilberger, 2010) indicating the existence of multiple protein export pathways in malaria parasites.

Table 2.1: Comprehensive list of J proteins across the *Plasmodium* species analyzed. The table is subdivided into parasite resident and exported J protein complements. New members identified are highlighted in bold for *P. falciparum*. PF; *P. falciparum,* PVX; *P. vivax*, PCHAS; *P. chabaudi*, PBANKA, *P. berghei*, PY; *P. yoelii*.

Key:

Color	Description
	Type I
	Type II Parasite Resident
	Type III Parasite Resident
	Type IV Parsite Resident
	Type II Exported
	Type III Exported
	Type IV Exported

----------Parasite resident J protein complement----------					
PF	PVX	PKH	PCHAS	PBANKA	PY
PFD0462w	PVX_000775	PKH_030520	PCHAS_100790	PBANKA_100700	PY04093
PF14_0359	PVX_084650	PKH_131140	PCHAS_061260	PBANKA_061090	PY02476
MAL13P1.277	PVX_114815	PKH_111430	PCHAS_113250	PBANKA_113300	
PF11_0099	PVX_091110	PKH_090590	PCHAS_090600	PBANKA_093830	PY07174
PF14_0137	PVX_085755	PKH_133370	PCHAS_102960	PBANKA_102880	PY05607
PFB0595w	PVX_002875	PKH_040690	PCHAS_031210	PBANKA_031000	PY02986
PFF1415c	PVX_114560	PKH_111970	PCHAS_112730	PBANKA_112780	PY03544
PFL0565w	PVX_084600	PKH_131040		PBANKA_060990	PY01224
PF07_0103	PVX_096125	PKH_031810	PCHAS_062240	PBANKA_062190	PY01612
PF08_0032	PVX_089170	PKH_050720	PCHAS_071610	PBANKA_070680	PY04500
PF10_0032	PVX_094340	PKH_080150	PCHAS_120190	PBANKA_120120	PY04382
PF10_0057a	PVX_094470	PKH_080420	PCHAS_120450	PBANKA_120380	PY01286
PF11_0273	PVX_091930	PKH_092390	PCHAS_092240	PBANKA_092200	
PF11_0380	PVX_092455	PKH_093470	PCHAS_071310	PBANKA_091180	PY05753
PF13_0036	PVX_122195	PKH_140610	PCHAS_140760	PBANKA_140570	PY00038
PF13_0102	PVX_122755	PKH_141800	PCHAS_141910	PBANKA_141730	PY03272
PF14_0700	PVX_116820	PKH_123210	PCHAS_134100	PBANKA_133640	PY03688
PFE0135w	PVX_097645	PKH_103070	PCHAS_110220	PBANKA_110250	PY04661
PFE1170w	PVX_080080	PKH_100880	PCHAS_123860	PBANKA_123820	PY03711
PFI0935w	PVX_099370	PKH_071630		PBANKA_082000	PY05339
PFI0985c	PVX_099420	PKH_071730		PBANKA_082100	PY05250
PFL0815w	PVX_123520	PKH_143400	PCHAS_143450	PBANKA_143250	PY01558
PF08_0115	PVX_088225	PKH_011190	PCHAS_122480	PBANKA_122420	PY02866
MAL13P1.162	PVX_082455	PKH_122240	PCHAS_134990	PBANKA_134530	PY04182
PF14_0213	PVX_085365	PKH_132680	PCHAS_102190	PBANKA_102110	PY00027
PF14_0111	PVX_085885	PKH_133630	PCHAS_103200	PBANKA_103120	PY00164
-	PVX_092765	PKH_094070			
PFI0855w	PVX_071480	PKH_071480	PCHAS_081880	PBANKA_081850	PY06081
PF11_0433	PVX_092710	PKH_093950	PCHAS_070810	PBANKA_090690	PY03538
PF11_0443			PCHAS_070700	PBANKA_090580	
PFF1010c	PVX_114160	PKH_112850	PCHAS_111940	PBANKA_111990	PY04223

----------Exported J protein complement----------					
PF	PVX	PKH	PCHAS	PBANKA	PY
PFB0090c					
PFE0055c	PVX_081840	PKH_021560	PCHAS_021330	PBANKA_021480	PY07104
PFA0660w					
	PVX_118690				
PF11_0513					
PF10_0378					
PFB0920w					
MAL8P1.204					
PFL0055c					
PF10_0381					
PF11_0034					
PF11_0509					
PF11_0512					
PF14_0013					
PFA0675w					
PFB0085c					
PFB0925w					
PFE0040c					
PFL2550w					
PFA0110w					

2.3.1.3.1 Chromosomal localization and phylogenetic analysis

The gene structure and synteny of parasite resident J proteins are highly conserved across the *Plasmodium* species. The chromosomal assignment of J proteins follows a similar pattern to that of Hsp70s with *P. berghei* and *P. chabaudi* homologous J proteins showing the same pattern of chromosomal localization. While homologous J proteins in *P. vivax* and *P. knowlesi* are located on the same chromosome, those present in *P. falciparum* have a unique chromosomal assignment pattern relative to the rest (Data not shown). Interestingly, genes encoding the exported J proteins are localized in the subtelomeric chromosomal regions compared to the unbiased distribution of the parasite resident counterparts (Figure 2.3) and encode for proteins that have been implicated in host cell remodelling and virulence (Maier, et al., 2009; Marti, et al., 2004; Sargeant, et al., 2006).

Phylogenetic clustering of the J protein complement had been carried out in a previous study (Botha, et al., 2007). Here, phylogenetic analysis was however conducted following an increase in the number of J proteins reported in this study and removal of two J proteins included in the previous study. This study consistently observed clustering of the exported J proteins as previously reported (Figure 2.5) following inclusion of the additional new J proteins identified. For example, MAL8P1.204, an additional member of the exported J protein members, clusters in the exported category, while all the other newly identified parasite resident J proteins cluster in the parasite resident cluster. Additionally, consistent with the study by Botha and colleagues, (2007), three members of the parasite resident J proteins clustered in the exported category (Figure 2.4).

2.3.1.3.2 Domain organization

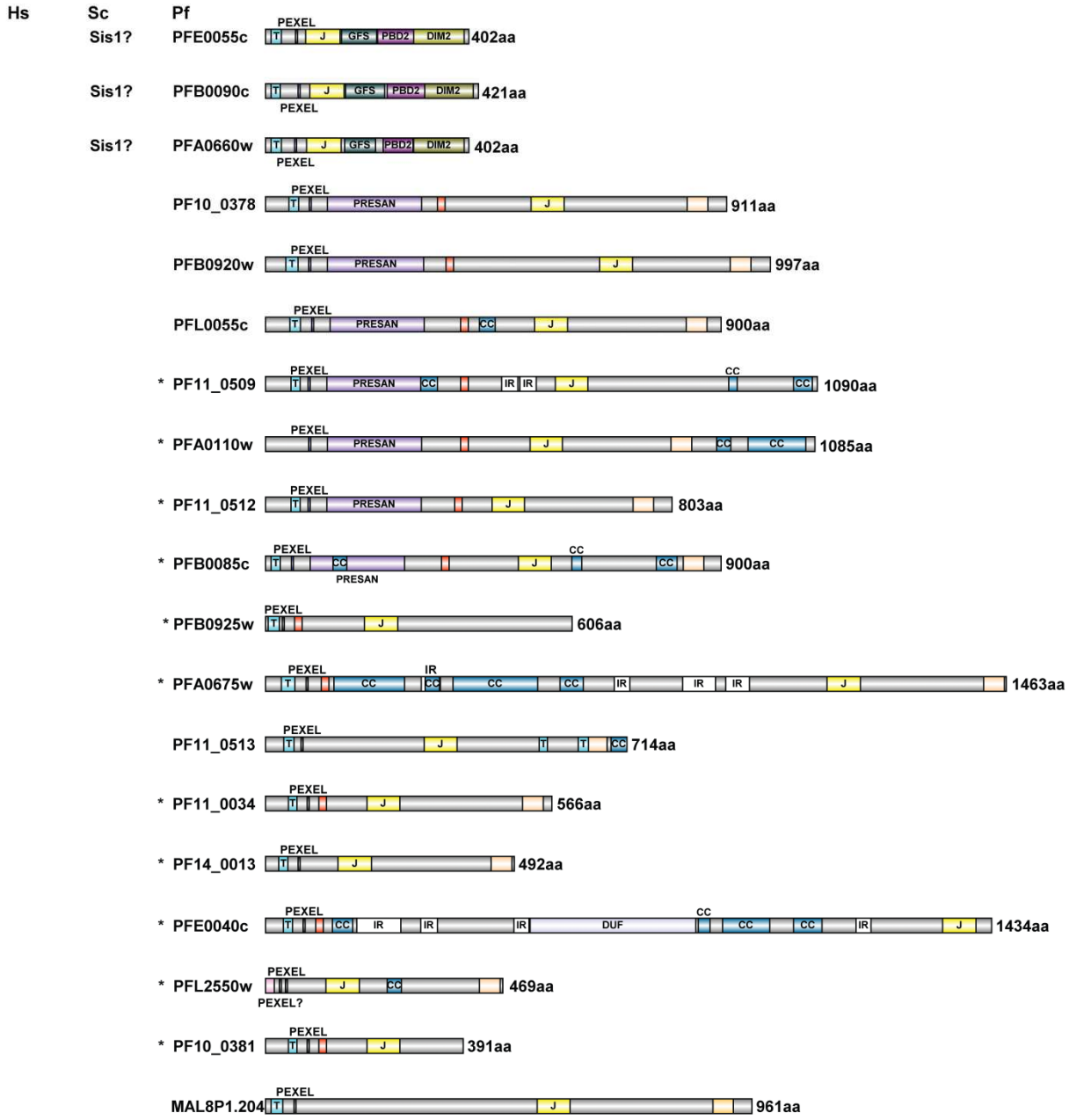

Figure 2.4: Schematic representation of the domain architecture of the *P. falciparum* J protein complement showing parasite resident J proteins followed by exported J proteins. Each protein sequence is represented by an open bar with the protein locus indicated on the left hand side along with the human (Hs) and the yeast (Sc) putative homologues. The number of amino acids in each protein is shown on the right hand side of the protein bar. J proteins designated by an asterisk (*) next to the sequence name indicate that they have a corrupted HPD motif in their J-domain. The various domains are depicted by blocks within the protein sequence bar using different colors. The key provides a short description of the various domains.

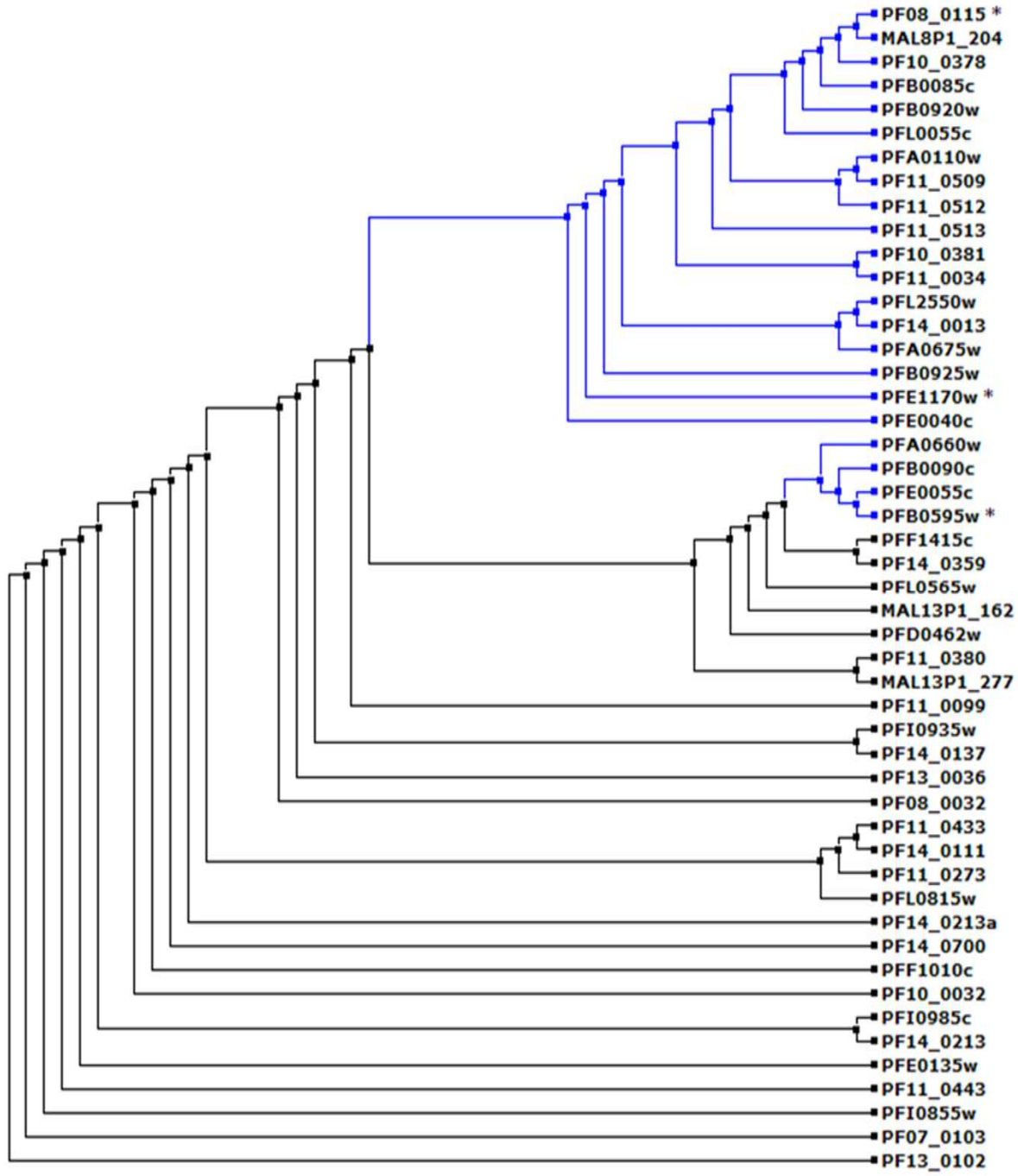

Figure 2.5: Phylogenetic clustering analysis of the J protein complement. The amino acid sequences used in this figure were retrieved from PlasmoDB version 8.1 (http://plasmodb.org/plasmo/) (Aurrecoechea, et al., 2009). Multiple protein sequence alignments were carried out using ClustalW (Larkin, et al., 2007) followed by phylogenetic tree construction. The exported J protein cluster is highlighted in the blue color. The "*" sign indicates a parasite resident J protein present in the exported J protein cluster.

The *P. falciparum* genome unlike other eukaryotes is AT-rich and characterized by nucleotide repeats (Gardner, et al., 2002). Additionally, relative to other eukaryotes, it

encodes for larger sized proteins composed of a biased amino acid composition and prevalence of low complexity regions (LCRs) (Pizzi and Frontali, 2001; Zilversmit, et al., 2010). *P. falciparum* proteins are highly divergent and characterized by insertions of non-globular regions that separate conserved adjacent domains in homologous proteins (Pizzi and Frontali, 2001). This feature makes domain identification in *Plasmodium* proteins difficult using commonly available software derived from domain analysis of well characterized eukaryotes.

There was an overall high percentage identity and similarity derived from multiple sequence alignment of each J protein with homologs across the *Plasmodium* species. This indicated that there was a high level of conservation at the protein sequence level and therefore domain identification was only carried out for *P. falciparum*. The domain organization of most parasite resident J proteins appeared to be generally conserved when compared to homologues from well studied eukaryotes such as yeast and humans (Figure 2.4). Unlike the high number of domains identified in humans and yeast (Kampinga and Craig, 2010), *P. falciparum* displayed relatively fewer domains probably reflecting the associated difficulty with domain identification. The exported J proteins contained peculiar domains and domain organization (Figure 2.4). For example, seven of the exported J proteins possess the *Plasmodium* RESA N-terminal domain (PRESAN) (Oakley, et al., 2007) also called PRESAC but previously referred to as the *Plasmodium* helical interspersed subtelomeric (PHIST) domain that has been reported only in *Plasmodium* species (Sargeant, et al., 2006). Six of the PRESAN-containing exported J proteins (PFB0920w, PFL0055c, PF10_0378, PF11_0509, PF11_0512, PFA0110w) also contain the MEC (MESA erythrocyte cytoskeleton-binding) domain (Kilili and LaCount, 2011). In addition to MESA, the MEC domain is also present in four (PFA0675w, PFB0925w, PF10_0381, PF11_0034) other exported J proteins (Bennett, et al., 1997; Kilili and LaCount, 2011) suggesting a possible role of these proteins in the regulation of cytoskeleton functions. Almost all exported J proteins encode a transmembrane domain upstream of the PEXEL motif. As the PEXEL motif represents a cleavage site for plasmepsin V (Boddey, et al., 2010; Russo, et al., 2010), the transmembrane domain functions as part of the signal sequence recruiting the proteins to the ER (Nilsson, et al., 1994).

Interestingly, when *P. falciparum* J proteins were submitted for analysis to the Multiple Expectation Maximization for Motif Elicitation (MEME; http://meme.nbcr.net) suite (Bailey and Elkan, 1994; Bailey, et al., 2006), a highly conserved unique 41-long amino acid stretch

(Figure 2.6) was identified in the C-terminus of 13 J proteins (Figure 2.5). This study has termed this motif as the 41aa unknown domain (Figure 2.4). All J proteins containing 41aa motif except PF08_0115, fall in the exported category. This domain was also found in several other *Plasmodium* proteins and the list is provided in (Table 2.2).

Figure 2.6: Alignment of the conserved 41 amino acid motif identified using the Multiple Expectation Maximization for Motif Elicitation (MEME) suite (http://meme.nbcr.net). **A)** Alignment of the J proteins sharing the identified domain. The names of the J proteins are indicated in the first column, the start indicates the start site of the domain in the protein. The *P*-values are also shown. **B)** The consensus amino acid sequence motif highlighting highly conserved residues.

Table 2.2: Comprehensive list of proteins possessing the 41aa unknown domain.

Name	Start	*p*-value	Sites
PFA0675w	1418	7.63e-46	EILRNILKII LCDVETTVRRSAQKVLQNAEGDTNLMLKRAKGLQSLGKMIL QKVN
PFC1075w	237	7.63e-46	EILRNILKII LCDVETTVRRSAQKVLQNAEGDTNLMLKRAKGLQSLGKMIL QKVN
PF11_0026	237	7.63e-46	EILRNILKII LCDVETTVRRSAQKVLQNAEGDTNLMLKRAKGLQSLGKMIL QKVN
PFB0980w	237	7.63e-46	EILRNILKII LCDVETTVRRSAQKVLQNAEGDTNLMLKRAKGLQSLGKMIL QKVN
PFF1520w	237	7.63e-46	EILRNILKII LCDVETTVRRSAQKVLQNAEGDTNLMLKRAKGLQSLGKMIL QKVN
PFF0065c	237	7.63e-46	EILRNILKII LCDVETTVRRSAQKVLQNAEGDTNLMLKRAKGLQSLGKMIL QKVN
PF07_0002	237	6.01e-45	EILRNILKII LCDVETTVRRSAQKVLQNAEGDTNLMLKRAKGLQSLGRMIL QKVN
PFA0070c	229	8.93e-45	EILRNILKII LCDVETTVRRSAQKVLQNAEGDTNLMFKRAKGLQSLGKMIL QKVN
PF10_0388	214	8.93e-45	EILRNILKII LCDVETTVRRSAQKVLQNAEGDTNLMFKRAKGLQSLGKMIL QKVN
PF11_0015	184	6.04e-44	EILRNILKII LCDVETTVRRSAQKVLQNAEGDTNLMFKRAKGLQSLGRMIL QKVN
PBANKA_122420	709	1.39e-37	SIIKNVLSLV LWDVESTTKGVAQKLVRDEGVDINTRLKRAYALKQLGDMML NLSKTEKDLF
PY02866	793	8.94e-37	SIIKNILSLV LWDIESTTKEVAQKLVRDEGVDINVRLKRAYALKQLGEMML NLSKTEKDLF
PKH_011190	685	8.94e-37	IIIKNVLKVV LWDIESTVRKVAEKVLRDEGVSIETRLQRAKALKLLGKIML RLSKTKKDMS
PVX_088225	750	2.97e-36	IIIKNVLKVV LWDIECTVRKVAEKVLRDEGVSIKVRLQRAKALKILGKTML KLSKTKKDMS
PCHAS_122480	725	3.35e-35	SIIKNILSLV LWDIESTTKEVAQKLVRDEGVDINTRLKRAYALKQLGEIMT NLSKTEKDLF
PFL0055c	830	3.75e-35	FMTMHILTLI LWDIEETTQYAASRVLRDEGVDENTRIKRAEALQILGKLMQ KWSLNVKSKK
PF08_0115	586	5.19e-34	VIIKNVLTLV LWDIESTVRQATEKVIRDEDVNIETRLKRAEGMKFLGKLMQ KWSKIKNDKC
MAL8P1.204	883	6.98e-33	SFIIELLTVI LYDIETTVRNASDKFLRDQGVDVYMRLKRAEGMCILGKLMQ KWVKTKKNDQ
PFB0920w	918	1.80e-31	DIICDALRLM LWDIESTVKDVAKRVLRDKAVRKKIRLKRAEAMLILGNLML EISGISGIDF
PF10_0378	833	4.24e-30	DILDDIFTIV LCDIELTVRYAADRVLRDEGCNKEIRLKRAEGIKIVGNLMN KWAKIKKQQM
PF11_0034	508	7.95e-30	TFVKTMTVYF LDIIESIVRVVAETVLYDESDDIKIRLKRARGMKKLGILMQ KVARIRSEQF
PF10_0382	100	7.95e-30	TFVKTMTVYF LDIIESIVRVVAETVLYDESDDIKIRLKRARGMKKLGILMQ KVARIRSEQF
PY03711	434	1.10e-28	TVVETMLNIC LIDIDQTIKGVCKKVFTDMSVDENVRKARAESLIVLAKIMK KVIQEYTKNN
PFB0085c	825	1.83e-28	FMIKNIKNVV QGDIELTIRYAAEKVLFDEGVDKETQLKRVEALEILGNIMK TCSKENKNWE
PF14_0013	446	2.16e-28	ELLKIILNIN LCDIEETIRECAYNVLKDKTVDASVHSKRAHRMNILGSLML ESSNE
PFL2550w	423	2.35e-28	DLLISILYIN VYDIEETVRNIAEVVLRDNDVNVNTRSKRAHRMRLLGSMIL QKINV
PBANKA_123820	457	2.56e-28	TVVETMLNIC LIDIDQTIKGVCKKVFTDMSVDENVRKTRAESLIVLAKIMK KVIQEYTKNN
PCHAS_123860	475	1.35e-27	TVVETMLNIC LIDIDQTIKGVCKKVFTDMSVDESVRKARAESLIVLAKVMK KVIQEYTKNN
PF11_0513	634	8.01e-27	SLMSTIVTLF LSIIEGTVRTSCKMVLVELDVDKDTLFKRAEGMKLLGQKMQ KLAKRKKEKS
PFA0110w	801	1.02e-23	KIVSYIVDIS LYDIENTALNAAEQLLSDNSVDEKTLKKRAQSLKKLSSIME RYAGGKRNDK
PF11_0512	726	1.55e-22	SFVKNLIKIA LSDIEYTIKTVCENILTEKGIDDITIKARAESLNKLGYIIR QNILKGKNIK

2.3.2 The intraerythrocytic *Plasmodial* Hsp70-J protein chaperone machinery

This study was biased towards the intraerythrocytic stage of parasite development; the stage associated with clinical malaria symptoms. Indeed, experimental investigations on the Hsp70-J protein chaperone machinery have mainly focused on the erythrocytic stage of the parasite life cycle. It is expected that various Hsp70-J protein partnerships occur in several cellular compartments present in the parasite and infected erythrocyte (Figure 2.7).

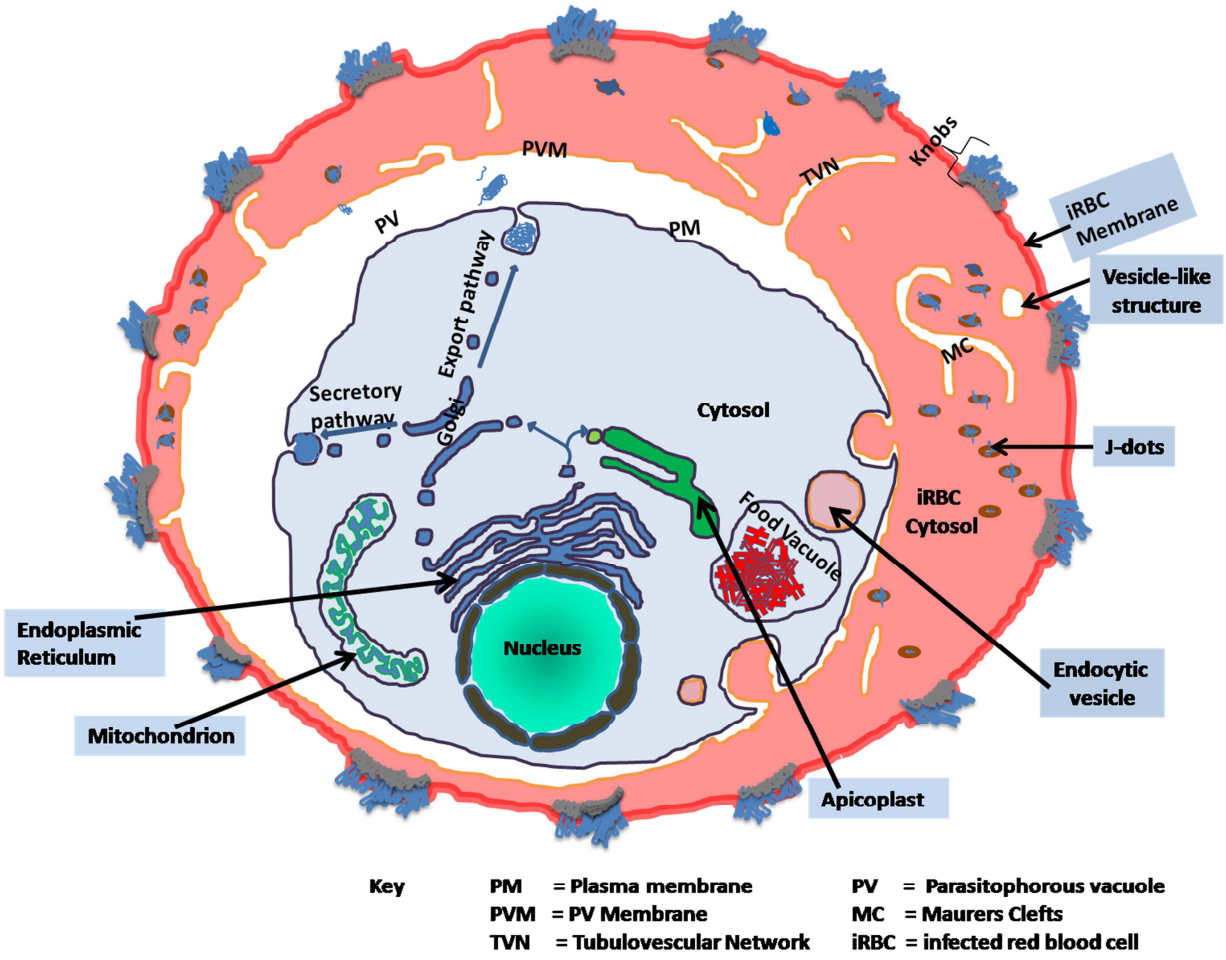

Figure 2.7: A diagrammatic representation of an infected erythrocyte depicting the various compartments and organelles present.

2.3.3 Cytoplasm and Nucleus

PfHsp70-1 is the most studied of the six Hsp70 homologues encoded by the genome of *P. falciparum*. It is highly expressed throughout the *P. falciparum* lifecycle and localizes to the parasite cytoplasm and nucleus (Biswas and Sharma, 1994; Joshi, et al., 1992; Pesce, et al., 2008). It potentially interacts with several cytosolic J proteins (Figure 2.8) in roles that may span protein synthesis, associated protein folding and refolding, protein translocation across membranes, and degradation of terminally misfolded proteins among others (Bell, et al., 2011; Mayer and Bukau, 2005; Meimaridou, et al., 2009). Previously, PfHsp70-1 chaperone activities have been extensively studied using *in vitro* and *in vivo* assays (Matambo, et al., 2004; Shonhai, et al., 2005; Shonhai, et al., 2008). Recently, using a yeast model, PfHsp70-1 was shown to be involved in cytosolic protein homeostasis including protein translocation,

ER-associated protein degradation and also protection from cellular oxidative stress (Bell, et al., 2011). These findings place PfHsp70-1 at the centre-stage of cytosolic proteostasis possibly playing a critical role in parasite survival. PfHsp70-z is predicted to be cytosolic thus potentially playing a role as a NEF for PfHsp70-1 (Shonhai, et al., 2007).

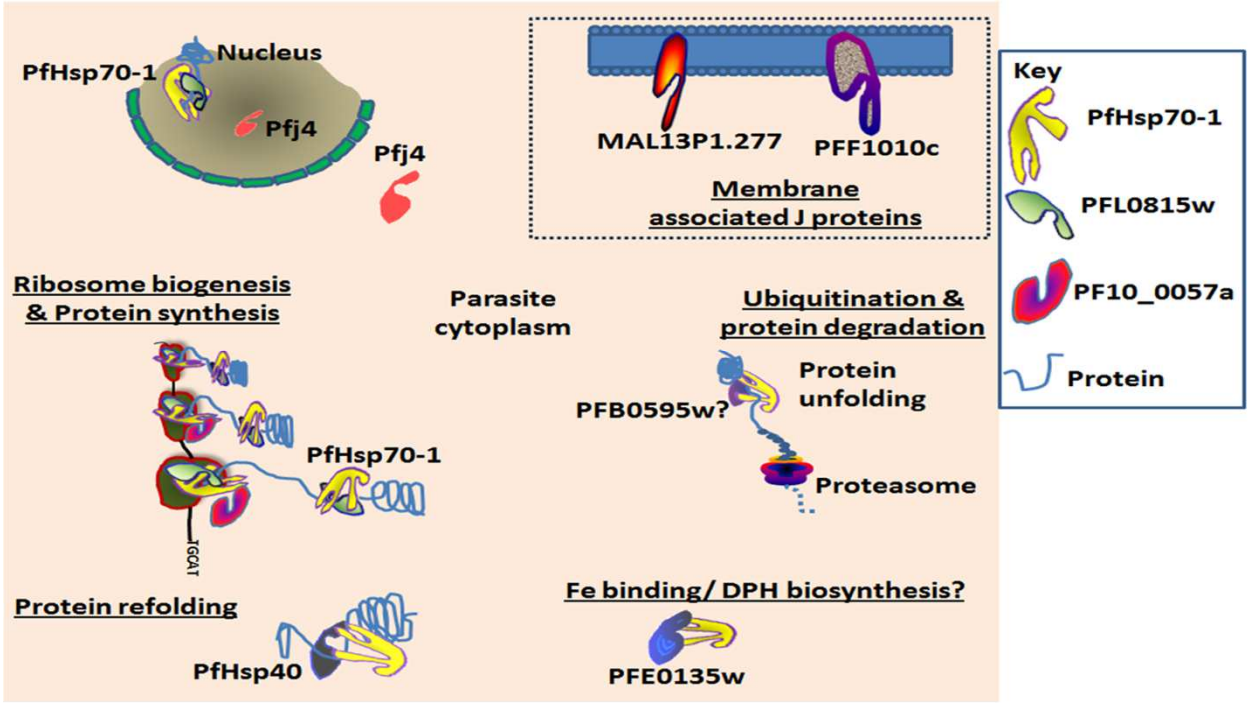

Figure 2.8: The roles of several J proteins in the cytoplasmic and nucleus. Diagrammatic representation of the J proteins predicted to reside in the cytosol and nucleus and their potential interactions with PfHsp70-1. The putative roles like protein synthesis, refolding, and degradation are shown. Intracellular membrane associated J proteins depicted in a dashed box enclosure could recruit PfHsp70-1 to distinct locations within the cytoplasm. A key is provided on the right hand side depicting the different unique drawings not labeled in the diagram.

A great number of J proteins are predicted to be cytosolic even though very few have been experimentally characterized. PF14_0359 (PfHsp40) is homologous to yeast Ydj1, and localizes in the cytosol and, similarly to PfHsp70-1, is upregulated upon heat shock (Botha, et al., 2011). Through in vitro assays, PfHsp40 was also shown to stimulate PfHsp70-1 ATPase activity and cooperatively assist its ability to suppress protein aggregation, indicating a possible functional interaction between the two chaperones (Botha, et al., 2011). Proteomic studies have revealed that both PfHsp70-1 and PfHsp40 are phosphorylated (Wu, et al.,

2009). PfHsp40 contains a C-terminal CAQQ motif which functions in protein isoprenylation (Clarke, 1992; Zhu, et al., 1993), a modification that mediates the association of yeast, Ydj1, and the plant *Atriplex nummularia* Anj1, J proteins, with different intracellular membranes (Caplan, et al., 1992; Zhu, et al., 1993). As Ydj1 has previously been shown to play a role in mitochondrial protein import (Caplan, et al., 1992) and PfHsp70-1 could functionally replace the yeast Hsp70 equivalent, it is tempting to speculate that PfHsp40 could represent the centre-stage for recruiting PfHsp70-1 to membranes for functions such as protein import in the ER (Figure 2.9) and mitochondrion (Figure 2.10).

PFL0565w (Pfj4) localizes to the parasite cytosol and nucleus and its expression is upregulated in response to heat shock (Pesce, et al., 2008; Watanabe, 1997). It has been shown to occur in a common complex with PfHsp70-1 suggesting a possible direct or indirect interaction (Pesce, et al., 2008). In addition, Pfj4 was upregulated in parasites isolated from clinical samples (Pallavi, et al., 2010). While the role of this J protein is not well understood, it has been suggested to be involved in cytoprotection against thermal stress, protein translocation across membranes, DNA replication and repair, and translation initiation (Pesce, et al., 2008). Using in silico analysis and yeast two-hybrid studies, the yeast Sis1p homolog, PFB0595w, has been predicted to interact directly with PfHsp70-1 and other putative proteins including antigen 332 (PF11_0507), myosin-like protein (PFF0675c), PfHsp40, and ubiquitin protein ligase (MAL8P1.23) (Pavithra, et al., 2007). The predicted interaction between MAL8P1.23 and PFB0595w may imply a role for this J protein in protein degradation via the proteasome (Figure 2.8). Whereas there is no functional data on this J protein, the yeast counterpart, Sis1, is required for the initiation of translation (Zhong and Arndt, 1993) and prion propagation (Higurashi, et al., 2008). MAL13P1.277 is another highly conserved J protein across the *Plasmodium* species although its homologue is absent in *P. yoelii*. It lacks a putative signal sequence but has a predicted transmembrane domain and it is likely that it is membrane associated (Figure 2.8).

PFL0815w is a homolog to the yeast Zuo1 J protein and has a predicted DNA binding domain at the C-terminus. It has been shown to be significantly upregulated in *P. falciparum* isolates from malaria patients (Pallavi, et al., 2010). Yeast-two hybrid and expression analyses indicated that PFL0815w was possibly involved in the transcriptional machinery and RNA processing (Figure 2.8) as it was predicted to interact directly or indirectly with several proteins (Pallavi, et al., 2010; Zhou, et al., 2008) including PF14_0230 (Ribosomal protein family L5, putative) (Bischoff and Vaquero, 2010) and MAL13P1.14 an ATP dependent

DEAD box helicase (Zhou, et al., 2008). Zuo1 has been characterized as an RNA-binding and ribosome-associated J protein that interacted with Ssb, a yeast Hsp70 homolog (Pfund, et al., 1998; Yan, et al., 1998). Zuo1 and another J protein, Jjj1, in partnership with Hsp70 have been shown to mediate the biogenesis of ribosomes in yeast (Albanèse, et al., 2010). PF10_0057a is the Jjj1 homolog in *P. falciparum* and possesses two zinc fingers (C2H2) at the C-terminus. Its function is not known but its expression is upregulated in sporozoites. PFE0135w is another J protein and an orthologue of the yeast Jjj3 and the human DnaJC24 (Dph4) J proteins. Jjj3 and Dph4 are specialized J proteins that play a role in the biosynthesis of diphthamide (DPH), a conserved posttranslational modification of translation elongation factor, eEF2 (Liu, et al., 2004; Thakur, et al., 2012). Recent studies have shown that Dph4 performs both J-domain dependent (possible recruitment of partner Hsp70 to specific cytoplasmic sites and stimulation of its ATPase activity) and independent (Fe-binding and oligomerization) cellular functions (Thakur, et al., 2012). It remains to be experimentally validated whether such functional interactions and roles potentially exist in *Plasmodium* species.

2.3.4 Endoplasmic reticulum (ER)

Through co-translational translocation, the ER functions as the site for synthesis and trafficking of secretory and plasma membrane proteins in eukaryotic cells. Newly synthesized proteins cross the ER membrane into the ER lumen where they are folded, assembled and posttranslationally modified to acquire a functional conformation (Kleizen and Braakman, 2004). However, as an ER quality control measure, terminally misfolded proteins are retrotranslocated from the ER into the cytosol for degradation via the ubiquitin-proteasome system through a process known as ER-associated degradation (ERAD) (Ellgaard and Helenius, 2003).

Processes carried out by the ER including protein synthesis, associated trafficking and degradation are carried out with the help of ER-resident molecular chaperones. BiP (immunoglobulin heavy chain binding protein) is an ER resident Hsp70 that cooperates with different ER J proteins in protein translocation, productive folding, and degradation of proteins through ER-associated degradation (ERAD) (Ellgaard and Helenius, 2003). There are two *P. falciparum* Hsp70 homologues that localize to the ER: PFI0875w (PfHsp70-2/

PfBiP) and MAL13P1.540 (PfHsp70-y) (Külzer, et al., 2009; Kumar, et al., 1991; Kumar, et al., 1988; Van Dooren, et al., 2005).

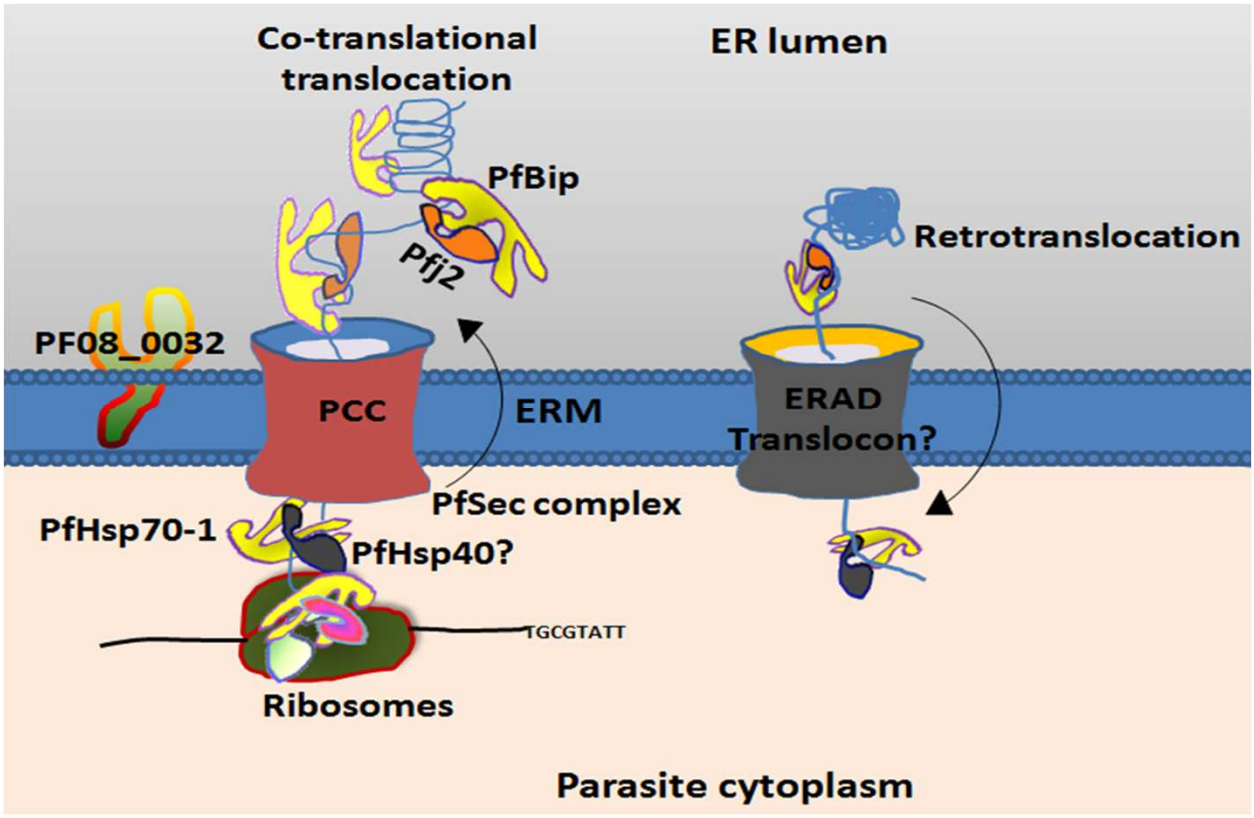

Figure 2.9: Protein co-translational translocation and retro-translocation between the cytoplasm and the ER. A diagram representing the co-translation translocation of proteins resident-in and trafficked-through the endoplasmic reticulum and the associated retrotranslocation of proteins targeted for degradation. PfHsp70-1 potentially interacts with J proteins like PfHsp40 and assists in the co-translational translocation of proteins to the ER through the protein conducting channel (PCC) embedded in the ER membrane (ERM). PfBip and Pfj2 potentially associate with the translocon on the ER lumen where they capture and pull translocating polypeptides and refold them. As an ER quality control mechanism, terminally misfolded proteins are retrotranslocated from the ER through an ER-associated degradation (ERAD) translocon to the cytosol with the help of both ER and cytosolic chaperones.

The passage of nascent polypeptide chains through the ER is mediated by a highly conserved protein conducting channel (PCC) (Simon and Blobel, 1991) (Figure 2.9). Several components of the protein translocation machinery have been identified in *P. falciparum* and an ER protein translocation model has been suggested (Tuteja, 2007). Similar to other eukaryotes, the *P. falciparum* PCC is composed of various proteins of which the PfSec

protein complex translocon is a major component (Tuteja, 2007). PfSec is a heteromeric protein complex comprising Sec61 (Sec61α; Mal13P1.231, Sec61β; Mal8P1.51, Sec61γ; PFB0450w), Sec62; (PF14_0361), and Sec63; (PF13_0102). PfSec63 is a conserved J protein across the *Plasmodium* species and other eukaryotic cellular systems. It has three predicted transmembrane domains and potentially interacts with PfBiP during the translocation of polypeptide chains across the ER membrane translocon (Tuteja, 2007).

PF11_0099 (Pfj2) and PF08_0032 are predicted ER resident J proteins, which contain a putative N-terminal signal sequence. Pfj2 additionally bears a possibly non-functional putative PEXEL motif that lies adjacent to the HPD motif of its J-domain and a C-terminal DDEL ER retention signal. PF08_0032 has an extended N-terminus before the J-domain that contains a predicted transmembrane domain downstream of the signal sequence indicating that it may be membrane bound (Figure 2.9). Both Pfj2 and PF08_0032 are predicted to have a thioredoxin domain whereby this domain is characterized by a -CHSC- motif present after the G/F rich region in Pfj2 that is similarly present in ERdj5, a human ER resident J protein. ERdj5, however, contains four thioredoxin-like domains and functions as a co-chaperone of BiP (Braakman and Otsu, 2008; Cunnea, et al., 2003; Hosoda, et al., 2003; Ushioda, et al., 2008). ERdj5 was shown to have disulfide bond reductase activity, and accelerated ERAD through its functional interactions with EDEM (ER degradation–enhancing alpha-mannosidase–like protein) and BiP. Both Pfj2 and PF08_0032 may interact with PfBiP and fulfill general ER protein folding, refolding, and ERAD (Figure 2.9). Experimental verification of the localization of these J proteins, their potential interactions with PfBiP, and possible roles are yet to be elucidated.

2.3.5 Mitochondrion

In eukaryotes, the mitochondrion is an essential organelle that houses a number of biochemical pathways including iron metabolism and oxidative phosphorylation (Hatefi, 1985). The structure of the *Plasmodium* mitochondrion consists of outer and inner membranes and two aqueous compartments of the intermembrane space (IMS) and the matrix (Rudzinska, 1969). The erythrocytic stage of *Plasmodium* displays a remodeled mitochondrial carbon and energy metabolism with down-regulation of mitochondrial enzymes and relies almost entirely on glycolysis (Mogi and Kita, 2010; Olszewski, et al.,

2010; van Dooren, et al., 2006). Since the ~6 kb mitochondrial genome has reportedly only three protein-coding genes (Feagin, 2000), the majority of the mitochondrial proteins are nuclear-encoded and synthesized by cytosolic ribosomes. Mitochondrial precursor proteins are delivered to the organelle by virtue of a specific targeting N-terminal leader presequence (Neupert, 1997; Pfanner and Geissler, 2001) or through other mechanisms (van Dooren, et al., 2006). A *P. falciparum* mitochondrial protein translocation model has previously been constructed based on homologues of well studied eukaryotic models (van Dooren, et al., 2006) (Figure 2.10).

Chaperones resident in the mitochondrial matrix assist in protein translocation across the mitochondrial membrane, their refolding, and assembly (Mayer and Bukau, 2005; Neupert and Brunner, 2002). They additionally help in protein sorting, removal of signal sequences, and degradation. The mitochondrial Hsp70-J protein chaperone machinery may therefore be involved in protein translocation to the mitochondria and assistance in their refolding (Figure 2.10). The *P. falciparum* mitochondrial matrix Hsp70 (PF11_0351/PfHsp70-3) and its putative co-chaperones such as Tim44 (PF11_0265), GrpE (PF11_0258) and PfPam18 (PF07_0103) provides the machinery required for the import of proteins into the matrix. In yeast, the mtHsp70 Ssc1 binds to short hydrophobic segments of the incoming polypeptide chains and is tethered to the protein import channel by the peripherally associated membrane protein Tim44, where it undergoes a regulated recycling at the protein import channel (Liu, et al., 2003). Unlike yeast which has two J proteins (Pam18/ Tim 14 and Mdj2) associated with the protein import motor on the mitochondrial matrix, *P. falciparum* appears to possess one; PF07_0103. This membrane associated J protein potentially cooperates with PfHsp70-3 during the import process.

Upon successful translocation, the leader peptide is cleaved by a mitochondrial processing peptidase (van Dooren, et al., 2002). A subset of imported proteins requires additional assistance by mitochondrial chaperonins Hsp60 (PF10_0153) and Hsp10 (PFL0740c/ Cpn10) (Sato and Wilson, 2005) (Figure 2.10). Indeed, PfHsp70-3 may interact with GrpE, Hsp60, Clpβ (PF08_0063), PFF1415c; a J protein, among other proteins as predicted using the STRING protein interaction network resource (http://string-db.org/) (Szklarczyk, et al., 2011). In yeast, Mdj1, a mitochondrion matrix J protein, primarily assists the mtHsp70 functions in protein folding, stress protection and degradation thereby modulating its substrate protein spectrum (Martin, 1997; Walsh, et al., 2004). In *P. falciparum*, PFD0462w (Pfj1), has previously been predicted to possess a mitochondrion import signal and therefore

thought to reside in the mitochondrion matrix (Watanabe, 1997). However, this has not been experimentally validated. JacI, is another yeast J protein that resides in the mitochondria matrix and is involved in the assembly of Fe/S clusters in proteins and iron metabolism (Craig and Marszalek, 2002; Voisine, et al., 2001). PFI0985c is proposed to be the JacI homolog in *P. falciparum* predicted to reside in the mitochondrion matrix (Figure 2.10). However, it has to be noted that the Fe/S cluster biogenesis has also been proposed to occur in the apicoplast (Kumar, et al., 2011; Seeber, 2002). The functional J partner(s) of PfHsp70-3 in the mitochondrion of *P. falciparum* remains to be experimentally elucidated.

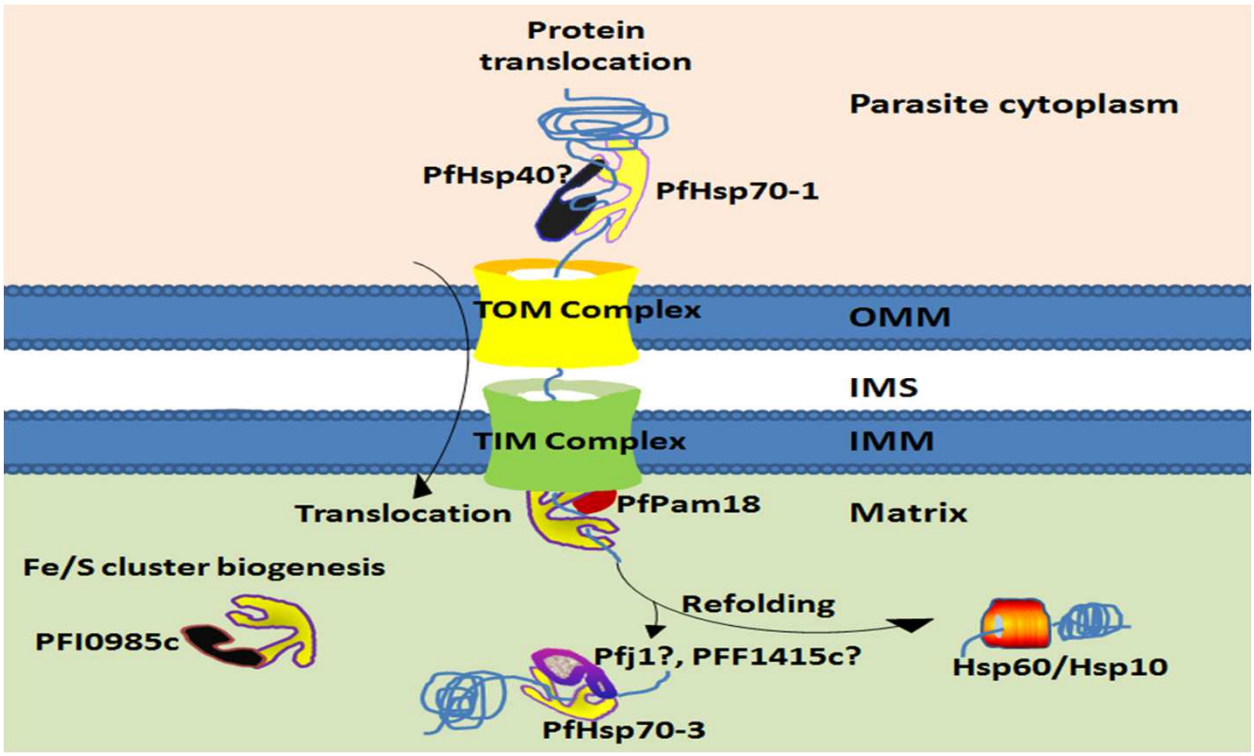

Figure 2.10: Protein import and refolding in the mitochondrion. Upon synthesis, mitochondrial preproteins are directed to the organelle by topogenic signals. The signals are recognized by receptors on the outer mitochondrial membrane (OMM) and unfolded possibly by the cytosolic Hsp70-J protein system then presented to the general import pore; a constituent of the translocase of the outer membrane (TOM) complex. The preproteins are then translocated from the TOM complex through the intermembrane space (IMS) into the translocase of the inner membrane (TIM) complex which is embedded in the inner mitochondrial membrane (IMM). PfHsp70-3 assists in the general protein import into the matrix in association with PfPam18 and refolding with mitochondrial resident J proteins. Protein refolding is also carried out by the Hsp60/Hsp10 chaperone complex.

2.3.6 Apicoplast

The apicoplast is a non-photosynthetic organelle and is evolutionarily homologous to the plant plastid that is found in most members of the phylum *Apicomplexa* (McFadden, et al., 1996). It is surrounded by four membranes (Kohler, et al., 1997) and provides essential functions to the parasite including heme biosynthesis, type II fatty acid biosynthesis, and deoxyxylulose-5-phosphate pathway for isoprenoid metabolism (Gardner, et al., 2002; Lim and McFadden, 2010; Ralph, et al., 2004). It is therefore indispensable (Dahl, et al., 2006; Fichera and Roos, 1997) and represents a validated anti-malarial drug target (Wiesner and Seeber, 2005). Different models have been suggested to explain how nuclear encoded apicoplast targeted (NEAT) proteins reach the apicoplast outer membrane, traffic through the four membranes, and enter the lumen of the apicoplast (Felsner, et al., 2011; Foth, et al., 2003; Karnataki, et al., 2007; Parsons, et al., 2007; Tonkin, et al., 2008; Waller and McFadden, 2005; Waller, et al., 2000) (Figure 2.11). Initial experiments showed that luminal apicoplast protein targeting is a two step process mediated by a bipartite N-terminal presequence that consists of a signal peptide for entry into the secretory pathway and a transit peptide for subsequent import into the apicoplast (Ralph, et al., 2004; Waller, et al., 1998; Waller, et al., 2000). This, however, may not be the case for the outer apicoplast membrane proteins (Karnataki, et al., 2007).

The involvement and possible role of Hsp70 chaperones in protein trafficking to the apicoplast has generated debate (Blatch and Przyborski, 2011; Misra and Ramachandran, 2010; Ramachandran, 2011). Previously, it has been suggested that enrichment of Hsp70 putative binding sites is an important feature of *P. falciparum* transit peptides (Foth, et al., 2003; Rudiger, et al., 1997). Of the six *P. falciparum* Hsp70 homologues, none have been experimentally detected or predicted to carry the apicoplast targeting signals. The correct folding, refolding and assembly of luminal apicoplast proteins mainly depends on the type I chaperonin system with Cpn60 and its co-chaperonin Cpn20 as its major components (Sato and Wilson, 2005; Sato and Wilson, 2004) (Figure 2.11). Pfj1 and PFF1415c are the only two J proteins that have been predicted to be targeted to the apicoplast. Recent experimental data suggested that Pfj1 localizes in the apicoplast (Kumar, et al., 2010) which contrasts with a previous mitochondrial prediction (Watanabe, 1997). Pfj1 has an elongated C-terminal domain that lacks any significant homology with known proteins. Kumar and coworker's proposed that Pfj1 is a DNA-binding protein capable of binding the apicoplast DNA origin of

replication sites thus fulfilling a role in DNA replication (Kumar, et al., 2010). Whether there is a Hsp70-J protein machinery in the apicoplast remains to be experimentally elucidated, especially in the light of an Fe/S cluster biogenesis (Kumar, et al., 2011) in this organelle.

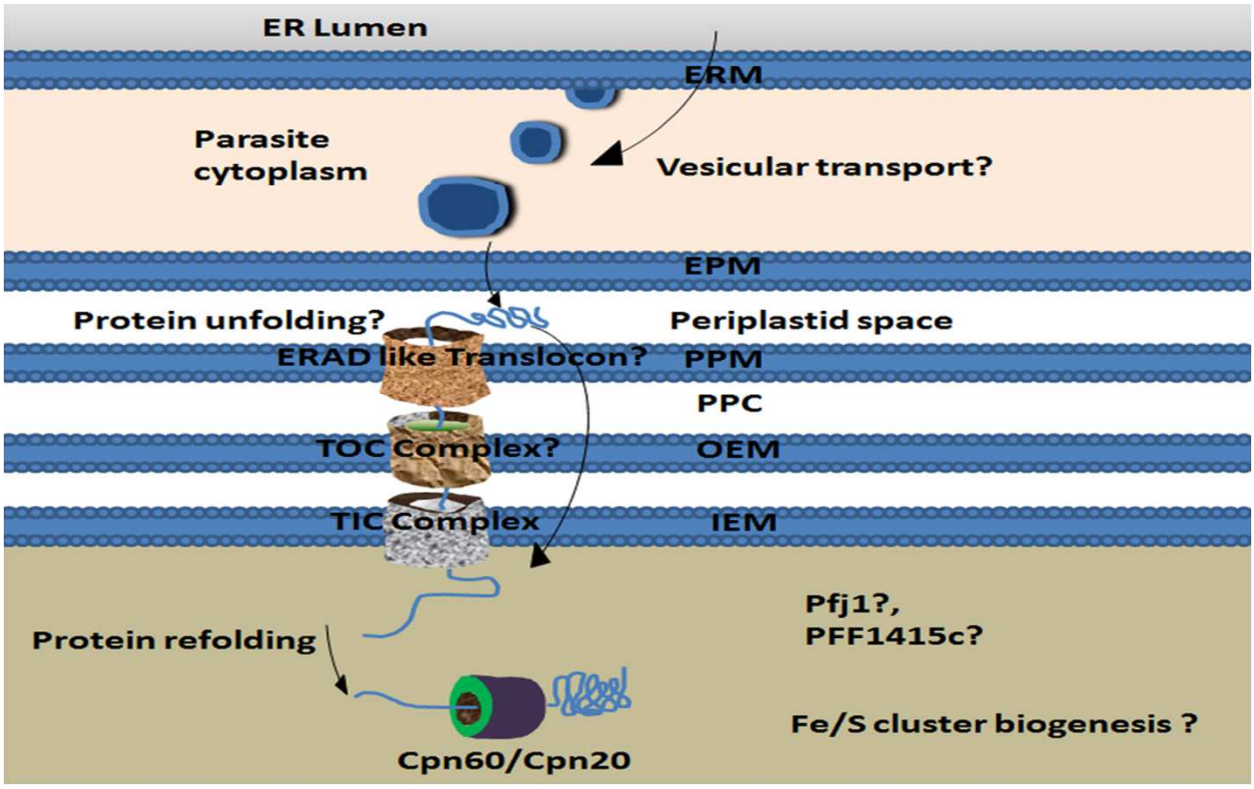

Figure 2.11: Protein import and refolding in the apicoplast. Proteins targeted to the apicoplast lumen usually possess an N-terminal topogenic signal comprised of signal peptide and a transit peptide (Lang, et al., 1998; Waller, et al., 2000). The signal peptide is responsible for cotranslational import into the ER lumen. Here, the signal peptide is cleaved off exposing the transit peptide that helps distinguish apicoplast proteins from secretory proteins. The proteins are then packaged into vesicles (van Dooren, et al., 2001) that bud from the ER membrane (ERM) and are delivered to the epiplastid membranes (EPM) also referred to as the outer plastid membrane. Following fusion of apicoplast targeted vesicles with the EPM, the proteins are delivered in the periplastid space where they are possibly unfolded and fed into an ERAD-like (ER-associated degradation) translocon (Sommer, et al., 2007; Spork, et al., 2009) located in the periplastid membrane (PPM). The transit peptide dictates translocation into the three inner membranes and is cleaved upon protein entry into the apicoplast lumen. Transport of proteins from the periplastid compartment (PPC) to the apicoplast lumen is most likely mediated by translocators similar to those found in chloroplast (Gould, et al., 2008). These comprise the translocator of the outer chloroplast membrane (TOC) and translocator of the inner chloroplast membranes (TIC) complexes localized in the outer envelope membrane (OEM) and the inner envelope membrane (IEM) respectively. Upon translocation, proteins are most likely refolded by the Cpn60/Cpn20 cochaperonin system.

2.3.7 Parasitophorous vacuole

Upon entry into erythrocytes, the parasite establishes itself within the parasitophorous vacuole (PV) surrounded by the PV membrane (PVM) that provides a biochemically permissive barrier between the parasite and the infected erythrocyte cytoplasm. It represents an avenue for trafficking of parasite proteins to the erythrocyte compartment. Alternative models have been suggested on how exported proteins, following entry into the classical ER secretory pathway, reach the PV compartment (Boddey, et al., 2009; Crabb, et al., 2010) (Figure 2.12). Proteins involved in infected erythrocyte remodelling traffic through PEXEL and non-PEXEL mediated export mechanisms that are conserved across the *Plasmodium* species (Hiller, et al., 2004; Sargeant, et al., 2006; Spielmann and Gilberger, 2010; van Ooij, et al., 2008). The exported proteins that lack a PEXEL motif are referred to as the PEXEL-negative exported proteins (PNEPs) (Spielmann and Gilberger, 2010). A model to explain how soluble and non-soluble PEXEL-containing proteins travel from the PV compartment to the erythrocyte cytoplasm has been developed following the discovery of the *Plasmodium* translocon of exported proteins (PTEX) that localizes at discrete foci in the PVM (de Koning-Ward, et al., 2009; Haase and de Koning-Ward, 2010). Whereas little is known about the roles of the highly abundant chaperones identified in the PV (Nyalwidhe and Lingelbach, 2006), it has been suggested that they maintain proteins en route to the infected erythrocyte in a translocation competent form. PfHsp101 (PF11_0175) is a ClpA/B-like ATPase from the AAA1 superfamily that was shown to be a core component of the PTEX translocon (de Koning-Ward, et al., 2009). PfHsp101 is thought to be responsible for unfolding of proteins destined for export, a requirement for exported proteins (Gehde, et al., 2009), and feeding them into the translocation pore (de Koning-Ward, et al., 2009). It is speculated that a human Hsp70 on the erythrocyte cytosol assists in the translocation and refolding of the exported proteins (de Koning-Ward, et al., 2009).

2.3.8 Infected erythrocyte cytosol

Mature erythrocytes are optimally adapted for oxygen and carbon dioxide transport and lack protein synthesis and trafficking machinery as well as most organelles. Using proteomic approaches, Hsps have been shown to be part of the erythrocyte proteome (Roux-Dalvai, et al., 2008) among them are the Hsp70s and the J proteins (Table 2.3). The Hsp70-J protein

machinery has been suggested to be part of several pathways including protein synthesis, folding, post-translational modification, as well as protein transport, metabolism, and erythrocyte cell death (D'Alessandro, et al., 2009). Whereas these functions fall well within the roles of chaperones, it is debatable whether all the identified Hsp70s and J proteins are all genuine components of mature erythrocytes or some are incompletely degraded during maturation of reticulocytes. Indeed, it has been suggested that some proteins that are not essential or may not be functional in the mature erythrocytes are not degraded due to energy costs (Roux-Dalvai, et al., 2008). HSPA1A, commonly referred to as host-Hsp70 (HsHsp70), is among the Hsp70 homologues present in the erythrocyte cytosol that is easily detected in both infected and uninfected erythrocytes (Banumathy, et al., 2002). It bears a C-terminal EEVD motif but lacks the GGMP repeats that are present in PfHsp70-1 (Banumathy, et al., 2002).

Table 2.3: The Hsp70 and the Hsp40 complement in mature uninfected erythrocytes. The names, molecular mass (Mm) in Daltons, and the Isoelectric points (pI) are listed.

Description	Mm	pI
Hsp70 family		
HSPA8 Isoform 1 of Heat shock cognate 71 kDa protein	71082.31	5.37
HSPB1 Heat shock protein beta-1	22825.51	5.98
HSPA1B;HSPA1A Heat shock 70 kDa protein 1	70294.14	5.48
HSPA4 Heat shock 70 kDa protein 4	95095.61	5.18
HSPBP1 Isoform 1 of Hsp70-binding protein 1	40189.83	5.13
HSPA1L Heat shock 70 kDa protein 1L	70730.47	5.76
HSPA6 Heat shock 70 kDa protein 6	71440.4	5.81
HSPA14 Heat shock 70 kDa protein 14	55444.31	5.41
HSPA2 Heat shock-related 70 kDa protein 2	70262.97	5.56
HSPH1 Isoform Beta of Heat shock protein 105 kDa	92969.79	5.42
J-protein family		
DNAJB2 Isoform 3 of DnaJ homolog subfamily B member 2	35672.45	5.69
DNAJA2 DnaJ homolog subfamily A member 2	46343.83	6.06
DNAJC9;MRPS16 DnaJ homolog subfamily C member 9	30062.16	5.58
DNAJB1 DnaJ homolog subfamily B member 1	38191.43	8.74
DNAJC17 DnaJ homolog subfamily C member 17	34780.18	8.61
DNAJB4 DnaJ homolog subfamily B member 4	38011.22	8.65
DNAJC8 DnaJ homolog subfamily C member 8	29823.42	9.04
DNAJC13 DnaJ homolog subfamily C member 13	256538.2	6.28
DNAJB6 Isoform A of DnaJ homolog subfamily B member 6	36121.89	9.17
DNAJA4 Putative uncharacterized protein DKFZp686G2074	48616.73	7.88
ZRF1 Isoform 2 of DnaJ homolog subfamily C member 2	66115.75	9.08

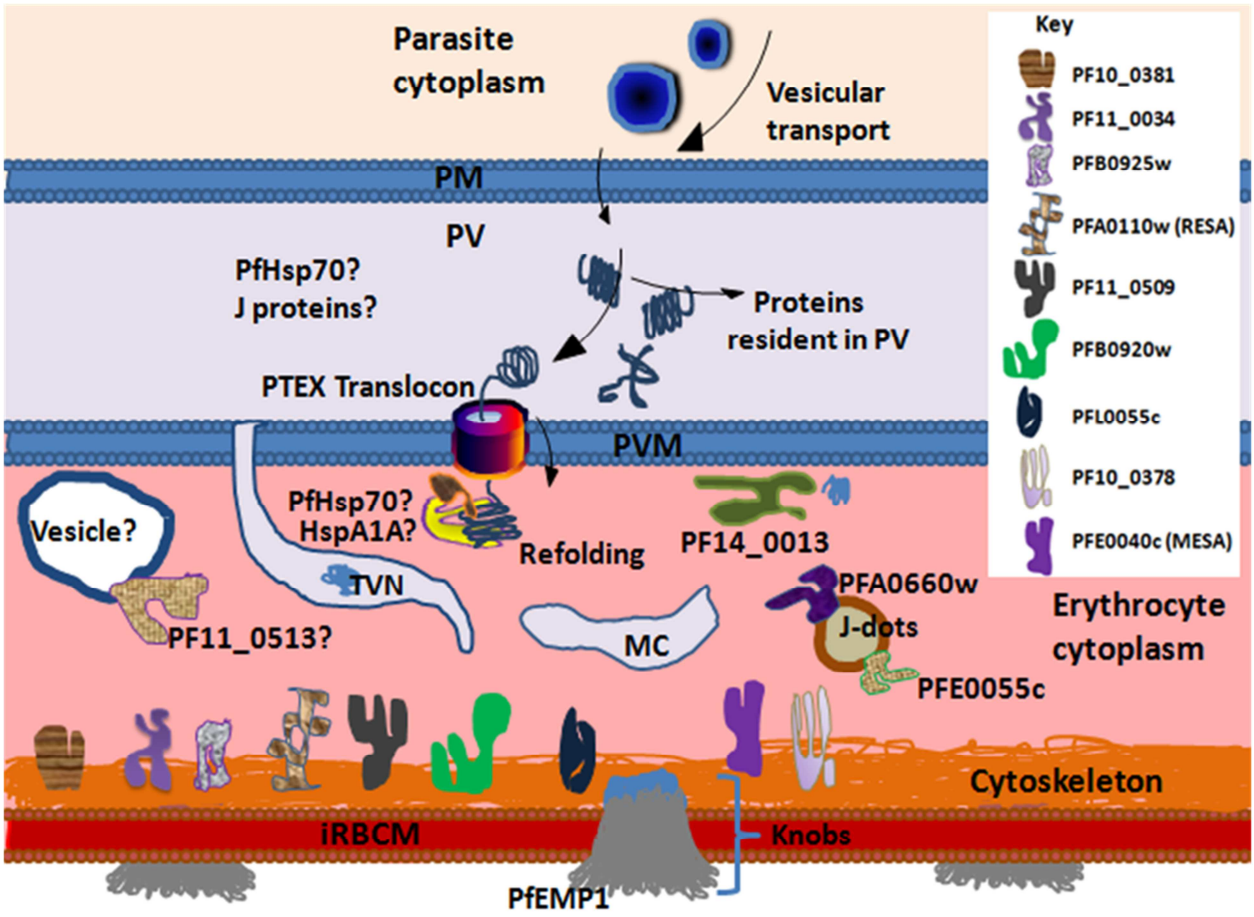

Figure 2.12: A diagrammatic representation of the structural components and protein trafficking machinery from parasite's cytoplasm to infected erythrocyte compartment. Proteins destined for export and secretion into the parasitophorous vacuole (PV) reach the parasite plasma membrane (PM) through vesicles. These vesicles fuse with the PM and release their contents into the PV. Here, a hypothetical chaperone machinery potentially exists that may assist in general proteostasis in the PV and may include Hsp70 and J proteins. Export proteins are then unfolded and fed into the translocon of exported proteins (PTEX) (de Koning-Ward, et al., 2009). Upon translocation into the erythrocyte cytosol, exported proteins are refolded and those destined for the membrane like PfEMP1 are shuttled through vesicles and maurer's clefts (MC) to the infected erythrocyte membrane (iRBCM). Several of the exported J proteins are potentially associated with vesicles, J-dots, MC, and the erythrocyte cytoskeleton. The refolding and transport process inside the infected erythrocyte cytosol involves interaction of several of the exported and host J proteins with host Hsp70s or potentially, an exported Hsp70. A key is provided depicting the different drawings not labeled within the diagram.

Following its entry into the uninfected erythrocyte, the parasite modifies the erythrocyte cytoplasm by generating various membranous structures including the tubulovescular network (TVN) (Elmendorf and Haldar, 1994), Maurer's clefts (MC) (Przyborski, et al., 2003; Tilley, et al., 2008), mobile vesicles (Hanssen, et al., 2010; Hibbs and Saul, 1994) and

J-dots (Külzer, et al., 2010) (Figure 2.12). Additionally, the surface of the plasma membrane of infected erythrocytes is characterized by parasite induced knobs comprising protein complexes of the knob associated histidine-rich protein (KAHRP) (Crabb, et al., 1997). The knobs anchor the antigenically diverse *P. falciparum* erythrocyte membrane protein (PfEMP1) (Leech, et al., 1984) to the erythrocyte cytoskeleton. The PfEMP1 protein family is responsible for the adherence of these parasitized erythrocytes to other erythrocytes and to the vascular endothelium (Baruch, et al., 1995; Su, et al., 1995) hence preventing splenic clearance (Miller, et al., 2002).

The biochemical characteristics of host Hsps in the erythrocyte cytosol and their distribution is significantly altered upon parasite entry (Banumathy, et al., 2002). Banumathy and co-workers observed that upon infection, host chaperones are recruited into membrane-bound, detergent-resistant complexes in infected cells unlike their soluble nature in normal uninfected erythrocytes (Banumathy, et al., 2002). The export of J proteins and PfHsp70-x (Külzer, et al., 2012) to the infected erythrocyte compartment expands the Hsp70-J protein partnerships inside the infected erythrocyte cytosol. PfHsp70-x is exported by the parasite through non-PEXEL mediated mechanisms to the erythrocyte cytoplasm compartment. The localization of PfHsp70-x in the PV and also in the infected erythrocyte cytoplasm allowed for the revision of the previous model. Previously it has been suggested that exported J proteins potentially associate with erythrocyte resident human Hsp70 and together the two chaperones regulate translocation and refolding of parasite exported proteins once they have crossed the PVM. However, the question of whether exported J proteins interact with erythrocyte Hsp70s is still speculation. Previously, it has been demonstrated that alteration of the signature HPD motif in J-domains abolishes Hsp70-J protein interaction thereby suggesting that the exported J proteins with this alteration would not interact with Hsp70s in a canonical manner (Botha, et al., 2007).

A significant number of the exported J proteins have a relatively high expression at both the merozoite and ring stages of parasite development including PFE0055c, PFB0090c, PFB0920w, PF11_0509, RESA, PFB0085c, PF11_0513, and PF14_0013. This timely expression appears to be in tandem with the need to establish trafficking machinery upon entry into the “new home”. Apart from playing a role in translocation of exported proteins, exported J proteins are important for the creation of parasite-derived structures in the cytoplasm of infected erythrocytes and remodelling of infected erythrocyte surface: processes considered essential for parasite virulence and survival. Two exported J-proteins, namely;

PFE0055c and PFA0660w, were found to be tightly associated with J-dots in a manner dependent on cholesterol (Külzer, et al., 2010). These J proteins potentially play a role in the loading and transport of exported proteins including PfEMP1 in these vesicle-like structures that were also shown to be highly mobile (Külzer, et al., 2010). Indeed, a role for cholesterol rich domains in the delivery of PfEMP1 to the infected erythrocyte surface has been previously reported (Frankland, et al., 2006). Recent experiments have observed that PFB0090c, another exported J protein, co-localized with KAHRP, PfEMP1 and PfEMP3 and suggested its potential involvement in chaperoning knob assembly (Acharya, et al., 2012). The crucial role played by certain exported J proteins in the architecture modulation of infected erythrocytes was recently observed through loss-of-function mutant studies (Maier, et al., 2008). Of interest in Maier and coworker's experiments was the finding that exported proteins are required to modify the physical properties of infected erythrocytes, in particular, the correct assembly of knobs and trafficking of PfEMP1 to the infected erythrocyte surface. They also observed that while the expression of 11 exported J proteins could be disrupted, *P. falciparum* knock out mutants of three other exported J proteins (PFA0660w, PF11_0034, and PF11_0509) were not viable suggesting that these three proteins may play essential roles. Furthermore, their analysis revealed that PF10_0381 is important for correct surface presentation of PfEMP1 and assembly of knobs at the infected erythrocyte surface.

RESA localizes to the erythrocyte membrane and binds to the repeat 16 of β-spectrin via a 48 residue long region and thereby stabilizes spectrin tetramers and thus increasing cytoskeleton and overall thermal stability of infected erythrocyte membranes (Da Silva, et al., 1994; Foley, et al., 1994; Pei, et al., 2007; Silva, et al., 2005). While targeted gene disruption of RESA resulted in a significant reduction in membrane rigidity of infected erythrocytes, the disruption of PFB0920w, caused a significant increase in membrane rigidity (Maier, et al., 2008). This indicates that certain exported J proteins are essential in determining the overall membrane architecture of infected erythrocytes. PFE0055c, PF14_0013, RESA, and RESA like J proteins have been found to be expressed in clinical isolates (Acharya, et al., 2009; Pallavi, et al., 2010) and additionally RESA expression is upregulated in placental parasites (Tuikue Ndam, et al., 2008). MESA is a 250 to 300 kDa phosphoprotein produced in the early trophozoite stage and is associated with the infected erythrocyte cytoskeleton (Coppel, et al., 1986; Coppel, et al., 1988). It colocalizes with parasite induced knobs but is not required for knob formation and cytoadherence (Petersen, et al., 1989). Mapping studies have shown that MESA associates with the erythrocyte cytoskeleton by binding to the

phosphorylated form of protein 4.1 (4.1 R; band 4.1; EPB41), a host protein that helps in regulating the erythrocyte membrane mechanical properties (Lustigman, et al., 1990). Prevention of MESA interaction with protein 4.1 has been shown to cause cytoplasmic accumulation leading to parasite death (Magowan, et al., 1995). MESA binds to protein 4.1 through the MEC domain present near its N-terminus (Bennett, et al., 1997; Kilili and LaCount, 2011). MESA has been recently shown to be preferentially upregulated in *P. falciparum* field isolates infecting children and pregnant women and may therefore play an important role in childhood malaria pathogenesis (Vignali, et al., 2011).

Apart from RESA and MESA, several other MEC domain containing J proteins may be anchored or associated with the erythrocyte cytoskeleton or membranes possibly playing additional specialized structural roles (Figure 2.12). Indeed, some J proteins are tightly bound to detergent resistant membranes in the erythrocyte cytosol implying that transmembrane domains may not be essential for membrane association as most of the exported ones do not possess any (Figure 2.5). Six MEC domain containing J proteins have a PRESAN domain that has previously been predicted to form a compact α-helical bundle (Oakley, et al., 2007). The PRESAN and the MEC domains which are located adjacent to each other on the N-terminus may provide the platform for association with the erythrocyte cytoskeleton. Adjacent to these two domains is the J-domain and the 41 kDa unknown domain which has a significant number of charged residues. It has been suggested that less conserved charged regions which lie mostly at the C-terminus of these J proteins comprise the exposed surface that may play a role in protein-protein interactions (Oakley, et al., 2007). It appears therefore that these J proteins localize to various foci at the cytoskeleton and at the parasite induced structures and they serve to recruit potential Hsp70 partner(s) for folding and transport of exported proteins to their destinations (Figure 2.12). They may additionally play a critical role in maintaining the infected erythrocyte cytoskeleton during heat stress.

Experimental studies on J proteins in *P. falciparum* have mostly focused on the intraerythrocytic (ring, trophozoite, and schizont) stages of parasite development. However, while certain J proteins will be expressed at all stages of parasite development, others may be stage specific or highly expressed at a particular stage. For example, PFL2550w (PfGECO; *P. falciparum* gametocyte erythrocyte cytosolic protein) is an exported gametocyte-specific J protein localized in the erythrocyte cytoplasm (Morahan, et al., 2011). Morahan and colleagues observed through gene disruption that PfGECO is not essential for both gametocytogenesis and targeting of other exported gametocyte proteins to the infected

erythrocyte (Morahan, et al., 2011). Other examples of highly expressed J proteins at the gametocyte stage include PF14_0213, PFF1010c, and PF13_0036 (Le Roch, et al., 2003). Overall, the parasite Hsp70-J protein machinery is essential for development of the parasite in both the host and the vector and that certain J proteins may have specialised roles at specific stages.

2.4 Conclusion

The comparative side-by-side analysis of the Hsp70s and J proteins of *Plasmodium* species infecting rodents and primates has served to highlight certain key features of the *P. falciparum* chaperone system. *P. falciparum* has an expanded and diverse J protein complement and an Hsp70 isoform that is not encoded on the genome of the other *Plasmodium* species (PfHsp70-x). The recent observation that PfHsp70-x is *laverania* sub-genus (sub-genus comprising *P. falciparum* and its sister species *P. reichenowi*) specific, is exported, and associates with exported J proteins prioritizes it for further studies on its role in protein export (Duval, et al., 2010; Külzer, et al., 2012). The biased localization of exported J proteins at the subtelomeric regions of chromosomes and the possession of unique domains raises questions about their potential roles and interactions with Hsp70s following export. Indeed, the exported J proteins appear to be better drug targets based on their uniqueness and the lack of human homologues. Overall, efforts geared towards the identification and validation of potential drug targets will require elucidation of the *Plasmodium* Hsp70-J protein chaperone partnerships and a detailed characterization of their structure and biological function. Additionally, investigations into the roles that this chaperone machinery plays in other lifecycle stages including the liver and mosquito stage of the parasite development will provide better insights into the role of this chaperone machinery. Further, the observed PEXEL containing J proteins in the other *Plasmodium* species relative to *P. falciparum* and the lack of an exported Hsp70 homologue raises questions related to the chaperoning of exported proteins in this species.

CHAPTER THREE

Cell biological and biochemical characterization of Pfj1

3.0 Introduction

The genome of *P. falciparum* encodes a large complement of J proteins, two of which have been classified as type I (Botha, et al., 2007). Of these, PfHsp40 is the canonical type I that was recently shown to reside in the cytosol and was proposed to be a cochaperone for PfHsp70-1 (Botha, et al., 2011). Pfj1, on the other hand, is considered atypical since it possesses an extended C-terminal domain that is not similar to other canonical homologues found in this class in other organisms including humans. The uniqueness of Pfj1 makes it a potential drug target. It also has an extended N-terminal region before the J-domain that is considered a signal sequence implying that Pfj1 may not reside in the cytosol. This J protein was recently shown to localize to the apicoplast thereby raising questions regarding its roles and interacting partners (Kumar, et al., 2010). Kumar and coworkers proposed Pfj1 to be a DNA-interacting protein that plays a role in the replication of the apicoplast genome and has very few if any chaperone roles in this organelle (Kumar, et al., 2010). Their experiments further proposed that Pfj1 is synthesized as a 160 kDa preprotein that is processed to a mature 69 kDa protein that was detected through western analysis, thereby suggesting that the current annotated gene model for Pfj1 in PlasmoDB is incorrect (Kumar, et al., 2010). However, as discussed in sections 2.3.5 and 2.3.6 of chapter two, the localization of Pfj1 is controversial and forms the basis of the study detailed in this chapter. The validation of its localization would pave way for further cell biological and biochemical characterization.

Earlier, Pfj1 had been proposed to reside in the mitochondrial matrix following in silico prediction of a mitochondrial import signal at the N-terminus (Watanabe, 1997). Pfj1 has also been suggested to be a homologue of Mdj1 in yeast and hTid-1 in humans and that its transcription is low but is slightly upregulated following heat shock (Acharya, et al., 2007; Botha, et al., 2007; Watanabe, 1997). Both Mdj1 and hTid-1 reside in the mitochondria with the former playing an important role in mitochondrial biogenesis and in the folding of imported proteins especially at high temperatures (Rowley, et al., 1994). Sequence analysis has shown that Pfj1 is highly conserved among *Plasmodium* species (Kumar, et al., 2010). Complementation experiments of the J-domain of Pfj1 in a *dnaJ cbpA* mutant *E. coli* strain have shown that it has a functional J-domain (Nicoll, et al., 2007). Additionally, through in vitro assays, Pfj1 was shown to functionally modulate the chaperone activities of PfHsp70-1 (Misra and Ramachandran, 2009). While Pfj1 may arguably not reside in the cytosol, the latter study implied that it may possess cochaperone properties and interact with an Hsp70.

This observation raises questions regarding its localization and potential Hsp70 partner in *P. falciparum*. To date, none of the Hsp70s encoded by the *P. falciparum* genome have been localized in the apicoplast. It is possible that Pfj1 would co-localize with an Hsp70 partner due to determination of chaperone activity. The purpose of this study was to verify the localization of Pfj1 for further functional characterization. Bases on the in silico prediction that Pfj1 may reside in the mitochondria (Watanabe, 1997), this study included a preliminary characterization of the mitochondrial Hsp70 (PfHsp70-3) as partner for Pfj1. PfHsp70-3 possesses a putative mitochondrial pre-sequence and has been shown to phylogenetically cluster with mitochondrial Hsp70s from other eukaryotic organisms and cytosolic Hsp70 homologues of prokaryotic origin (Shonhai, et al., 2007). However, to date, no experimental data exists regarding this Hsp70.

3.1 Objectives

This study aimed to verify the localization of Pfj1 and PfHsp70-3 in the intraerythrocytic stage of development of *P. falciparum*. Further, the study aimed to heterologously express and purify these proteins for biochemical characterization.

Specifically, this study aimed

i. To express and purify recombinant Pfj1 protein for antibody production and subsequent characterization.
ii. To engineer transfection plasmids that encode for Pfj1 fused with either GFP or strep-tag II to be subsequently used for localization.
iii. To engineer transfection plasmids that encode for PfHsp70-3 fused with GFP and determine the localization of PfHsp70-3.
iv. To express and purify recombinant PfHsp70-3 protein for subsequent characterization.

3.2 Materials and methods

3.2.1 Heterologous production of recombinant Pfj1 protein

3.2.1.1 Plasmid construct coding for 6xHis Pfj1 protein

To express and purify recombinant 6xHis-tagged Pfj1 protein, a plasmid construct, pQPfj1-Ntruncated was kindly provided by Dr Botha (Biomedical Biotechnology Research Unit, Rhodes University, South Africa). The pQPfj1-Ntruncated plasmid contains a codon optimized Pfj1 coding sequence and encodes for a 6xHis-tagged Pfj1 protein referred to here as Pfj1m (m for mature) that lacks the N-terminus region coding for the first sixty amino acids before the start of the J-domain (Appendix C). The integrity of the new pQPfj1-Ntruncated plasmid construct was confirmed through DNA sequencing.

3.2.1.2 Induction studies for the production of Pfj1m

Transformed *E. coli* M15[pREP4] cells containing the pQPfj1-Ntruncated plasmid were selected by plating onto 2x yeast tryptone (YT) agar plates containing 100 μg/ml ampicillin sodium salt (Sigma-Aldrich, Germany) and 50 μg/ml kanamycin sulfate (Sigma-Aldrich, Germany) (Appendix F7 and F8). Subsequently, one isolated colony from the YT agar plate was inoculated into 25 ml of YT broth containing 100 μg/ml ampicillin and 50 μg/ml kanamycin followed by overnight incubation at 37°C in a shaking incubator. The overnight culture was diluted 10x and incubated at 37°C in a shaking incubator. At A_{600} of 0.6, a pre-induction sample was collected and protein expression was induced with 1 mM isopropyl-β-D-1-thiogalactopyranoside (IPTG) (Peqlab, Germany). Post induction samples were collected at 1 hour intervals up to 5 hour and thereafter an overnight sample was also collected. In addition to the *E. coli* M15[pREP4] cells, the *E. coli* XL1-Blue (Stratagene, USA) and JM109 (NEB, UK) strains were also used for Pfj1m expression studies. The growth conditions such as temperature and IPTG concentration were also varied to optimize the expression. A negative control comprising of the pQE30 plasmid vector without any insert for the expression of Pfj1m was included.

Samples obtained were treated with sample buffer (10% glycerol, 2% SDS, 5% β–mercaptoethanol, 0.05% bromophenol blue, 0.0625 M Tris, pH 6.8) (Laemmli, 1970) and boiled for 5 min. They were then analyzed using 12% SDS–PAGE and Western blotting onto a nitrocellulose membrane (Dassel, Germany) according to standard protocols (Appendix F9 and F10) (De Blas and Cherwinski, 1983; Gershoni and Palade, 1982; Towbin, et al., 1979). The membrane was blocked for 1 hour at room temperature using 5% (w/v) non–fat powder milk in Tris–buffered saline–Tween (TBST); (50 mM Tris; pH 7.5, 150 mM NaCl, 0.1%

(v/v) Tween-20). The membrane was subsequently incubated in 5% (w/v) non–fat powder milk in TBST containing appropriate primary antibodies overnight at 4^{o}C on a rocking platform. The membrane was washed three times at 10 minute intervals with TBST followed by incubation in 5% (w/v) non–fat powder milk in TBST containing specific secondary antibodies for 1 hour at room temperature on a rocking platform. The membrane was washed as above and the proteins were detected by chemiluminescence using the enhanced chemiluminescence (ECL^{TM}) western blotting kit (GE Healthcare, UK) as per the manufacturer's instructions. Images were acquired using the Chemidoc imaging system equipped with Quantity one software version 4.4.1 (Bio-Rad, USA). For Western detection, the mouse anti-His (1:5000) (Santa Cruz, USA) primary antibody was used for the detection of Pfj1m. The detection of Pfj1m was also carried out using the mouse anti-Pfj1 polyclonal antibody (1:2500 dilution; see section 3.2.3.1 for details). Horseradish peroxidase (HRP)-conjugated goat anti-mouse (1:5000) (GE Healthcare, UK) secondary antibody was used.

3.2.2 Cell biological characterization of Pfj1 and PfHsp70-3

3.2.2.1 Peptide directed anti-Pfj1 antibody design and production

The amino acid sequence of Pfj1 was obtained from PlasmoDB version 8.1 (Aurrecoechea, et al., 2009) and aligned with other reported *P. falciparum* J proteins to identify potential regions for antibody production. Unique peptide regions, in particular within the C-terminus, comprising of 10-15 amino acids were identified. To avoid cross-reactivity of the antibody with human and other *P. falciparum* proteins, the identified peptides were used as queries for any local alignments with predicted proteomes of *P. falciparum* and *H. sapiens*. Strings of 5-6 amino acids were also used in the searches since antibodies normally recognize epitopes of short stretches of amino acids in a polypeptide chain. As a general criterion to choose the peptide, regions that are predicted to be surface exposed, soluble, have high peptide chain flexibility, possess hydrophilic amino acid stretches, and have high charge density were assessed.

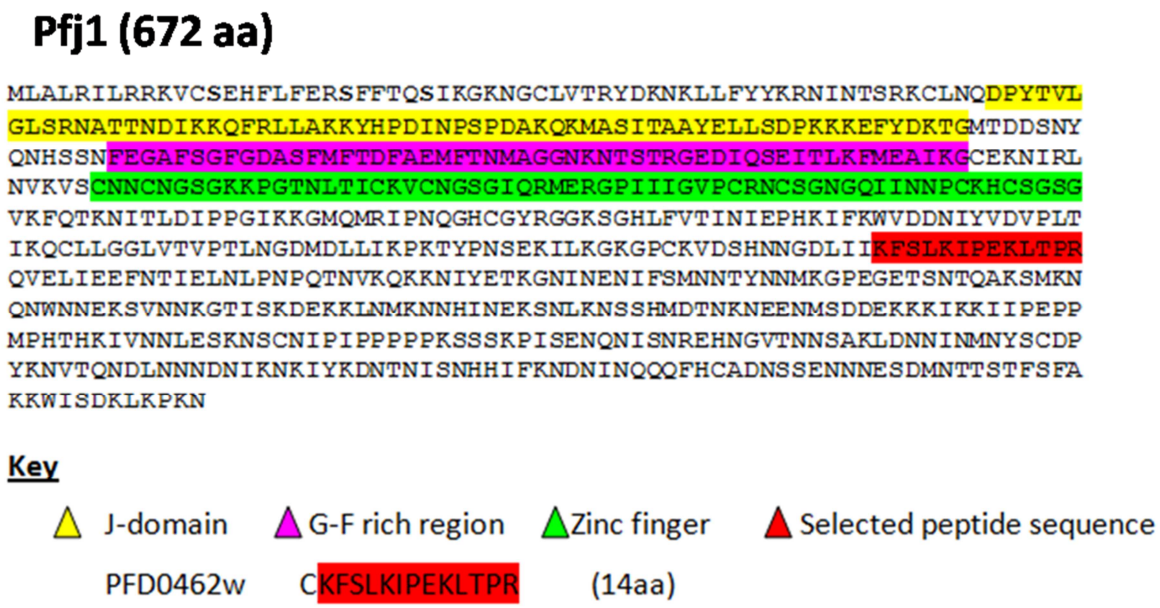

Figure 3.1: The amino acid sequence depicting the conserved domains and the identification of the unique peptide for the design of the Pfj1 antibody. Regions that are predicted to be surface exposed, soluble, have high peptide chain flexibility, possess hydrophilic amino acid stretches, and have high charge density were assessed using the GeneRunner software (version 3.05; Hastings Software Inc.). The peptide selected was used to query the predicted human and *P. falciparum* proteomes.

The protein sequence of Pfj1 was assessed using an algorithm for determining peptide antigenicity (Hofmann and Hadge, 1987; Hopp and Woods, 1981; Jameson and Wolf, 1988), surface probability (Emini, et al., 1985), hydropathy (Kyte and Doolittle, 1982) and chain flexibility (Karplus and Schulz, 1985) as provided by the GeneRunner software (version 3.05; Hastings Software Inc.). Regions rich in lysine and arginine were discarded as many malaria proteins are rich in these amino acids. An epitopic region in the C-terminus (Figure 3.1) was selected and synthesized by the GenScript Corporation (Piscataway, New Jersey, USA). The GenScript Corporation further used the synthesized peptide to raise antisera in mice after collection of pre-immune serum and subsequently purified the fractions using protein A.

3.2.2.2 Parasite culture

P. falciparum (clone 3D7) was cultured using vented flasks in a 37°C incubator that was supplied with nitrogen gas (N_2) mixture containing 5% (v/v) carbon dioxide (CO_2) and 5% (v/v) oxygen (O_2). The parasites we propagated in human erythrocytes at a hematocrit of 4%

in RPMI 1640 medium containing 25 mM hepes and L-Glutamine (Whitehead scientific, South Africa) supplemented with 0.5% AlbumaxII (Gibco, USA), 0.4% (w/v) glucose (Merck, USA), 200 mM hypoxanthine (Sigma-Aldrich, Germany) and 50 µg/ml gentamicin (Sigma-Aldrich, Germany) as described previously (Trager and Jensen, 1997). Human blood used for parasite culture was drawn by a nurse following informed consent from healthy donors at the Ampath laboratories (Grahamstown, South Africa). The serum and buffy coat from the whole blood was discarded following initial centrifugation (3200 xg, 5 min). The hematocrit was processed by washing it several times with RPMI 1640 medium lacking AlbumaxII. Asynchronous parasites were routinely synchronized to the ring stage through the sorbitol lysis method as previously described (Lambros and Vanderberg, 1979).

3.2.2.3 Preparation of *P. falciparum* lysates and detection of Pfj1

Synchronized parasites at the trophozoite stage were harvested through centrifugation (800 xg, 2 min) and treated on ice for 7 minutes with 0.1% (w/v) saponin (Sigma-Aldrich, Germany) in phosphate-buffered saline (PBS; 137 mM NaCl, 2.7 mM KCl, 10.3 mM Na_2HPO_4, 1.8 mM KH_2PO_4, pH 7.4), to enable lysis of erythrocyte membranes. Subsequently, intact parasites were collected by centrifugation (2800 xg, 5 min) and the supernatant discarded. The parasite pellet was washed several times with ice cold PBS to remove hemoglobin and saponin. This method of erythrocyte membrane lysis was maintained throughout the study unless otherwise stated. The pellet was then diluted in reducing and denaturing sample buffer (Laemmli, 1970) and boiled for 5 minutes. Proteins were resolved by 12% SDS–PAGE followed by Western blotting onto a nitrocellulose membrane (Dassel, Germany) according to standard protocols (Appendix F10) (De Blas and Cherwinski, 1983; Gershoni and Palade, 1982; Towbin, et al., 1979). The processing of the western membrane and subsequent detection was carried out as described in section 3.2.1.2 except that 3% (w/v) bovine serum albumin (BSA) in TBST was used in place of 5% (w/v) non–fat powder milk in TBST. Primary antibodies used included anti-Pfj1 (1:2500 dilution) and anti-PfHsp70-1 (1:5000 dilution) as a positive control. The anti-PfHsp70-1 antibody used here had been raised in rabbits and was a kind gift from Dr. Addmore Shonhai, Rhodes University (Shonhai, 2007). HRP-conjugated goat anti-mouse (1:5000 dilution) (GE Healthcare, UK) and goat anti-rabbit (1:5000 dilution) (Cell signaling technology, USA) secondary antibodies were used.

3.2.2.4 Pfj1 and PfHsp70-3 constructs for transfection

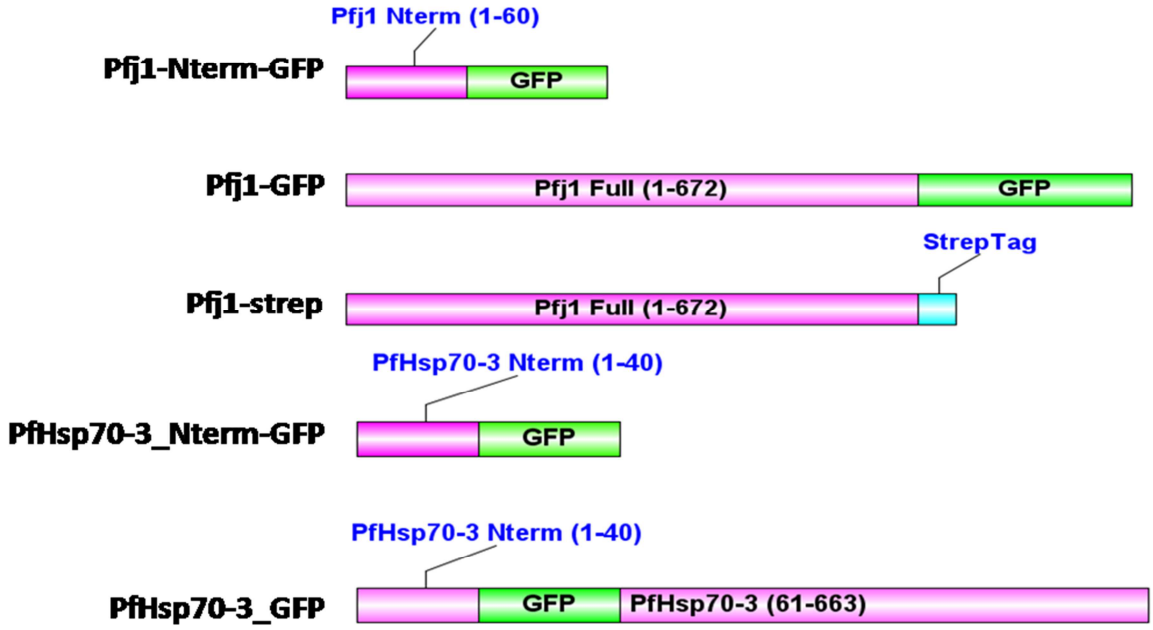

Figure 3.2: Schematics representation depicting the design of transfection constructs for Pfj1 and PfHsp70-3.

To engineer transfection plasmids for the localization of Pfj1 and PfHsp70-3, the predicted signal sequences were identified through in silico analysis conducted in section 2.3.1.3.2. The N-terminus regions before the J-domain of Pfj1 and before the ATPase domain of PfHsp70-3 were considered sufficient to carry the signal sequences and were used for fusion tagging with GFP at the C-terminus (Figure 3.2). Additionally, the full length sequences of both proteins were also tagged with GFP (Figure 3.2; see sections 3.2.2.4.1 and 3.2.2.4.2). However, the full length sequence of Pfj1 was considered for fusion tagging with the strep-tag II at the C-terminus.

3.2.2.4.1 Pfj1 constructs for transfection

Three plasmids were designed (Figure 3.2) and constructed for Pfj1 through PCR amplification from *P. falciparum* genomic DNA and subsequent cloning into the pARL2-GFP plasmid. The reverse primers were designed to amplify the coding sequence without the

stop codon to allow for the fusion of the tags at the C-terminus. The full length Pfj1 sequence encoding amino acid 1-672 was amplified using the forward primer (PFJ1_ATG_X; 5'-GG**CTCGAG**ATGTTAGCTTTAAGAATATTAAGAAGAAAGG-3') containing a *Xho*I site (highlighted in bold) and reverse primer (PFJ1_Full_A_R; 5'-GG**CCTAGG**ATTTTTTGGCTTTAACTTATCAGATATC-3') containing an *Avr*II site (highlighted in bold). The amplified Pfj1 PCR product was gel purified and digested with *Xho*I-*Avr*II and ligated into the *Xho*I-*Avr*II restricted pARL2-GFP vector creating pARL2_Pfj1$^{\boldsymbol{1\text{-}672}}$-GFP construct referred here in as Pfj1-GFP. The pARL2-GFP plasmid was kindly provided by Dr. Jude Przyborski, Philipps University, Marburg, Germany. This plasmid is under the control of the *P. falciparum* chloroquine resistance transporter (PfCRT) promoter. The predicted Pfj1 N-terminal signal sequence coding for amino acid 1-60 was also PCR amplified using the forward primer (PFJ1_ATG_X; 5'-GG**CTCGAG**ATGTTAGCTTTAAGAATATTAAGAAGAAAGG-3') containing a *Xho*I site (highlighted in bold) and the reverse primer (PFJ1+60_A_R; 5'-GG**CCTAGG**TTGATTTAAACATTTTCTTGAAGTATTTATATTTC-3') containing an *Avr*II site (highlighted in bold). The amplified Pfj1-N terminus PCR product was gel purified and digested with *Xho*I-*Avr*II and inserted into the *Xho*I-*Avr*II restricted pARL2-GFP vector, creating pARL2_Pfj1$^{\boldsymbol{1\text{-}60}}$-GFP plasmid herein referred as Pfj1-Nterm-GFP.

Further, to generate a construct coding for the full length Pfj1 fused to the strep-tag II at the C-terminus, the Pfj1 coding sequence was PCR amplified using the forward primer; PFJ1_ATG_X, and reverse primer; (Pfj1_Strep 5'-**CCCGGG**TCATTTTTCGAACTGCGGGTGGCTCCAATTTTTTGGCTTTAAC-3'). The *Xma*I restriction site in the Pfj1_Strep primer is highlighted in bold and the sequence coding for the strep-tag II is underlined. The amplified Pfj1 PCR product was gel purified and restricted with *Xho*I-*Xma*I and subsequently ligated into *Xho*I-*Xma*I restricted pARL2-GFP vector creating the pARL2-Pfj1-Strep plasmid construct herein referred as Pfj1-strep. Diagnostic restriction digests were conducted followed by DNA sequencing to confirm the integrity of the generated constructs.

3.2.2.4.2 PfHsp70-3 construct for transfection

Two plasmids were designed (Figure 3.2) and constructed for PfHsp70-3 through PCR amplification from *P. falciparum* genomic DNA and subsequently cloned into the pARL2-GFP plasmid. The plasmids for PfHsp70-3 were designed to encode for the signal sequence and the full length fused to GFP. Here, while the predicted signal sequence was fused to GFP at the C-terminus, the full length was engineered with an internal GFP sequence inserted between the signal sequence and the ATPase domain (Figure 3.2). Fusing the GFP towards the C-terminus was avoided as it could affect the lid domain and potential interaction with other proteins. To engineer a plasmid construct coding for the signal sequence fused to GFP, the N-terminus region coding for amino acid 1-40 was amplified through PCR using the forward primer; (PfHsp70-3_Nterm_ATG_*Xho*I 5'-CG**CTCGAG**ATGGCATCACTCAATAAAAAGAAC-3') containing a *Xho*I site (highlighted in bold) and the reverse primer; (PfHsp70-3_Nterm_Rev_*Kpn*I 5'-GC**GGTACC**GGAAGCTCTATTGCGATTTATC -3') containing a *Kpn*I site (highlighted in bold). The amplified PCR product was gel purified and digested with *Xho*I-*Kpn*I, and subsequently ligated into the *Xho*I-*Kpn*I restricted pARL2-GFP vector creating pARL2-PfHsp70-3$^{1\text{-}40}$-GFP plasmid herein referred as PfHsp70-3_Nterm-GFP.

To create a plasmid encoding the full length PfHsp70-3 described above, a *Pst*I restriction site was initially introduced before the *Sma*I restriction site in the pARL2-GFP vector. The GFP sequence was amplified through PCR using the forward primer (pARL2-GFP_ATG_ *Kpn*I 5'-GC**GGTACC**ATGAGTAAAGGAGAAGAACTTTTC-3') containing the *Kpn*I site (highlighted in bold) and the reverse primer (pARL2-GFP_Rev_*Pst*I 5'-GA<u>*CCCGGG*</u>**CTGCAG**TTTGTATAGTTCATCCATGCC-3') containing the *Pst*I site (highlighted in bold) and the *Sma*I site (underlined). The pARL2-GFP_Rev_*Pst*I lacked the stop codon present in the GFP sequence. The PCR product was gel purified and restricted using *Kpn*I-*Sma*I and ligated into *Kpn*I-*Sma*I restricted pARL2-GFP vector creating the pARL2-GFP-*Pst*I plasmid. The PfHsp70-3 signal sequence was then subcloned into this new vector using the primers PfHsp70-3_Nterm_ATG_*Xho*I (forward) and PfHsp70-3_Nterm_Rev_*Kpn*I as described above. This resulted into an intermediate plasmid referred to as pARL2-GFP-*Pst*I-PfHsp70-3Nterm. The PfHsp70-3 sequence lacking the signal sequence but with a stop codon was then PCR amplified using the forward primer (PfHsp70-

3_Full_ATG_*Pst*I 5'- GG**CTGCAG**GGAGATATCATAGGTATTGATTTAGG-3') containing the *Pst*I site (highlighted in bold) and the reverse primer (PfHsp70-3_Full_Rev_*Sph*I 5'-GC**GCATGC**TTATGCATTATCTTTATTTTCTTCAGC-3') containing the *Sph*I site (highlighted in bold). The amplified PCR product was subsequently gel purified, restricted using *Pst*I-*Sph*I and ligated into *Pst*I-*Sph*I restricted pARL2-GFP-*Pst*I-PfHsp70-3Nterm plasmid creating the pARL2_PfHsp70-3 (1-40_GFP_41-663) plasmid herein referred as PfHsp70-3_GFP. Diagnostic restriction digests were conducted followed by DNA sequencing to confirm the integrity of the generated plasmids.

3.2.2.5 Parasite transfection

Plasmid DNA for parasite transfection was prepared using the Qiagen plasmid maxi kit (Qiagen, Germany) according to the manufacturer's instructions. Plasmid DNA (150 µg) was resuspended in 300 µl of cytomix buffer (120 mM KCl, 0.15 mM CaCl, 2 mM EGTA, 5 mM $MgCl_2$, 10 mM K_2HPO_4, KH_2PO_4, 25 mM hepes, pH 7.6) (van den Hoff, et al., 1992; Wu, et al., 1995) and transferred to a 0.2 cm gapped electroporation cuvette (Bio-Rad, USA). Synchronized ring-stage parasitized erythrocytes at 5-10% parasitemia were collected by centrifugation (800 xg, 2 min) and washed once with cytomix buffer and subsequently transferred into the electroporation cuvette containing the plasmid DNA. The mixture (400 µl) was electroporated using the GenePulser Xcell^{TM} (Bio-Rad, USA) set to a voltage of 310V and a capacitance of 950 µF. Electroporated samples were immediately mixed with complete culture media and fresh erythrocytes were added to give a 5% hematocrit and transferred into a T25 culture flask. Cultures were maintained without drug selection for 5 hours and subsequently on 2.5 nM WR99210 drug (Sigma-Aldrich, Germany) permanently. As a positive control for the GFP line, the pARL2-GFP plasmid was also transfected and maintained under similar conditions. The integrity of the WR99210 drug was assessed using the parental 3D7 parasite line. The PFB0595w-GFP plasmid was used a positive control (see section 4.2.4 for details). Parasite transfection and imaging was carried out with the kind assistance of Dr. Jude Przyborski at the Department of Parasitology, Philipps University, Marburg, Germany).

3.2.2.6 Live cell imaging and western analysis of transfectants

For live imaging of GFP transfectant parasites, the cells were harvested from culture and washed once with pre-warmed incomplete media. They were then resuspended briefly in incomplete media containing 10 µg/ml Hoechst 33258 (Sigma-Aldrich, Germany) for DNA staining and with 20 nM MitoTracker red (Molecular Probes, USA). MitoTracker Red (chloromethyl-X-rosamine) is a mitochondrion-selective fluorescent probe (Terasaki, et al., 2001). They were subsequently resuspended into complete medium after centrifugation (800 xg, 2 min). The parasites were imaged at room temperature (25^{o}C) within 30 min of mounting under a coverslip on to a glass slide through 100x oil-immersion objective. Images were acquired using an Axio Observer inverse epifluorescence microscope system equipped with Axiovision 4 software (Zeiss, Jena, Germany) or an AxioVert.A1 equipped with Zeiss efficient navigation (ZEN) imaging software (Zeiss, Jena, Germany) with both microscopes being operated under the appropriate filter sets. Images of trophozoite stage parasites were captured even though parasites at the ring and schizont stages were also examined. Parasite lysates were generated from both the wild type and the transfectant lines and assessed through western blotting as described in section 3.2.3.3. Primary antibodies including rabbit anti-GFP (1:2000) (Santa Cruz, USA) and rabbit anti-PfHsp70-1 (1:5000) polyclonal antibodies were used for western detection. HRP-conjugated donkey anti-rabbit (1:5000) secondary antibody was used.

3.2.2.7 Indirect Immunofluorescence microscopy

To study the localization of GFP in the Pfj1 transfectant lines relative to the apicoplast, the acyl carrier protein (ACP) was used as a marker for the apicoplast. For indirect immunofluorescence microscopy, the 3D7 parental lines and GFP transfectants were cultured as described in section 3.2.3.5. The parasites were harvested at the trophozoite stage from culture by centrifugation (800 xg, 2 min). The parasite cell pellet was washed with PBS and the cells were fixed using the paraformaldehyde/glutaraldehyde method. Briefly, infected erythrocytes were fixed by resuspending the cell pellet in PBS containing 4% (w/v) paraformaldehyde and 0.0075% (v/v) glutaraldehyde and incubated at 37^{o}C for 30 minutes with gentle mixing. This was followed by quenching for 10 minutes with 125 mM glycine in

PBS and the pellet subsequently obtained by centrifugation (1800 xg, 2 min). The cell pellet was permeabilized by resuspending it in 0.1% TritonX-100 followed by mixing and centrifugation as above. The cell pellet was incubated briefly with 125 mM glycine in PBS with gentle mixing followed by a wash step with PBS. The cell pellet was then incubated in blocking buffer (3% (w/v) BSA in PBS) for 2 hours at room temperature. The parasite pellet was incubated overnight with rabbit anti-ACP (1:500) primary antibody (kind donation from Prof. Jude Przyborski, Philipps University, Marburg, Germany) diluted in the blocking buffer at 4^{o}C on a gentle rocking platform. The cells were then washed three times with PBS at 10 minute intervals on the same rocking platform. This was followed by incubation with goat anti-rabbit-Cy3 (Dako probes) secondary antibody (1:2000) diluted in blocking buffer in the dark for 1 hour at room temperature on the rocking platform. The cells were subsequently washed as described above and Hoechst 33258 (50 ng/ml) diluted in PBS was included in the last washing step to stain the nuclei. The cells were spotted onto a microscopy slide in the dark before a glass coverslip was mounted using a small drop of Dako mounting medium (Invitrogen, USA). Images were captured using an Axio Observer inverse epifluorescence microscope system equipped with Axiovision 4 software (Zeiss, Jena, Germany) operated under the appropriate filter sets. Controls used in this experiment included incubating the fixed parasites with either the primary antibody alone or secondary antibody alone. Additionally, wild type 3D7 parasites processed without inclusion of any antibodies were also used.

3.2.3 Heterologous production of recombinant PfHsp70-3 protein

3.2.3.1 Preparation of the plasmid coding for the 6xHis PfHsp70-3 protein

To generate a plasmid encoding 6xHis-tagged PfHsp70-3 protein, the coding sequence for PfHsp70-3 lacking the first forty amino acids at the N-terminus before the start of the ATPase domain, referred here as PfHsp70-3m, was codon optimized to allow for improved heterologous expression in *E. coli* (Appendix B). As described above, the N-terminus region before the ATPase domain was excluded in the design of the plasmid for protein expression since it is predicted to carry a mitochondrion import signal. The *Bam*HI and *Hind*III restriction sites were engineered at the 5' and 3' ends of the coding sequence to facilitate the ligation of the sequence into the pQE30 expression vector (Qiagen, Germany). The coding

sequence for PfHsp70-3 was subsequently synthesized and inserted into the pQE30 vector to produce the plasmid pQE30-PfHsp70-3 by the GenScript Corporation (Piscataway, New Jersey, USA). The integrity of the plasmid was verified by DNA sequencing (Appendix C).

3.2.3.1.1 Induction studies for the production of PfHsp70-3m

Induction studies were conducted to facilitate the purification of PfHsp70-3m, following the transformation of the pQE30-PfHsp70-3 plasmid into competent *E. coli* M15[pREP4] cells (Qiagen, Germany) as described in section 3.2.2.2. Western detection was carried out using the mouse anti-His (1:5000) (Santa Cruz, USA) primary antibody as described in the same section.

3.2.3.1.2 Solubility studies for PfHsp70-3m

Solubility studies for PfHsp70-3m were undertaken following inductions studies. The *E. coli* M15[pREP4] cells were transformed and colonies inoculated into cultures which were grown overnight as described in section 3.2.4.1.1. Overnight cultures were diluted 10x and incubated at 37°C in a shaking incubator followed by induction with 1 mM IPTG at A_{600} of 0.6. Three hours after induction, the cells were harvested by centrifugation (5000 xg, 20 min) at 4°C and the cell pellet resuspended in 5 ml of lysis buffer (10 mM Tris HCL pH 7.5, 300 mM NaCl and 50 mM imidazole, 1 mM phenylmethylsulphonylfluoride (PMSF) (Roche, Switzerland), and 1 mg/ml lysozyme (Sigma, Germany) and split into four separate fractions. Cell lysis was allowed to proceed for 20 min at room temperature (22^{o}C) after which the fractions were frozen overnight at -80^{o}C. The fractions were subsequently thawed and two of the samples were adjusted either with 7.5% (w/v; final concentration) N-lauroylsarcosine (Sarcosyl) (Sigma-Aldrich, Germany) prepared in Sodium-Tris-EDTA (STE) buffer (100 mM NaCl, 10 mM Tris-HCL; pH 8, 1 mM EDTA), or with 0.1% (v/v; final concentration) polyethylenimine (PEI) (Sigma-Aldrich, Germany) prepared in lysis buffer. Out of the remaining two samples, one was processed under denaturing conditions with urea (8M; final concentration) while the other received no treatment. The supernatant fraction was obtained by centrifugation (13000 xg, 30 min) at 4^{o}C and the pellet was subsequently resuspended in

an equivalent volume of PBS. Equal volumes of both the supernatant and pellet were treated with sample buffer (Laemmli, 1970), boiled for 5 min and analyzed through SDS-PAGE.

3.2.3.1.3 Purification of PfHsp70-3m

PfHsp70-3m was first overexpressed in *E. coli* M15[pREP4] cells as described in section 3.2.4.1.1. Three hours following induction of protein expression, the cells were harvested through centrifugation and the pellet obtained was resuspended in lysis buffer and frozen overnight at −80°C as described in section 3.2.4.1.2. Prior to sonication, the sample was treated with sarcosyl (7.5 w/v) as described in section 3.2.4.1.2. The PfHsp70-3m protein present in the soluble cell extract was allowed to bind to nickel charged sepharose beads (GE Healthcare, UK) overnight at 4°C. The beads were subsequently washed using wash buffer (10 mM Tris, pH 7.5, 300 mM NaCl, 50 mM imidazole, and 1 mM PMSF) and PfHsp70-3m was then eluted using elution buffer (10 mM Tris, pH 7.5, 300 mM NaCl, 1 M imidazole, and 1 mM PMSF). The eluted protein was extensively dialysed at 4°C against the storage buffer (10 mM Tris, pH 7.5, 300 mM NaCl, 50 mM imidazole, 0.8 mM DTT, 10% glycerol, and 1 mM PMSF) and frozen at -80^{o}C for future applications.

3.3 Results

3.3.1 Approaches to the expression of Pfj1m

The study aimed to produce recombinant Pfj1 protein that was to be subsequently used to raise anti-Pfj1 serum in mice. SDS-PAGE analysis of whole cell lysates showed slight induction of expression of the Pfj1m protein at the expected size (~70 kDa) as shown in Figure 3.3. Western analysis using the anti-His antibody confirmed that the protein expressed was Pfj1m. However, another major band at ~58 kDa was detected which was probably a major degradation product of Pfj1m. While there was very low expression prior to induction as determined by western analysis, Pfj1m protein appeared to be slightly induced between the third and fifth hours.

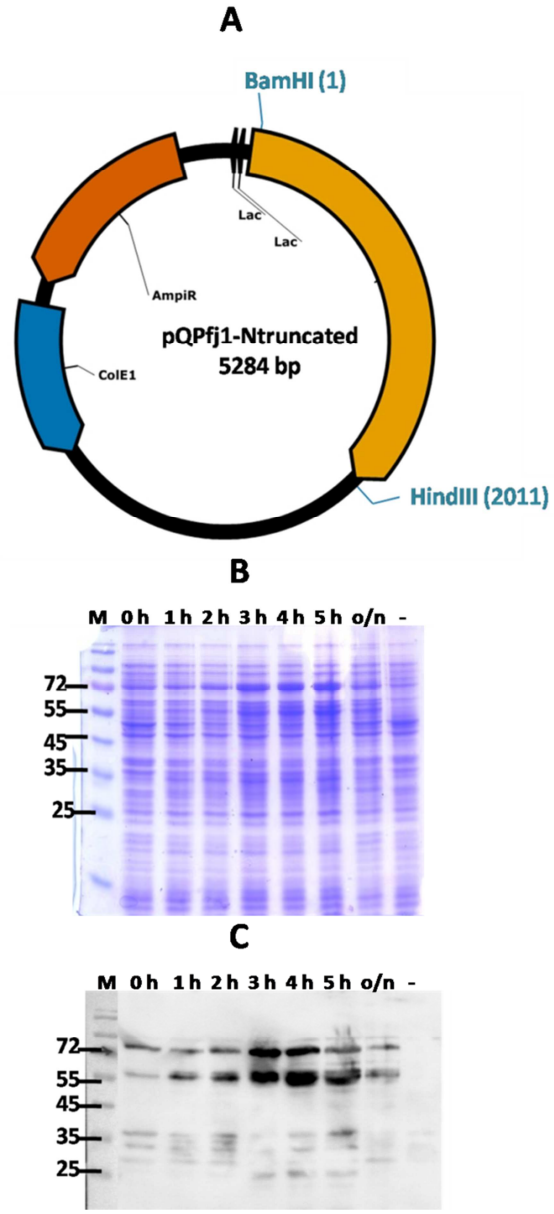

Figure 3.3: Heterologous expression of Pfj1m. A) Plasmid map for pQPfj1-Ntruncated designed using PlasmaDNA software (Angers-Loustau, et al., 2007). The plasmid confers ampicillin resistance when transformed in *E. coli* cells as indicated (AmpiR; β–lactamase coding sequence). The 6xHis-tag segment is upstream of the *Pfj1m* coding sequence inserted between *Bam*HI and *Hind*III restriction sites. The origin of replication (ColE1 origin) and region coding for LacZ alpha are also highlighted in the plasmid map. **B**) SDS–PAGE (12%) analysis of the Pfj1m total protein extracts prepared from *E. coli* M15[pREP4] cells transformed with pQPfj1-Ntruncated and induced with 1 mM IPTG. Lane M; molecular mass marker, lane 0 h; non–induced sample, lanes 1 h – 5 h; induced samples taken hourly for five hours, lane o/n; overnight induced sample, lane -; pQE30 plasmid negative control **C**) An associated western blot analysis for the detection of Pfj1m using anti-His antibody.

There was no observed difference in the production of Pfj1m when differing concentrations of IPTG were used (data not shown). The induction levels were not considered sufficient for purification purposes. Additionally, the presence of a major band at ~58 kDa implied that both the full length and the truncated protein lacking part of the C-terminus would be co-purified using the nickel affinity chromatography purification method. The low level of induction of Pfj1m expression prompted the use of *E. coli* XL1-Blue and JM109 strains (data not shown). However, these strains showed minimal induction compared to that observed for the M15[pREP4] strain implying that Pfj1m is potentially toxic to the *E. coli* cells. Other approaches attempted to improve expression was the induction of protein expression under lower temperatures such as 30^{o}C and 25^{o}C. However, both temperatures did not result in

increased expression of Pfj1m (data not shown). The difficulty associated with the expression of this J protein in the *E. coli* expression system did not allow for its purification and calls for further investigation.

3.3.2 Peptide anti-Pfj1 antibodies unsuitable for cell-biological studies

Following the unsuccessful production of the full length Pfj1m recombinant protein, the peptide directed approach for generation of the anti-Pfj1 antibody was considered. Serum directed against a unique peptide of Pfj1 (shown in Figure 3.1) was successfully raised in mouse and subsequently used for the detection of Pfj1 in the intraerythrocytic cycle of *P. falciparum* development. The antibody was intended for cell-biological characterization including localization, solubility, and immunoprecipitation studies. Western analysis of trophozoite stage parasites showed that the antibody detected a minor band at ~63 kDa and a major band at ~38 kDa (Figure 3.4). However, the predicted molecular mass of Pfj1 is 76 kDa that is supposedly processed to ~69 kDa (mature) following the cleavage of the predicted signal sequence before the J-domain. The detected bands contrasted the detection of the mature protein and were thought to result from the degradation of Pfj1 or the antibody was detecting another protein of that molecular mass. As such, the antibody could not be used for cell-biological analysis and experimentation. However, the antibody detected a band at the expected size (~ 70 kDa, Figure 3.4; iii) and other bands at lower molecular masses judged as degradation products when it was tested on *E. coli* whole cell lysates producing Pfj1m.

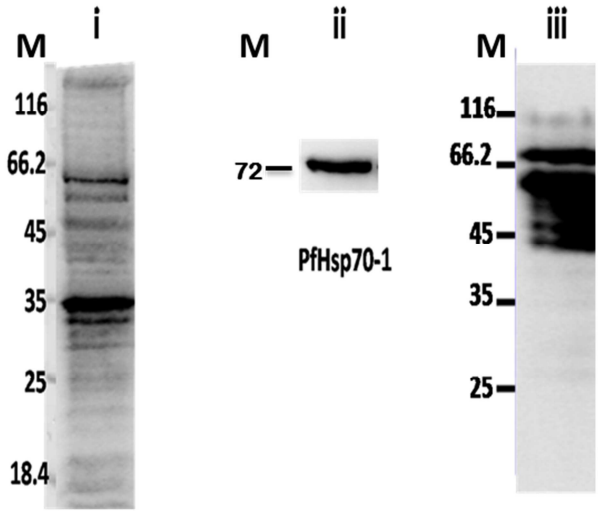

Figure 3.4: Pfj1-specific peptide based antibody detects native and recombinant Pfj1 proteins. i) Western detection of Pfj1 on lysates derived from the trophozoite stage of *P. falciparum* clone 3D7 parasites using the anti-Pfj1 antibody. M: molecular weight marker. **ii**) Detection of PfHsp70-1 using the anti-PfHsp70-1 antibody that served as a positive control. **iii**) Western detection of Pfj1m in *E. coli* M15 [pREP4] whole cell lysates transformed with pQPfj1-Ntruncated and induced with 1 mM IPTG.

3.3.3 The N-terminus of Pfj1 targets GFP to the mitochondrion

The lack of success with the anti-Pfj1 antibody prompted the generation of transfection plasmids coding for full length and N-terminus Pfj1 sequences fused with GFP that would enable localization studies to be conducted (Figure 3.5). The plasmids generated were transiently transfected and positive transfectants were selected through permanent drug pressure with WR99210. However, of the three plasmids transfected (Pfj1-GFP, Pfj1-strep, and Pfj1-Nterm-GFP), only the Pfj1-Nterm-GFP plasmid gave rise to viable transfectants. This transfectant parasite line was therefore used for subsequent localization studies. The other two plasmids did not give rise to transfectant lines following two transfection attempts.

Microscopy images were captured from live transfectant parasites at the trophozoite stage expressing GFP. The GFP fluorescence displayed ribbon-like structures indicating that the signal did not originate from the cytoplasm. The transfectant parasites were then stained with MitoTracker red to allow for the visualization of the mitochondria. GFP fluorescence was observed to colocalize with the MitoTracker red staining showing that Pfj1 localized to the mitochondrion (Figure 3.6A). To verify that Pfj1 did not localize to the apicoplast as previously shown (Kumar, et al., 2010), the GFP transfectants were fixed as described and immunostained with the anti-ACP antibody. Images subsequently captured from the fixed parasites showed that GFP did not colocalize with the signal from the anti-ACP antibody (Figure 3.6B). Indeed, the mitochondrion displayed a ribbon-like shape that had distinct morphology to the punctate nature observed with the apicoplast (Figure 3.6B). Pfj1 localized exclusively to the mitochondrion in all the parasites observed as well as those imaged. Western analysis of the Pfj1-Nterm-GFP transfectant line using the anti-GFP antibody detected a band at ~29 kDa. It has been shown that the topogenic signal or the mitochondrion transit peptide (Bender, et al., 2003) is cleaved off following import into the mitochondrion by the mitochondrial processing peptidase (Gakh, et al., 2002; Ito, 1999). This band appears to depict the processed form of the synthesized chimeric preprotein (~34 kDa) following import. A faint band at approximately 34 kDa was detected in all the three lanes indicated that the anti-GFP antibody was also detecting one or more proteins at that molecular weight. A band at the expected size (~66 kDa) was also detected for the PFB0595w-GFP that acted as a positive control (Figure 3.6C, see section 4.3.4 for a detailed description of PFB0595w-GFP)

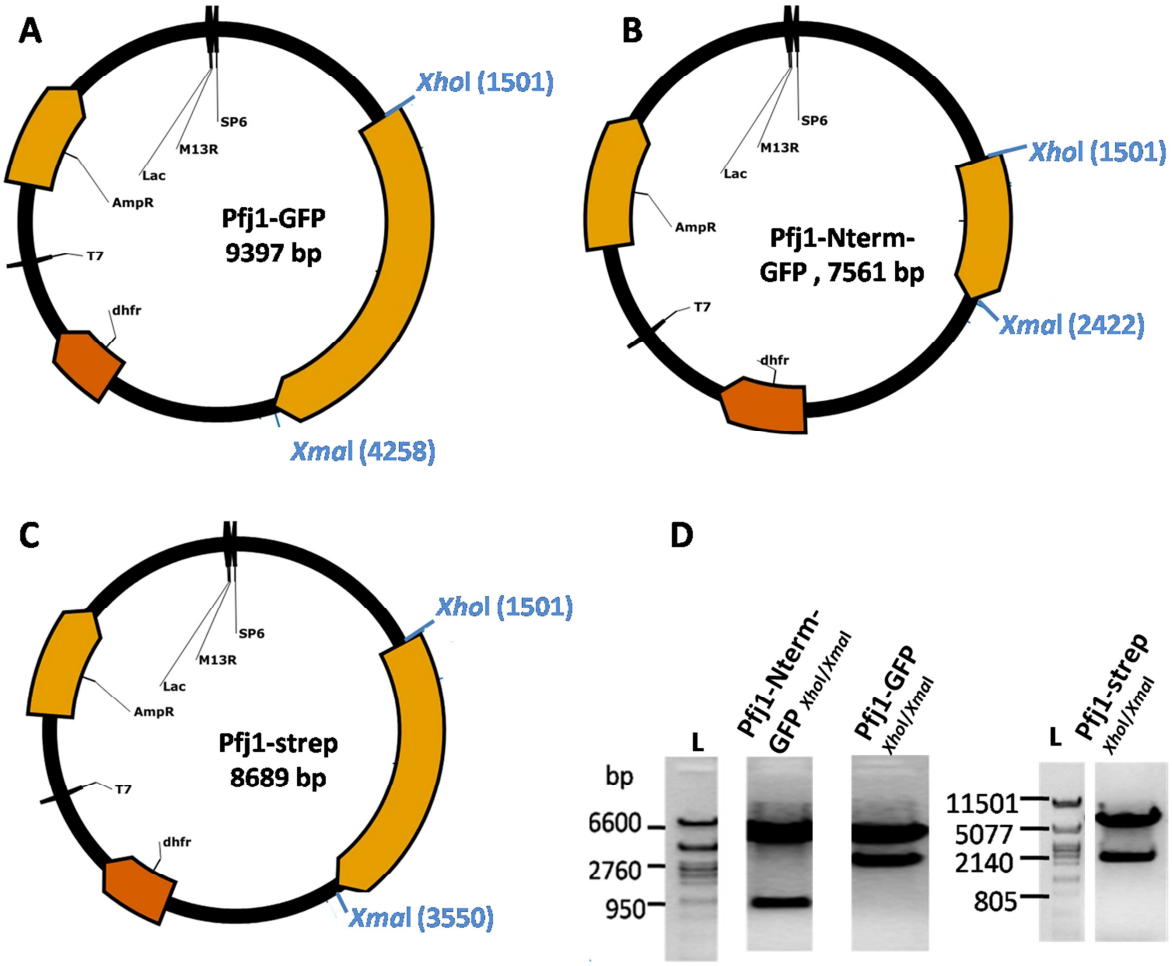

Figure 3.5: Pfj1 plasmids used for transfection. The plasmid maps (A-C) designed using the PlasmaDNA software (Angers-Loustau, et al., 2007) and associated diagnostic restriction analysis gels (D) for the Pfj1 plasmids used for parasite transfection. The plasmids confer ampicillin resistance when transformed into *E. coli* cells as indicated (AmpR; β-lactamase gene) and confer WR99210 resistance (dhfr; Dihydrofolate reductase gene) when transfected into *P. falciparum* parasites. A) **Pfj1-GFP**, plasmid map for the full length Pfj1 tagged with GFP on the C-terminus inserted between *Xho*I and *Xma*I. B) **Pfj1-Nterm-GFP**, plasmid map for Pfj1 signal sequence tagged with GFP on the C-terminus inserted between *Xho*I and *Xma*I. C) **Pfj1-strep**, plasmid map for the full length Pfj1 tagged with the strep-tag on the C-terminus inserted between *Xho*I and *Xma*I. Restriction digests of the respective plasmids in A –C resolved on a 1% agarose gel. L; DNA ladder, bp; basepairs.

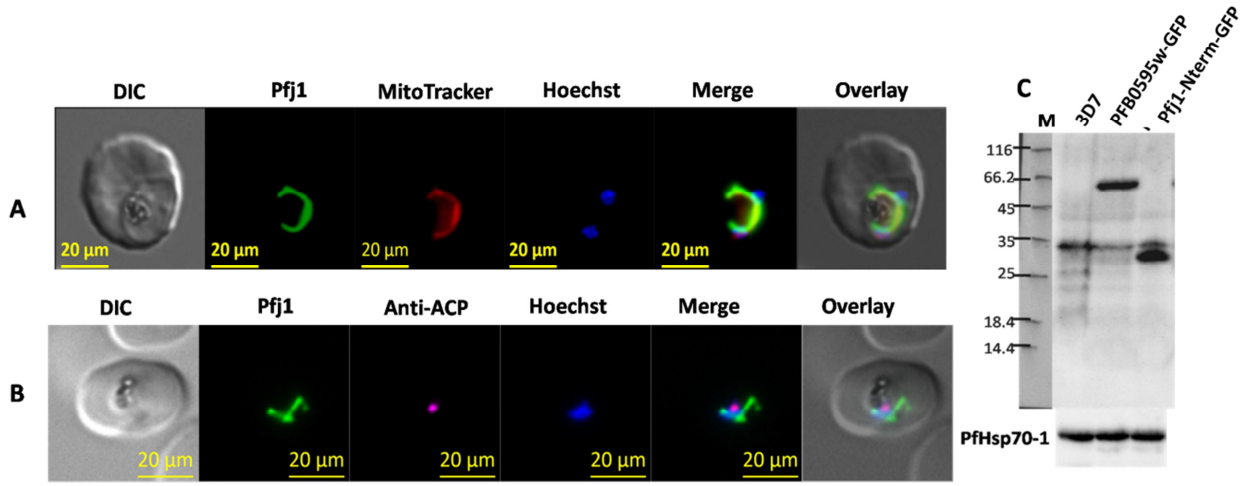

Figure 3.6: Microscopy images of the Pfj1-Nterm-GFP transfectants depicting the mitochondrial localization of Pfj1. A) Live-cell imaging of the Pfj1-Nterm-GFP transfectants stained with MitoTracker red to visualize the mitochondrion and with Hoechst to visualize nuclear staining. DIC, differential interference contrast; Merge: GFP with Hoechst and MitoTracker red, Overlay; DIC plus Merge. **B**) Immunolocalization of the ACP (Acyl carrier protein) using fixed Pfj1-Nterm-GFP transfectants stained with Hoechst. Merge: GFP plus Hoechst and anti-ACP, Overlay; DIC plus Merge. The images were pseudocoloured following capture. **C**) Western analysis of the Pfj1-Nterm-GFP transfectants. M, molecular mass marker; 3D7, *P. falciparum* 3D7 used as a negative control; PFB0595w-GFP, the PFB0595w-GFP transfectant parasite line used as a positive control; Pfj1-Nterm-GFP, the Pfj1-Nterm-GFP transfectant parasite line used for the localization of Pfj1. PfHsp70-1 acted as a control for the integrity of the lysates.

3.3.4 PfHsp70-3_Nterm-GFP localizes to the mitochondrion and cytoplasm

Following the mitochondrial localization of Pfj1, the localization of the putative mitochondrial Hsp70 (PfHsp70-3) was investigated. Transfection plasmids coding for the full length sequence and the N-terminus (comprised of the sequence before the ATPase domain) of PfHsp70-3 fused to GFP were designed and successfully generated (Figure 3.7). The design of the full-length plasmid was such that the GFP sequence was inserted between the N-terminus signal sequence and the start of the ATPase domain. As mentioned previously, fusing the GFP towards the C-terminus was avoided as it could affect the lid domain and potential interaction with other proteins. Transfectants were selected permanently through WR99210 drug selection pressure following transfection. However, of the two transfected plasmids, only the PfHsp70-3_NTerm-GFP plasmid gave rise to positive clones which were subsequently used for localization studies. Imaging of the PfHsp70-3_Nterm-GFP transfectants was carried out using live trophozoites and schizonts (Figure 3.8A-3.8C). The

GFP signal displayed ribbon-like structures in approximately 70% of the incidences observed while the rest displayed parasite cytoplasmic localization (Figure 3.8A-3.8C). When the transfectant parasites were stained with MitoTracker red, the GFP signal was observed to overlap with the MitoTracker red displaying mitochondrial localization. However, the images displayed here were captured using a fluorescent microscope and further studies are required to verify the colocalization of the GFP signal with that of the MitoTracker red using alternative approaches such as confocal microscopy. Western analysis detected two bands (Figure 3.8D) at ~32 kDa (upper band) and ~27 kDa (lower band) which could represent the PfHsp70-3_Nterm-GFP prior to and after processing by the mitochondrial processing peptidase (Gakh, et al., 2002; Ito, 1999). The predicted molecular mass of the signal sequence for PfHsp70-3 is ~4.55 kDa. The cytoplasmic localization of the GFP signal may be attributed to the unprocessed form of the PfHsp70-3_Nterm-GFP protein potentially following synthesis prior to import that is detected at ~32 kDa on the western blot (Figure 3.8D).

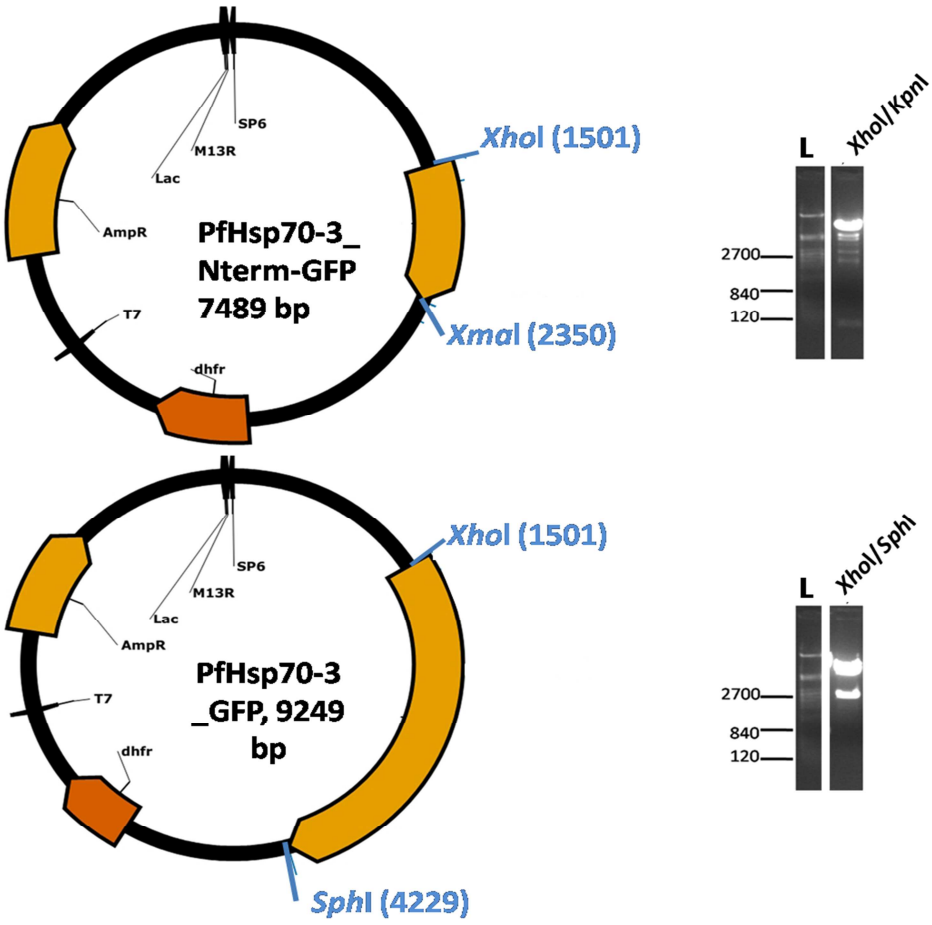

Figure 3.7: PfHsp70-3 plasmids used for transfection. The plasmid maps designed using the PlasmaDNA software (Angers-Loustau, et al., 2007) and associated diagnostic restriction analysis gels for the PfHsp70-3 transfection plasmids. Both plasmids confer ampicillin resistance when transformed into *E. coli* as indicated (AmpR; β-lactamase coding sequence) and confer WR99210 resistance (dhfr; Dihydrofolate reductase coding sequence) when transfected into *P. falciparum* parasites. Upper panel: plasmid map (left) for PfHsp70-3 signal sequence tagged to GFP on the C-terminus inserted between *Xho*I and *Kpn*I and an associated restriction digest. Lower panel: plasmid map for the full length PfHsp70-3 containing an internally fused GFP gene sequence and an associated restriction digest (right). Restriction digests of the two plasmids were ran on a 1% agarose gel. L, DNA ladder; bp, basepairs.

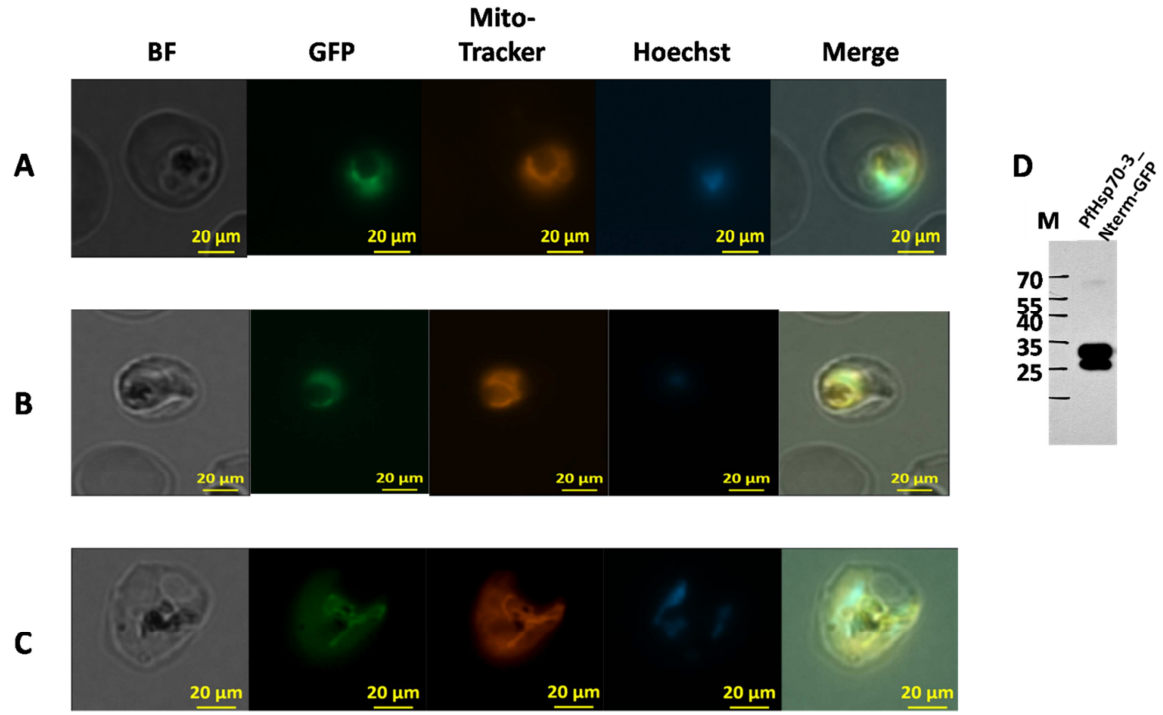

Figure 3.8: PfHsp70-3 localizes to the mitochondrion. (**A** and **B**) Live cell imaging of trophozoite stage and (**C**) schizont stage parasites stained with MitoTracker red to visualize the mitochondrion and with Hoechst 33258 to visualize nuclei staining. BF; bright field, Merge: GFP and Hoechst and MitoTracker red plus BF. The images were pseudocoloured following capture. **D**) Western analysis of the PfHsp70-3_NTerm-GFP transfectants using the anti-GFP antibody. Lane M, molecular mass marker.

3.3.5 Expression and purification of PfHsp70-3m

This study showed that both Pfj1 and PfHsp70-3 localized to the mitochondrion and lead to the hypothesis that Pfj1 is a potential cochaperone for PfHsp70-3. To examine such a hypothesis, the biochemical properties and interactions of the two proteins ought to be further investigated. Such characterization requires the availability of purified proteins that are

active. Indeed, the purification of PfHsp70-3 and Pfj1 would allow for the chaperone-cochaperone interactions to be studied using biochemical assays. The pQE30-PfHsp70-3 expression plasmid coding for the PfHsp70-3m protein was successfully engineered (Figure 3.9A) and subsequently used for protein expression studies. The coding sequence for the expression of this protein was codon optimized to improve expression in *E. coli* host cells.

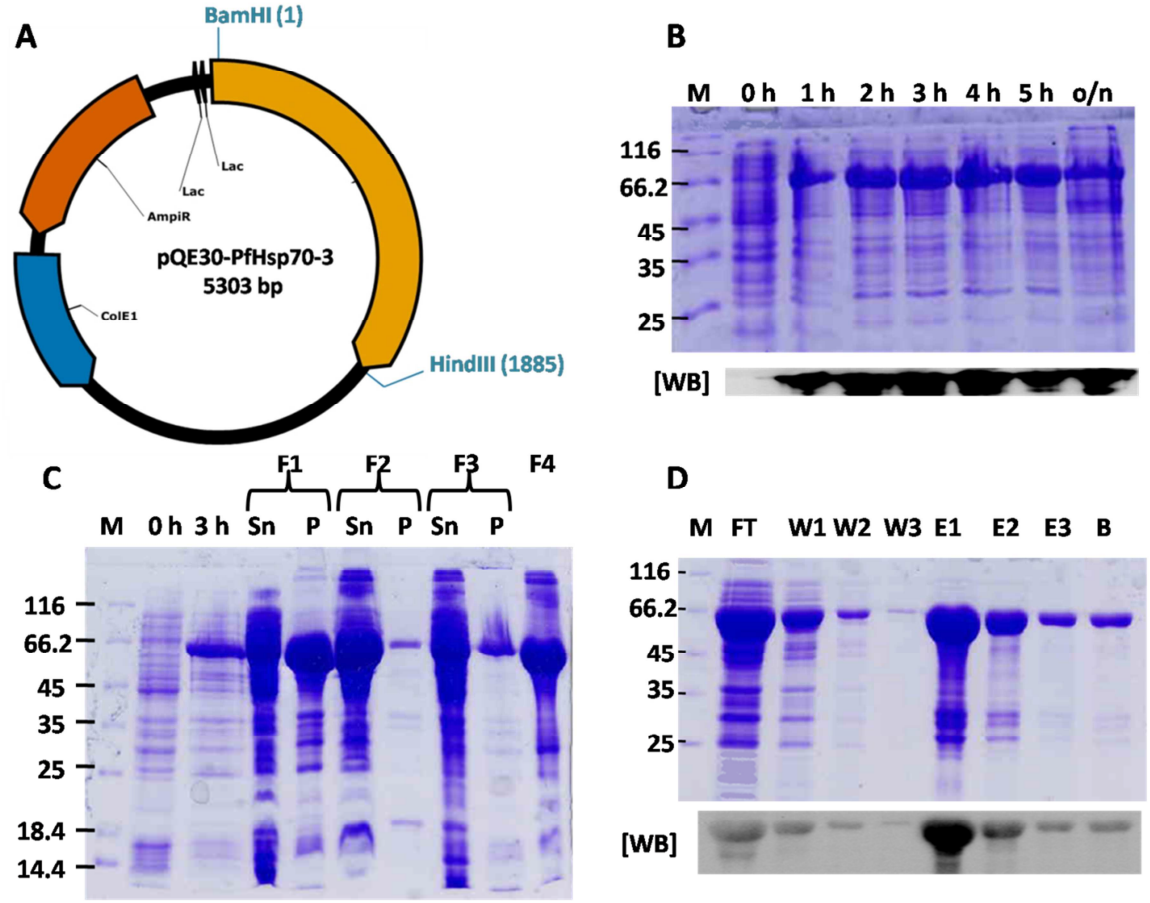

Figure 3.9: Heterologous expression and purification of PfHsp70-3m. A) Plasmid map for pQE30-PfHsp70-3 designed using PlasmaDNA software (Angers-Loustau, et al., 2007). The plasmid confers for ampicillin resistance when transformed in *E. coli* cells as indicated (AmpiR; β–lactamase coding sequence). The 6xHis-tag segment is upstream of the coding region with the genes inserted between *Bam*HI and *Hind*III restriction sites. The origin of replication (ColE1 origin) and the region coding for LacZ alpha are also shown in the plasmid map. **B**) SDS–PAGE (12%) analysis of the PfHsp70-3m total protein extracts prepared from *E. coli* M15[pREP4] cells transformed with pQE30-PfHsp70-3 and induced with 1 mM IPTG. Lane M; molecular mass marker, lane 0 h; non–induced sample, lanes 1 h – 5 h; induced samples taken hourly for five hours, lane o/n; overnight induced sample. An associated western blot [**WB**] analysis for the detection of PfHsp70-3m using anti-His antibody is provided. **C**) SDS–PAGE (12%) analysis of the solubility of PfHsp70-3m on total protein extracts prepared from *E. coli* M15[pREP4] transformed with pQE30-PfHsp70-3. Lane F1, no solubilizing agent used; lane F2, 7.5% sarcosyl; lane F3, 0.1% PEI; lane F4, 8M

urea. Sn = supernatant fraction, P = pellet fraction. **D**) SDS–PAGE (12%) and Western analysis of the fractions collected during PfHsp70-3m protein purification. Lane FT, flow-through; Lane W1 – W3, wash 1 up to wash 3; Lane E1 – E3, elution 1 up to elution 3; Lane B, bead fraction.

The successful engineering of the pQE30-PfHsp70-3 plasmid that encodes for the PfHsp70-3m protein allowed for expression studies to be conducted in the *E. coli* host system. SDS-PAGE analysis of whole cell lysates of the *E. coli* M15[pREP4] strain transformed with pQE30-PfHsp70-3 showed induction of a distinct band at ~70.4 kDa, the expected size of PfHsp70-3m (Figure 3.9B). Western analysis using the anti-His antibody confirmed that the induced protein observed on the SDS-PAGE was PfHsp70-3m. The successful induction of PfHsp70-3m, allowed for solubility studies to be conducted. The PfHsp70-3m protein was observed to associate with the pellet fraction (Figure 3.9C; lanes F1) and therefore solubilizing agents were used to enhance its solubility. The lysate fractions were sonicated in the presence of sarcosyl (Figure 3.9C; lane F2), or 0.1% PEI (Figure 3.9C; lane F3), or denatured through the use of 8 M urea (Figure 3.9C; lane F4) prepared in lysis buffer. SDS-PAGE analysis of the supernatant and pellets of the respective fractions showed that the solubilizing agents resulted in solubilization of PfHsp70-3m thereby allowing subsequent purification using sarcosyl. SDS-PAGE analysis of fractions collected during its purification showed that the protein bound to the nickel charged beads with almost no protein being lost at the third wash (lane W3). However, some of the produced protein was present in the flow through (Figure 3.9D, lane FT). The first and second elutions displayed a major band at ~70.4 kDa depicting good protein yields but contained other minor bands considered as degradation products or contaminants. Elution three also gave good protein yields and the purity was considered to be better than that of prior elutions as no other bands were observed hence resulting in its successful purification. Western analysis using the anti-His antibody confirmed that the protein purified was PfHsp70-3m (Figure 3.9D).

3.4 Discussion

The cellular localization of a protein provides the environment where a protein operates and can therefore be used for functional prediction and identification of interacting partners (Rost, et al., 2003). One of the objectives here was to validate the localization of Pfj1 and study its

expression in the intraerythrocytic stage of *P. falciparum* development. To fulfill this objective, the pQE30 protein expression system using a codon optimized sequence coding for Pfj1m was used for expression and purification studies of this protein. The purification of Pfj1m would have allowed for the production of an antibody against the full length mature protein that would be subsequently used for cell-biological experimentation and biochemical characterization. The Pfj1m protein proved recalcitrant to expression using the approaches adopted in this study. The low induction of expression of this J protein implies that it is potentially toxic to the *E. coli* host system. Pfj1 has previously been purified in two previous studies (Kumar, et al., 2010; Misra and Ramachandran, 2009). However, unlike this study, these two studies used the wild type *Pfj1* coding sequence cloned into a pQE30 expression system and the protein was successfully purified following co-transformation with the RIG plasmid that helps to overcome codon bias present in *P. falciparum* proteins (Baca and Hol, 2000).

The peptide directed approach for antibody production was sought following unsuccessful attempts with the purification of the full length Pfj1 protein. The anti-Pfj1 antibody, designed against a peptide region selected at the unique C-terminal region of Pfj1, was successfully raised in mice. The antibody detected two bands that ran at a lower molecular mass compared to that expected for the mature form of Pfj1 when tested on *P. falciparum* lysates prepared at the trophozoite stage. The bands detected by the antibody were considered to be degradation products of the mature protein and could imply that Pfj1 is highly unstable. Alternatively, the antibody might have been nonspecific, detecting other proteins running at the observed molecular masses. However, the anti-Pfj1 antibody specifically detected the Pfj1m recombinant protein derived from whole cell lysates of *E. coli* M15[pREP4] producing the protein. The anti-Pfj1 antibody could therefore not be used for the detection and further characterization studies related to Pfj1. Unlike the result from this study, the mature form of Pfj1 has previously been detected at the expected size (69 kDa) using antibodies raised against the Pfj1 protein (Kumar, et al., 2010). Kumar and colleagues additionally observed degradation products at different molecular masses and concluded that Pfj1 is a rather unstable protein (Kumar, et al., 2010).

In silico analysis of the upstream region of the *Pfj1* gene did not reveal any additional N-terminus region upstream of the start site of Pfj1 as suggested by Kumar and colleagues (2010). Indeed, analysis of the gene structure as detailed in chapter two showed that Pfj1 is conserved across the *Plasmodium* species whose genomes have been sequenced.

Additionally, the start site for Pfj1 as annotated in PlasmoDB has previously been shown (Aurrecoechea, et al., 2009; Watanabe, 1997). However, the protein sequence determined by Watanabe varies from the one reported in PlasmoDB in the number of amino acids and the amino acid sequence at the C-terminus (Watanabe, 1997). Watanabe showed that Pfj1 possesses 627 amino acids unlike the 672 amino acids depicted by PlasmoDB. Additionally, the last 24 amino acids in the Pfj1 sequence determined by Watanabe differ from those depicted by PlasmoDB. These discrepancies show the lack of consistency in the determined full length sequence for Pfj1. The gene sequencing results generated in this study from cloning experiments cannot be used to validate the upstream and downstream regions of the *Pfj1* gene since the primers were designed to anneal to the 5' start site and the 3' termination site. However, sequence alignment of the amplified fragment shows that it is entirely identical to that predicted by PlasmoDB thereby supporting the gene model depicted by PlasmoDB.

Determination of the localization of Pfj1 by transfection of plasmids expressing the full length Pfj1 protein fused to either GFP or the Strep-tag II constructs was not possible as no positive clones were obtained following transfection with these plasmids. Transfectant clones were only obtained using the Pfj1-Nterm-GFP plasmid construct implying that the other two plasmids may have encoded for proteins that possibly affected the survival of resistant clones. Indeed, the full length Pfj1 protein fused to GFP may have been unable to attain its native conformation thereby leading to its aggregation. Alternative explanations could be that the GFP tag impaired the localization of Pfj1, or the timing and levels of the expressed protein were incorrect and toxic. Such properties could lead to a toxic protein and therefore affect the survival of transfectants. The fusion of the C-terminus of Pfj1 with a smaller tag such as the strep-tag II used in this study was intended to circumvent the problems associated with a larger fusion tag such as GFP. The transfection of the Pfj1-strep plasmid did not give any positive clones either. This may highlight, among other reasons, the important role the C-terminal domain plays in the functioning of Pfj1. The pARL2-GFP plasmid used in this study is under the control of the *P. falciparum* chloroquine resistance transporter (PfCRT) promoter which could play an important role in the expression dynamics of fusion proteins and therefore affect the establishment of transfectant parasite populations. This can however be avoided by using the endogenous Pfj1 promoter in future studies. The mitochondrial localization of Pfj1 needs to be revisited using other approaches before solid conclusions can be made. This is based on the observation that antibodies that could be used for

immunofluorescence experiments as well as transfection with full length Pfj1 transfection constructs approaches were not successful. Additionally, for transfection, the constructs were not under the control of an endogenous promoter. As such, integration of the Pfj1 sequence fused with different tags into the parasite genome would ensure regulation of expression by the endogenous promoter and is more attractive in future studies and such an approach has been successfully applied for other proteins (Crabb and Cowman, 1996).

Localization studies conducted here revealed that Pfj1 resides in the mitochondrion and not in the apicoplast as previously shown (Kumar, et al., 2010). The apparent mitochondrial localization of the GFP signal was verified by co-staining with the MitoTracker red and immunolocalization of the ACP that is often used as an apicoplast marker (Waller, et al., 2000). Observations made in this study are not consistent with those previous made by Kumar and colleagues as well as those obtained using in silico prediction programs. The mitochondrial localization prediction program PlasMit (Bender, et al., 2003) predicts Pfj1 to be non-mitochondrial whereas Target P (Emanuelsson, et al., 2000; Nielsen, et al., 1997) predicts mitochondrial localization. Both PATs and PlasmoAP programs for the prediction of apicoplast-target sequences (Foth, et al., 2003; Zuegge, et al., 2001) support apicoplast localization albeit with shortfalls in the fulfillment of the required criteria. The luminal targeting of apicoplast proteins is described as a two step process mediated by a bipartite N-terminal presequence that consists of a signal peptide for entry into the secretory pathway and a transit peptide for subsequent import into the apicoplast (Ralph, et al., 2004; Waller, et al., 1998; Waller, et al., 2000). Pfj1 does not appear to fulfill the two requirements since the software depicts it to have a recessed transit peptide without a signal peptide. The localization of Pfj1 to the mitochondrial matrix was previously proposed by Watanabe (1997) who highlighted a putative mitochondrial import signal in Pfj1. However, a more elaborate study is required to verify whether Pfj1 localizes to the matrix as proposed. A search for putative Pfj1 homologs in other eukaryotic and prokaryotic systems proved daunting since its C-terminus bears an extended region that shows no significant homology with other proteins. Most of the hypothetical homologues of Pfj1 such as Mdj1 in yeast, Tid1 in humans, and Gametophytic Factor 2 (GFA2) in *Arabidopsis thaliana* have been shown to have less well conserved C-terminal domains (Christensen, et al., 2002; Lu, et al., 2006; Rowley, et al., 1994).

The mitochondrial localization of Pfj1 allowed the study to hypothesize PfHsp70-3 as a potential chaperone partner. Previous phylogenetic analysis has shown that PfHsp70-3

clusters with other mitochondrial Hsp70s from eukaryotic systems and with prokaryotic Hsp70 homologues (Shonhai, et al., 2007). This allowed the study to prioritize the localization of PfHsp70-3 in lieu of further cell-biological and biochemical characterization. Plasmids were engineered coding for GFP fused to either the signal sequence or the full length PfHsp70-3. However, for the full length PfHsp70-3 plasmid constructs, the GFP sequence was fused internally before the ATPase domain to avoid potential negative effects by the tag such as masking the lid domain present in the C-terminus. This study indicated that the predicted signal sequence for PfHsp70-3 was sufficient to localize the GFP to the mitochondria although partial fluorescence was also observed in the cytoplasm. However, the full-length fusion construct did not generate positive clones implying that the fusion protein may have led to a lethal phenotype. Further studies are required to validate the localization of PfHsp70-3 using alternative full length fusion constructs or through specific antibodies raised against it.

It is possible that Pfj1 is a cochaperone of PfHsp70-3 in the mitochondria and to investigate such partnership, PfHsp70-3 was purified. High levels of PfHsp70-3m protein production were observed following induction. However, the purification of this protein was only possible through the use of solubilizing agents. PfHsp70-3m appeared to have a high tendency to associate with the pellet fraction under the buffer conditions adopted. This observation is not unique since in yeast the mitochondrial Hsp70s (mtHsp70/Ssc1p) has been shown to have a high propensity for self aggregation that is normally prevented in the presence of mtHsp70 escort protein 1 (Hep1) (Sichting, et al., 2005). Hep1 resides in the mitochondrial matrix and has been shown to be important for the maintenance of mtHsp70 structure and function and has been used in co-expression studies with mtHsp70 to allow for solubilization, purification and maintenance of activity (Blamowska, et al., 2012; Sichting, et al., 2005; Zhai, et al., 2008). Through sequence searches (data not shown) using the yeast Hep1 (YNL310c) in PlasmoDB, this study has identified a putative *P. falciparum* mtHsp70 escort protein (PF14_0197) which we term PfHep1. Additionally, Hep1 has been shown to be conserved across eukaryotic systems, such co-expression with the putative protein should be prioritized and investigated.

3.5 Conclusion

This study has shown that Pfj1 and PfHsp70-3 localize to the mitochondria in the intraerythrocytic stage of *P. falciparum* development. Here, we propose that Pfj1 is a potential cochaperone for PfHsp70-3. The study has highlighted the difficulties associated with the transfection of plasmids coding for full length fusion proteins adopted in this study but has served to lay a foundation for further cell biological characterization. Indeed, a more elaborate study is required to understand the roles of these two proteins in the mitochondria. Further, different approaches from those adopted in this study may be required to enhance the heterologous expression and purification of Pfj1 and PfHsp70-3. The role of the putative PfHep1 in the purification and biochemical characterization of PfHsp70-3 should also be prioritized.

CHAPTER FOUR

Cell-biological characterization of PFB0595w

4.0 Introduction

The plasmodial Hsp70-J protein chaperone complement is thought to play an essential role in protein homeostasis during vector-host transitions that are associated with differences in temperature and general physiology (Oakley, et al., 2007; Pallavi, et al., 2010). Of the six Hsp70 homologues encoded by the genome of *P. falciparum*, the 74 kDa PfHsp70-1 is the most studied (Biswas and Sharma, 1994; Joshi, et al., 1992; Pesce, et al., 2008; Shonhai, et al., 2008). PfHsp70-1 is thought to play both basal and stress induced proteostatic roles in the cytosol and nucleus (Botha, et al., 2011; Joshi, et al., 1992; Pesce, et al., 2008). Characterization of such chaperone-cochaperone interactions and the identification of client proteins are essential for the understanding of the roles of PfHsp70-1 within the parasite. However, experimental characterization of the predicted J protein cochaperones for PfHsp70-1, which is crucial if any inferences on functional partnerships are to be made, is still in its infancy. Of the several J proteins predicted to reside in the cytosol, only two have been experimentally studied and implicated as cochaperones of PfHsp70-1 (Botha, et al., 2011; Pesce, et al., 2008).

PFB0595w is a typical type II J protein that does not have a putative targeting presequence and is proposed to reside in the parasite cytosol and act as a cochaperone for PfHsp70-1 (Botha, et al., 2007). Using in silico analysis and yeast two-hybrid studies, PFB0595w has been predicted to interact directly with PfHsp70-1 and other putative proteins such as antigen 332 (PF11_0507), myosin-like protein (PFF0675c), PfHsp40, and ubiquitin protein ligase (MAL8P1.23) (LaCount, et al., 2005; Pavithra, et al., 2007). PfHsp70-1 has recently been shown to complement for yeast mutants lacking two cytosolic Hsp70s, Ssa1 (71% identity and 97% similarity) and Ssa2 (69% identity and 83% similarity), under normal and stress conditions (Bell, et al., 2011). The orthologue of PFB0595w in yeast, Sis1, has been shown to functionally interact with Ssa1 (Aron, et al., 2005; Qian, et al., 2002). Sis1 is associated with translating ribosomes (Zhong and Arndt, 1993) and prion propagation (Higurashi, et al., 2008). Its human orthologue, DnaJB1 (Hdj1), has also been shown to reside in the cytosol (Kampinga and Craig, 2010).

This study proposed to determine the expression and localization of PFB0595w in the intraerythrocytic stages of *P. falciparum* development. The expression of a protein is important for cellular functioning and may provide clues to its functions (White, et al., 1999).

It may additionally provide clues to its interacting partners or pathways such as those related to normal and stress conditions. As discussed in chapter three, the localization of a protein is important if any inferences on function and/or interacting partners are to be made (Rost, et al., 2003).

4.1 Objectives

This study aimed to commercially raise peptide-directed antibodies and determine the expression and localization of PFB0595w in the intraerythrocytic stages of *P. falciparum* development. The study also sought to investigate PFB0595w as a cochaperone for PfHsp70-1.

Specifically, this study aimed

i. To design and commercially raise a peptide-directed antibody specific to PFB0595w.
ii. To confirm the presence of PFB0595w in the intraerythrocytic stage of *P. falciparum* development and assess the effect of induced heat shock on its expression.
iii. To determine the localization of PFB0595w through immunofluorescence microscopy.
iv. To generate transfection plasmids that encode for PFB0595w fused to either GFP or Strep-tag II.
v. To assess the solubility of PFB0595w and PfHsp70-1.

4.2 Materials and methods

4.2.1 Peptide directed anti-PFB0595w antibody design and production

Sequence analysis for the identification of an epitopic region in the C-terminus to be used for antibody design and production was carried out as described in section 3.2.3.1. The region selected (shown in Figure 4.1) was commercially synthesized by the GenScript Corporation (Piscataway, New Jersey, USA). The GenScript Corporation further used the synthesized peptide to raise antisera in mice after collection of pre-immune serum and subsequently purified the fractions using protein A.

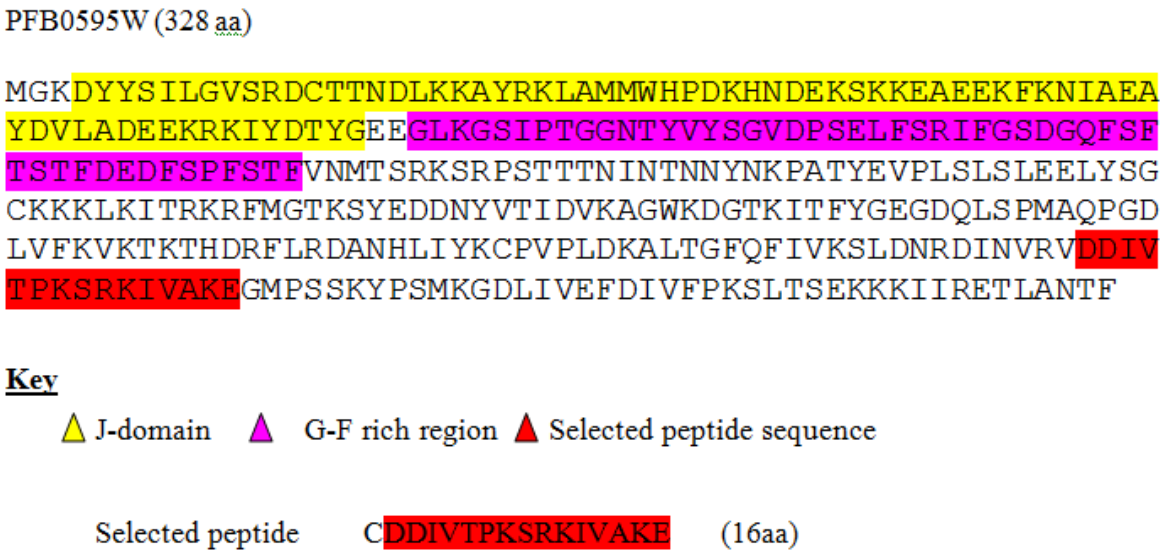

Figure 4.1: The amino acid sequence depicting the conserved domains and the identification of the unique peptide with potential for design of the PFB0595w antibody. As a general criterion to choose the peptide, regions that are predicted to be surface exposed, soluble, have high peptide chain flexibility, possess hydrophilic amino acid stretches, and have high charge density were assessed were assessed using GeneRunner software (version 3.05; Hastings Software Inc.). The peptide selected was used to query the predicted proteomes of *P. falciparum* and humans to avoid potential cross-reactivity.

4.2.2 Parasite culture

P. falciparum (clone 3D7) was cultured as described in section 3.2.3.2.

4.2.3 Preparation of *P. falciparum* lysates and detection of PFB0595w

Preparation of lysates from *P. falciparum* (clone 3D7) was carried out as described in section 3.2.3.3. Primary antibodies used included anti-PFB0595w (1:2500 dilution) while anti-PfHsp70-1 (1:5000 dilution) served as a positive control. HRP-conjugated goat anti-mouse (1:5000 dilution) (GE Healthcare, UK) and goat anti-rabbit (1:5000 dilution) (Cell signaling technology, USA) secondary antibodies were used.

4.2.4 PFB0595w plasmid constructs for transfection

The genomic sequence coding for PFB0595w contains two introns and therefore the coding sequence was amplified by polymerase chain reaction (PCR) from *P. falciparum* cDNA (clone 3D7). The reverse primers were designed to amplify the coding sequence without the stop codon to allow fusion of the GFP and strep-tag II tags at the C-terminus. The cDNA was amplified using a forward primer (Hsp40_F_*Xho*I: 5'-CC**CTCGAG**ATGGGGAAGGATTATTATTCAATATTAGG-3') with an *Xho*I restriction site (highlighted in bold) and a reverse primer (Hsp40_R_*Kpn*I: 5'-CC**GGTACC**GAATGTATTTGCCAATGTTTCTC-3') with a *Kpn*I restriction site (highlighted in bold). The amplified PFB0595w PCR product was gel purified and digested with *Xho*I-*Kpn*I and ligated into a *Xho*I-*Kpn*I restricted pARL2-GFP vector (Przyborski, et al., 2005), creating the pARL2_PFB0595w_GFP construct referred here as PFB0595w-GFP (Figure 4.4A). A diagnostic restriction digest (Figure 4.4A) was conducted and followed by DNA sequencing to confirm the integrity of the PFB0595w-GFP construct. To generate a plasmid construct coding for PFB0595w fused to the strep-tag II at the C-terminus, the PFB0595w coding sequence was PCR amplified as above using the Hsp40_F_*Xho*I forward primer and a reverse primer PFB0595w_strep: (5'-**CCCGGG***TCA*<u>TTTTTCGAACTGCGGGTGGCTCCA</u>GAATGTATTTGCC-3'). The *Sma*I restriction site in the PFB0595w_strep primer is highlighted in bold and the sequence coding for the strep tag underlined. A stop codon was introduced after the strep-tag sequence in the primer and is shown in italics. The amplified PFB0595w PCR product was gel purified and digested with *Xho*I-*Sma*I and ligated into a *Xho*I-*Sma*I restricted pARL2-GFP vector creating the pARL2-PFB0595w_strep-tag construct referred here as PFB0595w-strep (Figure 4.4B). This construct was also verified through restriction digest analysis and DNA sequencing.

4.2.5 Parasite transfection

Parasite transfection was carried out as described in section 3.2.3.5. As a positive control for the GFP line, the pARL2-GFP plasmid was also transfected and maintained under similar conditions. As mentioned previously, the integrity of the WR99210 drug was assessed using the parental 3D7 parasite line.

4.2.6 Live cell imaging and western analysis of transfectants

For live imaging of PFB0595w-GFP transfectant parasites, the cells were harvested from culture and washed once with pre-warmed incomplete media. They were then resuspended briefly in incomplete media containing 10 µg/ml Hoechst 33258 (Sigma-Aldrich, Germany) for DNA staining and subsequently resuspended into complete medium after centrifugation (800 xg, 2 min). The parasites were imaged as described in section 3.2.3.6. Images of trophozoite stage parasites were captured even though parasites at the ring and schizont stages were also examined. The pARL2-GFP transfectant parasites served as a positive control while the PFB0595w-strep transfectants and the wild type 3D7 parental strain served as negative controls. Parasite lysates were generated from both the wild type and the transfectants and assessed through western blotting as described in section 3.2.3. Primary antibodies including rabbit anti-GFP (1:2000) (Santa Cruz, USA), rabbit anti-PfHsp70-1 (1:5000), and anti-strep tag II (GenScript, New Jersey, USA) polyclonal antibodies were used for western detection. HRP-conjugated goat anti-mouse (1:5000) (KPL, USA) and donkey anti-rabbit (1:5000) secondary antibodies were used.

4.2.7 Indirect immunofluorescence microscopy

For indirect immunofluorescence microscopy, the 3D7 parental clone and PFB0595w-GFP transfectants were cultured as described above. The parasites were harvested and processed using the paraformaldehyde/glutaraldehyde method as described in section 3.2.3.7. Subsequently, the cell pellet was then incubated in blocking buffer (3% (w/v) BSA in PBS) for 2 hours at room temperature. The parasite pellet was incubated overnight with primary antibodies including mouse anti-PFB0595w (1:50 dilution) or rabbit anti-PfHsp70-1 (1: 500 dilution) diluted in the blocking buffer at 4^{o}C on a gentle rocking platform. The cells were then washed three times with PBS at 10 minute interval on the same rocking platform. This was followed by incubation with secondary antibodies including Alexa Fluor® 488 donkey anti–mouse IgG (Invitrogen, USA) or Alexa Fluor® 546 chicken anti–rabbit IgG (Invitrogen, USA) both at 1: 250 dilution in blocking buffer in the dark for 1 hour at room temperature on a rocking platform. The cells were subsequently washed as described above and Hoechst 33258 (50 ng/ml) diluted in PBS was included in the last washing step to stain the nuclei. The cells were mounted and images captured using an Axio Observer inverse epifluorescence

microscope system equipped with Axiovision 4 software (Zeiss, Jena, Germany) as described in section 3.2.3.7. Controls used in this experiment included incubating the fixed parasites with either the primary antibody alone or secondary antibody alone. Additionally, wild type 3D7 parasites processed without inclusion of any antibodies were also used as negative controls.

Methanol fixation of parasites (Wickham, et al., 2001) was also attempted as an alternative approach to the paraformaldehyde/glutaraldehyde fixation method. Here, microscopy smears prepared on glass slides were fixed briefly with cold methanol. The slides were then incubated with the blocking buffer and subsequently processed as described above.

4.2.8 Intraerythrocytic time course expression of PFB0595w

P. falciparum parasites (clone 3D7) were cultured as described above and synchronized by sorbitol lysis at the ring stage. For the time course experiment, the parasites were equally split into six flasks and incubated at 37°C. Parasite lysates were generated at 8 hour intervals of the 48 hour intraerythrocytic parasite development and frozen at -80°C until use. The expression of PFB0595w was analyzed by SDS-PAGE gel and western blotting as described in section 3.2.3.3. As a loading control, rabbit anti-glycophorin antibody (Thermo scientific, USA) (1:4000 dilution) and HRP-conjugated donkey anti-rabbit (1:5000 dilution) secondary antibodies were used.

4.2.9 Heat shock inducibility of PFB0595w

For the heat shock experiment, synchronized parasites were cultured as previously described and equally split in to 3 flasks at the trophozoite stage. Heat shock was applied by incubating subcultures at 37°C (control), 41°C (heat shock) and 43°C (heat shock) for 1 hour. The expression of PFB0595w was analyzed by SDS-PAGE gel and western blotting as described in section 3.2.3.3. Glycophorin was used as a loading control as described in section 4.2.8.

4.2.10 Solubility study

For the solubility study, parasitized erythrocytes at 5-10% parasitemia were harvested and saponin lysed as described in section 3.2.3. The parasite pellet obtained was resuspended in lysis buffer (150mM NaCl, 50mM Tris HCL pH 7.5, 0.1% NP-40 (Nonidet P40; Roche, Switzerland), 1 mM PMSF (Roche, Switzerland), and protease inhibitor cocktail (Sigma, Germany) as described (Gitau, et al., 2012; Pesce, et al., 2008). Cell lysis was enhanced through three freeze/thaw cycles using liquid nitrogen followed by separation of the soluble fraction from the pellet through centrifugation (13000 xg, 30 min) at 4°C. The pellet was washed once with ice cold PBS and both fractions analyzed through SDS-PAGE and Western blotting as described in section 3.2.3.3. Detection of PfHsp70-1 was used as a control for the supernatant fraction while detection of glycophorin was used as a control for the pellet fraction.

4.3 Results

4.3.1 PFB0595w is expressed in the intraerythrocytic stage of parasite development

As a starting point for the cell-biological characterization of PFB0595w, the study sought to determine whether PFB0595w was expressed in the intraerythrocytic stage of parasite development. To this end, trophozoite stage parasites were subjected to western analysis and the antibody generated against PFB0595w was used for detection. A protein was detected at 39 kDa, the expected molecular mass for PFB0595w (Figure 4.2A). To verify that the detected protein was PFB0595w and not any other protein running at a similar molecular mass, a control lysate generated from transfectants expressing PFB0595w fused with strep tag II at the C-terminus (PFB0595w-strep) was used. The expected molecular mass for the PFB0595w-strep protein is 40 kDa since the strep-tag II used comprised of eight amino acids (WSHPQFEK) bearing a molecular mass of 1 kDa. Two bands with approximately 1 kDa separation on the same western blot were detected when the anti-PFB0595w antibody was used for detection of the PFB0595w-strep parasite lysate (Figure 4.2A). The lower and the upper bands detected would reflect the endogenous PFB0595w and the PFB0595w-strep proteins respectively. When the anti-strep tag antibody was used for detection on the same set

of lysates, a single band from the PFB0595w-strep parasite lysates was detected (Figure 4.2B) reflecting the specificity of both antibodies. PfHsp70-1 was used as a positive control for the lysates used (Figure 4.2, middle panel).

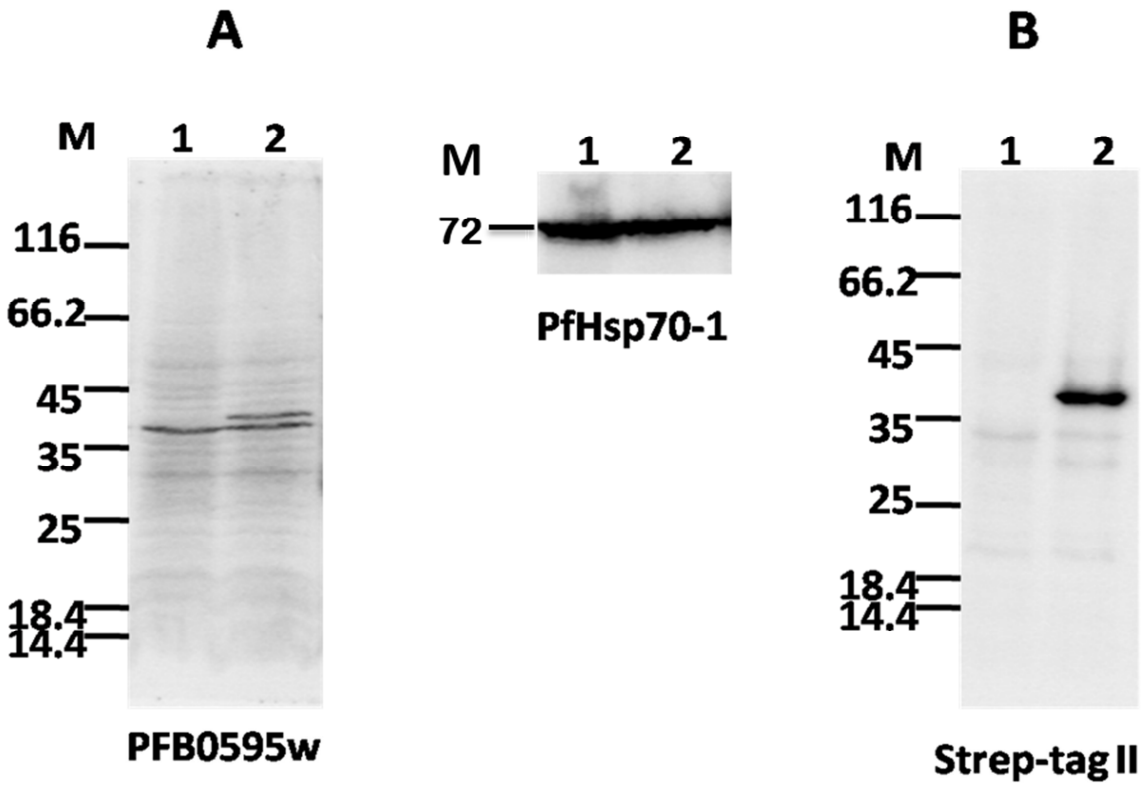

Figure 4.2: PFB0595w is expressed in the intraerythrocytic stage of *P. falciparum* development. The detection of PFB0595w in *P. falciparum* strain 3D7 (lane 1) and PFB0595w-strep transfectant line (lane 2) by western analysis using the anti-PFB0595w (**A**) and anti-strep-tag II antibodies (**B**). The middle panel shows western detection of PfHsp70-1 using anti-PfHsp70-1 antibody.

4.3.2 The expression of PFB0595w is slightly induced by heat shock treatment

Following detection of PFB0595w, the study sought to find out whether the expression of this J protein is upregulated by heat shock. Parasites in the trophozoite stage were incubated under normal (37^{o}C) and heat-shock (41^{o}C and 43^{o}C) conditions and an equal number of infected erythrocytes were analyzed using SDS-PAGE (Figure 4.3A) and western analysis (Figure 4.3B). PfHsp70-1 was used as a positive control for heat-shock associated upregulation while glycophorin, a glycoprotein present on the membranes of erythrocytes, was used as a loading control as previously described (Botha, et al., 2011; Tomita and

Marchesi, 1975). The levels of glycophorin did not change across the lanes suggesting that the cells loaded per lane were equivalent. PFB0595w was consistently detected at 37^{o}C and its expression was slightly upregulated following heat shock at 41^{o}C and 43^{o}C (Figure 4.3B) as quantified using densitometry. The observed upregulation of PfHsp70-1 relative to the loading control at the mentioned temperatures confirmed that the heat-shock treatment had been effective.

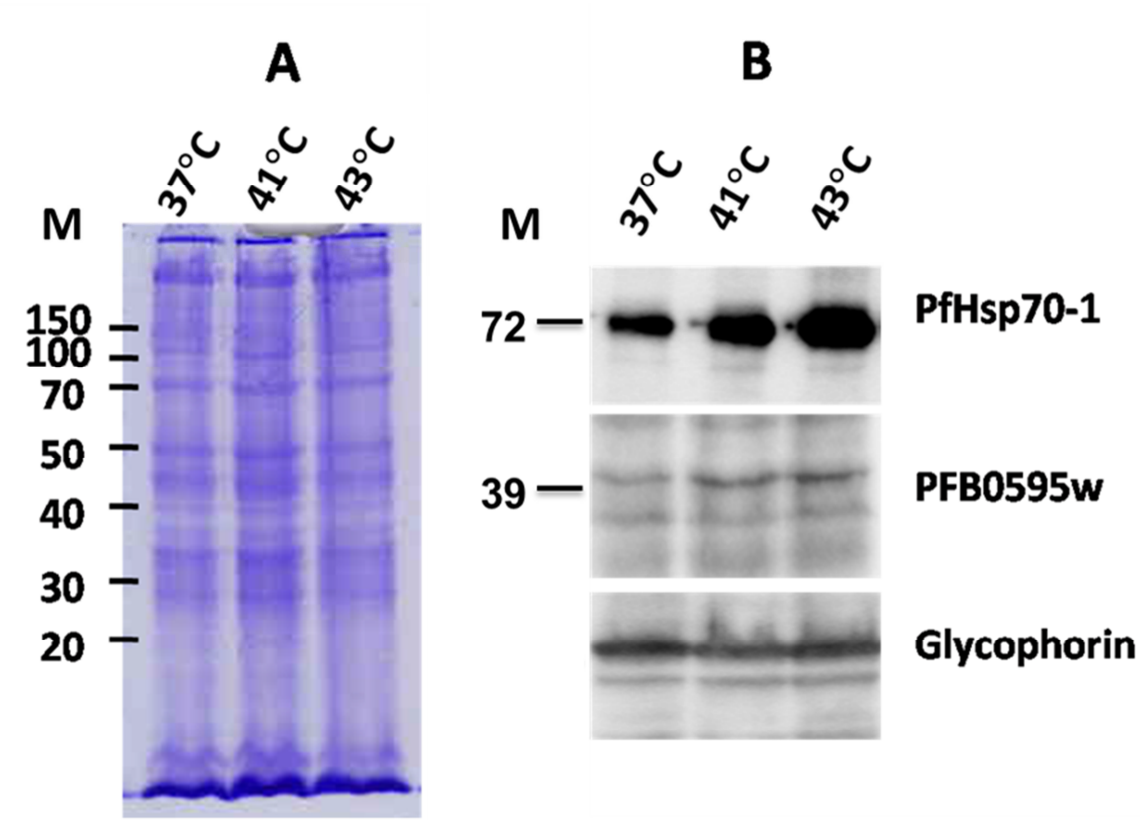

Figure 4.3: PFB0595w is slightly upregulated following heat-shock. A) SDS-PAGE (12%) protein profiles of parasite incubated at 37^{o}C, 41^{o}C, and 43^{o}C for 1 hour. B) Western analysis: detection of PFB0595w, PfHsp70-1 and glycophorin on the same panel of parasite lysates using anti-PFB0595w, anti-PfHsp70-1, and anti-glycophorin antibodies respectively. Note: an equal number of infected erythrocytes were loaded per lane and three independent experiments were carried out.

4.3.3 Preparation of transfection constructs

The detection of PFB0595w at the intraerythrocytic stage allowed this study to validate the predicted cytosolic localization of PFB0595w. Transfection plasmids coding for PFB0595w-

GFP and PFB0595w-strep were successfully obtained and verified using restriction analysis and DNA sequencing (Figure 4.4).

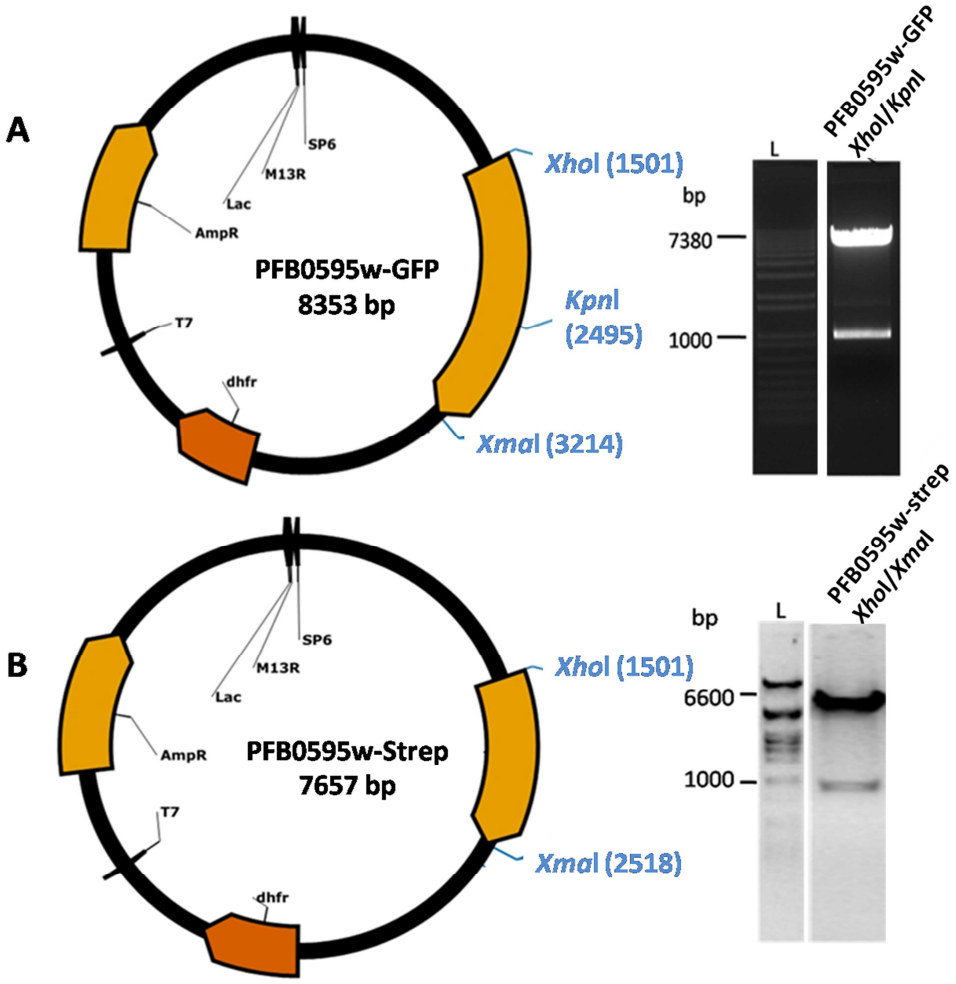

Figure 4.4: PFB0595w constructs used for transfection. The plasmid maps designed using the PlasmaDNA software (Angers-Loustau, et al., 2007) and associated diagnostic restriction analysis agarose gels for the plasmids used for transfection. Both plasmids confer ampicillin resistance when transformed into *E. coli* cells as indicated (AmpR; β-lactamase gene) and confer WR99210 resistance (dhfr; dihydrofolate reductase coding sequence) when transfected into *P. falciparum* clone 3D7 parasites. **A**) Plasmid map for PFB0595w-GFP inserted between *Xho*I and *Xma*I and a restriction digest of the plasmid with *Xho*I and *Kpn*I ran on a 1% agarose gel: L; Ladder, bp; basepairs. **B**) Plasmid map for PFB0595w-strep inserted between *Xho*I and *Xma*I and a restriction digest of the plasmid with *Xho*I and *Xma*I ran on a 1% agarose gel.

The PFB0595w-strep plasmid construct was also used as the strep tag II is arguably smaller in size and may therefore pose less deleterious effects on the functioning of the C-terminal domain in comparison to the GFP tag. The transfectant lines appeared 3-5 weeks following transfection and permanent WR99210 drug selection. The PFB0595w-strep transfectant

parasite line appeared earlier than the PFB0595w-GFP parasite line and multiplied more rapidly relative to the GFP line.

4.3.4 PFB0595w and PfHsp70-1 localize to the parasite cytosol in the infected erythrocyte

For localization purposes, the PFB0595w-GFP transfectant line was used. However, as an additional approach, the antibody raised against PFB0595w was used in indirect immunofluorescence localization studies since it would provide for the detection of the endogenously expressed PFB0595w protein. Microscopy images captured from live transfectant parasites expressing PFB0595w-GFP showed that PFB0595w localizes in the cytosol and potentially to the nucleus of the parasite (Figure 4.5C). A similar localization pattern was observed when the anti-PFB0595w antibody was used in immunofluorescence localization experiments (Figure 4.5B). In both approaches, no fluorescence signal was observed outside the parasite cytoplasm. However, the signal detected could potentially mask staining of intracellular organelles within the cytoplasm. The cytoplasmic localization of PFB0595w was observed in all the parasites examined and at least 20 independent observations were captured. PfHsp70-1 was detected in the parasite cytosol as previously reported (Botha, et al., 2011; Pesce, et al., 2008) (Figure 4.5D). The GFP signal was observed in all the stages of the intraerythrocytic cycle but was more pronounced at the trophozoite stage. No staining was observed on the parental 3D7 parental line that served as a negative control (data not shown). Cytoplasmic localization of the GFP signal was observed for the pARL2-GFP transfectant parasite line that served as a positive control (Figure 4.5A). To confirm that the observed fluorescence was originating from the expression of PFB0595w-GFP and not cross contamination with the vector, western analysis of the transfectant lines was carried out. Western analysis of the PFB0595w-GFP transfectant line using the anti-GFP antibody detected a single band at ~66 kDa, the expected molecular mass of PFB0595w-GFP (Figure 4.5E). No signal was detected in both negative controls (wild type 3D7 clone and PFB0595w-strep parasite lines) (Figure 4.5E). Additionally, a single band was also detected at ~30 kDa for the positive control (pARL-GFP) (Figure 4.5E). PfHsp70-1, used as a control to assess the integrity of the parasite lysates, was detected in all the parasite lines using the anti-PfHsp70-1 antibody (Figure 4.5E).

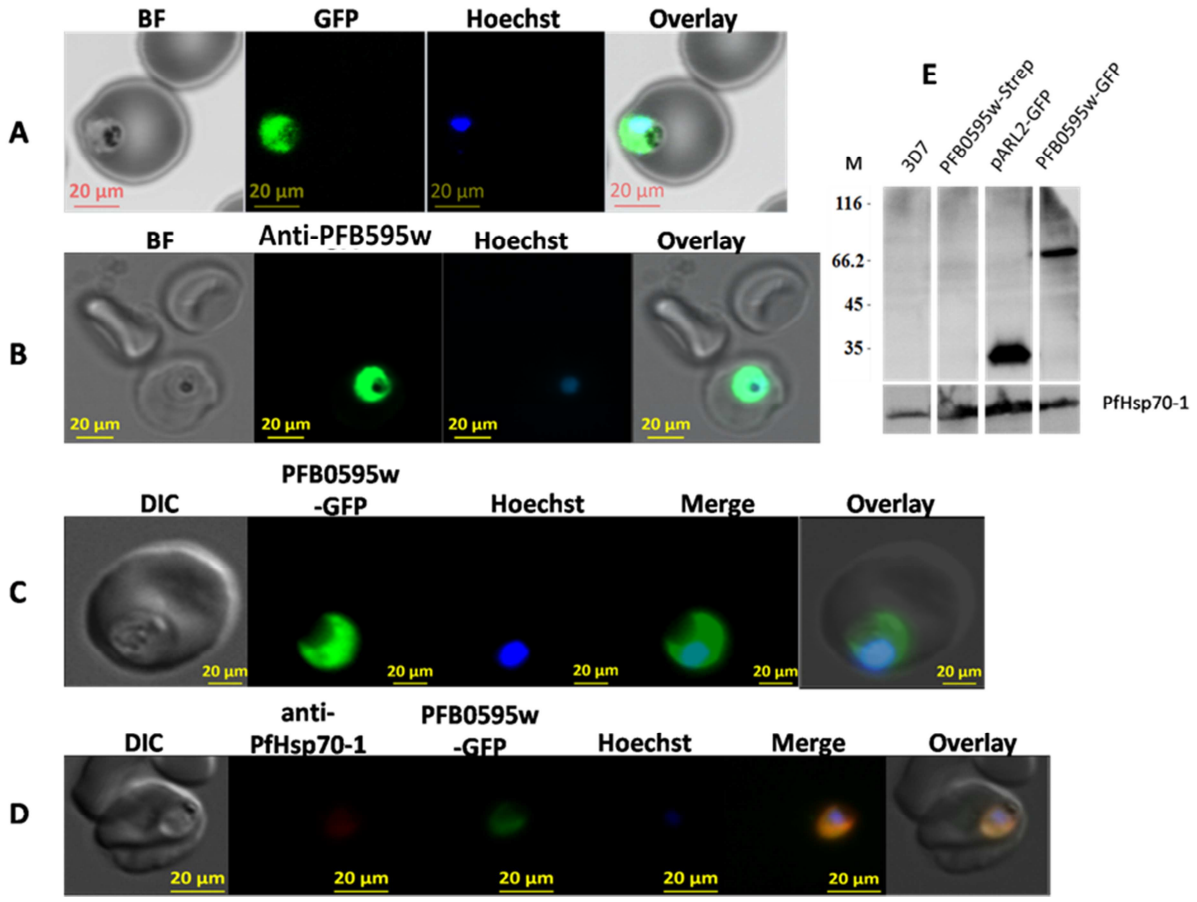

Figure 4.5: PFB0595w localizes to the parasite cytosol in the infected erythrocyte. A) Localization of the GFP signal through live cell imaging of pARL2-GFP transfectants stained with Hoechst 33258 (to visualize the nucleus). BF, Bright field; Overlay, BF plus GFP and Hoechst 33258. **B**) Immunolocalization of PFB0595w using the anti-PFB0595w antibody on fixed wild type clone 3D7 parasites stained with Hoechst 33258. **C**) Localization of the GFP signal through live cell imaging of PFB0595w-GFP transfectants stained with Hoechst 33258. DIC, Differential interference contrast; Merge, PFB0595w-GFP plus Hoechst; Overlay, DIC plus merge. **D**) Indirect immunofluorescence localization of GFP and PfHsp70-1 in PFB0595w-GFP transfectants using the anti-PfHsp70-1 antibody. Merge, anti-PfHsp70-1 plus PFB0595w-GFP and Hoechst; Overlay, DIC plus merge. The images were pseudocoloured following capture. **E**) Western analysis of PFB0595w-GFP transfectants using the anti-GFP antibody. M, Molecular mass marker (kDa); 3D7, wild type clone 3D7 parasites (negative control); PFB0595w-strep, PFB0595w-strep transfectant parasite line (negative control); pARL2-GFP, pARL2-GFP vector transfectant line (positive control); PFB0595w-GFP; PFB0595w-GFP transfectant parasite line.

4.3.5 PFB0595w is expressed maximally at the trophozoite stage

The purpose of the time course experiment was to determine when the maximum expression of PFB0595w occurred during the 48 hour intraerythrocytic cycle. Parasite lysates generated from sorbitol synchronized parasites were generated at six time points in the cycle starting

with the ring-stage of parasite development. Following sorbitol synchronization, at least 90% of the infected erythrocytes contained rings and synchronization was carried out one 48h cycle prior to the experiment. Equal numbers of infected erythrocytes were loaded per lane and subjected to SDS-PAGE and Western analysis. Glycophorin which was used as a loading control confirmed that the loading was equivalent across the lanes (Figure 4.6A). The antiglycophoring A antibody detected a band at 72 kDa that represented the dimer and another band at ~35 kDa representing the monomer (Data not shown). The 72 kDa band was adopted in all the experiments described. SDS-PAGE showed different protein profiles at the different stages of parasites development in the intraerythrocytic stage (Figure 4.6A). The ring stage appeared to have the least amount of protein while the trophozoite and schizont stages appeared to have the highest overall protein levels. In general, parasite progression from the ring stage to the schizont stage is associated with an increase in both parasite protein levels and overall volume. Western analysis using the anti-PFB0595w antibody indicated that PFB0595w is maximally detected at the trophozoite stage of parasite development (Figure 4.6A). PFB0595w was not detected in the ring stage and this may have resulted from low expression of PFB0595w at this stage where overall low parasite protein abundance was observed. Lower levels of expression were observed at the late trophozoite and schizont stages. However, a band (~34kDa) was detected at the 24h and 48h of the intra-erythrocytic development which may represent degradation products of PFB0595w or detection of another protein at that stage. No further experiments were carried out to validate the identity of the lower bands. While the mRNA levels of PFB0595w cannot be directly compared with protein expression, the result from this study show that peak levels of PFB0595w expression coincided with those from the mRNA expression profile (Figure 4.6B). The expression profile as adapted from the PlasmoDB genomic resource shows that PFB0595w is maximally expressed at the trophozoite stage (Figure 4.6B). When the same parasite lysates were probed with the anti-PfHsp70-1 antibody, it was found that PfHsp70-1 was present throughout the parasite intraerythrocytic cycle with higher abundance being observed from the trophozoite to the schizont stage (Figure 4.6A).

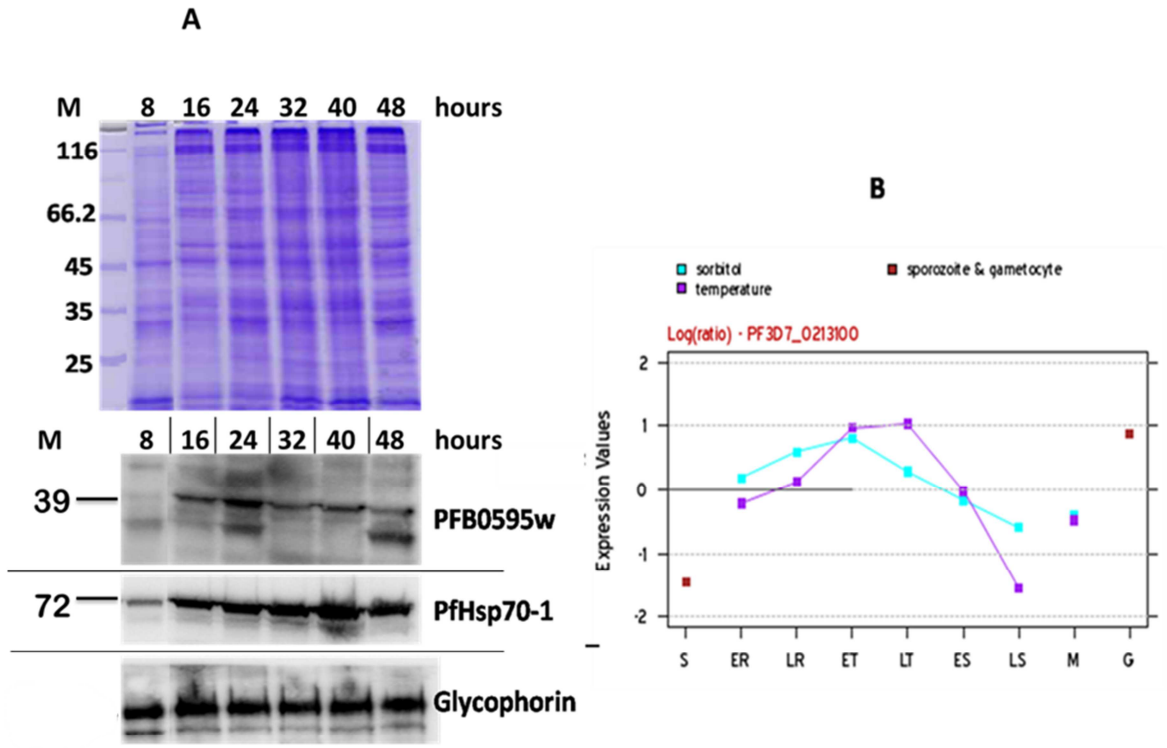

Figure 4.6: Time course expression of PFB0595w and PfHsp70-1 in the intraerythrocytic cycle of parasite development. A) Upper panel: 12% SDS-PAGE gel showing the protein profiles of the highly synchronized parasites at 6 different time points. Lower panel: Associated western blots probed for PFB0595w, PfHsp70-1, and glycophorin. **B**) The transcription profile of PFB0595w at the different stages of parasite development as adapted from PlasmoDB version 8.1 (Aurrecoechea, et al., 2009). Sorbitol, indicates parasite synchronized via sorbitol lysis synchronization. Note: an equal number of infected erythrocytes were loaded per lane and two independent experiments were carried out.

4.3.6 Solubility studies

The solubility study was carried out to investigate whether PFB0595w may be associated with intracellular membranes in the cytosol. Parasites in the trophozoite stage were saponin lysed and the pellet fraction treated with lysis buffer as previously described. Western analysis of the soluble and pellet fraction indicated that PFB0595w was present in the supernatant fraction similarly PfHsp70-1 was also largely present in the supernatant (Figure 4.7). However, PfHsp70-1 was not entirely in the supernatant fraction as some was also observed in the pellet fraction. As expected, glycophorin was present in the pellet fraction even though a minor fraction was also observed in the supernatant (Figure 4.7).

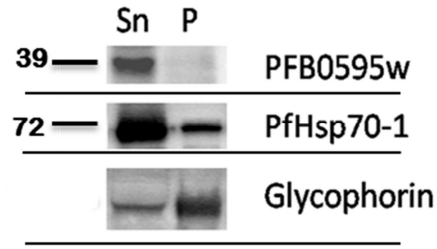

Figure 4.7: Solubility study of PFB0595w. Western analysis of parasite fractions derived from the supernatant and pellet using antibodies specific to PFB0595w, PfHsp70-1, and glycophorin. Sn, supernatant; P, pellet. Note: an equal number of infected erythrocytes were loaded per lane.

4.4 Discussion

Very few J proteins from malaria have been characterized creating a large knowledge-gap in the understanding of the Hsp70-J protein interactions in *P. falciparum*. Cell-biological characterization of predicted Hsp70 and J proteins is crucial for gaining better insights into the expression, localization and interactions of these proteins. Notable differences between the Hsp70-J protein chaperone machinery in parasitic systems relative to the human system will be of interest for the development of drug targets. Previous in silico protein-protein interaction analysis prediction indicated that PFB0595w interacts directly with PfHsp70-1 (LaCount, et al., 2005; Pavithra, et al., 2007). Results from this study confirm that PFB0595w is expressed during the intraerythrocytic cycle of parasite development with maximal levels at the trophozoite stage. The mRNA transcript profile of PFB0595w has been shown to be maximal at the trophozoite stage but with low abundance in the other stages of parasite development (Bozdech, et al., 2003; Llinás, et al., 2006). Taken together, these two observations may point to a correlation between the mRNA and protein profiles. As mentioned previously, Sis1 has been implicated in translation initiation in yeast (Zhong and Arndt, 1993) and while such a role has yet to be investigated for PFB0595w, its maximum expression coincides with high expression activity present during the trophozoite stage of parasite development (Bozdech, et al., 2003; Mamoun, et al., 2001). Proteomic analysis has shown that PFB0595w is also expressed during the sporozoite stage (Lasonder, et al., 2008). Whether its expression at this stage reflects an indirect role of this J protein in sporozoite maturation, motility, infection of the human host or associated metabolic adjustments remains to be determined. The protein profiles presented from the expression analysis highlighted the

low protein levels at the ring stage that increase with parasite development into the schizont stages. Following this observation, the study proceeded to ascertain whether the basal expression is upregulated during heat associated stress. The heat shock experiments were intended to simulate responses by parasites during febrile episodes in malaria patients where temperatures above 37^{o}C are experienced. Experiments relating to heat shock have only been previously been reported for PfHsp40 which was shown to be upregulated following heat shock (Botha, et al., 2011). Here, the expression of PFB0595w was slightly upregulated following heat shock. However, PfHsp70-1 was highly upregulated following heat shock as previously reported (Botha, et al., 2011; Pesce, et al., 2008). The induced expression of both PFB0595w and PfHsp70-1 may imply that these two proteins are involved in heat-stress associated response pathways. However, complementary approaches are needed to support the induced expression of PFB0595w such as determination of mRNA levels following heat shock. Further, whether the slight upregulation of PFB0595w may result in a change of localization deserves further studies.

This study showed PfHsp70-1 to localize to the cytosol which is consistent with previous observations (Kumar, et al., 1991; Pesce, et al., 2008). This study additionally showed that PFB0595w localizes in the cytosol hence validating previous in silico predictions. Indeed, the cytosolic localization was expected since PFB0595w does not possess a putative targeting sequence. PFB0595w displayed a cytosolic localization in a similar fashion to that of PfHsp70-1 suggesting a possible co-localization and association pattern. Orthologues of PFB0595w in different cellular systems such as yeast, human, and *Toxoplasma gondii* have been experimentally shown to localize in the cytosol (Figueras, et al., 2012; Kampinga and Craig, 2010; Walsh, et al., 2004). Additionally, this study showed that PFB0595w was soluble, while PfHsp70-1 was not entirely in the soluble fraction as protein was observed to be present in the pellet fraction implying possible association with membrane or membrane associated proteins. However, PfHsp70-1 is quite abundant in the intraerythrocytic stage of *P. falciparum* development and may contaminate the different fractions during such experiments. The occurrence of PFB0595w only in the soluble fraction may indicate that PFB0595w may not associate with intracellular membranes or such association may be transient. Indeed, the solubility of PFB0595w was expected since it does not have a predicted transmembrane domain or a membrane associating motif and was therefore predicted to be in the soluble fraction. This was similarly observed for *T. gondii* Sis1 (TgSis1) which was shown to be present in the soluble fraction (Figueras, et al., 2012).

This study explored the interaction and partnership of PfHsp70-1 with PFB0595w using immunoprecipitation technique (Data not shown). This approach was however unsuccessful as a result of the non-specific binding of PfHsp70-1 in the appropriate negative controls that appeared to be unaffected by the presence or absence of ATP. As mentioned above, the presence of PfHsp70-1 in the different fractions obtained during immunoprecipitation may arise from contamination related to its high abundance. Previously, Pfj4 was shown to interact with PfHsp70-1 using immunoprecipitation and occur in the same fraction using size exclusion chromatography implying a direct or indirect interaction (Pesce, et al., 2008). An association was however not reported for PfHsp40 thereby highlighting possible differences in their interactions with PfHsp70-1 (Botha, et al., 2011). Additionally, co-immunoprecipitation experiments by Figueras and colleagues in *T. gondii*, recently showed that TgSis1 was associated or occurred in a common complex with Hsp70 and Hsp90 suggesting that its interaction with Hsp70 may be more stable (Figueras, et al., 2012). Further optimization is however required to study the in vivo interaction between PfHsp70-1 and J proteins. These observations point to further evaluation of possible chaperone - cochaperone interactions between PfHsp70-1 and PFB0595w by in vitro approaches.

4.5 Conclusion

This study has shown that PFB0595w resides in the cytosol and that it is expressed in the intraerythrocytic stage of parasite development, similarly to PfHsp70-1. This study has additionally demonstrated that the expression of this J protein is upregulated following heat induced stress and that it occurs in the same soluble fraction as PfHsp70-1. These observations point to further evaluation of possible chaperone - cochaperone interaction between PfHsp70-1 and PFB0595w through in vitro approaches.

CHAPTER FIVE

Biochemical interaction studies of PFB0595w with PfHsp70-1

5.0 Introduction

The cell-biological studies detailed in chapter four showed that PFB0595w localized to the cytosol of the parasite. These studies also showed a similar localization for PfHsp70-1, which is consistent with analyses made in previous reports (Kumar, et al., 1991; Pesce, et al., 2008). Additionally, the expression of PFB0595w and PfHsp70-1 was observed during the intraerythrocytic stage and was shown to be upregulated following heat shock (Figure 4.2 and 4.3). These observations imply possible co-localization and association patterns. Unlike PFB0595w, the biochemical properties of PfHsp70-1 have previously been studied in vitro thereby providing avenues for further characterization (Botha, et al., 2011; Matambo, et al., 2004; Misra and Ramachandran, 2009; Ramya, et al., 2006; Shonhai, et al., 2008). Through such biochemical assays, PfHsp70-1 has been reported to be relatively stable under temperatures higher than those experienced physiologically and also towards chemical denaturants (Misra and Ramachandran, 2009; Shonhai, et al., 2008). This Hsp70 has also been shown to have ATPase activity that is stimulated by J proteins (Botha, et al., 2011; Misra and Ramachandran, 2009; Shonhai, et al., 2008). Additionally, PfHsp70-1 displays aggregation-suppression properties which are enhanced in the presence of a J protein (Botha, et al., 2011; Misra and Ramachandran, 2009). It is worth noting that results detailed in chapter three showed that Pfj1 localized to the mitochondrion of the parasite thereby discounting the cell biological relevance of in vitro experiments detailed by Misra and Ramachandran relating to its interaction with PfHsp70-1 (Misra and Ramachandran, 2009).

Of interest in this study was the heterologous expression and purification of PFB0595w and PfHsp70-1 proteins to be subsequently used for in vitro assays. Here, their interaction was explored through ATPase assays and surface plasmon resonance (SPR) spectroscopy. As described previously, the N-terminus of Hsp70s is comprised of the nucleotide binding domain that binds and hydrolyzes ATP during its interaction cycles with client proteins (McCarty, et al., 1995). Additionally, the J-domain present in J proteins stimulates the ATPase activity of Hsp70s and therefore the ATPase assay was intended to examine such an interaction between PFB0595w and PfHsp70-1. The ATPase activity involving the conversion of ATP to ADP and inorganic phosphate can be assessed in vitro using assays that monitor the amount of inorganic phosphate released using a variety of methods such as colorimetry (Carter and Karl, 1982; Chifflet, et al., 1988; Lanzetta, et al., 1979). The stimulation of the Hsp70 ATPase activity by a certain J protein can be used to indirectly infer

functional interaction in vitro. The SPR spectroscopy technology on the other hand allows for the label free detection of specific biomolecular interactions (adsorption) between an immobilized ligand with an interacting partner (analyte) in real time (Liedberg, et al., 1983; Schuck, 1997). Here, the interaction between PfHsp70-1 and PFB0595w was analyzed using SPR spectroscopy.

Studies regarding protein structure have shown that J proteins belonging to the canonical type I and type II have a dimerization domain at their C-terminus and function as homodimers (Li, et al., 2006; Sha, et al., 2000). These dimers form a cleft that is involved in efficient client binding and transfer to Hsp70 (Li, et al., 2003). PFB0595w has a predicted dimerization domain as determined by in silico analyses conducted in chapter two. In this chapter, the ability of PFB0595w to dimerize was investigated using size exclusion chromatography.

5.1 Objectives

This study aimed to examine the interaction of PFB0595w with PfHsp70-1 using in vitro approaches.

Specifically, the aims were:

i. To design and commercially generate a codon optimized His-tagged PFB0595w expression plasmid. Note: His-tagged PfHsp70-1 expression plasmid which had been codon optimized had been produced in a related study in the Biomedical Biotechnology Research Unit (BioBRU, Department of Biochemistry, Microbiology, and Biotechnology, Rhodes University, South Africa).
ii. To heterologously express and purify recombinant 6xHis-PFB0595w and 6xHis-PfHsp70-1 referred to here as PFB0595w and PfHsp70-1 respectively using a suitable *E. coli* expression system.
iii. To carry out in vitro assays including ATPase assays and SPR spectroscopy.
iv. To determine whether PFB0595w dimerizes using size exclusion chromatography.

5.2 Materials and methods

5.2.1 Heterologous expression and purification of PFB0595w and PfHsp70-1

5.2.1.1 Expression plasmids coding for PFB0595w and PfHsp70-1

The coding sequences for PFB0595w and PfHsp70-1 were codon optimized to enhance their yields in the *E. coli* heterologous expression system. To facilitate insertion of the coding regions into the pQE30 expression vector (Qiagen, Germany), *Bam*HI and *Hind*III restriction sites were engineered into the 5' and 3' ends of the coding sequence respectively. The codon-optimized coding sequence was synthesized and inserted into pQE30 expression vector (Qiagen, Germany) to produce the plasmids pQE30-PFB0595w and pQE30-PfHsp70-1 by GenScript Corporation (Piscataway, New Jersey, USA). DNA sequencing was employed to verify the integrity of the two constructs.

5.2.1.2 Induction studies for the production of PFB0595w and PfHsp70-1

To purify PFB0595w, the pQE30-PFB0595w plasmid was first transformed into competent *E. coli* M15[pREP4] cells and induction studies conducted as described in section 3.2.2.2. A similar protein induction study was adopted for the pQE30-PfHsp70-1 plasmid encoding PfHsp70-1 except that the plasmid was transformed into competent *E. coli* XL1 Blue strain and 100 μg/ml ampicillin was used. The induction and expression of both recombinant proteins was analyzed by SDS-PAGE and detected by western blot analysis as described in section 3.2.2.2. For western detection, the mouse anti-His primary antibody was used for both proteins. Alternatively, PFB0595w was also detected using mouse anti-PFB0595w polyclonal antibody (1:2500 dilution) while PfHsp70-1 was detected using rabbit anti-PfHsp70-1 polyclonal antibody (1:5000 dilution). HRP-conjugated goat anti-mouse (1:5000 dilution) (GE Healthcare, UK) and goat anti-rabbit (1:5000 dilution) (Cell signaling technology, USA) secondary antibodies were used. Chemiluminescence–based protein detection and image acquisition were carried out as described in section 3.2.2.2.

5.2.1.3 Solubility studies for PFB0595w and PfHsp70-1

Solubility studies were undertaken following inductions studies. The competent *E. coli* M15[pREP4] cells were first transformed and subsequently colonies were inoculated into 2x YT broth and grown overnight as described in section 5.2.1.2. The overnight cultures were diluted 10x and incubated at 37°C in a shaking incubator followed by induction with 1 mM IPTG at OD_{600} of 0.6. Three hours after induction, the cells were harvested by centrifugation (5000 xg, 20 min) at 4°C and the cell pellet resuspended in 5 ml of lysis buffer (10 mM Tris HCL pH 7.5, 300 mM NaCl and 50 mM imidazole, 1 mM PMSF (Roche, Switzerland), and 1 mg/ml lysozyme (Sigma-Aldrich, Germany). Cell lysis was allowed to proceed for 20 min at room temperature (22^oC) after which the sample was frozen overnight at -80^oC. The cells were thawed and sonicated at 4^oC. The supernatant fraction was obtained by centrifugation (13000 xg, 30 min) at 4^oC and the pellet was subsequently resuspended in PBS to a volume equivalent to that of the supernatant. Equal volumes of both the supernatant and pellet were treated with sample buffer (Laemmli, 1970), boiled for 10 min and analyzed through SDS-PAGE and western blotting.

5.2.1.4 Heterologous purification of PFB0595w and PfHsp70-1

To purify PFB0595w recombinant protein, the protein was overexpressed in *E. coli* M15[pREP4] cells as described in section 5.2.1.2. Three hours after induction, the cells were harvested by centrifugation and re-suspended in lysis buffer and frozen overnight at −80°C as described above in section 5.2.1.3. After sonication, the supernatant was separated from the cell debris by centrifugation. PFB0595w present in the soluble cell extract was allowed to bind to sepharose beads (GE Healthcare, UK) charged with $NiSO_4$, overnight at 4°C. The beads were subsequently washed using wash buffer (10 mM Tris, pH 7.5, 300 mM NaCl, 50 mM imidazole, and 1 mM PMSF) and PFB0595w was then eluted using elution buffer (10 mM Tris, pH 7.5, 300 mM NaCl, 1 M imidazole, and 1 mM PMSF). The eluted protein was extensively dialysed at 4°C against the assay buffer of interest. However, proteins were also dialysed against the storage buffer (10 mM Tris, pH 7.5, 300 mM NaCl, 50 mM imidazole, 0.8 mM DTT, 10% glycerol, and 1 mM PMSF) and frozen at -80^oC for future applications.

PfHsp70-1 was over-expressed in *E. coli* XL1 Blue cells and the same purification protocol to that for PFB0595w was adopted.

5.2.2 ATPase assay

The colorimetric ammonium molybdate ATPase activity assay for inorganic phosphate determination was performed as previously described (Chifflet, et al., 1988) but as modified by others (Matambo, et al., 2004). Briefly, purified proteins were prepared in the ATPase assay buffer (10 mM $MgCl_2$, 10 mM Hepes (pH 7.4), 20 mM KCl, and 0.5 mM DTT). Separate and combined reactions for PfHsp70-1 and PFB0595w were prepared with the chaperones to a final concentration of 0.4 μM and the final reaction volumes adjusted to 1000 μl with phosphate free water. The reactions were equilibrated at 37°C prior to initiating the ATPase reaction through the addition of 600 μM ATP (Roche, Switzerland). Triplicate samples (50 μl) were taken from the reaction at 0, 15, 30, 45, 60, 120, and at 180 min after the start of the reactions and added to 50 μl of 10 % SDS present in a 96 well flat bottomed microtitre plate to stop the reaction at these time points. For color development, 50 μl of 1% solution of ammonium molybdate dissolved in 1M HCl was added to the microtitre plate wells containing the sample mixture. This was followed by the addition of 50 μl of 6% ascorbic acid prepared in phosphate free water that resulted in the formation of a blue color in the presence of inorganic phosphate. Finally, 150 μl of 2% (w/v) sodium citrate in 2% (v/v) acetic acid was added to the microtitre plate wells containing the sample mixture to complex the excess of molybdate and prevent further increase in color if hydrolysis of ATP took place. A standard curve to determine phosphate concentration in the samples was generated using KH_2PO_4.

The levels of inorganic phosphate generated by the enzymatic reactions and phosphate standards were determined at an absorbance of 850 nm using a microtitre plate reader (Powerwavex, Biotek Instruments Inc., USA). The ATPase assays were performed in triplicate each with three independent batches of natively purified proteins. The ATPase activity was reported as a function of the nanomoles of inorganic phosphate released per min per mg of Hsp70 (nmolPi/min/mg of Hsp70). Control reactions included individual reactions containing PfHsp70-1 and PFB0595w without ATP to detect any contaminating inorganic phosphate in the reactions. A reaction containing ATP alone was used to estimate the amount

of inorganic phosphate released into the reaction solution through spontaneous ATP hydrolysis which was subsequently subtracted from all time points. *Medicago sativa* (alfalfa) Hsp70 (Alfa Biogene International, Germany) served as a positive control.

5.2.3 Surface plasmon resonance spectroscopy

Kinetic measurements related to the interaction between PFB0595w and PfHsp70-1 over time were performed using the ProteOn™ XPR36 protein interaction array system (Bio-Rad, USA). The array system provides for the parallel immobilization of up to six ligands and allows for the simultaneous measurement of 36 biomolecular interactions since up to six parallel analytes can be injected on to the chip perpendicular to the immobilized ligands. However, no ligand was immobilized on channel 4 which served as a negative control. The experimental set-up including monitoring the running of ProteOn™ XPR36 machine and subsequent data analysis was conducted using the *ProteOn Manager™ software* version 3.1.0.6 (Bio-Rad, USA). Unless stated otherwise, all the reagents and GLC sensor chips were purchased from the manufacturer. Analytes used in this study including purified proteins, BSA, and ATP were prepared in PBST, pH 7.4 (PBS with 0.005% Tween 20) that also acted as the running buffer. The analytes and running buffers were filtered, degassed, and allowed to equilibrate to 25^{o}C: the temperature used to conduct the experiments.

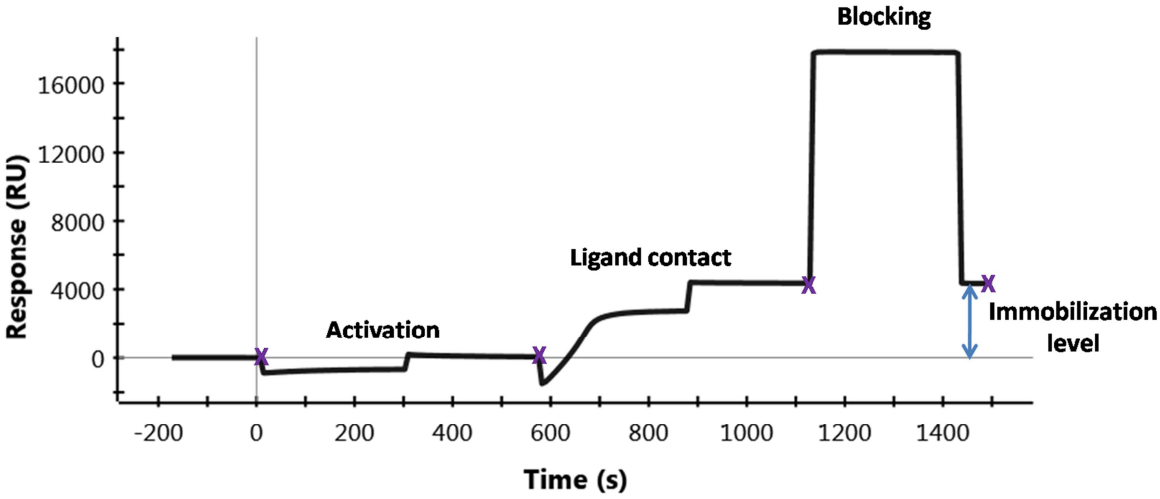

Figure 5.1: The immobilization of PfHsp70-1 on the surface of the GLC sensor chip. The immobilization of PfHsp70-1 was carried out by activation of the carboxymethyl groups on the dextran matrix by reaction with hydroxysuccinimide. The activated carboxyl groups were covalently bonded to free amino groups present in PfHsp70-1 following ligand contact. The

excess of activated carboxyl groups were blocked using 1 M ethanolamine. The surface was subsequently regenerated with 10 mM glycine (pH 1.5) and the immobilization level determined following channel referencing. The points labeled x on the graph represent the injection points.

The immobilization of the PfHsp70-1 was conducted as shown in figure 5.1. Briefly, the GLC sensor chip was initialized using 50% glycerol. Subsequently, it was preconditioned by performing sequential injections of 0.5% SDS, 50 mM NaOH, and then 100 mM HCl at a flow rate of 30 µl/min for 60 seconds each. The surface was afterward activated using a 1:1 mixture of 40 mM EDC (N-ethyl-N-(dimethylaminopropyl) carbodiimide) and 10 mM sulfo-NHS (N-hydroxysuccinimide) diluted to 1:5 in deionized water and injected at a similar flow rate and time. The EDC/NHS allows for the covalent immobilization of the ligand on the surface of the sensor chip. Activation of the chip surface was followed by a preconcentration test to determine the optimal pH and concentration required to reach the target level of response for each ligand to be immobilized. The tests were carried out through injection in a perpendicular orientation of 10 µg/ml of PfHsp70-1 (pI, 5.5; final pH used, 4.5) prepared in 10 mM sodium acetate buffer at differing pH over the desired channels at a flow rate of 30 µl/min for 5 minutes. The reference channel (channel 4) was injected with buffer alone and hence no ligand was immobilized on that channel. The channels were subsequently regenerated using 10 mM glycine pH 1.5.

The remaining active carboxyl groups were inactivated using 1 M ethanolamine at a flow rate of 30 µl/min for 5 minutes. The chip was washed thoroughly with PBST until a stable baseline was attained. A standard procedure for analyte injection was adopted involving an initial wash step with the assay buffer (PBST), followed by an interaction step through injection with the analyte of interest, and a subsequent regeneration step with 10 mM glycine (pH 1.5). Firstly, PFB0595w (0.6 µM) was injected in the presence and absence of molar excess ATP (1 µM) carried out at a flow rate of 60 µl/min for 90 seconds followed by a dissociation phase of 5 minutes using the assay buffer. As a control, buffer lacking any ATP was also injected under similar conditions. ATP is an interacting partner of Hsp70 through binding to its ATPase domain and the high concentration of ATP used would favor chaperone-cochaperone interaction and potentially hinder chaperone-substrate interaction. Further, using a similar flow rate and contact time, PFB0595w (1 µM) was injected at differing protein concentrations (0.2 µM, 0.4 µM, 0.6 µM, 0.8 µM, and 1 µM) in the presence of ATP (1 µM). The injection of PFB0595w at a range of differing concentrations would

allow the study to determine whether the interaction was concentration dependent. The data obtained from the concentration analysis would subsequently be used for kinetic analysis. Control experiments employed in the study included BSA (1 μM) to assess whether the interactions observed were specific and hence act as a negative control. The reactions were carried out in triplicate on the same channel and double referencing was adopted for all experiments. Data was monitored and manipulated using the *ProteOn Manager™ software* version 3.1.0.6 (Bio-Rad, USA). Additionally, data fitting was attempted using the models provided by the *ProteOn Manager™ software.* Seven models are provided by the ProteOn manager software of which the Langmuir model is the most common data fitting model and follows a pseudo first-order kinetics based on simple 1:1 biomolecular interaction. The model assumes that the binding is equivalent and independent for all binding sites and the reaction is not limited by mass transport. The other six models are more complex and take into account different experimental conditions that deviate from the Langmuir model.

5.2.4 Size exclusion chromatography of PFB0595w

Size exclusion chromatography of PFB0595w was carried out using the GE ÄKTA FPLC™ (fast protein liquid chromatography) system equipped with a Superdex 200 HR 10/30 gel filtration column (10 mm x 30-31 cm; bed volume of 24 ml; Amersham Pharmacia Biotech) and monitored using the Unicorn software version 4.11. Proteins at differing concentrations (8 mg/ml, 4 mg/ml, and 1.5 mg/ml) were diluted in the mobile phase (20 mM Hepes, pH 7.4 and 150 mM NaCl) which served as the column equilibration buffer as previously described (Boshoff, et al., 2008; Sha, et al., 2000). Proteins were injected at 1 ml/min and retention times were monitored at 280 nm. Molecular mass standards used included blue dextran (2000 kDa; void volume), catalase (240 kDa, 3 mg/ml), BSA (68 kDa, 4 mg/ml), ovalbumin (45 kDa, 4 mg/ml), and lysozyme (14.3 kDa; 3 mg/ml). The fractions collected were precipitated with 20% trichloroacetic acid and the protein pellet collected through centrifugation (13000 xg, 10 min). The pellet was subsequently washed twice with cold acetone and resuspended in laemmli sample buffer (Laemmli, 1970) after briefly evaporating off the acetone on a heating block and proteins were assessed by SDS-PAGE.

5.3 Results

5.3.1 Non-denaturing purification of PFB0595w and PfHsp70-1

The codon optimized coding sequences for PFB0595w and PfHsp70-1 were successfully synthesized and inserted into pQE30 expression vectors by GenScript Corporation (Piscataway, New Jersey, USA).

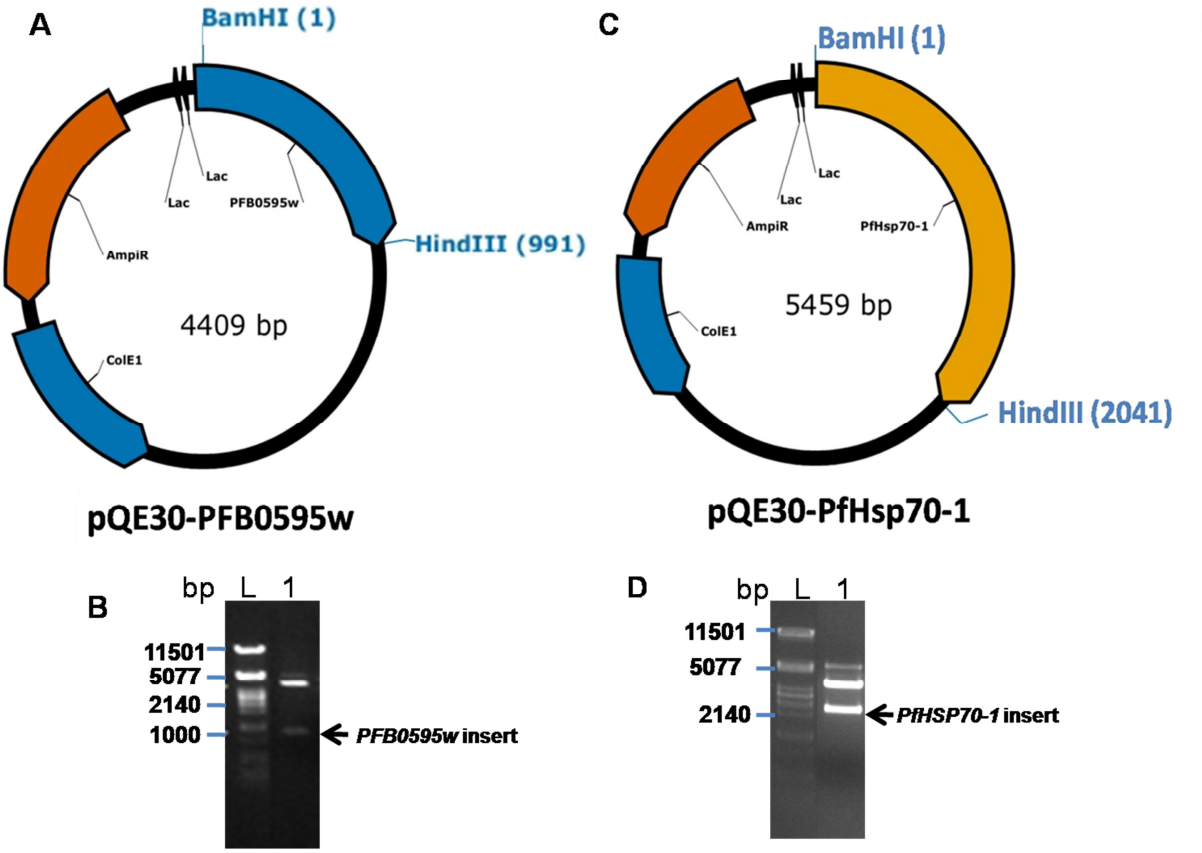

Figure 5.2: Plasmid maps and associated diagnostic restriction analyses of pQE30-PFB0595w and pQE30-PfHsp70-1 plasmids. Both plasmids (**A** and **C**) confer ampicillin resistance when transformed in *E. coli* cells as indicated (AmpiR; β–lactamase coding sequence). The 6xHis-tag segments are upstream of the coding regions inserted between *Bam*HI and *Hind*III restriction sites. The origin of replication (ColE1 origin) and regions coding for LacZ alpha are also shown. Agarose gels (1%) displaying double restriction enzyme analysis of the pQE30-PFB0595w (**B**) and pQE30-PfHsp70-1 (**D**) plasmids with *Bam*HI and *Hind*III restriction enzymes. Lane L, lambda DNA molecular ladder digested with *Pst*I; lane 1, plasmid double digested with *Bam*HI and *Hind*III restriction enzymes; Arrows indicates the position of the digested DNA fragments. The expected sizes of the *PFB0595w* and *PfHSP70-1* DNA fragment are 990 bp and 2040 bp respectively.

As mentioned earlier, the plasmids allow for the expression and purification of PFB0595w and PfHsp70-1 that are 6xHis-tagged at the N-terminus. The codon optimization strategy was adopted since both wild-type genes are AT rich: PFB0595w and PfHsp70-1 have 31% and 34% GC content respectively.

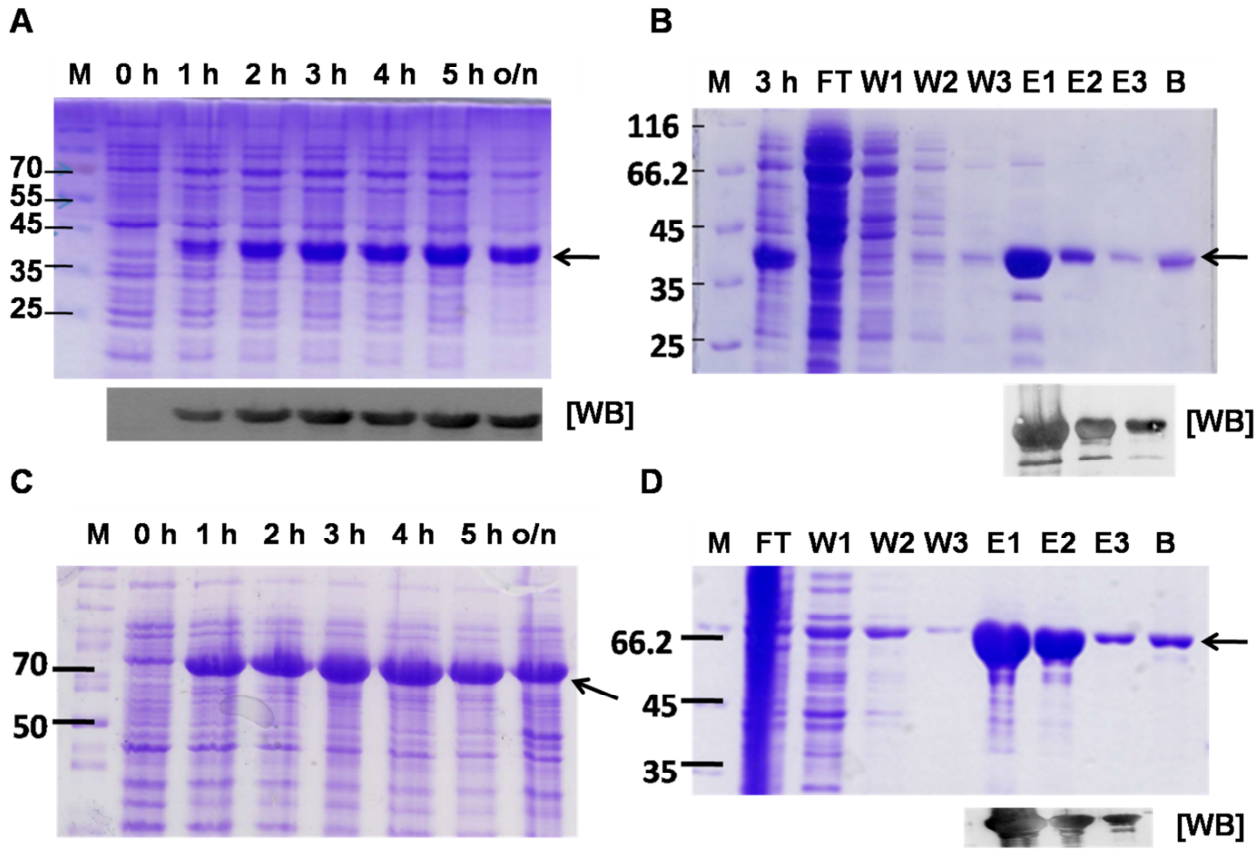

Figure 5.3: Heterologous over-expression and purification of PFB0595w and PfHsp70-1. **A**) SDS–PAGE (12%) analysis of total protein extracts prepared from *E. coli* M15[pREP4] cells transformed with pQE30-PFB0595w and producing PFB0595w during induction studies. Lane M, molecular mass marker; lane 0, non–induced sample; lanes 1–5, induced samples taken hourly; lane o/n, induced sample taken overnight. The arrow indicates the position of PFB0595w. An associated western blot [WB] analysis for the detection of PFB0595w induction study is provided. **B**). SDS–PAGE (12%) analysis of PFB0595w in the fractions collected during the purifications. Lane M, molecular mass marker; lane 3h, third hour post induction sample; Lane FT, flow-through; Lane W1 – W3, wash 1 up to wash 3; Lane E1 – E3, elution 1 up to elution 3; Lane B, bead fraction. **C**). SDS–PAGE (12%) analysis of total protein extracts prepared from *E. coli* XL1Blue cells transformed with pQE30-PfHsp70-1 and producing PfHsp70-1 during induction studies. **D**). SDS–PAGE (12%) analysis of PfHsp70-1 in the fractions collected during the purification. The arrow indicates the position of PfHsp70-1 protein. An associated western blot [WB] is provided below each SDS-PAGE analysis of the purification.

Following the verification of the integrity of the expression plasmids through DNA sequencing and restriction digestion (Figure 5.2), the induction of protein production over time was examined. The plasmid expressing PFB0595w was successfully transformed into competent *E. coli* M15[pREP4] cells. Analysis of induction of PFB0595w through SDS-PAGE of the whole cell lysates showed that the protein was not expressed prior to induction. Following induction, there was a significant increase in protein production (Figure 5.3A) at the expected molecular mass (39 kDa) which was further confirmed through western analysis. The high protein expression was sustained as assessed by samples taken at different time points of induction (Figure 5.3 A).

Similarly, PfHsp70-1 was found to be significantly overexpressed following induction (Figure 5.3C). The overexpression was sustained throughout the time points analyzed. For both proteins, the third hour post-induction was chosen as the point for cell harvest and purification. Prior to purification of both proteins, solubility studies were prioritized to investigate whether they were soluble. To this end, cells harvested at the third hour post-induction were treated with native lysis buffer and subsequently subjected to SDS-PAGE and Western analysis. Examination of the supernatant and pellet fractions showed that both proteins were soluble (data not shown). Based on the outcome of the solubility studies, purifications of both proteins under native conditions was chosen. SDS-PAGE analysis of the different fractions collected during the purification process showed that both proteins bound strongly to the nickel charged beads due to the presence of the 6xHis-tag giving high protein yields (>5mg per liter of culture) in the first elution with little contaminants (Figure 5.3B and 5.3D). Very little amount of protein was lost during the three wash steps included during the purification of both proteins. Most protein was found to be present in the first and second elutions with little being bound to the beads following the third elution. Additionally, the purified proteins were found to contain very low levels of DnaK (*E. coli* Hsp70) contamination, as assessed through western blot analysis of the eluted fractions, which become insignificant following subsequent dilution to working concentrations with the assay buffers (data not shown). It was observed that unlike PfHsp70-1, PFB0595w had a high propensity to precipitate at high protein concentrations.

5.3.2 PFB0595w stimulates the ATPase activity of PfHsp70-1

The successful purification of recombinant proteins allowed this study to examine whether PFB0595w could stimulate the basal ATPase activity of PfHsp70-1 using the colorimetric ammonium molybdate assay. Purified PfHsp70-1 was shown to have a basal ATPase activity of ~7 nmolPi/min/mg (Figure 5.4). No ATPase activity was observed for purified PFB0595w (Figure 5.4). PFB0595w stimulated the basal ATPase activity of PfHsp70-1 by approximately 5 orders of magnitude (~ 33 nmolPi/min/mg) (Figure 5.4). As mentioned previously, control reactions were included to account for the spontaneous hydrolysis of ATP while a phosphate standards curve was used to calculate the concentration of inorganic phosphate in the assay (data not shown).

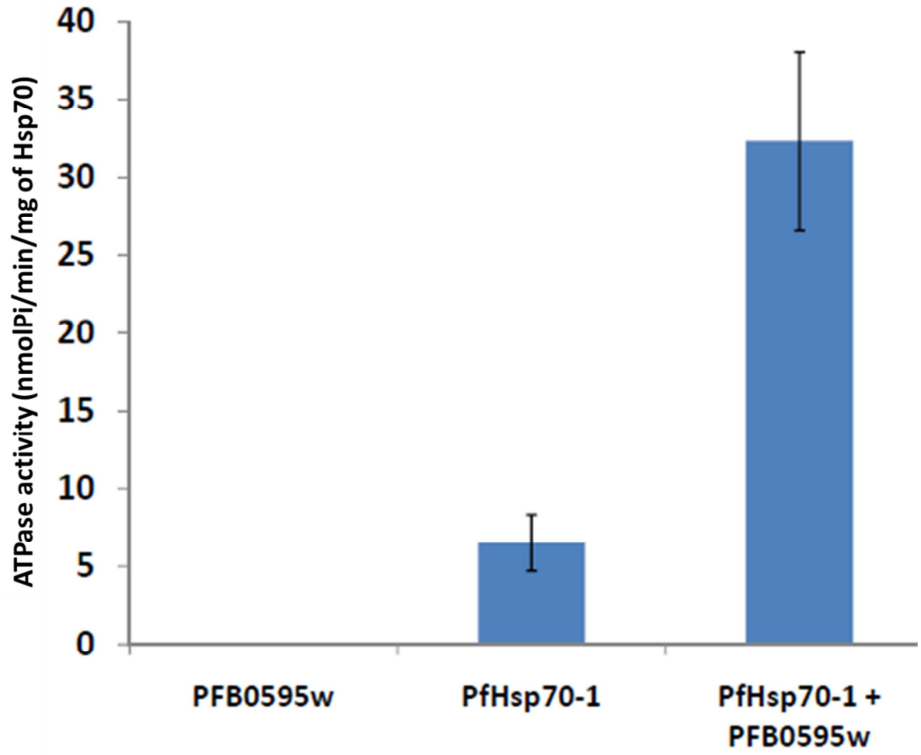

Figure 5.4: Bar graph showing that PFB0595w stimulated the ATPase activity of PfHsp70-1. The ATPase activity, in nmolPi/min/mg of Hsp70, is represented on the Y axis while the chaperones are shown on the X axis. Separate and combined reactions of PFB0595w and PfHsp70-1 each at 10 µM were used.

5.3.3 PFB0595w interacts with PfHsp70-1 as depicted by SPR spectroscopy

To examine the biophysical interaction of PfHsp70-1 with PFB0595w, PfHsp70-1 was successfully immobilized via covalent amine coupling to the sensor chip surface (Figure 5.1). The final level of PfHsp70-1 immobilization determined following reference subtraction was found to be ~ 4333 RU (Figure 5.1). This value was comparable to the *Rmax* (the theoretical maximum binding response of the surface ligand in RU) for PfHsp70-1 which was calculated to be 4519 RU using the equation 1 where, 1 000 RU equals a change in mass of 1 ng/mm^2 (Karlsson, et al., 1994). MW is the molecular weight, RL is the ligand response on immobilization, and V (valency), is the number of binding sites on the ligand.

$$Rmax = ({}^{Analyte\ MW}/_{Ligand\ MW}) \times RL \times V \quad (1)$$

Following the immobilization of PfHsp70-1, the study examined the nature of interaction between PFB0595w and PfHsp70-1 in the presence and absence of ATP (1 µM). ATP binds to PfHsp70-1 on a 1:1 ratio since PfHsp70-1 has one ATP binding domain while J proteins stimulate the ATPase activity of Hsp70s. The response obtained following the injection of ATP alone with immobilized PfHsp70-1 was subtracted from all assays where ATP was included during injection with different analytes. Responses (approximately 400 RU) were obtained when PFB0595w (0.6 µM) was injected in the absence of ATP (Figure 5.5). Further, responses (approximately 350 RU) were obtained when PFB0595w (0.6 µM) was injected in the presence of molar excess ATP (Figure 5.5). PFB0595w appeared to adsorb strongly to the surface of the chip since less dissociation was observed following the injection of the buffer alone in the dissociation phase. To examine whether the observed interaction was not due to non-specific adsorption of any protein injected on to the sensor chip, BSA was used as a negative control. BSA (1 µM) injected in the absence and presence of ATP (1 mM) did not adsorb onto the sensor chip implying that it did not interact with PfHsp70-1 (Figure 5.5). While results obtained here for PFB0595w are preliminary and deserve further investigation, they point to specific interaction with PfHsp70-1.

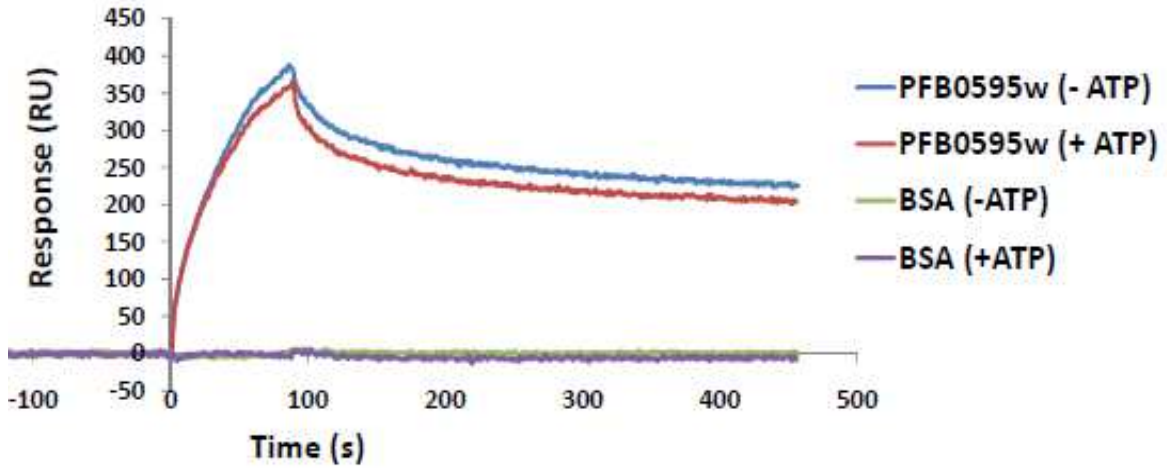

Figure 5.5: SPR sensorgrams showing PFB0595w and not BSA interacts with immobilized PfHsp70-1 in the presence and absence of ATP. PFB0595w (0.6 µM) and BSA (1 µM) were injected in the presence and absence of ATP (1 µM) at a flow rate of 60 µl/min for 90 second followed by a dissociation phase of 5 minute using the assay buffer. The final level of PfHsp70-1 immobilization following reference subtraction was ~ 4333 RU.

To investigate whether the interaction of PFB0595w with PfHsp70-1 was dependent on the concentration of protein injected, PFB0595w (0.2 µM to 1 µM) was injected on to the sensor chip surface at a flow rate of 60 µl/min and a contact time of 90s. PFB0595w adsorbed to the surface of the sensor chip in a concentration dependent manner with higher concentrations resulting in greater adsorption (Figure 5.6A). Here, less dissociation was observed with higher concentrations of PFB0595w injected on to the chip. When the maximum response units for the association phase were plotted against the amount of PFB0595w injected, a plot that did not appear to reach saturation was observed (Figure 5.6B). A plot reaching saturation would imply that the interaction was specific and as such, further studies are required to examine such interactions at higher PFB0595w protein concentrations than those employed here to assess whether saturation would be reached.

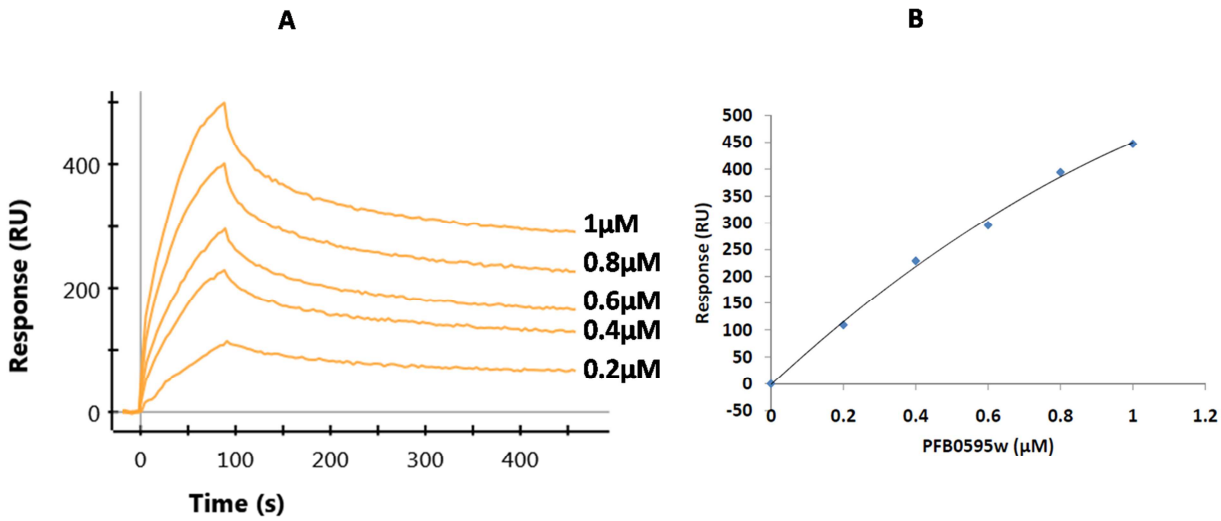

Figure 5.6: SPR analysis showing that PFB0595w, at differing concentrations, interacts with PfHsp70-1 in the presence of ATP. A) PFB0595w was injected at differing concentration (0.2 µM - 1 µM) in the presence of ATP (1 µM) at a flow rate of 60 µl/min for 90 s followed by a dissociation phase of 5 minute using the assay buffer. **B**) Associated saturation plot derived from plotting maximum response units for the association phase obtained in A against the concentration of PFB0595w injected.

Of interest in this study was the kinetic analysis of association (association rate constant; k_a) and dissociation (dissociation rate constant; k_d) of the interaction between PFB0595w and PfHsp70-1. Kinetic analysis involves fitting of sensorgrams to biochemical interaction models of well characterized systems thereby allowing estimated values associated with the kinetic parameters to be identified. However, data fitting for both the injection of PFB0595w in the presence of ATP and that for the concentration dependent interaction of PFB0595w with PfHsp70-1 could not be carried out as the results obtained here are preliminary and deserve further investigation. Overall, results obtained here calls for further studies that would enhance the understanding of the nature of the interaction and allow kinetic analysis. Indeed, further experiments with injections of PFB0595w over a range of concentrations are required to assess affinity of interaction between PFB0595w and PfHsp70-1 in the presence and absence of ATP.

5.3.4 PFB0595w exists as a homodimer

In silico predictions detailed in chapter two showed that PFB0595w does have a putative dimerization domain at the C-terminus. This study therefore sought to investigate whether PFB0595w dimerizes or forms higher order oligomers in solution through molecular exclusion chromatography. The calculated monomeric molecular mass of 6xHis-PFB0595w is 39 kDa.

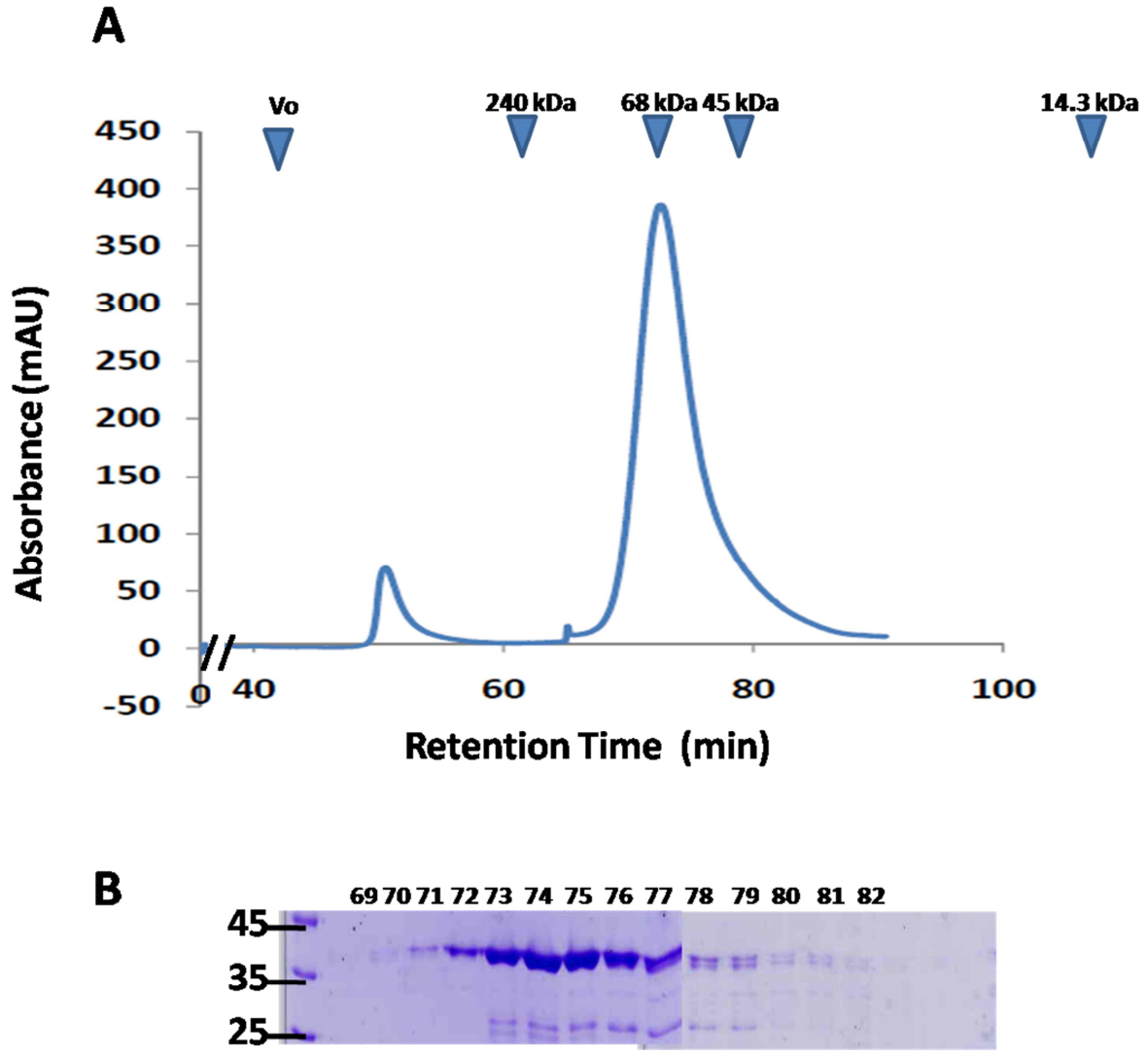

Figure 5.7: Gel filtration analysis of purified PFB0595w. A) Chromatogram for the resolution of purified PFB0595w at a concentration of 8 mg/ml injected at a flow rate of 1 ml/min. **B**) An associated SDS-PAGE analysis of the 1 ml elution fractions collected. The mobile phase comprised of 20 mM Hepes, pH 7.4 and 150 mM NaCl and served as the column equilibration buffer. The size exclusion standards used (Catalase; 240 kDa, BSA; 68 kDa, Ovalbumin; 45 kDa, and Lysozyme; 14.3 kDa) are indicated by blue arrows. Vo indicates the void volume.

A single major peak was observed at ~ 70 kDa (calculated molecular mass) that was interpreted as the homodimeric species of PFB0595w (Figure 5.7A). SDS-PAGE (12%) analysis of the 1 ml fractions collected displayed a molecular mass of ~ 40 kDa, the expected molecular mass of a monomer (Figure 5.7B). The SDS-PAGE profile additionally showed a minor band at ~ 27 kDa that was considered as degradation products of PFB0595w.

5.4 Discussion

Characterization of proteins through biochemical and biophysical approaches can provide greater insights into the nature of interactions between two or more proteins. The main objective of this study was to characterize the interaction between PfHsp70-1 and PFB0595w. As detailed in chapter four, the two proteins were shown to localize in the parasite cytosol. As described for most *Plasmodium* proteins, the coding regions for PFB0595w and PfHsp70-1 are AT rich and to enhance protein expression, their coding regions were codon optimized. Both optimized constructs encoding PFB0595w and PfHsp70-1 gave good protein expression and sufficient protein yields without the addition of denaturants. The advantage of native purification over the denaturation method is that the purified protein may not lose associated activity (Misra and Ramachandran, 2009). However, PfHsp70-1 has previously been purified in several studies using the native coding sequence inserted into pQE30 and other related protein expression vectors (Chiang, et al., 2009; Matambo, et al., 2004; Misra and Ramachandran, 2009; Shonhai, et al., 2008).

The ATPase activity of PfHsp70-1 is important in its interaction cycles with client proteins and it is tightly regulated through interaction with J proteins and nucleotide exchange factors (Langer, et al., 1992). This study showed that PfHsp70-1 has basal ATPase activity that is stimulated by PFB0595w by 5 orders of magnitude. This observation implied that PFB0595w potentially interacts with PfHsp70-1 since they both reside in the cytosol. A similar observation with PfHsp40, another cytosolic J protein, was made in a recent study (Botha, et al., 2011). The observed basal ATPase activity of purified PfHsp70-1 reported here is close to the levels reported by Misra and Ramachandran, (2009) (8.9 nmol Pi/min/mg of protein) and Matambo, et al. (2004) (14.6 nmol Pi/min/mg) but lower than those reported by Shonhai, et al. (2008) (29.2 nmol Pi/min/mg). These values are relatively high compared to those reported for Hsp70s from other species such as human, bovine, and *E. coli* DnaK (less than 4

nmol Pi/min/mg) (Bimston, et al., 1998; Liberek, et al., 1991; O'Brien and McKay, 1993). However, *Trypanosoma cruzi* Hsp70 has been reported to have high basal ATPase activity greater than 60 nmol Pi/min/mg (Edkins, et al., 2004; Olson, et al., 1994). Based on such values, it has been suggested that Hsp70s of parasitic origin may have relatively high basal ATPase activities (Shonhai, et al., 2008). The magnitude of Hsp70 ATPase activity stimulation by PFB0595w obtained here is comparable with previous reports. PfHsp40 was reported to stimulate the ATPase activity of PfHsp70-1 and human Hsp70 by a magnitude of ~ 4 and ~ 15 times respectively (Botha, et al., 2011). In *E. coli*, DnaJ has been shown to stimulate the ATPase activity of DnaK ranging approximately 2 to 13 fold (Liberek, et al., 1991; McCarty, et al., 1995).

This study aimed at understanding the biophysical nature of interaction between PfHsp70-1 with PFB0595w using the SPR spectroscopy technology (Malmqvist, 1993). PfHsp70-1 immobilized on the chip was judged as active since its interaction with PFB0595w resulted in a significant increase in response signal that was absent upon the injection of BSA. When PFB0595w was injected in the absence of ATP, interaction with PfHsp70-1 was observed and this calls for further studies. The difficulty in interpretation arises from the fact that PFB0595w was natively purified and could not potentially be recognized as a substrate by PfHsp70-1. In the absence of ATP, PfHsp70-1 was likely in the ADP bound state, and Hsp70s have a high affinity for client proteins in the ADP-bound conformation (Dragovic, et al., 2006; Kampinga and Craig, 2010). The subsequent inclusion of molar excess ATP in the injection of PFB0595w resulted in responses that would likely depict chaperone-cochaperone interactions since ATP would hinder potential chaperone-substrate interactions. However, the observations detailed here are preliminary and further studies are required to validate these results.

It is worth noting that only full length proteins were included in all the SPR spectroscopic experiments conducted in this study and therefore minor interactions between different domains may have been masked by major interactions. To better study such interactions, mutant proteins in which certain key residues are modified to disrupt the interaction between PFB0595w and PfHsp70-1 could be employed in future experiments. In such a scanning mutagenesis approach, residues present in the J-domain such as the HPD motif of PFB0595w could be mutated so as to disrupt its interaction with the ATPase domain of PfHsp70-1 without compromising its integrity. Further, preliminary results obtained indicated that PFB0595w interacted with PfHsp70-1 in a concentration dependent manner. However, the

concentrations of PFB0595w injected on to the chip were not sufficient to reach saturation as demonstrated by a secondary plot and hence the specificity of the interaction remains to be determined. During injections, low levels of dissociation were observed following complex formation between PFB0595w and PfHsp70-1. Indeed, the interaction did not appear to reach equilibrium under conditions used in this study (data not shown). The data obtained could not be fitted to exponential equations as provided by the ProteOn manager software and therefore the affinity associated with such interactions remains to be quantified. The interpretation of such data may however be confounded by other technical factors associated with the experimental set-up and prompts further investigations. Quite important is the purity of the analytes used in the study and the ligand immobilized. Natively purified proteins as used in this study may co-purify with minor contaminants or even contain degradation products from the analyte before use which may influence the experimental outcome making it difficult to interpret data. However, both influences were considered negligible as assessed by SDS-PAGE analysis of purified proteins and subsequent dilutions to working concentrations. Additionally, proteins used in this study were freshly purified and used within a week to minimize for the effects of degradation. Complex formation between PfHsp70-1 and PFB0595w can be evaluated using the Blue Native PAGE approach in future studies.

Sequence alignment and homology modeling of the peptide binding region in PFB0595w (data not shown) depicts the presence of a dimerization domain. Results detailed here depict PFB0595w to exist as a homodimeric protein species at protein concentrations used in this study. Previously, Sha and colleagues observed a single homodimeric species and suggested that the cleft formed by the dimer allows for peptide binding and transfer to Hsp70s (Sha, et al., 2000). Dimer formation is crucial for functionality of type I and II J proteins (Langer, et al., 1992; Li, et al., 2009). However, future experiments conducted at different protein concentrations other than those employed here are required to determine if PFB0595w also exists as a monomer or other oligomeric states. Further, a complimentary approach using Blue Native PAGE could also be employed to validate complex formation (Claeys, et al., 2005). Related studies could also explore the existence of protein complexes between PFB0595w and PfHsp70-1 following co-injections of both purified proteins.

5.5 Conclusion

The study showed that PFB0595w interacts with PfHsp70-1 and stimulates its ATPase activity. It has provided preliminary evidence of a biophysical interaction between these two proteins and highlighted the need for further experiments and analysis of the kinetics of this interaction. Additionally, while PFB0595w was shown to exist as a homodimer, suggestions have been made for future experiments to examine the existence of monomers and oligomers. Further, the ability of PFB0595w to modulate the chaperone properties of PfHsp70-1 such as protein folding and aggregation-suppression ought to be prioritized in future studies.

CHAPTER SIX

Conclusions and Future perspectives

This thesis details research addressing several knowledge gaps in the *Plasmodial* Hsp70 and J protein chaperone complements. Broadly, the objectives of this research were to identify and conduct a side-by-side comparative analysis of the Hsp70s and J proteins across the *Plasmodium* species. Secondly, the study aimed to verify the localization of Pfj1 and PfHsp70-3 in the intraerythrocytic stage of development of *P. falciparum*. Additionally, the study aimed to heterologously express and purify these proteins for biochemical characterization. Thirdly, this research aimed to determine the expression and localization of PFB0595w in the intraerythrocytic stages of *P. falciparum* development. Lastly, the study sought to investigate PFB0595w as a cochaperone for PfHsp70-1 using in vitro approaches.

One of the aims of this study was to identify and compare the Hsp70 and J protein complements across the *Plasmodium* species including human- and primate- (*P. falciparum 3D7* and *P. vivax SaI-1, P. knowlesi strain H*), and rodent-infecting species (*P. berghei ANKA, P. chabaudi chabaudi,* and *P. yoelii yoelii 17XNL*). This side-by-side analysis highlighted certain key features of the *P. falciparum* chaperone system. It showed that Hsp70s are highly conserved across these species with the exception of PfHsp70-x that is only present in *P. falciparum*. The export of PfHsp70-x was recently experimentally confirmed where it was found to be present in the PV and infected erythrocyte cytosol (Grover, et al., 2013; Külzer, et al., 2012). However, while the study by Külzer et al. (2012) localized PfHsp70-x in the J-dots and not in Maurer's clefts, that by Grover, et al. (2013) localized it to the Maurer's clefts. This discrepancy may have arisen from the differences in the Maurer's clefts marker used (SBP1 and STEVOR; Külzer, et al., 2012, MAHRP1; Grover, et al., 2013) and highlights the need for further studies. Overall, these observations highlighted the uniqueness of the *P. falciparum* chaperone system relative to the other species and calls for further studies regarding the role of PfHsp70-x in protein export in malaria parasites present in the *laverania* sub-genus. It further raises questions of whether and how protein trafficking occurs in host cells in the rodent and primate *Plasmodium* species.

Several features showed that the J protein complement is unique in *P. falciparum* relative to other *Plasmodium* species. *P. falciparum* possesses the highest overall number of J proteins displaying an expanded complement of PEXEL containing J proteins relative to the other *Plasmodium* species. This is in contrast to the parasite resident J proteins that displayed high conservation with almost all *P. falciparum* J proteins having homologues in the other *Plasmodium* species. Indeed, the domain organization of most parasite resident J proteins appeared to be generally conserved when compared to homologues from well studied

eukaryotes such as yeast and humans. The conserved nature of these J proteins may imply retention of similar functionality through evolution. The putative exported proteins had a biased localization towards the subtelomeric chromosomal regions occurring mostly after the synteny break-points. The reduced number of PEXEL containing J proteins in the other *Plasmodium* species points to differences in the virulence mechanism and general host-parasite interactions. Domain mapping of exported J proteins highlighted peculiar domains and domain organization not present in the human J protein complement. Recent research has revealed that some J proteins in *P. falciparum* have evolved to acquire intriguing domains that have been associated with non-canonical functions such as cytoskeletal stability, knob formation, and infected erythrocyte surface architecture (Bennett, et al., 1997; Kilili and LaCount, 2011; Maier, et al., 2008; Oakley, et al., 2007). What role the unique domains such as the MEC and PRESAN domains play for example, is still an open question. This study also identified a conserved motif of approximately 41 amino acids at the C-terminus of most exported J proteins in *Plasmodium* species analyzed. The role of this motif warrants further research. Overall, the unique features present in the exported J proteins allows them to be prioritized for future studies including drug targeting since most lack homologues in the human system.

The fact that a large number of J proteins in the export category have a corrupted HPD motif in their J-domain has raised questions regarding whether they do interact with Hsp70s. Indeed, the question of whether most of these J proteins are involved in chaperoning of exported proteins calls for further studies in light of the fact that few have been experimentally studied. Another important question relates to what roles the J proteins play at the different stages of parasite development. Expression studies have highlighted that some J proteins are expressed uniquely at some stages while others are generally expressed at most if not all of the stages. This may imply that some of the J proteins have unique or specialized roles at particular stages of the parasite life cycle while others play a more generalized homeostatic role.

Protein localization can assist in the prediction of pathways that a protein may participate and also highlight its potential partners (Rost, et al., 2003). However, there are very few J proteins whose localization has been experimentally validated. Here, in silico approach was adopted to predict the subcellular localization and carry out domain mapping of Hsp70s and J proteins in *P. falciparum*. The study enumerated potential subcellular localizations and partnerships of J proteins with Hsp70s. However, while in silico analysis is quite useful and can process

large datasets over a short period of time, it is often hampered by false positives. This constraint is more pronounced in eukaryotes such as *P. falciparum* that lack specific software as those widely available have mainly been developed based on well studied eukaryotes. Indeed, relative to other eukaryotes, the *P. falciparum* proteins display a biased amino acid composition, have a high prevalence of low complexity regions (LCRs), and the proteins encoded by this genome are larger in size compared with homologues from other eukaryotes (Pizzi and Frontali, 2001; Zilversmit, et al., 2010). Additionally, *P. falciparum* proteins are characterized by insertions of non-globular regions that separate well-conserved adjacent domains in homologous protein (Pizzi and Frontali, 2001). These features indicate high divergence of *P. falciparum* proteins and makes domain identification and subcellular localization prediction in *Plasmodium* proteins difficult using commonly available software programs. Overall, while many predictions made need to be experimentally confirmed, in silico analysis plays an important role in helping select unique proteins for further studies.

The second major aim of this study was the characterization of Pfj1. This molecule has been suggested as a drug target due to its structural uniqueness and lacks homologues in other eukaryotes including humans (Pesce, et al., 2010). The uniqueness of Pfj1 coupled with the controversy regarding its localization formed the basis of the experimental work conducted in chapter three. This is the first study showing that Pfj1 localizes to the mitochondrion in the intraerythrocytic stage of development of *P. falciparum*. This observation is consistent with predictions made by Watanabe and discounts the previously described apicoplast localization by Kumar and co-workers (Kumar, et al., 2010; Watanabe, 1997). It is worth noting that while the study by Kumar and co-workers (2010) employed serum raised against Pfj1, results detailed here relied on transfection of plasmids coding for Pfj1 fused to GFP. The serum employed in the study by the Kumar and co-workers (2010) had been raised against a region covering the conserved DnaJ domains (aa 61–419 of Pfj1) that contains a conserved J-domain, Zn finger-like domain (four CxxCxG repeats) and a DnaJ C-terminal domain. All or some of these domains are also present in J proteins or other proteins encoded by the *P. falciparum* genome raising the possibility for cross-reactivity. The peptide directed antibody approach employed in this study was considered attractive since it would help lower chances of possible cross-reactivity. Preliminary data obtained from testing the serum raised from the peptide selected in the unique C-terminus was inconclusive. It is against such a background that the transfection approach was successfully employed. However, the antibodies specific

to Pfj1 would have helped answer questions regarding its expression and localization. Further, such antibodies could effectively be used for immunoprecipitation experiments.

Preliminary results detailed here showed that PfHsp70-3 localizes to the mitochondrion and Pfj1 was thereby proposed as a potential cochaperone for PfHsp70-3. Analysis carried out in chapter two (section 2.3.5) suggests that both proteins may reside in the mitochondrial matrix. It is worth noting that images represented for localization were produced using a fluorescence microscope without confocal abilities which may lead to misinterpretation of data. However, the Axio Observer inverse epifluorescence microscope system used here captured the images through deconvolution of Z-stack sections of the infected erythrocyte under study; the same properties employed by a Confocal microscope. Further, more experiments are required to determine whether they both localize to the mitochondrial matrix. The localization experiments laid a foundation regarding further cell biological characterization for Pfj1 and PfHsp70-3 and highlighted some of the difficulties associated with the transfection of plasmids coding for full length fusion proteins. Fusing the coding regions at either terminus with a fluorescent protein has the advantage that transfectant cells can be imaged live without need for further treatment that may introduce artifacts. However, such proteins are usually large in size and may have deleterious effects on the phenotype. Smaller tags comprising of few amino acids on the other hand have the advantage of their small size but require the use of antibodies for detection. Further, this study employed the chloroquine resistant promoter to drive the expression of proteins in transfected cells and endogenous promoters therefore need to be considered in future studies.

It is notable that the study was unable to detect the endogenous levels of Pfj1 mainly attributed to the lack of success with the antibodies generated in this study. Future efforts therefore include the design, synthesis and use of alternative antibodies for such detection and localization experiments. For example, the unique C-terminal domain of Pfj1 may be heterologously purified and used to generate antibodies. This accounts for the initial approach of peptide-directed antibody design and synthesis detailed in this study based on this domain. Additionally, antibodies specific to PfHsp70-3 should be prioritized that would allow for the cell biological characterization of this Hsp70. Here, the peptide directed antibody design approach would be more feasible due to the high level of conservation of the Hsp70s present in *P. falciparum*.

Data obtained here suggests that different approaches from those adopted in this study may be used to enhance the heterologous expression and purification of Pfj1. Pfj1 appears to be recalcitrant to heterologous expression as demonstrated by this study and is supposedly toxic to the *E. coli* expression system. Indeed, Pfj1 does not possess an equivalent homologue in the *E. coli* system and its overexpression may lead to a toxic phenotype. However, future studies may consider yeast, mammalian or baculovirus/insect cell lines as alternative expression systems that may satisfy any post-translational modification requirements. Further, while this study used pQE30 as the expression vector of choice, other vectors that contain the His-tag or other tags may be employed in future Pfj1 expression studies. Additionally, studies should be prioritized to understand the role of the putative PfHep1 in the purification and biochemical characterization of PfHsp70-3.

The purification of both Pfj1 and PfHsp70-3 would have allowed the study to conduct chaperone-cochaperone interaction studies. As described previously, the N-terminus of PfHsp70-3 is comprised of the nucleotide binding domain that supposedly binds and hydrolyzes ATP during its interaction cycles with client proteins. To this end, the basal ATPase activity of PfHsp70-3 and whether Pfj1 plays any role in stimulating this activity is yet to be determined. Further, biochemical studies on the chaperone-cochaperone interaction using the suppression of aggregation assays may be undertaken to provide preliminary information on the interaction of PfHsp70-3 with client proteins and what role Pfj1 may play during such interactions. Previously, Pfj1 has been shown to have a functional J-domain implying the potential to stimulate the ATPase activity of Hsp70s.

Another major aim of this study was the cell biological and biochemical characterization of PFB0595w, a typical type II J protein. This is the first study to show that this J protein resides in the cytosol and is expressed in the intraerythrocytic stage of parasite development similarly to PfHsp70-1. The imaging however could not resolve whether PFB0595w also localizes to the nuclei owing to the fluorescent microscope used. Transfection was successful with plasmids encoding full length PFB0595w fused to either the GFP or the strep-tag: approaches that were not successful with full length Pfj1 transfection plasmids. Further, PFB0595w displayed low levels of expression that showed slight upregulation following heat shock. However, alternative approaches other than those employed here are required to verify (i) whether PFB0595w localizes to the nuclei in a similar fashion to that previously described for PfHsp70-1 by Pesce and colleagues (2008), (ii) validate the expression of PFB0595w following heat shock using other approaches such as northern blotting to determine mRNA

levels after heat shock conditions, (iii) determine the localization of PFB0595w under heat shock conditions. Of interest in this study was to explore the interaction and partnership of PfHsp70-1 with PFB0595w using immunoprecipitation experiments. This approach was however unsuccessful as a result of the non-specific binding of PfHsp70-1 in the appropriate negative controls that appeared to be unaffected by the presence or absence of ATP (data not shown). PfHsp70-1 is quite abundant in the intraerythrocytic stage of *P. falciparum* and may contaminate the different fractions during the immunoprecipitation experiments. However, such contamination may also be attributed to the experimental set-up. Previously, Pfj4 was shown to interact with PfHsp70-1 using the immunoprecipitation approach and occur in the same fraction using size exclusion chromatography implying a direct or indirect interaction (Pesce, et al., 2008). Further optimization is therefore required to study such potential interactions between PfHsp70-1 and PFB0595w.

The evaluation of chaperone - cochaperone interactions between PfHsp70-1 and PFB0595w was conducted through in vitro approaches. PFB0595w and PfHsp70-1 proteins were successfully purified and used for biochemical interaction assays as detailed in chapter five. The codon optimization approach employed in this study proved successful and resulted in high protein production. This is the first study to show that PFB0595w stimulates the ATPase activity of PfHsp70-1 implying functional interaction between the two proteins. Further, the study has provided preliminary evidence of a biophysical interaction between these two proteins using SPR spectroscopy studies. However, further experiments are required to support such preliminary data. Future studies may for example use the scanning mutagenesis approach to characterize the biophysical interaction of PfHsp70-1 with PFB0595w. Here, the HPD motif present in the J domain of PFB0595w may for example be replaced with non-functional residues followed by interaction analysis. PFB0595w may also be immobilized onto the sensor chip and PfHsp70-1 injected as the analyte. Other alternative approaches may include (i) the Quartz Crystal Microbalance with Dissipation monitoring (QCM-D) approach that may help understand the chaperone – cochaperone interaction and conformational changes associated with such interactions which the SPR spectroscopy is less capable of determining, (ii) the Isothermal Titration Calorimetry (ITC) which may help determine the thermodynamics of interactions in solution hence avoiding the need to immobilize protein molecules as is the case with SPR spectroscopy. Further, other in vitro approaches such as the protein refolding assays and the suppression of protein aggregation may be employed in

future to provide insights on how these two proteins interact with each other to enhance protein folding.

Overall, the identification and validation of potential drug targets will require the elucidation of the *Plasmodium* Hsp70-J protein chaperone partnerships and a detailed characterization of their structure and biological function. As detailed in this thesis, very few partnerships have been experimentally investigated. Indeed, to date, there is not a single crystal structure of a J protein from *Plasmodium* species submitted to the protein data bank. This thesis has highlighted features unique to the *P. falciparum* Hsp70 and J protein complement relative to that of humans and this may form the basis for future investigations. Indeed, several J proteins such as Pfj1, PF10_0381, and RESA have been predicted as potential drug targets since they are unique to the parasite and the latter two have been shown to fulfil important tasks (Maier, et al., 2008). Indeed, their mechanism of action is not known and it remains to be tested if they are able to interact with Hsp70s. Therefore, such proteins deserve further investigation both in structure, function and partnerships with Hsp70s. Further, while several chaperone – cochaperone partnerships have been proposed here, preliminary data from Pfj1 and PFB0595w has been presented paving the way for future studies. It is worth noting that the recent implication of PfHsp70-x in partnership with PEXEL containing J proteins in the chaperoning of the exportome represents as an attractive frontier in the Hsp70-J protein biology of malaria parasites. Such investigations will pave the way for the testing of small molecules inhibitors that may abrogate partnerships and hence act as antimalarial therapeutics.

References

.

Acharya, P., *et al.* (2012) An exported heat shock protein 40 associates with pathogenesis-related knobs in *Plasmodium falciparum* infected erythrocytes, *PLOS One*, **7**, e44605.

Acharya, P., Kumar, R. and Tatu, U. (2007) Chaperoning a cellular upheaval in malaria: Heat shock proteins in *Plasmodium falciparum*, *Molecular and Biochemical Parasitology*, **153**, 85-94.

Acharya, P., *et al.* (2009) A glimpse into the clinical proteome of human malaria parasites *Plasmodium falciparum* and *Plasmodium vivax*, *Proteomics - Clinical Applications*, **3**, 1314-1325.

Achtman, A.H., *et al.* (2005) Longevity of the immune response and memory to blood-stage malaria infection immunology and immunopathogenesis of malaria. In Langhorne, J. (ed). Springer Berlin Heidelberg, pp. 71-102.

Albanèse, V., Reissmann, S. and Frydman, J. (2010) A ribosome-anchored chaperone network that facilitates eukaryotic ribosome biogenesis, *The Journal of Cell Biology*, **189**, 69-81.

Alonso, P.L., *et al.* (2011) A research agenda to underpin malaria eradication, *PLOS Medicine*, **8**, e1000406.

Alonso, P.L., *et al.* (2004) Efficacy of the RTS,S/AS02a vaccine against *Plasmodium falciparum* infection and disease in young African children: Randomised controlled trial, *The Lancet*, **364**, 1411-1420.

Altieri, D.C., *et al.* (2012) Trap-1, the mitochondrial Hsp90, *BBA Molecular Cell Research*, **1823**, 767-773.

Anfinsen, C.B. (1973) Principles that govern the folding of protein chains, *Science*, **181**, 223-230.

Angers-Loustau, A., Rainy, J. and Wartiovaara, K. (2007) PlasmaDNA: A free, cross-platform plasmid manipulation program for molecular biology laboratories, *BMC Molecular Biology*, **8**, 77.

Aravind, L., *et al.* (2003) *Plasmodium* biology: Genomic gleanings, *Cell*, **115**, 771-785.

Aron, R., *et al.* (2005) In vivo bipartite interaction between the Hsp40 Sis1 and Hsp70 in *Saccharomyces cerevisiae*, *Genetics*, **169**, 1873-1882.

Aunpad, R., *et al.* (2009) The effect of mimicking febrile temperature and drug stress on malarial development, *Annals of Clinical Microbiology and Antimicrobials*, **8**, 19.

Aurrecoechea, C., *et al.* (2009) PlasmoDB: A functional genomic database for malaria parasites, *Nucleic Acids Research*, **37**, D539-543.

Ayisi, J.G., *et al.* (2003) The effect of dual infection with HIV and malaria on pregnancy outcome in western Kenya, *AIDS*, **17**, 585-594.

Baca, A.M. and Hol, W.G.J. (2000) Overcoming codon bias: A method for high-level overexpression of *Plasmodium* and other AT-rich parasite genes in *Escherichia coli*, *International Journal for Parasitology*, **30**, 113-118.

Baer, K., *et al.* (2007) Release of hepatic *Plasmodium yoelii* merozoites into the pulmonary microvasculature., *PLOS Pathogens*, **3**, e171.

Bailey, T.L. and Elkan, C. (1994) Fitting a mixture model by expectation maximization to discover motifs in biopolymers, *Proceedings of the International Conference on Intelligent Systems for Molecular Biology*, **2**, 28-36.

Bailey, T.L., *et al.* (2006) MEME: Discovering and analyzing DNA and protein sequence motifs, *Nucleic Acids Research*, **34**, W369-W373.

Bairwa, M., *et al.* (2012) Malaria vaccine: A bright prospect for elimination of malaria, *Human Vaccines & Immunotherapeutics*, **8**.

Baker, D.A. (2010) Malaria gametocytogenesis, *Molecular and Biochemical Parasitology*, **172**, 57-65.

Banumathy, G., *et al.* (2003) Heat shock protein 90 function is essential for *Plasmodium falciparum* growth in human erythrocytes, *The Journal of Biological Chemistry*, **278**, 18336-18345.

Banumathy, G., Singh, V. and Tatu, U. (2002) Host chaperones are recruited in membrane-bound complexes by *Plasmodium falciparum*, *The Journal of Biological Chemistry*, **277**, 3902-3912.

Barral, J.M., *et al.* (2004) Roles of molecular chaperones in protein misfolding diseases, *Seminars in Cell & Developmental Biology*, **15**, 17-29.

Baruch, D.I., *et al.* (1995) Cloning the *P. falciparum* gene encoding PfEMP1, a malarial variant antigen and adherence receptor on the surface of parasitized human erythrocytes, *Cell*, **82**, 77-87.

Bell, S.L., Chiang, A.N. and Brodsky, J.L. (2011) Expression of a malarial Hsp70 improves defects in chaperone-dependent activities in Ssa1 mutant yeast, *PLoS One*, **6**, e20047.

Bender, A., *et al.* (2003) Properties and prediction of mitochondrial transit peptides from *Plasmodium falciparum*, *Molecular and Biochemical Parasitology*, **132**, 59-66.

Bennett, B.J., Mohandas, N. and Coppel, R.L. (1997) Defining the minimal domain of the *Plasmodium falciparum* protein MESA involved in the interaction with the red cell membrane skeletal protein 4.1, *The Journal of Biological Chemistry*, **272**, 15299-15306.

Bimston, D., *et al.* (1998) Bag-1, a negative regulator of Hsp70 chaperone activity, uncouples nucleotide hydrolysis from substrate release., *The EMBO Journal*, **17**, 6871–6878.

Birnboim, H.C. and Doly, J. (1979) A rapid alkaline extraction procedure for screening recombinant plasmid DNA, *Nucleic Acids Research*, **7**, 1513-1523.

Bischoff, E. and Vaquero, C. (2010) In silico and biological survey of transcription-associated proteins implicated in the transcriptional machinery during the erythrocytic development of *Plasmodium falciparum*, *BMC Genomics*, **11**, 34.

Biswas, S. and Sharma, Y.D. (1994) Enhanced expression of *Plasmodium falciparum* heat shock protein PfHsp70-I at higher temperatures and parasite survival, *FEMS Microbiology Letters*, **124**, 425-429.

Blamowska, M., Neupert, W. and Hell, K. (2012) Biogenesis of the mitochondrial Hsp70 chaperone, *The Journal of Biological Chemistry*, **199**, 125-135.

Blatch, G.L. and Przyborski, J.M. (2011) Protein biochemistry: Don't forget the cell biology, *BBA Proteins and Proteomics*, **1814**, 456.

Bloland, P.B., *et al.* (1993) Beyond chloroquine: Implications of drug resistance for evaluating malaria therapy efficacy and treatment policy in Africa, *The Journal of Infectious Diseases*, **167**, 932-937.

Boddey, J.A., *et al.* (2010) An aspartyl protease directs malaria effector proteins to the host cell, *Nature*, **463**, 627-631.

Boddey, J.A., *et al.* (2009) Role of the *Plasmodium* export element in trafficking parasite proteins to the infected erythrocyte, *Traffic*, **10**, 285-299.

Boorstein, W.R., Ziegelhoffer, T. and Craig, E.A. (1994) Molecular evolution of the Hsp70 multigene family, *Journal of Molecular Evolution*, **38**, 1-17.

Boshoff, A., Stephens, L.L. and Blatch, G.L. (2008) The *Agrobacterium tumefaciens* DnaK: ATPase cycle, oligomeric state and chaperone properties, *The International Journal of Biochemistry & Cell Biology*, **40**, 804-812.

Botha, M., *et al.* (2011) *Plasmodium falciparum* encodes a single cytosolic type I Hsp40 that functionally interacts with Hsp70 and is upregulated by heat shock, *Cell Stress and Chaperones*, 389-401.

Botha, M., Pesce, E.R. and Blatch, G.L. (2007) The Hsp40 proteins of *Plasmodium falciparum* and other apicomplexa: Regulating chaperone power in the parasite and the host, *The International Journal of Biochemistry & Cell Biology*, **39**, 1781-1803.

Bozdech, Z., *et al.* (2003) The transcriptome of the intraerythrocytic developmental cycle of *Plasmodium falciparum*, *PLOS Biology*, **1**, e5.

Braakman, I. and Otsu, M. (2008) Cargo load reduction, *Science*, **321**, 499-500.

Breman, J.G., Egan, A. and Keusch, G.T. (2001) The intolerable burden of malaria: A new look at the numbers, *The American Journal of Tropical Medicine and Hygiene*, **64**, iv-vii.

Brodsky, J.L. (1999) Selectivity of the molecular chaperone-specific immunosuppressive agent 15-Deoxyspergualin: Modulation of Hsc70 ATPase activity without compromising DnaJ chaperone interactions, *Biochemical Pharmacology*, **57**, 877-880.

Buchner, J. (1999) Hsp90 & Co. – a holding for folding, *Trends in Biochemical Sciences*, **24**, 136-141.

Bukau, B., Weissman, J. and Horwich, A. (2006) Molecular chaperones and protein quality control, *Cell*, **125**, 443-451.

Caplan, A.J., Cyr, D.M. and Douglas, M.G. (1992) Ydj1p facilitates polypeptide translocation across different intracellular membranes by a conserved mechanism, *Cell*, **71**, 1143-1155.

Carlton, J.M., *et al.* (2008) Comparative genomics of the neglected human malaria parasite *Plasmodium vivax*, *Nature*, **455**, 757-763.

Carlton, J.M., *et al.* (2002) Genome sequence and comparative analysis of the model rodent malaria parasite *Plasmodium yoelii yoelii*, *Nature*, **419**, 512-519.

Carpenter, D.O., Arcaro, K. and Spink, D.C. (2002) Understanding the human health effects of chemical mixtures, *Environmental Health Perspectives*, **110 Suppl 1**, 25-42.

Carruthers, V.B. and Sibley, L.D. (1997) Sequential protein secretion from three distinct organelles of *Toxoplasma gondii* accompanies invasion of human fibroblasts, *European Journal of Cell Biology*, **73**, 114-123.

Carter, R. (2001) Transmission blocking malaria vaccines, *Vaccine*, **19**, 2309-2314.

Carter, R. and Diggs, C.L. (1977) Plasmodia in rodents., *In: Kreier J (ed) Parasitic Protozoa*. Academic Press, New York, pp. 359-465.

Carter, S.G. and Karl, D.W. (1982) Inorganic phosphate assay with malachite green: An improvement and evaluation, *Journal of Biochemical and Biophysical Methods*, **7**, 7-13.

Cavalier-Smith, T. (1993) Kingdom protozoa and its 18 phyla, *Microbiology and Molecular Biology Reviews*, **57**, 953-994.

Cheetham, M.E. and Caplan, A.J. (1998) Structure, function and evolution of DnaJ: Conservation and adaptation of chaperone function, *Cell Stress and Chaperones*, **3**, 28-36.

Chiang, A.N., *et al.* (2009) Select pyrimidinones inhibit the propagation of the malarial parasite, *Plasmodium falciparum*, *Bioorganic & Medicinal Chemistry*, **17**, 1527-1533.

Chifflet, S., *et al.* (1988) A method for the determination of inorganic phosphate in the presence of labile organic phosphate and high concentrations of protein: Application to lens ATPases, *Analytical Biochemistry*, **168**, 1-4.

Chirenda, J., Siziya, S. and Tshimanga, M. (2000) Association of HIV infection with the development of severe and complicated malaria cases at a rural hospital in Zimbabwe, *Central African Journal of Medicine*, **46**, 5-9.

Christensen, C.A., *et al.* (2002) Mitochondrial Gfa2 is required for synergid cell death in Arabidopsis, *The Plant Cell*, **14**, 2215-2232.

Claeys, D., Geering, K. and Meyer, B.J. (2005) Two-dimensional blue native/sodium dodecyl sulfate gel electrophoresis for analysis of multimeric proteins in platelets, *Electrophoresis*, **26**, 1189-1199.

Clarke, S. (1992) Protein isoprenylation and methylation at carboxyl-terminal cysteine residues, *Annual Review of Biochemistry*, **61**, 355-386.

Cockburn, I.L., *et al.* (2011) Screening for small molecule modulators of Hsp70 chaperone activity using protein aggregation suppression assays: Inhibition of the plasmodial chaperone PfHsp70-1, *Biological Chemistry*, **392**, 431-438.

Coetzee, M. (2004) Distribution of the African malaria vectors of the *Anopheles gambiae* complex, *The American Journal of Tropical Medicine and Hygiene*, **70**, 103-104.

Collins, F.H. and Paskewitz, S.M. (1995) Malaria: Current and future prospects for control, *Annual Review of Entomology*, **40**, 195-219.

Coppel, R.L., *et al.* (1986) Variable antigen associated with the surface of erythrocytes infected with mature stages of *Plasmodium falciparum*, *Molecular and Biochemical Parasitology*, **20**, 265-277.

Coppel, R.L., *et al.* (1988) MESA is a *Plasmodium falciparum* phosphoprotein associated with the erythrocyte membrane skeleton, *Molecular and Biochemical Parasitology*, **31**, 223-231.

Cowman, A.F. and Crabb, B.S. (2006) Invasion of red blood cells by malaria parasites, *Cell*, **124**, 755-766.

Cox, M.J., *et al.* (1994) Dynamics of malaria parasitaemia associated with febrile illness in children from a rural area of Madang, Papua New Guinea, *Transactions of the Royal Society of Tropical Medicine and Hygiene*, **88**, 191-197.

Crabb, B.S., *et al.* (1997) Targeted gene disruption shows that knobs enable malaria-infected red cells to cytoadhere under physiological shear stress, *Cell*, **89**, 287-296.

Crabb, B.S. and Cowman, A.F. (1996) Characterization of promoters and stable transfection by homologous and nonhomologous recombination in *Plasmodium falciparum*, *Proceedings of the National Academy of Sciences*, **93**, 7289-7294.

Crabb, B.S., de Koning-Ward, T.F. and Gilson, P.R. (2010) Protein export in *Plasmodium* parasites: From the endoplasmic reticulum to the vacuolar export machine, *International Journal for Parasitology*, **40**, 509-513.

Craig, E.A. and Marszalek, J. (2002) A specialized mitochondrial molecular chaperone system: A role in formation of Fe/S centers, *Cellular and Molecular Life Sciences*, **59**, 1658-1665.

Cunnea, P.M., *et al.* (2003) Erdj5, an endoplasmic reticulum (ER)-resident protein containing DnaJ and thioredoxin domains, is expressed in secretory cells or following ER stress, *The Journal of Biological Chemistry*, **278**, 1059-1066.

D'Alessandro, A., Righetti, P.G. and Zolla, L. (2009) The red blood cell proteome and interactome: An update, *Journal of Proteome Research*, **9**, 144-163.

Da Silva, E., *et al.* (1994) The *Plasmodium falciparum* protein RESA interacts with the erythrocyte cytoskeleton and modifies erythrocyte thermal stability, *Molecular and Biochemical Parasitology*, **66**, 59-69.

Dahl, E.L., *et al.* (2006) Tetracyclines specifically target the apicoplast of the malaria parasite *Plasmodium falciparum*, *Antimicrobial Agents and Chemotherapy*, **50**, 3124-3131.

Daily, J.P., *et al.* (2007) Distinct physiological states of *Plasmodium falciparum* in malaria-infected patients, *Nature*, **450**, 1091-1095.

De Blas, A.L. and Cherwinski, H.M. (1983) Detection of antigens on nitrocellulose paper immunoblots with monoclonal antibodies, *Analytical Biochemistry*, **133**, 214-219.

de Koning-Ward, T.F., *et al.* (2009) A newly discovered protein export machine in malaria parasites, *Nature*, **459**, 945-949.

Delves, M., *et al.* (2012) The activities of current antimalarial drugs on the life cycle stages of *Plasmodium*: A comparative study with human and rodent parasites, *PLOS Medicine*, **9**, e1001169.

Den, R.B. and Lu, B. (2012) Heat shock protein 90 inhibition: Rationale and clinical potential, *Therapeutic Advances in Medical Oncology*, **4**, 211-218.

Deuerling, E. and Bukau, B. (2004) Chaperone-assisted folding of newly synthesized proteins in the cytosol, *Critical Reviews in Biochemistry and Molecular Biology*, **39**, 261-277.

Dinglasan, R.R. and Jacobs-Lorena, M. (2008) Flipping the paradigm on malaria transmission-blocking vaccines, *Trends in Parasitology* **24**, 364-370.

Dobson, C.M. (2001) The structural basis of protein folding and its links with human disease, *Philosophical Transactions: Biological Sciences*, **356**, 133-145.

Dobson, C.M. (2004) Principles of protein folding, misfolding and aggregation, *Seminars in Cell & Developmental Biology*, **15**, 3-16.

Doolan, D.L., Dobaño, C. and Baird, J.K. (2009) Acquired immunity to malaria, *Clinical Microbiology Reviews*, **22**, 13-36.

Dragovic, Z., *et al.* (2006) Molecular chaperones of the Hsp110 family act as nucleotide exchange factors of Hsp70s, *The EMBO Journal*, **25**, 2519-2528.

Dragovic, Z., *et al.* (2006) Fes1p acts as a nucleotide exchange factor for the ribosome-associated molecular chaperone Ssb1p. *Biological Chemistry*. Berlin ; New York : W. De Gruyter, Biological chemistry., pp. 1593.

Duval, L., *et al.* (2010) African apes as reservoirs of *Plasmodium falciparum* and the origin and diversification of the laverania subgenus, *Proceedings of the National Academy of Sciences*, **107**, 10561-10566.

Easton, D.P., Kaneko, Y. and Subjeck, J.R. (2000) The Hsp110 and Grp170 stress proteins: Newly recognized relatives of the Hsp70s, *Cell Stress and Chaperones*, **5**, 276-290.

Edkins, A.L., Ludewig, M.H. and Blatch, G.L. (2004) A *Trypanosoma cruzi* heat shock protein 40 is able to stimulate the adenosine triphosphate hydrolysis activity of heat shock protein 70 and can substitute for a yeast heat shock protein 40., *The International Journal of Biochemistry & Cell Biology*, **36**, 1585-1598.

Eggers, D.K., Welch, W.J. and Hansen, W.J. (1997) Complexes between nascent polypeptides and their molecular chaperones in the cytosol of mammalian cells, *Molecular Biology of the Cell*, **8**, 1559-1573.

Elcock, A.H. (2010) Models of macromolecular crowding effects and the need for quantitative comparisons with experiment, *Current Opinion in Structural Biology*, **20**, 196-206.

Ellgaard, L. and Helenius, A. (2003) Quality control in the endoplasmic reticulum, *Nature Reviews Molecular Cell Biology*, **4**, 181-191.

Ellis, J. (1987) Proteins as molecular chaperones, *Nature*, **328**, 378-379.

Ellis, R.D., *et al.* (2010) Blood stage vaccines for *Plasmodium falciparum*: Current status and the way forward, *Human Vaccine*, **6**, 627-634.

Ellis, R.J. and van der Vies, S.M. (1991) Molecular chaperones, *Annual Review of Biochemistry* **60**, 321-347.

Elmendorf, H.G. and Haldar, K. (1994) *Plasmodium falciparum* exports the golgi marker sphingomyelin synthase into a tubovesicular network in the cytoplasm of mature erythrocytes, *The Journal of Cell Biology*, **124**, 449-462.

Emanuelsson, O., *et al.* (2000) Predicting subcellular localization of proteins based on their N-terminal amino acid sequence, *Journal of Molecular Biology*, **300**, 1005-1016.

Emini, E.A., *et al.* (1985) Induction of hepatitis A virus-neutralizing antibody by a virus-specific synthetic peptide, *Journal of Virology*, **55**, 836-839.

Evans, C.G., Chang, L. and Gestwicki, J.E. (2010) Heat shock protein 70 (Hsp70) as an emerging drug target, *Journal of Medicinal Chemistry*, **53**, 4585-4602.

Fast, N.M., *et al.* (2001) Nuclear-encoded, plastid-targeted genes suggest a single common origin for apicomplexan and dinoflagellate plastids, *Molecular Biology and Evolution*, **18**, 418-426.

Feagin, J.E. (2000) Mitochondrial genome diversity in parasites, *International Journal for Parasitology*, **30**, 371-390.

Feder, M.E. and Hofmann, G.E. (1999) Heat-shock proteins, molecular chaperones, and the stress response: Evolutionary and ecological physiology, *Annual Review of Physiology*, **61**, 243-282.

Felsner, G., *et al.* (2011) Erad components in organisms with complex red plastids suggest recruitment of a preexisting protein transport pathway for the periplastid membrane, *Genome Biology and Evolution*, **3**, 140-150.

Ferreira, M.U., da Silva Nunes, M. and Wunderlich, G. (2004) Antigenic diversity and immune evasion by malaria parasites, *Clinical and Diagnostic Laboratory Immunology*, **11**, 987-995.

Fewell, S.W., *et al.* (2004) Small molecule modulators of endogenous and co-chaperone-stimulated Hsp70 ATPase activity, *The Journal of Biological Chemistry*, **279**, 51131-51140.

Fichera, M.E. and Roos, D.S. (1997) A plastid organelle as a drug target in apicomplexan parasites, *Nature*, **390**, 407-409.

Fidock, D.A., *et al.* (2008) Recent highlights in antimalarial drug resistance and chemotherapy research, *Trends in Parasitology*, **24**, 537-544.

Fidock, D.A., *et al.* (2004) Antimalarial drug discovery: Efficacy models for compound screening, *Nature Reviews Drug Discovery*, **3**, 509-520.

Figueras, M.J., *et al.* (2012) Toxoplasma gondii Sis1-like J-domain protein is a cytosolic chaperone associated to Hsp90/Hsp70 complex, *International Journal of Biological Macromolecules*, **50**, 725-733.

Florens, L., *et al.* (2002) A proteomic view of the *Plasmodium falciparum* life cycle, *Nature*, **419**, 520-526.

Foley, M., *et al.* (1994) *Plasmodium falciparum*: Mapping the membrane-binding domain in the ring-infected erythrocyte surface antigen, *Experimental Parasitology*, **79**, 340-350.

Foth, B.J., *et al.* (2003) Dissecting apicoplast targeting in the malaria parasite *Plasmodium falciparum*, *Science*, **299**, 705-708.

Frankland, S., *et al.* (2006) Delivery of the malaria virulence protein PfEMP1 to the erythrocyte surface requires cholesterol-rich domains, *Eukaryotic Cell*, **5**, 849-860.

Frech, C. and Chen, N. (2011) Genome comparison of human and non-human malaria parasites reveals species subset-specific genes potentially linked to human disease, *PLOS Computational Biology*, **7**, e1002320.

Fujioka, H. and Aikawa, M. (2002) Structure and life cycle. In Perlmann, P. and Troye-Blomberg, M. (eds), *Malaria immunology*. Karger, Basel, pp. 1-26.

Fulda, S., *et al.* (2010) Cellular stress responses: Cell survival and cell death, *International Journal of Cell Biology*, **2010**, 214074.

Gakh, O., Cavadini, P. and Isaya, G. (2002) Mitochondrial processing peptidases, *BBA - Molecular Cell Research*, **1592**, 63-77.

Gallup, J.L. and Sachs, J.D. (2001) The economic burden of malaria, *The American Journal of Tropical Medicine and Hygiene*, **64**, 85-96.

Gamble, C., *et al.* (2007) Insecticide-treated nets for the prevention of malaria in pregnancy: A systematic review of randomised controlled trials, *PLOS Medicine*, **4**, e107.

Gardner, M.J., *et al.* (2002) Genome sequence of the human malaria parasite *Plasmodium falciparum*, *Nature*, **419**, 498-511.

Gatton, M.L. and Cheng, Q. (2004) Modeling the development of acquired clinical immunity to *Plasmodium falciparum* malaria, *Infection and Immunity*, **72**, 6538-6545.

Gehde, N., *et al.* (2009) Protein unfolding is an essential requirement for transport across the parasitophorous vacuolar membrane of *Plasmodium falciparum*, *Molecular Microbiology*, **71**, 613-628.

Genevaux, P., *et al.* (2002) Scanning mutagenesis identifies amino acid residues essential for the in vivo activity of the *Escherichia coli* DnaJ (Hsp40) J-domain, *Genetics*, **162**, 1045-1053.

Gershoni, J.M. and Palade, G.E. (1982) Electrophoretic transfer of proteins from Sodium Dodecyl Sulfate-Polyacrylamide gels to a positively charged membrane filter, *Analytical Biochemistry*, **124**, 396-405.

Gething, M.-J. and Sambrook, J. (1992) Protein folding in the cell, *Nature*, **355**, 33-45.

Gething, P., *et al.* (2011) A new World malaria map: *Plasmodium falciparum* endemicity in 2010, *Malaria Journal*, **10**, 378.

Gitau, G.W., *et al.* (2012) Characterisation of the *Plasmodium falciparum* Hsp70-Hsp90 organising protein (PfHop), *Cell Stress and Chaperones*, **17**, 191-202.

Goloudina, A.R., Demidov, O.N. and Garrido, C. (2012) Inhibition of Hsp70: A challenging anti-cancer strategy, *Cancer Letters*, **325**, 117-124.

Good, M.F. (2001) Towards a blood-stage vaccine for malaria: Are we following all the leads?, *Nature Reviews Immunology*, **1**, 117-125.

Good, M.F., Kaslow, D.C. and Miller, L.H. (1998) Pathways and strategies for developing a malaria blood-stage vaccine, *Annual Reviews of Immunology*, **16**, 57-87.

Gould, S.B., Waller, R.F. and McFadden, G.I. (2008) Plastid evolution, *Annual Review of Plant Biology*, **59**, 491-517.

Greene, M.K., Maskos, K. and Landry, S.J. (1998) Role of the J-domain in the cooperation of Hsp40 with Hsp70, *Proceedings of the National Academy of Sciences*, **95**, 6108-6113.

Greenwood, B.M., *et al.* (2008) Malaria: Progress, perils, and prospects for eradication, *The Journal of Clinical Investigation*, **118**, 1266-1276.

Grimberg, B.T. and Mehlotra, R.K. (2011) Expanding the antimalarial drug arsenal-now, but how?, *Pharmaceuticals (Basel)*, **4**, 681-712.

Grover, M., *et al.* (2013) Identification of an exported heat shock protein 70 in *Plasmodium falciparum*, *Parasite*, **20**.

Gupta, S., *et al.* (1999) Immunity to non-cerebral severe malaria is acquired after one or two infections, *Nature Medicine*, **5**, 340-343.

Haas, L.F. (1999) Charles louis Alphonse Laveran (1845-1922), *Journal of Neurology, Neurosurgery & Psychiatry*, **67**, 520.

Haase, S. and de Koning-Ward, T.F. (2010) New insights into protein export in malaria parasites, *Cellular Microbiology*, **12**, 580-587.

Haigis, M.C. and Yankner, B.A. (2010) The aging stress response, *Molecular Cell*, **40**, 333-344.

Hanssen, E., *et al.* (2010) Whole cell imaging reveals novel modular features of the exomembrane system of the malaria parasite, *Plasmodium falciparum*, *International Journal for Parasitology*, **40**, 123-134.

Harrison, C.J., *et al.* (1997) Crystal structure of the nucleotide exchange factor Grpe bound to the ATPase domain of the molecular chaperone DnaK, *Science*, **276**, 431-435.

Hartl, F.U. (1996) Molecular chaperones in cellular protein folding, *Nature*, **381**, 571-580.

Hartl, F.U., Bracher, A. and Hayer-Hartl, M. (2011) Molecular chaperones in protein folding and proteostasis, *Nature*, **475**, 324-332.

Hartl, F.U. and Hayer-Hartl, M. (2002) Molecular chaperones in the cytosol: From nascent chain to folded protein, *Science*, **295**, 1852-1858.

Hartl, F.U. and Hayer-Hartl, M. (2009) Converging concepts of protein folding in vitro and in vivo, *Nature Structural & Molecular Biology*, **16**, 574-581.

Hatefi, Y. (1985) The mitochondrial electron transport and oxidative phosphorylation system, *Annual Review of Biochemistry*, **54**, 1015-1069.

Hawley, W.A., *et al.* (2003) Community-wide effects of permethrin-treated bed nets on child mortality and malaria morbidity in western Kenya, *The American Journal of Tropical Medicine and Hygiene*, **68**, 121-127.

Henderson, B. (2010) Integrating the cell stress response: A new view of molecular chaperones as immunological and physiological homeostatic regulators, *Cell Biochemistry and Function*, **28**, 1-14.

Hennessy, F., *et al.* (2005) Not all J domains are created equal: Implications for the specificity of Hsp40-Hsp70 interactions, *Protein Science*, **14**, 1697-1709.

Hibbs, A.R. and Saul, A.J. (1994) *Plasmodium falciparum*: Highly mobile small vesicles in the malaria-infected red blood cell cytoplasm, *Experimental Parasitology*, **79**, 260-269.

Higurashi, T., *et al.* (2008) Specificity of the J-protein Sis1 in the propagation of 3 yeast prions, *Proceedings of the National Academy of Sciences*, **105**, 16596-16601.

Hill, R.B., Flanagan, J.M. and Prestegard, J.H. (1995) 1H and 15N magnetic resonance assignments, secondary structure, and tertiary fold of *Escherichia coli* DnaJ (1-78), *Biochemistry*, **34**, 5587-5596.

Hiller, N.L., *et al.* (2004) A host-targeting signal in virulence proteins reveals a secretome in malarial infection, *Science*, **306**, 1934-1937.

Hirai, M. and Mori, T. (2010) Fertilization is a novel attacking site for the transmission blocking of malaria parasites, *Acta Tropica*, **114**, 157-161.

Ho, M. and White, N.J. (1999) Molecular mechanisms of cytoadherence in malaria, *American Journal of Physiology - Cell Physiology*, **276**, C1231-C1242.

Hoffman, S.L., *et al.* (2002) Protection of humans against malaria by immunization with radiation-attenuated *Plasmodium falciparum* sporozoites, *Journal of Infectious Diseases*, **185**, 1155-1164.

Hofmann, G.E. and Todgham, A.E. (2010) Living in the now: Physiological mechanisms to tolerate a rapidly changing environment, *Annual Review of Physiology*, **72**, 127-145.

Hofmann, H.J. and Hadge, D. (1987) On the theoretical prediction of protein antigenic determinants from amino acid sequences, *Biomedica Biochimica Acta*, **46**, 855-866.

Holder, A.A. (2009) The carboxy-terminus of merozoite surface protein 1: Structure, specific antibodies and immunity to malaria, *Parasitology*, **136**, 1445-1456.

Hopp, T.P. and Woods, K.R. (1981) Prediction of protein antigenic determinants from amino acid sequences, *Proceedings of the National Academy of Sciences*, **78**, 3824-3828.

Hosoda, A., *et al.* (2003) Jpdi, a novel endoplasmic reticulum-resident protein containing both a Bip-interacting J-domain and thioredoxin-like motifs, *The Journal of Biological Chemistry*, **278**, 2669-2676.

Ishino, T., *et al.* (2004) Cell-passage activity is required for the malarial parasite to cross the liver sinusoidal cell layer, *PLOS Biology*, **2**, e4.

Ito, A. (1999) Mitochondrial processing peptidase: Multiple-site recognition of precursor proteins, *Biochemical and Biophysical Research Communications*, **265**, 611-616.

Jackson, S. (2012) Hsp90: Structure and function. In. Springer Berlin / Heidelberg, pp. 1-86.

Jameson, B.A. and Wolf, H. (1988) The antigenic index: A novel algorithm for predicting antigenic determinants, *Computer Applications in the Biosciences*, **4**, 181-186.

Johnson, E.O., *et al.* (1992) Mechanisms of stress: A dynamic overview of hormonal and behavioral homeostasis, *Neuroscience & Biobehavioral Reviews*, **16**, 115-130.

Johnson, J.L. (2012) Evolution and function of diverse Hsp90 homologs and cochaperone proteins, *BBA Molecular Cell Research*, **1823**, 607-613.

Joshi, B., Biswas, S. and Sharma, Y.D. (1992) Effect of heat-shock on *Plasmodium falciparum* viability, growth and expression of the heat-shock protein '*PfHsp70-1*' gene, *FEBS Letters*, **312**, 91-94.

Juan, D., Pazos, F. and Valencia, A. (2008) High-confidence prediction of global interactomes based on genome-wide coevolutionary networks, *Proceedings of the National Academy of Sciences*, **105**, 934-939.

Kabani, M., *et al.* (2002) Hsp-bp1, a homologue of the yeast Fes1 and Sis1 proteins, is an Hsc70 nucleotide exchange factor, *FEBS Letters*, **531**, 339-342.

Käll, L., Krogh, A. and Sonnhammer, E.L.L. (2004) A combined transmembrane topology and signal peptide prediction method, *Journal of Molecular Biology*, **338**, 1027-1036.

Kampinga, H.H. and Craig, E.A. (2010) The Hsp70 chaperone machinery: J proteins as drivers of functional specificity, *Nature Reviews Molecular Cell Biology*, **11**, 579-592.

Karlin, S. and Brocchieri, L. (1998) Heat shock protein 70 family: Multiple sequence comparisons, function, and evolution, *Journal of Molecular Evolution*, **47**, 565-577.

Karlsson, R., *et al.* (1994) Kinetic and concentration analysis using bia technology, *Methods*, **6**, 99-110.

Karnataki, A., *et al.* (2007) Cell cycle-regulated vesicular trafficking of *Toxoplasma* Apt1, a protein localized to multiple apicoplast membranes, *Molecular Microbiology*, **63**, 1653-1668.

Karplus, P.A. and Schulz, G.E. (1985) Prediction of chain flexibility in proteins - a tool for the selection of peptide antigens, *Naturwissenschaften*, **72**, 212-213.

Karunamoorthi, K. (2011) Vector control: A cornerstone in the malaria elimination campaign, *Clinical Microbiology and Infection*, **17**, 1608-1616.

Kassahn, K.S., *et al.* (2009) Animal performance and stress: Responses and tolerance limits at different levels of biological organisation, *Biological Reviews*, **84**, 277-292.

Khan, S.M., *et al.* (2005) Proteome analysis of separated male and female gametocytes reveals novel sex-specific *Plasmodium* biology, *Cell*, **121**, 675-687.

Kilili, G.K. and LaCount, D.J. (2011) An erythrocyte cytoskeleton-binding motif in exported *Plasmodium falciparum* proteins, *Eukaryotic Cell*, 1439-1447.

Kleizen, B. and Braakman, I. (2004) Protein folding and quality control in the endoplasmic reticulum, *Current Opinion in Cell Biology*, **16**, 343-349.

Kohler, S., *et al.* (1997) A plastid of probable green algal origin in apicomplexan parasites, *Science*, **275**, 1485-1489.

Kondoh, Y. and Osada, H. (2012) High-throughput screening identifies small molecule inhibitors of molecular chaperones, *Current Pharmaceutical Design*.

Kültz, D. (2003) Evolution of the cellular stress proteome: From monophyletic origin to ubiquitous function, *Journal of Experimental Biology*, **206**, 3119-3124.

Kültz, D. (2005) Molecular and evolutionary basis of the cellular stress response, *Annual Review of Physiology*, **67**, 225-257.

Külzer, S., *et al.* (2012) *Plasmodium falciparum*-encoded exported Hsp70/Hsp40 chaperone/co-chaperone complexes within the host erythrocyte, *Cellular Microbiology*, **14**, 1784–1795.

Külzer, S., Gehde, N. and Przyborski, J.M. (2009) Return to sender: Use of *Plasmodium* ER retrieval sequences to study protein transport in the infected erythrocyte and predict putative ER protein families, *Parasitology Research*, **104**, 1535-1541.

Külzer, S., *et al.* (2010) Parasite-encoded Hsp40 proteins define novel mobile structures in the cytosol of the *P. falciparum*-infected erythrocyte, *Cellular Microbiology*, **12**, 1398-1420.

Kumar, A., *et al.* (2010) Nuclear-encoded DnaJ homologue of *Plasmodium falciparum* interacts with replication ori of the apicoplast genome, *Molecular Microbiology*, **75**, 942-956.

Kumar, B., *et al.* (2011) Interaction between sulphur mobilisation proteins Sufb and Sufc: Evidence for an iron–sulphur cluster biogenesis pathway in the apicoplast of *Plasmodium falciparum*, *International Journal for Parasitology*, **41**, 991-999.

Kumar, N., *et al.* (1991) Induction and localization of *Plasmodium falciparum* stress proteins related to the heat shock protein 70 family, *Molecular and Biochemical Parasitology*, **48**, 47-58.

Kumar, N., *et al.* (1988) *Plasmodium falciparum* gene encoding a protein similar to the 78-kDa rat glucose-regulated stress protein, *Proceedings of the National Academy of Sciences*, **85**, 6277-6281.

Kyte, J. and Doolittle, R.F. (1982) A simple method for displaying the hydropathic character of a protein, *Journal of Molecular Biology*, **157**, 105-132.

LaCount, D.J., *et al.* (2005) A protein interaction network of the malaria parasite *Plasmodium falciparum*, *Nature*, **438**, 103-107.

Laemmli, U.K. (1970) Cleavage of structural proteins during the assembly of the head of bacteriophage T4, *Nature*, **227**, 680-685.

Laishram, D., *et al.* (2012) The complexities of malaria disease manifestations with a focus on asymptomatic malaria, *Malaria Journal*, **11**, 29.

Lambros, C. and Vanderberg, J.P. (1979) Synchronization of *Plasmodium falciparum* erythrocytic stages in culture, *The Journal of Parasitology*, **65**, 418-420.

Lang, M., Apt, K.E. and Kroth, P.G. (1998) Protein transport into "complex" diatom plastids utilizes two different targeting signals, *The Journal of Biological Chemistry*, **273**, 30973-30978.

Langer, T., *et al.* (1992) Successive action of DnaK, DnaJ and Groel along the pathway of chaperone-mediated protein folding, *Nature*, **356**, 683-689.

Langhorne, J., *et al.* (2011) The relevance of non-human primate and rodent malaria models for humans, *Malaria Journal*, **10**, 23.

Lansbury, P.T. and Lashuel, H.A. (2006) A century-old debate on protein aggregation and neurodegeneration enters the clinic, *Nature*, **443**, 774-779.

Lanzetta, P.A., *et al.* (1979) An improved assay for nanomole amounts of inorganic phosphate, *Analytical Biochemistry*, **100**, 95-97.

Larkin, M.A., *et al.* (2007) Clustal W and clustal X version 2.0, *Bioinformatics*, **23**, 2947-2948.

Lasonder, E., *et al.* (2008) Proteomic profiling of *Plasmodium* sporozoite maturation identifies new proteins essential for parasite development and infectivity, *PLOS Pathogens*, **4**, e1000195.

Lavazec, C. and Bourgouin, C. (2008) Mosquito-based transmission blocking vaccines for interrupting *Plasmodium* development, *Microbes and Infection*, **10**, 845-849.

Le Roch, K.G., *et al.* (2003) Discovery of gene function by expression profiling of the malaria parasite life cycle, *Science*, **301**, 1503-1508.

Lee, S. and Tsai, F.T.F. (2005) Molecular chaperones in protein quality control, *Journal of Biochemistry and Molecular Biology*, **38**, 259-265.

Leech, J.H., *et al.* (1984) Identification of a strain-specific malarial antigen exposed on the surface of *Plasmodium falciparum*-infected erythrocytes, *The Journal of Experimental Medicine*, **159**, 1567-1575.

Lengeler, C. (2004) Insecticide-treated bed nets and curtains for preventing malaria, *Cochrane database of Systematic reviews*, CD000363.

Lengeler, C., *et al.* (1998) Relative versus absolute risk of dying reduction after using insecticide-treated nets for malaria control in Africa, *Tropical Medicine & International Health*, **3**, 286-290.

Lengeler, C. and Sharp, B. (2003) Indoor residual spraying and insecticide-treated nets. In reducing malaria's burden: Evidence of effectiveness for decision makers. In Murphy, C., *et al.* (eds). Global Health Council, Washington, D.C.

Lengeler, C. and Snow, R.W. (1996) From efficacy to effectiveness: Insecticide-treated bednets in Africa, *Bulletin of the World Health Organization*, **74**, 325-332.

Letunic, I., Doerks, T. and Bork, P. (2012) Smart 7: Recent updates to the protein domain annotation resource, *Nucleic Acids Research*, **40**, D302-D305.

Lewis, A.C.F., Saeed, R. and Deane, C.M. (2010) Predicting protein-protein interactions in the context of protein evolution, *Molecular BioSystems*, **6**, 55-64.

Li, J., Qian, X. and Sha, B. (2003) The crystal structure of the yeast Hsp40 Ydj1 complexed with its peptide substrate, *Structure*, **11**, 1475-1483.

Li, J., Soroka, J. and Buchner, J. (2012) The Hsp90 chaperone machinery: Conformational dynamics and regulation by co-chaperones, *BBA Molecular Cell Research*, **1823**, 624-635.

Li, J., *et al.* (2006) Crystal structure of yeast Sis1 peptide-binding fragment and Hsp70 Ssa1 C-terminal complex, *Biochemical Journal*, **398**, 353-360.

Li, J.Z., Qian, X.G. and Sha, B.D. (2009) Heat shock protein 40: Structural studies and their functional implications, *Protein Peptide Letters*, **16**, 606-612.

Liberek, K., *et al.* (1991) The *Escherichia coli* DnaK chaperone, the 70-kDa heat shock protein eukaryotic equivalent, changes conformation upon ATP hydrolysis, thus triggering its dissociation from a bound target protein., *The Journal of Biological Chemistry*, **266**, 14491-14496.

Liedberg, B., Nylander, C. and Lunström, I. (1983) Surface plasmon resonance for gas detection and biosensing, *Sensors and Actuators*, **4**, 299-304.

Lim, L. and McFadden, G.I. (2010) The evolution, metabolism and functions of the apicoplast, *Philosophical transactions of the Royal Society of London. Series B, Biological sciences*, **365**, 749-763.

Lima, T., *et al.* (2009) Hamap: A database of completely sequenced microbial proteome sets and manually curated microbial protein families in UniProtKB/Swiss-Prot, *Nucleic Acids Research*, **37**, D471-D478.

Lindquist, S. (1986) The heat-shock response, *Annual Review of Biochemistry* **55**, 1151-1191.

Lindquist, S. and Craig, E.A. (1988) The heat-shock proteins, *Annual Review of Genetics*, **22**, 631-677.

Liu, Q., *et al.* (2003) Regulated cycling of mitochondrial Hsp70 at the protein import channel, *Science*, **300**, 139-141.

Liu, S., *et al.* (2004) Identification of the proteins required for biosynthesis of diphthamide, the target of bacterial ADP-ribosylating toxins on translation elongation factor 2, *Molecular and Cellular Biology*, **24**, 9487-9497.

Llinás, M., *et al.* (2006) Comparative whole genome transcriptome analysis of three *Plasmodium falciparum* strains, *Nucleic Acids Research*, **34**, 1166-1173.

Logan-Klumpler, F.J., *et al.* (2011) GeneDB—an annotation database for pathogens, *Nucleic Acids Research*, D98-D108.

Lu, B., *et al.* (2006) Tid1 isoforms are mitochondrial DnaJ-like chaperones with unique carboxyl termini that determine cytosolic fate, *The Journal of Biological Chemistry*, **281**, 13150-13158.

Lustigman, S., *et al.* (1990) The mature-parasite-infected erythrocyte surface antigen (MESA) of *Plasmodium falciparum* associates with the erythrocyte membrane skeletal protein, band 4.1, *Molecular and Biochemical Parasitology*, **38**, 261-270.

Magowan, C., *et al.* (1995) Role of the *Plasmodium falciparum* mature-parasite-infected erythrocyte surface antigen (MESA/PfEMP-2) in malarial infection of erythrocytes, *Blood*, **86**, 3196-3204.

Maier, A.G., *et al.* (2009) Malaria parasite proteins that remodel the host erythrocyte, *Nature Reviews Microbiology*, **7**, 341-354.

Maier, A.G., *et al.* (2008) Exported proteins required for virulence and rigidity of *Plasmodium falciparum*-infected human erythrocytes, *Cell*, **134**, 48-61.

Malmqvist, M. (1993) Biospecific interaction analysis using biosensor technology, *Nature*, **361**, 186-187.

Mamoun, C.B., *et al.* (2001) Co-ordinated programme of gene expression during asexual intraerythrocytic development of the human malaria parasite *Plasmodium falciparum* revealed by microarray analysis, *Molecular Microbiology*, **39**, 26-36.

Marsh, K., *et al.* (1995) Indicators of life-threatening malaria in African children, *The New England Journal of Medicine*, **332**, 1399-1404.

Marti, M., *et al.* (2004) Targeting malaria virulence and remodeling proteins to the host erythrocyte, *Science*, **306**, 1930-1933.

Martin, J. (1997) Molecular chaperones and mitochondrial protein folding, *Journal of Bioenergetics and Biomembranes*, **29**, 35-43.

Marzec, M., Eletto, D. and Argon, Y. (2012) Grp94: An Hsp90-like protein specialized for protein folding and quality control in the endoplasmic reticulum, *BBA Molecular Cell Research*, **1823**, 774-787.

Matambo, T.S., *et al.* (2004) Overproduction, purification, and characterization of the *Plasmodium falciparum* heat shock protein 70, *Protein Expression and Purification*, **33**, 214-222.

Matuschewski, K. (2006) Getting infectious: Formation and maturation of *Plasmodium* sporozoites in the Anopheles vector, *Cellular Microbiology*, **8**, 1547-1556.

Maurer-Stroh, S. and Eisenhaber, F. (2005) Refinement and prediction of protein prenylation motifs, *Genome Biology* **6**, R55.

Mayer, M.P. (2010) Gymnastics of molecular chaperones, *Molecular cell*, **39**, 321-331.

Mayer, M.P. and Bukau, B. (2005) Hsp70 chaperones: Cellular functions and molecular mechanism, *Cellular and Molecular Life Sciences*, **62**, 670-684.

McCarty, J.S., *et al.* (1995) The role of ATP in the functional cycle of the DnaK chaperone system, *Journal of Molecular Biology*, **249**, 126-137.

McClellan, A.J., *et al.* (2005) Protein quality control: Chaperones culling corrupt conformations, *Nature cell biology*, **7**, 736-741.

McFadden, G.I., *et al.* (1996) Plastid in human parasites, *Nature*, **381**, 482.

Meimaridou, E., Gooljar, S.B. and Chapple, J.P. (2009) From hatching to dispatching: The multiple cellular roles of the Hsp70 molecular chaperone machinery, *Journal of Molecular Endocrinology*, **42**, 1-9.

Miller, L.H., *et al.* (2002) The pathogenic basis of malaria, *Nature*, **415**, 673-679.

Mills, A., Lubell, Y. and Hanson, K. (2008) Malaria eradication: The economic, financial and institutional challenge, *Malaria Journal*, **7 Suppl 1**, S11.

Misra, G. and Ramachandran, R. (2009) Hsp70-1 from *Plasmodium falciparum*: Protein stability, domain analysis and chaperone activity, *Biophysical Chemistry*, **142**, 55-64.

Misra, G. and Ramachandran, R. (2010) Exploring the positional importance of aromatic residues and lysine in the interactions of peptides with the *Plasmodium falciparum* Hsp70-1, *BBA Proteins and Proteomics*, **1804**, 2146-2152.

Mogi, T. and Kita, K. (2010) Diversity in mitochondrial metabolic pathways in parasitic protists *Plasmodium* and *Cryptosporidium*, *Parasitology International*, **59**, 305-312.

Moorthy, V.S., Good, M.F. and Hill, A.V. (2004) Malaria vaccine developments, *The Lancet*, **363**, 150-156.

Morahan, B.J., *et al.* (2011) Functional analysis of the exported type IV Hsp40 protein PfGECO in *P. falciparum* gametocytes, *Eukaryotic Cell*, EC.05155-05111.

Mota, M.M., Hafalla, J.C.R. and Rodriguez, A. (2002) Migration through host cells activates *Plasmodium* sporozoites for infection, *Nature Medicine*, **8**, 1318-1322.

Muchowski, P.J. (2002) Protein misfolding, amyloid formation, and neurodegeneration: A critical role for molecular chaperones?, *Neuron*, **35**, 9-12.

Murphy, S.C. and Breman, J.G. (2001) Gaps in the childhood malaria burden in Africa: Cerebral malaria, neurological sequelae, anemia, respiratory distress, hypoglycemia, and

complications of pregnancy, *The American Journal of Tropical Medicine and Hygiene*, **64**, 57-67.

Murray, C.J.L., *et al.* (2012) Global malaria mortality between 1980 and 2010: A systematic analysis, *The Lancet*, **379**, 413-431.

Mutabingwa, T.K. (2005) Artemisinin-based combination therapies (ACTs): Best hope for malaria treatment but inaccessible to the needy!, *Acta Tropica*, **95**, 305-315.

Neupert, W. (1997) Protein import into mitochondria, *Annual Review of Biochemistry*, **66**, 863-917.

Neupert, W. and Brunner, M. (2002) The protein import motor of mitochondria, *Nature Reviews Molecular Cell Biology*, **3**, 555-565.

Nicholas, K.B., Nicholas, H.B. and Deerfield, D.W. (1997) GeneDoc: Analysis and visualization of genetic variation, *EMBNET news*, **4**, 14.

Nicoll, W.S., *et al.* (2007) Cytosolic and ER J-domains of mammalian and parasitic origin can functionally interact with DnaK, *The International Journal of Biochemistry & Cell Biology*, **39**, 736-751.

Nielsen, H., *et al.* (1997) Identification of prokaryotic and eukaryotic signal peptides and prediction of their cleavage sites, *Protein Engineering*, **10**, 1-6.

Nilsson, I., Whitley, P. and von Heijne, G. (1994) The COOH-terminal ends of internal signal and signal-anchor sequences are positioned differently in the ER translocase, *The Journal of Cell Biology*, **126**, 1127-1132.

Nussenzweig, R.S., *et al.* (1967) Protective immunity produced by the injection of x-irradiated sporozoites of *Plasmodium berghei*, *Nature*, **216**, 160-162.

Nyalwidhe, J. and Lingelbach, K. (2006) Proteases and chaperones are the most abundant proteins in the parasitophorous vacuole of *Plasmodium falciparum*-infected erythrocytes, *Proteomics*, **6**, 1563-1573.

O'Brien, M.C. and McKay, D.B. (1993) Threonine 204 of the chaperone protein Hsc70 influences the structure of the active site, but is not essential for ATP hydrolysis, *The Journal of Biological Chemistry*, **268**, 24323-24329.

Oakley, M.S., *et al.* (2007) Molecular factors and biochemical pathways induced by febrile temperature in intraerythrocytic *Plasmodium falciparum* parasites, *Infection and Immunity*, **75**, 2012-2025.

Olliaro, P. and Wells, T.N.C. (2009) The global portfolio of new antimalarial medicines under development, *Clinical Pharmacology & Therapeutics*, **85**, 584-595.

Olson, C.L., *et al.* (1994) Molecular and biochemical comparison of the 70-kDa heat shock proteins of *Trypanosoma cruzi*, *The Journal of Biological Chemistry*, **269**, 3868-3874.

Olszewski, K.L., *et al.* (2010) Branched tricarboxylic acid metabolism in *Plasmodium falciparum*, *Nature*, **466**, 774-778.

Pain, A., *et al.* (2008) The genome of the simian and human malaria parasite *Plasmodium knowlesi*, *Nature*, **455**, 799-803.

Pallavi, R., *et al.* (2010) Chaperone expression profiles correlate with distinct physiological states of *Plasmodium falciparum* in malaria patients, *Malaria Journal*, **9**, 236.

Pallavi, R., *et al.* (2010) Heat shock protein 90 as a drug target against protozoan infections, *The Journal of Biological Chemistry*, **285**, 37964-37975.

Parsons, M., *et al.* (2007) Protein trafficking to the apicoplast: Deciphering the apicomplexan solution to secondary endosymbiosis, *Eukaryotic Cell*, **6**, 1081-1088.

Pavithra, S.R., Kumar, R. and Tatu, U. (2007) Systems analysis of chaperone networks in the malarial parasite *Plasmodium falciparum*, *PLOS Computational Biology*, **3**, e168.

Pearl, L.H. and Prodromou, C. (2006) Structure and mechanism of the Hsp90 molecular chaperone machinery, *Annual Review of Biochemistry*, **75**, 271-294.

Pei, X., *et al.* (2007) The ring-infected erythrocyte surface antigen (RESA) of *Plasmodium falciparum* stabilizes spectrin tetramers and suppresses further invasion, *Blood*, **110**, 1036-1042.

Perkins, D.J., *et al.* (2011) Severe malarial anemia: Innate immunity and pathogenesis, *International Journal of Biological Sciences*, **7**, 1427-1442.

Pesce, E.R., *et al.* (2008) The *Plasmodium falciparum* heat shock protein 40, Pfj4, associates with heat shock protein 70 and shows similar heat induction and localisation patterns, *The International Journal of Biochemistry & Cell Biology*, **40**, 2914-2926.

Pesce, E.R., *et al.* (2010) Malaria heat shock proteins: Drug targets that chaperone other drug targets, *Infectious Disorders - Drug Targets*, **10**, 147-157.

Petersen, C., *et al.* (1989) The mature erythrocyte surface antigen of *Plasmodium falciparum* is not required for knobs or cytoadherence, *Molecular and Biochemical Parasitology*, **36**, 61-65.

Pfanner, N. and Geissler, A. (2001) Versatility of the mitochondrial protein import machinery, *Nature Reviews Molecular Cell Biology*, **2**, 339-349.

Pfund, C., *et al.* (1998) The molecular chaperone SSB from *Saccharomyces cerevisiae* is a component of the ribosome-nascent chain complex, *The EMBO Journal*, **17**, 3981-3989.

Pizzi, E. and Frontali, C. (2001) Low-complexity regions in *Plasmodium falciparum* proteins, *Genome Research*, **11**, 218-229.

Planche, T., *et al.* (2005) Metabolic complications of severe malaria, *Current Topics in Microbiology and Immunology*, **295**, 105-136.

Planche, T. and Krishna, S. (2006) Severe malaria: Metabolic complications, *Current Molecular Medicine*, **6**, 141-153.

Plattner, F. and Soldati-Favre, D. (2008) Hijacking of host cellular functions by the apicomplexa, *Annual Review of Microbiology*, **62**, 471-487.

Pluess, B., *et al.* (2010) Indoor residual spraying for preventing malaria, *Cochrane database of Systematic reviews*, CD006657.

Polier, S., *et al.* (2008) Structural basis for the cooperation of Hsp70 and Hsp110 chaperones in protein folding, *Cell*, **133**, 1068-1079.

Pratt, W.B., *et al.* (2004) Role of Hsp90 and the Hsp90-binding immunophilins in signalling protein movement, *Cellular Signalling*, **16**, 857-872.

Pratt, W.B. and Toft, D.O. (2003) Regulation of signaling protein function and trafficking by the Hsp90/Hsp70-based chaperone machinery, *Experimental Biology and Medicine*, **228**, 111-133.

Prodromou, C., *et al.* (1999) Regulation of Hsp90 ATPase activity by tetratricopeptide repeat (TPR)-domain co-chaperones, *The EMBO Journal*, **18**, 754-762.

Przyborski, J.M., *et al.* (2005) Trafficking of stevor to the maurer's clefts in *Plasmodium falciparum*-infected erythrocytes, *The EMBO Journal*, **24**, 2306-2317.

Przyborski, J.M., *et al.* (2003) Maurer's clefts--a novel secretory organelle?, *Molecular and Biochemical Parasitology*, **132**, 17-26.

Qian, X., *et al.* (2002) Direct interactions between molecular chaperones heat-shock protein (Hsp) 70 and Hsp40: Yeast Hsp70 Ssa1 binds the extreme C-terminal region of yeast Hsp40 Sis1, *Biochemical Journal*, **361**, 27-34.

Rajan, V.B. and D'Silva, P. (2009) *Arabidopsis thaliana* J-class heat shock proteins: Cellular stress sensors, *Functional & Integrative Genomics*, **9**, 433-446.

Ralph, S.A., *et al.* (2004) Tropical infectious diseases: Metabolic maps and functions of the *Plasmodium falciparum* apicoplast, *Nature Reviews Microbiology*, **2**, 203-216.

Ramachandran, R. (2011) Exploring the positional importance of aromatic residues and lysine in the interactions of peptides with the *Plasmodium falciparum* Hsp70-1, *BBA-Proteins Proteom*, **1814**, 457.

Ramirez, J.L., Garver, L.S. and Dimopoulos, G. (2009) Challenges and approaches for mosquito targeted malaria control, *Current Molecular Medicine*, **9**, 116-130.

Ramya, T.N., *et al.* (2007) 15-deoxyspergualin primarily targets the trafficking of apicoplast proteins in *Plasmodium falciparum*, *The Journal of Biological Chemistry*, **282**, 6388-6397.

Ramya, T.N., Surolia, N. and Surolia, A. (2006) 15-deoxyspergualin modulates *Plasmodium falciparum* heat shock protein function, *Biochemical and Biophysical Research Communications*, **348**, 585-592.

Ranjit, M.R. and Sharma, Y.D. (1999) Genetic polymorphism of *falciparum* malaria vaccine candidate antigen genes among field isolates in India, *The American Journal of Tropical Medicine and Hygiene*, **61**, 103-108.

Ray, P.D., Huang, B.-W. and Tsuji, Y. (2012) Reactive oxygen species (ROS) homeostasis and redox regulation in cellular signaling, *Cellular Signalling*, **24**, 981-990.

Riezman, H. (2004) Why do cells require heat shock proteins to survive heat stress?, *Cell Cycle*, **3**, 60-62.

Riggs, D.L., *et al.* (2004) Functional specificity of co-chaperone interactions with Hsp90 client proteins, *Critical Reviews in Biochemistry and Molecular Biology*, **39**, 279-295.

Ritossa, F. (1962) A new puffing pattern induced by temperature shock and DNP in Drosophila, *Cellular and Molecular Life Sciences*, **18**, 571-573.

Ritossa, F. (1996) Discovery of the heat shock response, *Cell Stress and Chaperones*, **1**, 97-98.

Roe, S.M., *et al.* (1999) Structural basis for inhibition of the Hsp90 molecular chaperone by the antitumor antibiotics Radicicol and Geldanamycin, *The Journal of Medicinal Chemistry*, **42**, 260-266.

Rønn, A.M., *et al.* (1996) High level of resistance of *Plasmodium falciparum* to sulfadoxine-pyrimethamine in children in Tanzania, *Transactions of the Royal Society of Tropical Medicine and Hygiene*, **90**, 179-181.

Rost, B., *et al.* (2003) Automatic prediction of protein function, *Cellular and Molecular Life Sciences* **60**, 2637-2650.

Roux-Dalvai, F., *et al.* (2008) Extensive analysis of the cytoplasmic proteome of human erythrocytes using the peptide ligand library technology and advanced mass spectrometry, *Molecular & Cellular Proteomics*, **7**, 2254-2269.

Rowley, N., *et al.* (1994) Mdj1p, a novel chaperone of the DnaJ family, is involved in mitochondrial biogenesis and protein folding, *Cell*, **77**, 249-259.

Rozendaal, J.A. (1997) *Vector control. Methods for use by individuals and communities*. World Health Organization, Geneva.

Rudiger, S., *et al.* (1997) Substrate specificity of the DnaK chaperone determined by screening cellulose-bound peptide libraries, *The EMBO Journal*, **16**, 1501-1507.

Rudzinska, M.A. (1969) The fine structure of malaria parasites, *International Review of Cytology*, **25**, 161-199.

Rug, M. and Maier, A.G. (2011) The heat shock protein 40 family of the malaria parasite *Plasmodium falciparum*, *IUBMB Life*, **63**, 1081-1086.

Russo, I., *et al.* (2010) Plasmepsin V licenses *Plasmodium* proteins for export into the host erythrocyte, *Nature*, **463**, 632-636.

Sachs, J. and Malaney, P. (2002) The economic and social burden of malaria, *Nature*, **415**, 680-685.

Sakahira, H., *et al.* (2002) Molecular chaperones as modulators of polyglutamine protein aggregation and toxicity, *Proceedings of the National Academy of Sciences*, **99**, 16412-16418.

Sargeant, T.J., *et al.* (2006) Lineage-specific expansion of proteins exported to erythrocytes in malaria parasites, *Genome Biology*, **7**, R12.

Sato, S. and Wilson, R.J. (2005) Organelle-specific cochaperonins in apicomplexan parasites, *Molecular and Biochemical Parasitology*, **141**, 133-143.

Sato, S. and Wilson, R.J.M. (2004) The use of Dsred in single- and dual-color fluorescence labeling of mitochondrial and plastid organelles in *Plasmodium falciparum*, *Molecular and Biochemical Parasitology*, **134**, 175-179.

Scherf, A., Lopez-Rubio, J.J. and Riviere, L. (2008) Antigenic variation in *Plasmodium falciparum*, *Annual Review of Microbiology*, **62**, 445-470.

Scheufler, C., *et al.* (2000) Structure of TPR domain–peptide complexes: Critical elements in the assembly of the Hsp70–Hsp90 multichaperone machine, *Cell*, **101**, 199-210.

Schofield, L. and Grau, G.E. (2005) Immunological processes in malaria pathogenesis, *Nature Reviews Immunology*, **5**, 722-735.

Schuck, P. (1997) Use of Surface Plasmon Resonance to probe the equilibrium and dynamic aspects of interactions between biological macromolecules, *Annual Review of Biophysics and Biomolecular Structure*, **26**, 541-566.

Schwenk, R.J. and Richie, T.L. (2011) Protective immunity to pre-erythrocytic stage malaria, *Trends in Parasitology*, **27**, 306-314.

Seeber, F. (2002) Biogenesis of iron–sulphur clusters in amitochondriate and apicomplexan protists, *International Journal for Parasitology*, **32**, 1207-1217.

Sha, B., Lee, S. and Cyr, D.M. (2000) The crystal structure of the peptide-binding fragment from the yeast Hsp40 protein Sis1, *Structure*, **8**, 799-807.

Shaner, L. and Morano, K.A. (2007) All in the family: Atypical Hsp70 chaperones are conserved modulators of Hsp70 activity, *Cell Stress and Chaperones*, **12**, 1-8.

Shapiro, A.L., Vinuela, E. and Maizel, J.V., Jr. (1967) Molecular weight estimation of polypeptide chains by electrophoresis in SDS-polyacrylamide gels, *Biochemical and Biophysical Research Communications*, **28**, 815-820.

Sharma, M., Dash, A. and Das, A. (2010) Evolutionary genetic insights into *Plasmodium falciparum* functional genes, *Parasitology Research*, **106**, 349-355.

Shiau, A.K., *et al.* (2006) Structural analysis of *E.coli* Hsp90 reveals dramatic nucleotide-dependent conformational rearrangements, *Cell*, **127**, 329-340.

Shomura, Y., *et al.* (2005) Regulation of Hsp70 function by HspBP1: Structural analysis reveals an alternate mechanism for Hsp70 nucleotide exchange, *Molecular Cell*, **17**, 367-379.

Shonhai, A. (2007) Molecular characterisation of the chaperone properties of *Plasmodium falciparum* heat shock protein 70. *Biochemistry, Microbiology, and Biotechnology*. Rhodes University.

Shonhai, A. (2010) Plasmodial heat shock proteins: Targets for chemotherapy, *FEMS Immunology and Medical Microbiology*, **58**, 61-74.

Shonhai, A., Boshoff, A. and Blatch, G. (2005) *Plasmodium falciparum* heat shock protein 70 is able to suppress the thermosensitivity of an *Escherichia coli* DnaK mutant strain, *Molecular Genetics and Genomics*, **274**, 70-78.

Shonhai, A., Boshoff, A. and Blatch, G.L. (2007) The structural and functional diversity of Hsp70 proteins from *Plasmodium falciparum*, *Protein Science*, **16**, 1803-1818.

Shonhai, A., *et al.* (2008) Structure-function study of a *Plasmodium falciparum* Hsp70 using three dimensional modelling and in vitro analyses, *Protein Peptide Letters*, **15**, 1117-1125.

Sibley, L.D. (2004) Intracellular parasite invasion strategies, *Science*, **304**, 248-253.

Sichting, M., *et al.* (2005) Maintenance of structure and function of mitochondrial Hsp70 chaperones requires the chaperone Hep1, *The EMBO Journal*, **24**, 1046-1056.

Sigrist, C.J.A., *et al.* (2010) Prosite, a protein domain database for functional characterization and annotation, *Nucleic Acids Research*, **38**, D161-D166.

Silva, M.D., *et al.* (2005) A role for the *Plasmodium falciparum* RESA protein in resistance against heat shock demonstrated using gene disruption, *Molecular Microbiology*, **56**, 990-1003.

Simon, S.M. and Blobel, G. (1991) A protein-conducting channel in the endoplasmic reticulum, *Cell*, **65**, 371-380.

Sinka, M., *et al.* (2010) The dominant *Anopheles* vectors of human malaria in Africa, Europe and the middle East: Occurrence data, distribution maps and bionomic precis, *Parasites & Vectors*, **3**, 117.

Sinka, M., *et al.* (2012) A global map of dominant malaria vectors, *Parasites & Vectors*, **5**, 69.

Snow, R.W. and Marsh, K. (2002) The consequences of reducing transmission of *Plasmodium falciparum* in Africa. In, *Advances in parasitology*. Academic Press, pp. 235-264.

Snow, R.W. and Omumbo, J.A. (2006) Malaria. In Jamison, D.T., *et al.* (eds), *Disease and mortality in sub-Saharan Africa*. The International Bank for Reconstruction and Development, Washington, DC 20433, pp. 414.

Snow, R.W., *et al.* (1997) Relation between severe malaria morbidity in children and level of *Plasmodium falciparum* transmission in Africa, *The Lancet*, **349**, 1650-1654.

Sommer, M.S., *et al.* (2007) Der1-mediated preprotein import into the periplastid compartment of *Chromalveolates*?, *Molecular Biology and Evolution*, **24**, 918-928.

Sonna, L.A., *et al.* (2002) Invited review: Effects of heat and cold stress on mammalian gene expression, *Journal of Applied Physiology*, **92**, 1725-1742.

Spielmann, T. and Gilberger, T.W. (2010) Protein export in malaria parasites: Do multiple export motifs add up to multiple export pathways?, *Trends in Parasitology*, **26**, 6-10.

Spork, S., *et al.* (2009) An unusual Erad-like complex is targeted to the apicoplast of *Plasmodium falciparum*, *Eukaryotic Cell*, **8**, 1134-1145.

Steel, G.J., *et al.* (2004) Coordinated activation of Hsp70 chaperones, *Science*, **303**, 98-101.

Stevenson, M.M. and Riley, E.M. (2004) Innate immunity to malaria, *Nature Reviews Immunology*, **4**, 169-180.

Stewart, M.J., *et al.* (1986) *Plasmodium berghei* sporozoite invasion is blocked in vitro by sporozoite-immobilizing antibodies, *Infection and Immunity*, **51**, 859-864.

Stoute, J.A., *et al.* (1997) A preliminary evaluation of a recombinant circumsporozoite protein vaccine against *Plasmodium falciparum* malaria, *The New England Journal of Medicine*, **336**, 86-91.

Struik, S.S. and Riley, E.M. (2004) Does malaria suffer from lack of memory?, *Immunological Reviews*, **201**, 268-290.

Sturm, A., *et al.* (2006) Manipulation of host hepatocytes by the malaria parasite for delivery into liver sinusoids, *Science*, **313**, 1287-1290.

Su, X.Z., *et al.* (1995) The large diverse gene family var encodes proteins involved in cytoadherence and antigenic variation of *Plasmodium falciparum*-infected erythrocytes, *Cell*, **82**, 89-100.

Szklarczyk, D., *et al.* (2011) The string database in 2011: Functional interaction networks of proteins, globally integrated and scored, *Nucleic Acids Research*, **39**, D561-D568.

Taipale, M., Jarosz, D.F. and Lindquist, S. (2010) Hsp90 at the hub of protein homeostasis: Emerging mechanistic insights, *Nature Reviews Molecular Cell Biology*, **11**, 515-528.

Tamura, Y., *et al.* (2012) New paradigm for intrinsic function of heat shock proteins as endogenous ligands in inflammation and innate immunity, *Current Molecular Medicine*, **12**, 1198-1206.

Terasaki, M., *et al.* (2001) Fluorescent staining of subcellular organelles: ER, golgi complex, and mitochondria. In, *Current protocols in cell biology*. John Wiley & Sons, Inc.

Thakur, A., *et al.* (2012) Structure and mechanistic insights into novel iron-mediated moonlighting functions of human J-protein cochaperone, Dph4, *Journal of Biological Chemistry*, **287**, 13194-13205.

Thera, M.A. and Plowe, C.V. (2012) Vaccines for malaria: How close are we?, *Annual Review of Medicine*, **63**, 345-357.

Thomas, P.J., Qu, B.-H. and Pedersen, P.L. (1995) Defective protein folding as a basis of human disease, *Trends in Biochemical Sciences*, **20**, 456-459.

Tilley, L., *et al.* (2008) The twists and turns of maurer's cleft trafficking in *P. falciparum*-infected erythrocytes, *Traffic*, **9**, 187-197.

Tomita, M. and Marchesi, V.T. (1975) Amino-acid sequence and oligosaccharide attachment sites of human erythrocyte glycophorin, *Proceedings of the National Academy of Sciences*, **72**, 2964-2968.

Tonkin, C.J., Kalanon, M. and McFadden, G.I. (2008) Protein targeting to the malaria parasite plastid, *Traffic*, **9**, 166-175.

Toso, M.A. and Omoto, C.K. (2007) *Gregarina niphandrodes* may lack both a plastid genome and organelle, *Journal of Eukaryotic Microbiology*, **54**, 66-72.

Towbin, H., Staehelin, T. and Gordon, J. (1979) Electrophoretic transfer of proteins from polyacrylamide gels to nitrocellulose sheets: Procedure and some applications, *Proceedings of the National Academy of Sciences*, **76**, 4350-4354.

Trager, W. and Jensen, J.B. (1997) Continuous culture of *Plasmodium falciparum*: Its impact on malaria research, *International Journal for Parasitology*, **27**, 989-1006.

Trape, J.F. (2001) The public health impact of chloroquine resistance in Africa, *The American Journal of Tropical Medicine and Hygiene*, **64**, 12-17.

Tuikue Ndam, N., *et al.* (2008) *Plasmodium falciparum* transcriptome analysis reveals pregnancy malaria associated gene expression, *PLOS One*, **3**, e1855.

Tuteja, R. (2007) Unraveling the components of protein translocation pathway in human malaria parasite *Plasmodium falciparum*, *Archives of Biochemistry and Biophysics*, **467**, 249-260.

Tyedmers, J., Mogk, A. and Bukau, B. (2010) Cellular strategies for controlling protein aggregation, *Nature Reviews Molecular Cell Biology*, **11**, 777-788.

Uehara, Y. (2003) Natural product origins of Hsp90 inhibitors, *Current Cancer Drug Targets*, **3**, 325-330.

Ushioda, R., *et al.* (2008) Erdj5 is required as a disulfide reductase for degradation of misfolded proteins in the ER, *Science*, **321**, 569-572.

van den Hoff, M.J.B., Moorman, A.F.M. and Lamers, W.H. (1992) Electroporation in 'intracellular' buffer increases cell survival, *Nucleic Acids Research*, **20**, 2902.

Van Dooren, G.G., *et al.* (2005) Development of the endoplasmic reticulum, mitochondrion and apicoplast during the asexual life cycle of *Plasmodium falciparum*, *Molecular Microbiology*, **57**, 405-419.

van Dooren, G.G., *et al.* (2001) Translocation of proteins across the multiple membranes of complex plastids, *BBA Molecular Cell Research*, **1541**, 34-53.

van Dooren, G.G., Stimmler, L.M. and McFadden, G.I. (2006) Metabolic maps and functions of the *Plasmodium* mitochondrion, *FEMS Microbiology Reviews*, **30**, 596-630.

van Dooren, G.G., *et al.* (2002) Processing of an apicoplast leader sequence in *Plasmodium falciparum* and the identification of a putative leader cleavage enzyme, *The Journal of Biological Chemistry*, **277**, 23612-23619.

van Ooij, C., *et al.* (2008) The malaria secretome: From algorithms to essential function in blood stage infection, *PLoS Pathogens*, **4**, e1000084.

Vaughan, A.M., Aly, A.S.I. and Kappe, S.H.I. (2008) Malaria parasite pre-erythrocytic stage infection: Gliding and hiding, *Cell Host & Microbe*, **4**, 209-218.

Vaughan, A.M., Wang, R.B. and Kappe, S.H.I. (2010) Genetically engineered, attenuated whole-cell vaccine approaches for malaria, *Human Vaccines*, **6**, 107-113.

Vignali, M., *et al.* (2011) NSR-seq transcriptional profiling enables identification of a gene signature of *Plasmodium falciparum* parasites infecting children, *The Journal of Clinical Investigation*, **121**, 1119-1129.

Voisine, C., *et al.* (2001) Jac1, a mitochondrial J-type chaperone, is involved in the biogenesis of Fe/S clusters in *Saccharomyces cerevisiae*, *Proceedings of the National Academy of Sciences*, **98**, 1483-1488.

Voisine, C., Pedersen, J.S. and Morimoto, R.I. (2010) Chaperone networks: Tipping the balance in protein folding diseases, *Neurobiology of Disease*, **40**, 12-20.

Waller, R.F., *et al.* (1998) Nuclear-encoded proteins target to the plastid in *Toxoplasma gondii* and *Plasmodium falciparum*, *Proceedings of the National Academy of Sciences*, **95**, 12352-12357.

Waller, R.F. and McFadden, G.I. (2005) The apicoplast: A review of the derived plastid of apicomplexan parasites, *Current Issues in Molecular Biology*, **7**, 57-79.

Waller, R.F., *et al.* (2000) Protein trafficking to the plastid of *Plasmodium falciparum* is via the secretory pathway, *The EMBO Journal*, **19**, 1794-1802.

Walsh, P., *et al.* (2004) The J-protein family: Modulating protein assembly, disassembly and translocation, *EMBO Reports*, **5**, 567-571.

Warrell, D.A. and Gilles, H.M. (2002) *Bruce-chwatt's essential malariology*. Edward Arnold, London.

Waruiru, C.M., *et al.* (1996) Epileptic seizures and malaria in Kenyan children, *Transactions of the Royal Society of Tropical Medicine and Hygiene*, **90**, 152-155.

Wasmuth, J., *et al.* (2009) The origins of apicomplexan sequence innovation, *Genome Research*, **19**, 1202-1213.

Watanabe, J. (1997) Cloning and characterization of heat shock protein DnaJ homologues from *Plasmodium falciparum* and comparison with ring infected erythrocyte surface antigen, *Molecular and Biochemical Parasitology*, **88**, 253-258.

Wells, T.N.C., Burrows, J.N. and Baird, J.K. (2010) Targeting the hypnozoite reservoir of *Plasmodium* vivax: The hidden obstacle to malaria elimination, *Trends in Parasitology*, **26**, 145-151.

White, K.P., *et al.* (1999) Microarray analysis of *Drosophila* development during metamorphosis, *Science*, **286**, 2179-2184.

White, N. (1999a) Antimalarial drug resistance and combination chemotherapy, *Philosophical transactions of the Royal Society of London. Series B, Biological Sciences*, **354**, 739-749.

White, N.J. (1999b) Delaying antimalarial drug resistance with combination chemotherapy, *Parassitologia*, **41**, 301-308.

White, N.J. (2011) A vaccine for malaria, *The New England Journal of Medicine*, **365**, 1926-1927.

White, N.J. and Olliaro, P.L. (1996) Strategies for the prevention of antimalarial drug resistance: Rationale for combination chemotherapy for malaria, *Parasitology Today*, **12**, 399-401.

Whitesell, L., *et al.* (1994) Inhibition of heat shock protein Hsp90-pp60v-src heteroprotein complex formation by benzoquinone ansamycins: Essential role for stress proteins in oncogenic transformation, *Proceedings of the National Academy of Sciences*, **91**, 8324-8328.

WHO (1999) Making a difference. The World Health Report 1999, *Health Millions*, **25**, 3-5.

WHO (2003) The Africa Malaria Report Geneva.

WHO (2003) The Africa Malaria Report 2003. pp. 122.

WHO (2005) The World Health Report 2005 - make every mother and child count Geneva.

WHO (2010a) World Malaria Report 2010.

WHO (2010b) Guidelines for the treatment of malaria. WHO, Geneva.

WHO (2011a) World Malaria Report 2011.

WHO (2011b) Global plan for artemisinin resistance containment (GPARC). Geneva.

WHOPES (2009) Who pesticides evaluation scheme (WHOPES). WHO recommended insecticides for indoor residual spraying against malaria vectors. Geneva.

Wickham, M.E., *et al.* (2001) Trafficking and assembly of the cytoadherence complex in *Plasmodium falciparum*-infected human erythrocytes, *The EMBO Journal*, **20**, 5636-5649.

Wiesner, J. and Seeber, F. (2005) The plastid-derived organelle of protozoan human parasites as a target of established and emerging drugs, *Expert Opinion on Therapeutic Targets*, **9**, 23-44.

Winzeler, E.A. (2008) Malaria research in the post-genomic era, *Nature*, **455**, 751-756.

Wittung-Stafshede, P., *et al.* (2003) The J-domain of Hsp40 couples ATP hydrolysis to substrate capture in Hsp70, *Biochemistry*, **42**, 4937-4944.

Wu, Y., *et al.* (2009) Identification of phosphorylated proteins in erythrocytes infected by the human malaria parasite *Plasmodium falciparum*, *Malaria Journal*, **8**, 105.

Wu, Y., *et al.* (1995) Transfection of *Plasmodium falciparum* within human red blood cells, *Proceedings of the National Academy of Sciences*, **92**, 973-977.

Yan, W., *et al.* (1998) Zuotin, a ribosome-associated DnaJ molecular chaperone, *The EMBO Journal*, **17**, 4809-4817.

Zhai, P., *et al.* (2008) The human escort protein hep binds to the ATPase domain of mitochondrial Hsp70 and regulates ATP hydrolysis, *The Journal of Biological Chemistry*, **283**, 26098-26106.

Zhang, Y., *et al.* (2011) Redox control of the survival of healthy and diseased cells, *Antioxidants & Redox Signaling*, **15**, 2867-2908.

Zhong, T. and Arndt, K.T. (1993) The yeast Sis1 protein, a DnaJ homolog, is required for the initiation of translation, *Cell*, **73**, 1175-1186.

Zhou, H.X., Rivas, G. and Minton, A.P. (2008) Macromolecular crowding and confinement: Biochemical, biophysical, and potential physiological consequences, *Annual Review of Biophysics*, **37**, 375-397.

Zhou, Y., *et al.* (2008) Evidence-based annotation of the malaria parasite's genome using comparative expression profiling, *PLOS One*, **3**, e1570.

Zhu, G., Marchewka, M.J. and Keithly, J.S. (2000) *Cryptosporidium parvum* appears to lack a plastid genome, *Microbiology*, **146**, 315-321.

Zhu, J.K., Bressan, R.A. and Hasegawa, P.M. (1993) Isoprenylation of the plant molecular chaperone Anj1 facilitates membrane association and function at high temperature, *Proceedings of the National Academy of Sciences*, **90**, 8557-8561.

Zilversmit, M.M., *et al.* (2010) Low-complexity regions in *Plasmodium falciparum*: Missing links in the evolution of an extreme genome, *Molecular Biology and Evolution*, **27**, 2198-2209.

Zinkernagel, R.M. (2001) Maternal antibodies, childhood infections, and autoimmune diseases, *The New England Journal of Medicine*, **345**, 1331-1335.

Zuegge, J., *et al.* (2001) Deciphering apicoplast targeting signals--feature extraction from nuclear-encoded precursors of *Plasmodium falciparum* apicoplast proteins, *Gene*, **280**, 19-26.

Zylicz, M., *et al.* (1989) Initiation of lambda-DNA replication with purified host-encoded and bacteriophage-encoded proteins - the role of the DnaK, DnaJ and Grpe heat-shock proteins, *The EMBO Journal*, **8**, 1601-1608.

APPENDICES

Appendix A: Amino Acid and Nucleotide Nomenclature

One and three-letter codes were used to represent amino acids, and single letter codes were used to represent nucleotides as set forward by the Joint Commission of Biochemical Nomenclature (JBNC) of IUPAC (International Union of Pure and Applied Chemistry) and the IUBMB (International Union of Biochemistry and Molecular Biology):

Table 1

NUCLEOTIDE	SINGLE-LETTER CODE
Adenine	A
Cytosine	C
Guanine	G
Thymine	T
Uracil	U
Any Nucleotide (A, C, G, T or U)	N

AMINO ACID	1-LETTER CODE	3-LETTER CODE	DNA CODONS
Alanine	A	Ala	GCT, GCC, GCA, GCG
Arginine	R	Arg	CGT, CGC, CGA, CGG, AGA, AGG
Asparagine	N	Asn	AAT, AAC
Aspartic acid	D	Asp	GAT, GAC
Cysteine	C	Cys	TGT, TGC
Glutamine	Q	Gln	CAA, CAG
Glutamic acid	E	Glu	GAA, GAG
Glycine	G	Gly	GGT, GGC, GGA, GGG
Histidine	H	His	CAT, CAC
Isoleucine	I	Ile	ATT, ATC, ATA
Leucine	L	Leu	CTT, CTC, CTA, CTG, TTA, TTG
Lysine	K	Lys	AAA, AAG
Methionine	M	Met	ATG
Phenylalanine	F	Phe	TTT, TTC
Proline	P	Pro	CCT, CCC, CCA, CCG
Serine	S	Ser	TCT, TCC, TCA, TCG, AGT, AGC
Threonine	T	Thr	ACT, ACC, ACA, ACG
Tryptophan	W	Trp	TGG
Tyrosine	Y	Tyr	TAT, TAC
Valine	V	Val	GTT, GTC, GTA, GTG
Stop	-	-	TAA, TAG, TGA
Any Amino Acid	X	-	-

Appendix B: Nucleotide sequences in Fasta format

>PFB0595w optimized coding sequence

ATGGGCAAAGATTACTACTCGATTCTGGGCGTGTCCCGCGACTGTACCACCAACGACCTGAAAAAAGCCTACCGC
AAACTGGCAATGATGTGGCATCCGGATAAACACAACGACGAAAAAAGCAAAAAAGAAGCGGAAGAAAAATTCAAA
AACATTGCGGAAGCCTATGATGTGCTGGCCGACGAAGAAAAACGTAAAATCTACGATACCTACGGCGAAGAAGGT
CTGAAAGGCTCTATCCCGACGGGCGGTAACACCTATGTTTACAGTGGTGTCGATCCGTCGGAACTGTTCAGCCGC
ATCTTTGGTAGTGATGGCCAGTTTTCATTCACGTCGACCTTTGATGAAGACTTTAGCCCGTTCTCTACGTTTGTC
AACATGACCAGTCGTAAATCCCGCCCGTCAACCACGACCAACATCAACACGAACAACTACAACAAACCGGCAACC
TACGAAGTTCCGCTGAGTCTGTCCCTGGAAGAACTGTACTCGGGTTGCAAGAAAAAACTGAAAATCACGCGTAAA
CGCTTCATGGGCACCAAAAGCTATGAAGATGACAACTACGTGACCATTGATGTTAAAGCAGGTTGGAAAGACGGC
ACGAAAATCACCTTTTATGGCGAAGGTGATCAGCTGTCTCCGATGGCTCAACCGGGTGATCTGGTCTTCAAAGTG
AAAACGAAAACCCATGATCGTTTTCTGCGCGACGCAAATCACCTGATTTACAAATGTCCGGTGCCGCTGGATAAA
GCTCTGACGGGCTTTCAATTCATCGTTAAAAGCCTGGATAACCGTGACATTAATGTGCGCGTTGATGACATCGTT
ACCCCGAAATCCCGTAAAATTGTCGCCAAAGAAGGTATGCCGAGCTCTAAATATCCGTCAATGAAAGGCGATCTG
ATTGTCGAATTCGACATCGTGTTTCCGAAATCCCTGACCTCCGAAAAAAAAAAAAATTATCCGCGAAACCCTGGCT
AATACCTTC

>Pfj1 optimized coding sequence

ATGAGAGGATCGCATCACCATCACCATCACGGATCCAACCAGGACCCGTACACCGTTCTGGGTCTGTCTCGTAAC
GCGACCACCAACGACATCAAAAAACAGTTCAGGCTGCTGGCGAAAAAATACCACCCGGACATCAACCCGTCTCCG
GACGCGAAACAGAAAATGGCGTCTATCACCGCGGCGTACGAACTGCTGTCTGACCCGAAAAAGAAAGAATTCTAC
GACAAAACCGGTATGACCGACGACTCTAACTACCAGAACCACTCTTCTAACTTCGAAGGTGCGTTCTCTGGTTTC
GGTGACGCGTCTTTCATGTTCACCGACTTCGCGGAAATGTTCACCAACATGGCGGGTGGTAACAAAAACACCTCT
ACCCGTGGTGAAGACATCCAGTCTGAAATCACCCTGAAATTCATGGAAGCGATCAAAGGTTGCGAAAAAAACTCG
CGACTGAACGTTAAAGTTTCTTGCAACAACTGCAACGGTTCTGGTAAAAAACCGGGCACCAACCTGACCATCTGC
AAAGTTTGCAACGGTTCTGGTATCCAGCGTATGGAACGTGGTCCGATCATCATCGGTGTTCCGTGCCGTAACTGC
TCTGGTAACGGTCAGATCATCAACAACCCGTGCAAACACTGCTCTGGTTCTGGTGTTAAATTCCAGACCAAAAAC
ATCACCCTGGACATCCCGCCCGGGATCAAAAAAGGTATGCAGATGCGTATCCCGAACCAGGGTCACTGCGGTTAC
CGTGGTGGTAAATCTGGTCACCTGTTCGTTACCATCAACATCGAACCGCACAAAATCTTCAAATGGGTTGACGAC
AACATCTACGTTGACGTTCCGCTGACCATCAAACAGTGCCTGCTGGGTGGTCTGGTTACCGTTCCGACCCTGAAC
GGTGACATGGACCTGCTGATCAAACCGAAAACCTACCCGAACTCTGAAAAAATCCTGAAAGGTAAAGGTCCGTGC
AAAGTTGACTCTCACAACAACGGTGACCTGATCATCAAATTCTCTCTGAAAATCCCGGAAAAACTGACCCCGCGT
CAGGTTGAACTGATCGAAGAATTCAACACCATCGAACTGAACCTGCCGAACCCGCAGACCAACGTTAAACAGAAA
AAAAACATCTACGAAACCAAAGGTAACATCAACGAAAACATCTTCTCTATGAACAACACCTACAACAACATGAAA
GGTCCGGAAGGTGAAACCTCTAACACCCAGGCGAAATCTATGAAAAACCAGAACTGGAACAACGAAAAATCTGTT
AACAACAAAGGCACCATCTCTAAAGACGAAAAAAAACTGAACATGAAAAACAACCACATCAACGAAAAATCTAAC
CTGAAAAACTCTTCTCACATGGACACCAACAAAAACGAAGAAAACATGTCTGACGACGAAAAAAAAAAAATCAAA
AAAATCATCCCGGAACCGCCGATGCCGCACACCCACAAAATCGTTAACAACCTGGAATCTAAAAACTCTTGCAAC
ATCCCGATCCCGCCGCCGCCGCCGAAATCTTCTTCTAAACCGATCTCTGAAAACCAGAACATCTCTAACCGTGAA
CACAACGGTGTTACCAACAACTCTGCGAAACTGGACAACAACATCAACATGAACTACTCTTGCGACCCGTACAAA
AACGTTACCCAGAACGACCTGAACAACAACGACAACATCAAAAACAAAATCTACAAAGACAACACCAACATCTCT
AACCACCACATCTTCAAAAACGACAACATCAACCAGCAGCAGTTCCACTGCGCGGACAACTCTTCTGAAAACAAC
AACGAATCTGACATGAACACCACCTCTACCTTCTCTTTCGCCAAAAAATGGATCTCTGACAAACTGAAACCGAAA
AACTAAGGTA

>PfHsp70-3 optimized coding sequence

ATGTCGGGTGATATTATTGGCATTGACCTGGGCACCACGAACTCCTGCGTCGCTATTATGGAAGGCAAACAAGGC
AAAGTGATTGAAAACAGTGAAGGCTTTCGTACCACGCCGTCCGTGGTTGCGTTCACCAACGATAATCAGCGTCTG
GTCGGTATTGTGGCCAAACGCCAAGCAATCACGAACCCGGAAAATACCGTTTATGCTACGAAACGTTTTATTGGC
CGCAAATACGATGAAGACGCGACCAAAAAAGAACAGAAAAACCTGCCGTATAAAATTGTGCGTGCCAGCAATGGT
GATGCTTGGATCGAAGCGCAGGGCAAAAAATACAGCCCGTCTCAAATTGGCGCATGCGTTCTGGAAAAAATGAAA
GAAACCGCTGAAAACTATCTGGGTCGCAAAGTGCATCAGGCGGTTATTACCGTCCCGGCCTACTTTAATGACAGT
CAGCGTCAAGCCACGAAAGATGCAGGTAAAATCGCTGGCCTGGACGTGCTGCGCATTATCAATGAACCGACCGCC
GCGGCACTGGCATTTGGTCTGGAAAAATCCGATGGCAAAGTGATTGCAGTTTATGACCTGGGCGGTGGCACCTTT
GATATTTCAATCCTGGAAATCCTGTCGGGTGTCTTCGAAGTGAAAGCAACCAACGGCAATACGTCACTGGGTGGC
GAAGATTTTGACCAGCGCATTCTGGAATACTTCATCTCGGAATTCAAGAAAAAAGAAAACATCGACCTGAAAAAC
GATAAACTGGCTCTGCAGCGTCTGCGCGAAGCTGCGGAAACCGCGAAAATCGAACTGAGCTCTAAAACCCAAACG
GAAATTAACCTGCCGTTCATCACCGCCAATCAGACGGGCCCGAAACATCTGCAAATTAAACTGACCCGTGCAAAA

CTGGAAGAACTGTGTCACGATCTGCTGAAGGGTACGATTGAACCGTGCGAAAAATGTATCAAAGATGCGGACGTC
AAAAAAGAAGAAATCAACGAAATCATCCTGGTGGGTGGCATGACCCGCATGCCGAAAGTTACCGATACGGTCAAA
CAGATCTTTCAAAACAATCCGAGCAAAGGTGTTAATCCGGATGAAGCGGTTGCACTGGGTGCAGCAATTCAGGGT
GGCGTTCTGAAAGGTGAAATCAAAGACCTGCTGCTGCTGGATGTCATTCCGCTGTCACTGGGTATCGAAACCCTG
GGTGGCGTGTTCACGAAACTGATTAACCGTAATACCACGATCCCGACCAAAAAATCACAGATTTTTAGCACCGCT
GCGGATAACCAGACGCAAGTTAGTATCAAAGTTTTCCAAGGCGAACGTGAAATGGCTAGCGATAATAAACTGCTG
GGTTCTTTTGATCTGGTGGGCATTCCGCCGGCGCCGCGCGGTGTTCCGCAGATCGAAGTCACCTTCGATGTGGAC
GCTAACGCGATTATCAATATTAGCGCCATCGATAAAATGACCAACAAAAAACAGCAAATCACGATCCAGAGTTCC
GGTGGCCTGAGCAAAGAAGAAATCGAAAAAATGGTTCAGGAAGCCGAACTGAATCGCGAAAAAGATCAACTGAAG
AAAAACCTGACCGACTCTAAAAATGAAGCAGAAACGCTGATTTATTCATCGGAAAAACAGCTGGAAGACTTCAAA
GATAAAATCAGTGATTCCGACAAAGATGAACTGCGTCAGAAAATCACCGTGCTGCGCGAAAAACTGACGAGTGAA
GACCTGGATTCCATTAAAGATGCGACCAAACAGCTGCAAGAAAAAAGCTGGGCCATCTCTCAGGAAATGTACAAA
AACAATGCACAGCAAGGTGCCCAACAGGAACAACCGAACAACGAAAACAAAGCCGAAGAAAACAAAGACAACGCA
TAA

Appendix C: Amino acid sequences in Fasta format

>PFB0595w
MGKDYYSILGVSRDCTTNDLKKAYRKLAMMWHPDKHNDEKSKKEAEEKFKNIAEAYDVLADEEKRKIYDTYGEEG
LKGSIPTGGNTYVYSGVDPSELFSRIFGSDGQFSFTSTFDEDFSPFSTFVNMTSRKSRPSTTTNINTNNYNKPAT
YEVPLSLSLEELYSGCKKKLKITRKRFMGTKSYEDDNYVTIDVKAGWKDGTKITFYGEGDQLSPMAQPGDLVFKV
KTKTHDRFLRDANHLIYKCPVPLDKALTGFQFIVKSLDNRDINVRVDDIVTPKSRKIVAKEGMPSSKYPSMKGDL
IVEFDIVFPKSLTSEKKKIIRETLANTF

>6xHis-PfHsp70-3 (PfHsp70-3m)
MRGSHHHHHHGSMSGDIIGIDLGTTNSCVAIMEGKQGKVIENSEGFRTTPSVVAFTNDNQRLVGIVAKRQAITNP
ENTVYATKRFIGRKYDEDATKKEQKNLPYKIVRASNGDAWIEAQGKKYSPSQIGACVLEKMKETAENYLGRKVHQ
AVITVPAYFNDSQRQATKDAGKIAGLDVLRIINEPTAAALAFGLEKSDGKVIAVYDLGGGTFDISILEILSGVFE
VKATNGNTSLGGEDFDQRILEYFISEFKKKENIDLKNDKLALQRLREAAETAKIELSSKTQTEINLPFITANQTG
PKHLQIKLTRAKLEELCHDLLKGTIEPCEKCIKDADVKKEEINEIILVGGMTRMPKVTDTVKQIFQNNPSKGVNP
DEAVALGAAIQGGVLKGEIKDLLLLDVIPLSLGIETLGGVFTKLINRNTTIPTKKSQIFSTAADNQTQVSIKVFQ
GEREMASDNKLLGSFDLVGIPPAPRGVPQIEVTFDVDANAIINISAIDKMTNKKQQITIQSSGGLSKEEIEKMVQ
EAELNREKDQLKKNLTDSKNEAETLIYSSEKQLEDFKDKISDSDKDELRQKITVLREKLTSEDLDSIKDATKQLQ
EKSWAISQEMYKNNAQQGAQQEQPNNENKAEENKDNA

>6xHis-Pfj1 (Pfj1m)
MRGSHHHHHHGSNQDPYTVLGLSRNATTNDIKKQFRLLAKKYHPDINPSPDAKQKMASITAAYELLSDPKKKEFY
DKTGMTDDSNYQNHSSNFEGAFSGFGDASFMFTDFAEMFTNMAGGNKNTSTRGEDIQSEITLKFMEAIKGCEKNS
RLNVKVSCNNCNGSGKKPGTNLTICKVCNGSGIQRMERGPIIIGVPCRNCSGNGQIINNPCKHCSGSGVKFQTKN
ITLDIPPGIKKGMQMRIPNQGHCGYRGGKSGHLFVTINIEPHKIFKWVDDNIYVDVPLTIKQCLLGGLVTVPTLN
GDMDLLIKPKTYPNSEKILKGKGPCKVDSHNNGDLIIKFSLKIPEKLTPRQVELIEEFNTIELNLPNPQTNVKQK
KNIYETKGNINENIFSMNNTYNNMKGPEGETSNTQAKSMKNQNWNNEKSVNNKGTISKDEKKLNMKNNHINEKSN
LKNSSHMDTNKNEENMSDDEKKKIKKIIPEPPMPHTHKIVNNLESKNSCNIPIPPPPPKSSSKPISENQNISNRE
HNGVTNNSAKLDNNINMNYSCDPYKNVTQNDLNNNDNIKNKIYKDNTNISNHHIFKNDNINQQQFHCADNSSENN
NESDMNTTSTFSFAKKWISDKLKPKN

Appendix D: Recipes

Yeast-Tryptone (YT) Broth growth medium

Tryptone	16g/L
Yeast Extract	10g/L

NaCl 5g/L
Make up to 1L with water and autoclave (121°C and 119 kPa for 20 minutes)

Yeast-Tryptone (YT) Agar

A similar recipe to that of YT broth except 15g bacteriological agar was added per liter of broth. Autoclave the solution (121°C and 119 kPa for 20 minutes)

RF1 250 ml(pH 5.8) (Store at 4 °C)

(100 mM KCl, 50 mM $MnCl_2$, 30mM CH_3COOK, 10mM $CaCl_2$, 15% glycerol)

- 2.45 g or 7.5 ml of 1M CH_3COOK and pH to 5.8 with HCl or acetic acid
- Add 37.5ml glycerol and make up to a final volume of 202.5 ml and Autoclave (121 °C, 119 kPa for 15 to 20 minutes).

Subsequent to autoclaving, add the following autoclaved stocks:

- 25 ml 1M KCl
- 12.5 ml 1M $MnCl_2$
- 2.5 ml 1M $CaCl_2$

RF2 150 ml (pH 6.8) (Store at 4 °C)

(10 mM MOPS buffer pH 6.8, 10 mM KCl, 75 mM $CaCl_2$, 15% glycerol)

- 0.313 g or 1 ml 1M MOPS (pH to 6.8 with KOH)
- Add 22.5 ml glycerol
- Make up to 150 ml with distilled water and autoclave (121 °C, 119 kPa for 15 to 20 minutes.

Subsequent to autoclaving, add the following autoclaved stocks:

- 1.5 ml 1M KCl
- 11.25 ml 1M $CaCl_2$

Appendix E: Organisms

Table 2

Organism	Strain	Genotype
E. coli	JM109	*recA*1 *supE*44 *endA*1*hsdR*17*gyrA*96 *relA*1*thi* _(*lac-proAB*) F'[*TraD*36 *proAB*+ *lacI*q *lacZ* _M15]
E. coli	XL1blue	*supE*44 *hsdR*17 *recA*1 *endA*1 *gyrA*46 *thi relA*1 *lac*- F' [*pro*AB+ *lacI*q *lacZ* _M15 *Tn10* (*tet*r)]
E. coli	M15[pREP4]	
P. falciparum	3D7	Wild type laboratory strain

Appendix F: common protocols for standard molecular biology techniques

F1: Isolation of plasmid DNA

The protocol for isolation of plasmid DNA was adapted from that described for alkaline lysis (Birnboim and Doly, 1979). In brief, *E. coli* cells transformed with the plasmid of interest were grown overnight (37°C, 200 rpm) in 5 ml cultures of 2x YT (1.6% tryptone, 1% yeast extract, 0.5% NaCl) or LB media (1% tryptone, 0.5% yeast extract, 1% NaCl) supplemented with the appropriate antibiotic for plasmid selection (100 μg/ml ampicillin for pQE30-based plasmids). The cells were harvested in a microcentrifuge (16 000 xg, 1 minute) and resuspended in 250 μl of Solution I (2 mg/ml lysozyme, 10 mM EDTA, 50 mM Glucose, 25 mM Tris-Cl, pH 8.0). To the resuspended cells, 250 μl of Solution II (1% (w/v) SDS, 0.2 M NaOH) was added and mixed by inversion, and subsequently 350 μl of Solution III (1.5 M potassium acetate, 12% (v/v) glacial acetic acid) was similarly added. This was followed by centrifugation (16 000 xg, 10 minutes) and precipitation of the DNA from the resulting supernatant with 500 μl of 100% isopropanol (10 minutes, room temperature). The precipitated DNA was pelleted by centrifugation (16000 xg, 10 minutes) and washed with 800 μl of 70% ethanol (4°C). The ethanol was discarded and the pellet was allowed to dry for 20 minutes at room temperature, prior to resuspension in 50 μl of TE buffer (10 mM Tris, 20 μg/ml RNAse A, 1 mM EDTA, pH 8.0). The purified DNA was quantified at 260 nm in a Helios Alpha UV-Vis Spectrophotometer (Thermo Scientific).

F2: DNA digestion with restriction enzymes

Plasmid DNA was digested with the appropriate restriction endonuclease(s) for two or more hours at the appropriate optimal temperature (37°C unless otherwise stated) in a digestion reaction comprising: 200 - 500 ng of plasmid DNA, 2 μl of the appropriate 10x restriction buffer, 1 - 2 U of restriction endonuclease enzyme(s) and distilled water to a final volume of 20 μl. The digested DNA was resolved by agarose gel electrophoresis as described in section F3. Restriction buffers for single and double restriction enzyme digestions were selected as per the supplier's recommendations. *Pst*I-digested λDNA marker was prepared by the digestion of 20 μl of 526 μg/ml λDNA (Promega) for two hours at 37°C in a reaction containing 5 U of *Pst*I restriction enzyme (Fermentas), 20 μl of the appropriate 10x restriction enzyme buffer (Fermentas) and distilled water to a final volume of 200 μl. The digested λDNA was treated with 6x DNA gel loading buffer (0.25% (w/v) bromophenol blue, 30% (v/v) glycerol) for use in subsequent agarose gel electrophoresis (Section F3).

F3: Agarose gel electrophoresis

Agarose gels were prepared by melting molecular grade agarose (0.8% or 1.5% (w/v)) in TBE Buffer (45 mM Borate, 1 mM EDTA, 45 mM Tris-Cl, pH 8.3) and supplementing ethidium bromide to a final concentration of 0.5 μg/ml on cooling prior to casting. DNA samples for electrophoresis were treated with 6x DNA gel loading buffer in a ratio of 5:1 respectively and loaded onto the gel with an appropriate marker of *Pst*I-digested λDNA (prepared as per section F2). The samples were resolved at 90 - 120 V for one hour, and visualized under ultra-violet light with the Chemidoc Imaging System (Bio-Rad). For the visualization of DNA fragments smaller than 500 bp, ethidium bromide staining (0.5 μg/ml in TBE Buffer) was achieved subsequent to electrophoresis.

F4: Extraction and purification of DNA from an agarose gel

Resolved DNA fragments were isolated subsequent to agarose gel electrophoresis using the DNA Clean & Concentrator™-5 kit (Zymo Research) as per the manufacturer's instructions. In brief, the DNA fragment of interest was identified by brief exposure to long-wave UV light, excised from the gel and incubated in 3 volumes of capture buffer ADB (*e.g.* for 100 μl (mg) of agarose gel slice add 300 μl of ADB**)** at 60°C for 5 – 10 minutes until the gel slice is completely dissolved. The melted agarose solution was transferred to a Zymo-Spin™ Column in a Collection Tube and centrifuged at 16 000 xg for 1 minute. Bound DNA was washed twice with 200 μl of DNA wash buffer passed through the column by centrifugation (16 000 xg, 1 minute). The DNA was eluted from the column with 20-30 μl of Elution buffer by further centrifugation (16 000 xg, 1 minute). Quantification of the purified DNA was achieved in a Helios Alpha UV-Vis spectrophotometer (Thermo Scientific) at 260 nm.

F5: Ligation of DNA fragments

DNA fragments intended for ligation (typically 500 ng of insert fragment to 100 ng of target plasmid) were incubated at room temperature for 1 hour followed by overnight at 4°C in a ligation reaction comprising 1 μl of 10x ligation buffer (Roche Applied Sciences), 1 U of T4 DNA Ligase (Roche Applied Sciences) and distilled water to a final volume of 10 μl. The ligation mixture was subsequently transformed into competent *E. coli* cells as described in section F8).

F6: DNA sequencing

Plasmid DNA was isolated for DNA sequencing using the QiaPrep Miniprep Kit (Qiagen) as per the manufacturer's instructions, with the exception that the final DNA elution was achieved with an equal volume of distilled water. DNA Sequencing was carried out

commercially by Inqaba biotech. DNA sequencing results were analyzed using either the BioEdit Sequence Alignment Editor (version 7.0.4.1) or Chromas pro software.

F7: Preparation of competent *E. coli* cells

The strain of interest was grown overnight (37°C, 200 rpm) in 5 ml of 2x YT (1.6% tryptone, 1% yeast extract, 0.5% NaCl) or LB media (1% tryptone, 0.5% yeast extract, 1% NaCl) supplemented with the appropriate antibiotic for strain selection if required. The resulting overnight culture was diluted into 50 ml of 2x YT or LB media to an A_{600} of 0.1 and growth was allowed to proceed until early log phase (A_{600} of 0.3 - 0.6). The cells were harvested by centrifugation (5000 xg, 5 minutes, 4°C) and resuspended in 50 ml of ice-cold 0.1 M $MgCl_2$ (4°C). Following two minutes of incubation at 4°C the cells were pelleted by centrifugation as before and resuspended in 25 ml of ice-cold 0.1 M $CaCl_2$ (4°C). Following incubation at 4°C for one hour the cells were harvested by centrifugation as before and resuspended in 5 ml of 0.1 M $CaCl_2$ and 5 ml of 30% (v/v) glycerol. The competent cells were divided into aliquots and stored at -80°C prior to use.

F8: Transformation of competent *E. coli* cells

Competent *E. coli* cells (100 µl; Section F7) were incubated with 50 - 100 ng of the plasmid DNA of interest (or 2 µl of ligation product) at 4°C for 30 minutes, followed by heat shock (42°C for 45 seconds) and subsequent cold shock (4°C for 2 minutes). The cells were diluted 1:10 with 2x YT (1.6% tryptone, 1% yeast extract, 0.5% NaCl) or LB media (1% tryptone, 0.5% yeast extract, 1% NaCl) pre-warmed to 37°C, and were subsequently incubated for 1 hour with shaking (200 rpm, 37°C). The bacterial suspension (100 µl) was plated onto 2x YT- or LB-agar plates (1.5% agar in 2x YT or LB media) supplemented with the appropriate antibiotics (100 µg/ml ampicillin for pQE30-based plasmid selection; 50 µg/ml kanamycin for *E. coli* M15[pREP4] cells). The plates were incubated overnight at 37°C. Transformation controls included a sterile control with sterile distilled water replacing the plasmid DNA in the incubation mixture, and a competence control with plasmid DNA of known concentration (10 ng of plasmid pUC18; Promega) transformed into the *E. coli* cells.

F9: Sodium dodecyl sulphate – polyacrylamide gel electrophoresis (SDS-PAGE)

The protocol for SDS-PAGE analysis is adapted from that previously described (Shapiro, et al., 1967). Protein samples were treated with 5x SDS-PAGE sample buffer (10% glycerol, 2% SDS, 5% β-mercaptoethanol, 0.05% bromophenol blue, 0.0625 M Tris, pH 6.8) in a ratio of 4:1 respectively and loaded onto a polyacrylamide gel constituted by a resolving gel (12%

(w/v) acrylamide, 0.1% (w/v) SDS, 0.05% (w/v) ammonium persulphate (APS), 0.005% (v/v) N,N,N',N'-tetramethylethylenediamine (TEMED), 0.375 M Tris, pH 8.8) and a stacking gel (4% (w/v) acrylamide, 0.1% (w/v) SDS, 0.05% (w/v) APS, 0.005% (v/v) TEMED, 0.125 M Tris, pH 6.8). The gel was resolved in a Mini ProteanR II system (Bio-Rad) at 150 V for one hour and stained or used for Western analysis (Section F10). Staining of the SDS-PAGE gel was achieved in Coomassie Blue stain (40% (v/v) methanol, 7% (v/v) acetic acid, 0.25% (w/v) Coomassie Blue R250 in distilled water) for 30 minutes and subsequent destaining was achieved overnight in destain solution (40% (v/v) methanol, 7% (v/v) acetic acid in distilled water).

F10: Protein detection by western analysis

The protocol for the detection of proteins by Western analysis was adapted from that described (Towbin, et al., 1979). Proteins were resolved by SDS-PAGE and transferred onto nitrocellulose membrane in transfer buffer (20% (v/v) methanol, 192 mM glycine, 25 mM Tris) at 100 V for 90 minutes in a Mini ProteanR III Western trans-blot system (Bio-Rad). Protein transfer was verified with Ponceau S stain (0.5 % (w/v) Ponceau S, 1% (v/v) glacial acetic acid). The membrane was subsequently destained with distilled water and incubated overnight at 4°C in blocking solution comprised of 5% (w/v) fat-free milk powder in Tris Buffered Saline (TBS; 50 mM Tris, 150 mM NaCl, pH 7.5). The membrane was incubated with appropriate primary antibody (1:5000 in blocking solution unless otherwise stated in the text) for one hour at room temperature and subsequently washed three times with Tris Buffered Saline-Tween buffer (TBS-T; TBS containing 0.1% (v/v) Tween 20). The membrane was similarly incubated with the appropriate horse-radish peroxidise (HRP)-conjugated secondary antibody (1:5000 in blocking solution unless otherwise stated in the text) for one hour at room temperature and washed with TBS-T as before. Chemiluminescence-based protein detection was achieved using the ECL^{TM} Western blotting kit (GE Healthcare) as per the manufacturer's instructions, and captured with a Chemidoc chemiluminescence imaging system (Bio-Rad).

F11: analysis of recombinant protein expression

A colony of the specified *E. coli* strain transformed with the appropriate plasmid was inoculated into 100 ml of the appropriate growth media containing antibiotic selection pressure to the specified final concentration, and incubated overnight for approximately 16 hours at 200 rpm at the stated temperature. The overnight culture was diluted to an A_{600} of 0.1 in 1000 ml of the appropriate growth media supplemented with the appropriate concentration of antibiotic and incubated as before to a specified cell density (A_{600}). Protein expression was induced with 0.5 mM to 1 mM IPTG in the presence of selection pressure as indicated and 1 ml aliquots of the induced cells were harvested at hourly intervals between 0

– 5 hours post-induction and overnight at 16 hours post-induction. The harvested cells were pelleted by centrifugation (16 000 xg; 1 minute) and resuspended in phosphate buffered saline (PBS; 137 mM NaCl, 2.7 mM KCl, 10.3 mM Na2HPO4, 1.8 mM KH_2PO4, pH 7.4) in volumes dependent on the cell density (150 µl of PBS per 0.5 recorded A_{600} absorbance units). Samples were analyzed for recombinant protein expression by SDS-PAGE and Western analysis using appropriate antibodies.

Appendix F: Output

James M. Njunge, Michael H. Ludewig, Aileen Boshoff, Eva-Rachele Pesce, and Gregory L. Blatch. Hsp70s and J Proteins of *Plasmodium* Parasites Infecting Rodents and Primates: Structure, Function, Clinical Relevance, and Drug Targets. Current Pharmaceutical Design, 2013, 19, 387-403. Attached